Synthesis of Polyene Natural Products

MADDEN, KATRINA,SOPHIE

Synthesis of Polyene Natural Products

A thesis submitted as partial fulfilment of the requirements for the degree of Doctor of Philosophy at the Department of Chemistry, Durham University, UK

Submitted by

Katrina Sophie Madden

Under the supervision of

Professor Andy Whiting

Supported by the EPSRC

2016

Declaration

The work described in this thesis was carried out by the author unless stated otherwise or referenced. The material contained has not been submitted previously for any qualification. The copyright of this thesis rests with the author and any information derived from it should be correctly acknowledged.

Table of Contents

For Dad, who is my inspiration in everything I do.

Acknowledgements

I would first like to thank Professor Andy Whiting for offering me a chance to work on this project, for his endless patience, his constant support, and for his limitless supply of wisdom, wit and coffee. In addition, I would like to thank Dr Jonathan Knowles for his guidance, without which I would have struggled to master the skills required to isolate such unstable compounds.

Special thanks must go to Matthew Harris, who has been unwavering in his support throughout my PhD, and who I am grateful for every day (except for the days when I received drafts of this thesis after his proof-reading). Additional thanks go to my parents who, as chemists themselves, have been so enthusiastic throughout this project, if a little amused on days when practical chemistry hasn't gone too well.

I would like to thank the members of the Whiting group, both past and present. Special thanks go to Daniel Thompson, Sylvain David and Yoann Bouchard for their contributions to this project. In addition, I would like to extend my gratitude to Dr Adam Calow, who remains a valued mentor and friend. Other members I would like to thank (in no particular order) are Dr Alex Gehre, Dr Wade Leu, Dr Farhana Ferdousi, Dr Garr-Layy Zhou, Dr Hesham Haffez, Dave Chisholm, Alba Pujol, Sergey Arkhipenko, Dr Mona Al-Batal, Dr Ludovic Eberlin, Enrico La Cascia, Dr Duangduan "Nim" Chaiyaveij and Hannah Wilson.

The analytical services have been outstanding, in particular the NMR and Mass Spectrometry services, which have been so accommodating in running unstable samples. The fantastic service of the EPSRC Mass Spectrometry Service at Swansea should also be acknowledged.

I would also like to thank all of those who have collaborated on this project; Professor Conrad Mullineaux for his work on the bacteriology of *Xanthomonas* bacteria, Professor Monica Höfte and Dr Bart Cottyn for their donation of *Xanthomonas* strains that could be transported across borders and to Dr Jean-François Halet for his computational insight.

Finally, I would like to thank the friends and colleagues from other groups who have made working in this department such a pleasure, particularly Laura Smith, Dr Tony Harsanyi, Chris Jennings, Dr Luke Wilkinson, Jack Pike, and Jasmine Cross.

Abstract

A convergent approach was applied to the synthesis of a range of *Xanthomonas* pigments and a number of selected analogues, with a view to understanding more about their photoprotective properties, and utilising the group's iterative Heck-Mizoroki/ iododeboronation cross-coupling methodology to access polyenyl intermediates. This involved the synthesis of a number of key arenyl building blocks. Three polyenyl building blocks were accessed *via* sequential Heck-Mizoroki and iododeboronation reactions, providing flexibility in the construction of the pigments and their analogues. Following some optimisation of final cross-coupling reactions, two truncated bacterial pigment analogues were successfully synthesised, with evidence of the synthesis of one of the natural product pigments also obtained. The key challenges in these syntheses lay in the considerable instability of many of the polyenyl intermediates (particularly the polyenyl iodides) and in the successful coupling onto the arenyl intermediates.

Extensive NMR analysis, along with UV-Vis analysis provided insight into the photochemical behaviour of the truncated model compounds, and also corroborated the initial characterisation obtained by Andrewes *et al.* when they isolated xanthomonadin in 1976.

Studies were also undertaken into novel methods of polyene synthesis, with vinyl iodide established as a potential Heck-Mizoroki coupling partner, providing access to a key dienyl boronate building block. This dienyl boronate was used to access a range of terminal dienes and trienes, providing a versatile route to such compounds. The group's Heck-Mizoroki cross-coupling conditions were also re-optimised to operate at room temperature, at low catalyst loadings, and on much shorter timescales than had been utilised previously.

Abbreviations

4 Å MS 4 angstrom molecular sieves

Ar argon

ASAP atmospheric solids analysis probe

Bpin- 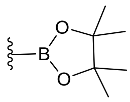

BHT 2,6-di-*tert*-butyl-4-methylphenol

Boc *tert*-butyloxycarbonyl protecting group

CCD countercurrent distribution

CD circular dichromism

$CDCl_3$ deuterated chloroform

$CHCl_3$ chloroform

COSY correlation spectroscopy

d days

DBU 1,8-diazabicycloundec-7-ene

DCM dichloromethane

DIBAL di-*iso*butyl aluminium hydride

DMAP 4-dimethylaminopyridine

DME 1,2-dimethoxyethane

DMF dimethylformamide

DMSO dimethylsulfoxide

DMSO-d_6 deuterated dimethylsulfoxide

DOSY diffusion ordered spectroscopy

dppf 1,1'-bis(diphenylphosphino)ferrocene

EI electron ionisation

ESI electrospray ionisation

Et_2O diethyl ether

EtOAc ethyl acetate

GC gas chromatography

GCMS gas chromatography mass spectrometry

H hours

HIV human immunodeficiency virus

HM Heck-Mizoroki (Use of this abbreviation within schemes indicates use of the group's iterative cross-coupling conditions i.e. $Pd(OA)_2$, $P(o\text{-tol})_3$, AgOAc and MeCN, unless otherwise stated)

HMBC heteronuclear multiple-bond correlation spectroscopy

HPLC high pressure liquid chromatography

HRMS high resolution mass spectrometry

HSQC heteronuclear single quantum coherence

HSV herpes simplex virus

HWE Horner-Wadsworth Emmons

Hz hertz

ICC iterative cross-coupling

IDB iododeboronation (Use of this abbreviation within schemes indicates use of the group's iterative cross-coupling conditions i.e. NaOMe, ICl, THF and DCM, unless otherwise stated)

IR Infra-red Spectroscopy

J coupling constant, NMR

LCMS liquid chromatography mass spectrometry

M molar

MeOH methanol

MeOD-d_4 deuterated methanol

MIDA N-methyliminodiacetic acid

min minutes

mmol millimoles

mol moles

mp melting point

MS mass spectrometry

NBS *N*-bromosuccinimide

NIS *N*-iodosuccinimide

NMR nuclear magnetic resonance spectroscopy

NOESY nuclear overhauser enchancement spectroscopy

o/n overnight

Ph phenyl

ppm parts per million

ROS reactive oxygen species

rt room temperature

SM Suzuki-Miyaura

TBAF tetrabutylammonium fluoride

TBS tert-butyldimethylsilyl

^{t}Bu *tert*-butyl

THF tetrahydrofuran

TLC thin layer chromatography

TMB 1,3,5-trimethoxybenzene

TMS trimethylsilane

UPLC ultra performance liquid chromatography

UV ultraviolet

Xantphos 4,5-bis(diphenylphosphino)-9,9-dimethylxanthene

Introduction

The term 'polyene natural product' encompasses a large group of compounds with a variety of interesting structures and properties. Of particular interest are those natural products which display biological activity. Whilst a large number of polyenes have been discovered, with over 200 polyenes in the polyene macrolide class alone,[1] they still present a considerable challenge in terms of total synthesis.[2] The construction of longer conjugated polyenes presents a number of obstacles in terms of stereoselectivity, reactivity and product stability. Those natural products containing all-*trans* polyene moieties tend to be more stable, whilst those containing all-*cis* olefins, or a mixture of *cis* and *trans* double bonds are much more prone to isomerisation and therefore present a greater challenge in terms of their synthesis.[3]

Polyenes can be unstable to light and heat, and strongly acidic or basic conditions, often resulting in a need for mild reaction conditions.[4] The traditional method of double bond formation has been achieved using ylide-based Wittig chemistry, with the Horner-Wadsworth Emmons (HWE) employing the mildest conditions.[5] Reasonable levels of stereoselective control are well established within ylide chemistry. There is, though, a need to either separate or subject stereoisomers to isomerisation conditions. With the ever expanding scope of palladium cross coupling chemistry, it has become possible to assemble highly complex conjugated systems with high efficiency and stereoselectivity.[1,2] In addition, olefin cross metathesis has been used more recently in polyene construction.[6]

An interesting question is whether transition metal-based strategies are beginning to take over as the method of choice for polyene construction. This review aims to provide an insight into some of the non-isoprenoid polyene structures discovered to date, and highlight attempts to complete their total synthesis. These non-isoprenoid polyene natural products will be discussed in classes determined by the length of the polyene moieties, with the total synthesis of at least one example in each class discussed in detail. Particular focus is given to the construction of the polyene chains within these natural products, and the strategies and synthetic methods which have been employed to make them. As the class of triene non-isoprenoid natural products is quite large, reasonably simple to construct, and provides enough scope for a review in its own right, this review will begin its focus from tetraene-containing natural products and longer.

Tetraenes

There are a large number of compounds containing the tetraene moiety. These have been isolated from a wide variety of natural sources and display a number of different types of biological activity.

Macrocyclic tetraenes

Polyene macrolide structures are often strongly associated with antifungal activity. There are a large number of tetraene polyene macrolides, produced by many different organisms, but often with very similar structures. Some important tetraene polyene macrolides are discussed below and all share common features. The macrocycles are bicyclic, with a larger ring of varied size and a six-membered cyclic ether. In addition, they also all possess an oxygen-linked cyclic six-membered ether substituent, the structure of which is highly conserved. Seven tetraene natural products share the same general structure. One difference, however, is the nature of the amine. Lucensomycin **1**, otherwise known as etruscomycin, is produced by *S. lucensis*[7] and contains an epoxide. Arenomycin B **2** is produced by *A. tumemacerans var. griseoarenicolor*.[8] The family of tetrins A-C have similar structures, with tetrin A **3** and B **4** produced by *Streptomyces sp.*[9,10]and tetrin C **5** produced by *Streptomyces sp.* GK9244.[11] Tetromycin A **6** and B **7** are both produced by *S. noursei var. jenensis*.[12] Similar structures to these tetraenes include pimaricin **8**, AB-400 **9**, rimodicin **10** and rimodicin B **11**, C **12**, CE-108 A **13**, B **14** and C **15**. Pimaricin **8**, otherwise known as natamycin, is a polyene macrolide produced by *S. natalensis, S. chattanoogensis,* and *S. gilveosporus* and is used as a natural preservative in the food industry.[13] It is also used as a treatment for fungal keratitis, as well as cutaneous, vaginal and intestinal cancer,[14] and antimalarial activity.[15] AB-400 **9** is a closely related analogue, produced by *Streptomyces sp. RGU5.3*.[16] Rimocidin **10** and rimocidin B **11** and C **12** are all produced by *S. diastaticus*, and rimocidin is also produced by *S. rimosus*.[17,18]CE-108 A **13**, B **14** and C **15** are all produced by *S. diastaticus* var. 108.[19] Larger macrocycles with similar structures include amphotericin A

16 and nystatin **17**. Amphotericin A **16** is produced by *S. nodosus*.[20] Nyastatin **17** is produced by *S. noursei* and displays broad spectrum antifungal activity[21] and possesses antimalarial activity.[15]

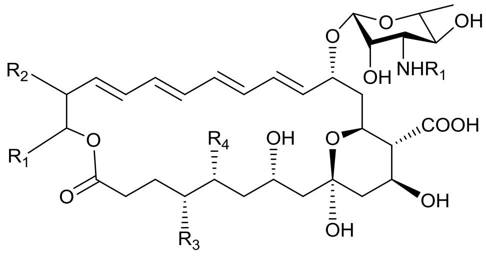

	R_1	R_2	R_3	R_4
lucensomycin **1**	n-C_4H_9	H	-O-	(epoxy)
arenomycin B **2**	n-C_4H_9	H	H	OH
tetrin A **3**	CH_3	CH_3	H	OH
tetrin B **4**	CH_3	CH_3	OH	OH
tetrin C **5**	CH_3	CH_3	H	H
tetramycin A **6**	CH_3	C_2H_5	H	OH
tetramycin B **7**	CH_3	C_2H_5	OH	OH

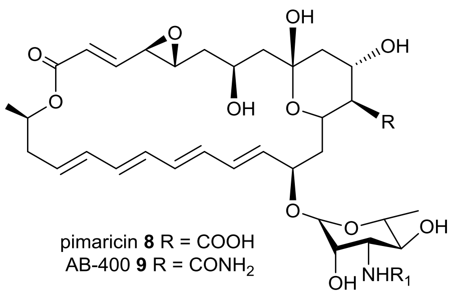

pimaricin **8** R = COOH
AB-400 **9** R = $CONH_2$

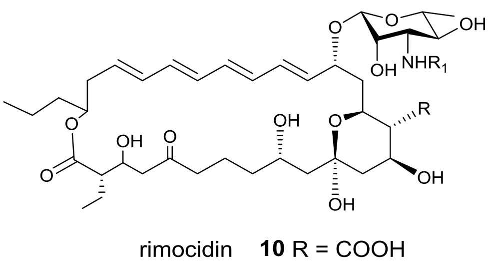

rimocidin **10** R = COOH
rimocidin B **11** R = $CONH_2$
rimocidin C **12** R = CH_3

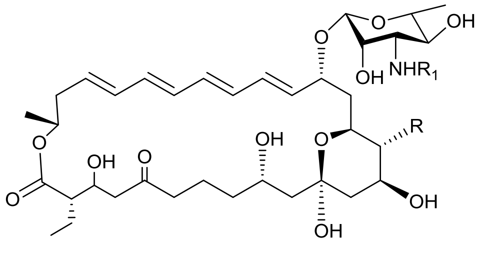

CE-108 **13** R = COOH
CE-108B **14** R = $CONH_2$
CE-108C **15** R = CH_3

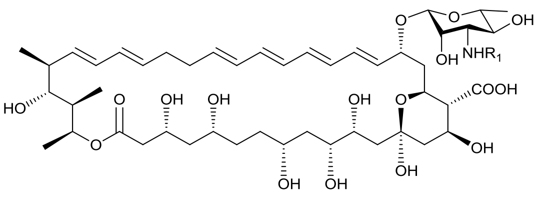

amphotericin A **16**

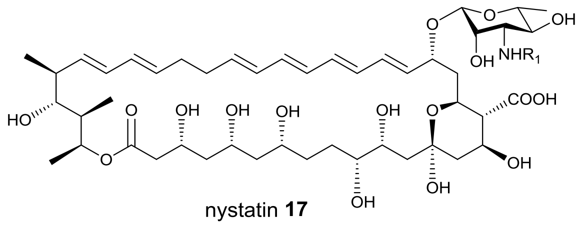

nystatin **17**

Common to all of the macrocycles above are the all-*E* configuration of the polyene moieties. Other macrocyclic polyenes are viridenomycin **18** and the marinomycins A-C **19-21**, whose total syntheses will be discussed in due course and whose structures are very different to those discussed above.

Linear tetraenes

There are a number of linear tetraene natural products and these include fumigillin **22** and lajollamycin **23**. These structures share far fewer similarities than those discussed in the macrocyclic tetraenes section above. Fumigillin **22** is produced by *Aspergillus fumigans* and displays amebicidal, anticancer, antiparasitic and antibacterial properties. It is also an angiogenesis inhibitor.[1,22] Its structure contains an all *E*-tetraene and a highly functionalised cyclohexane ring, as well as two epoxide rings. Lajollamycin **23** is produced by *Streptomyces nodosus* and displays antimicrobial and antitumour activities.[23] Its structure contains an *E:E:Z:Z*-tetraene, an amide linkage and a conjoined lactam and lactone.

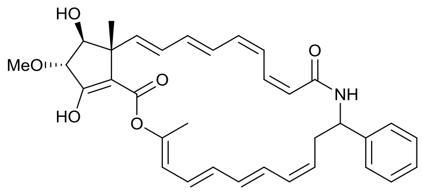

viridenomycin **18**

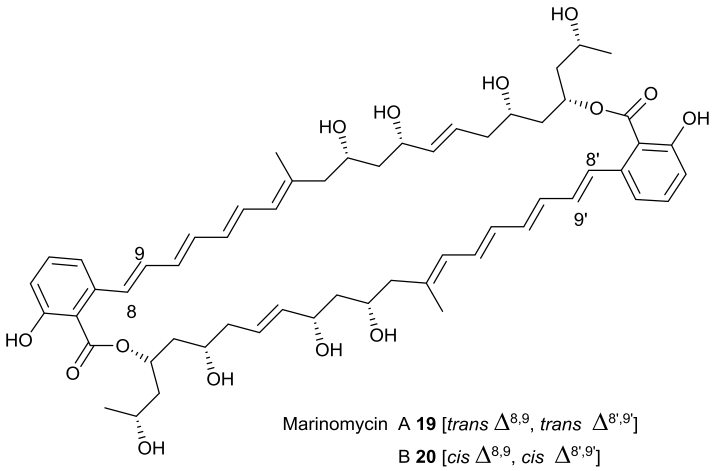

Marinomycin A **19** [*trans* $\Delta^{8,9}$, *trans* $\Delta^{8',9'}$]
B **20** [*cis* $\Delta^{8,9}$, *cis* $\Delta^{8',9'}$]
C **21** [*trans* $\Delta^{8,9}$, *cis* $\Delta^{8',9'}$]

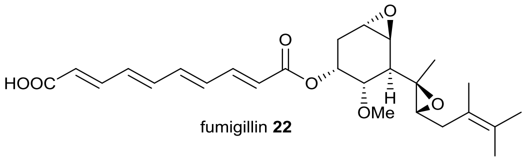

fumigillin **22**

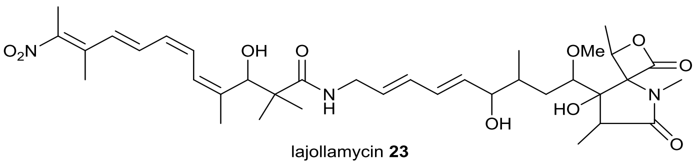

lajollamycin **23**

Viridenomycin

Viridenomycin **18** was first reported as a polyene natural product in 1975 by Hasegawa *et al.*, who isolated it from *S. viridochromogenes*. This compound was shown to have activity against *Trichomonas vaginalis* and Gram-positive bacteria.[24] In 1991, a compound was also reported to be isolated from *S. gannmycicus* and was shown to be identical to **18**. The absolute stereochemistry of the compound was not determined, with only the relative stereochemistry of the cyclopentene core known and the relative stereochemistry between the core and benzylic stereocentre.[25] This macrocycle also contains two tetraenes, one with an *E:E:E:Z*-configuration and the other being *E:E:Z:Z*. Additionally, the macrocycle contains a functionalised cyclopentene ring and is connected together by a lactam and enol ester. Shortly after, **18** was shown to have anticancer properties, prolonging the lives of mice affected by B16 melanoma and P388 leukaemia.[26] Two groups have published work pertaining to the synthesis of the polyene portions of viridenomycin **18**. Kruger and Meyers attempted two routes,[27,28] with their disconnection of the macrocycle giving three fragments **24-26** (**Scheme 1**). The intention was to install the lower (*E:E:E:Z*)-tetraene using a Julia olefination and the upper (*E:E:Z:Z*)-tetraene by a palladium catalysed cross coupling and subsequent alkyne reduction. Diene **30** was synthesised successfully using the Stork-Zhao Wittig homologation and then a Stille coupling. The aryl sulfonate was then successfully installed to give **31**, ready for an olefination reaction to give the lower tetraene (**Scheme 2**).

Scheme 1 Kruger and Meyers disconnection of **18**

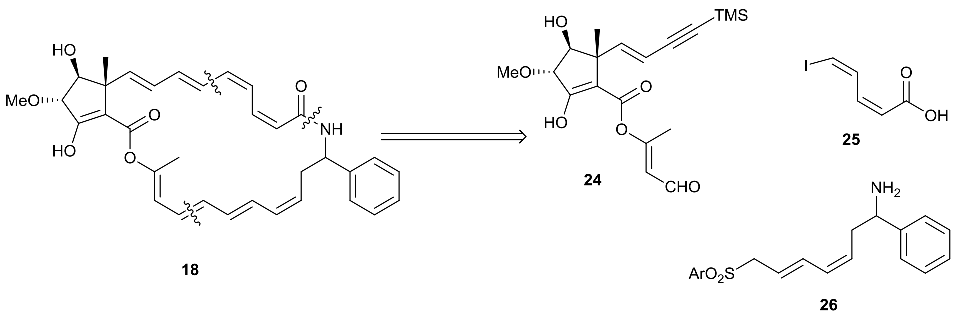

Scheme 2 Synthesis of sulfonate **31**

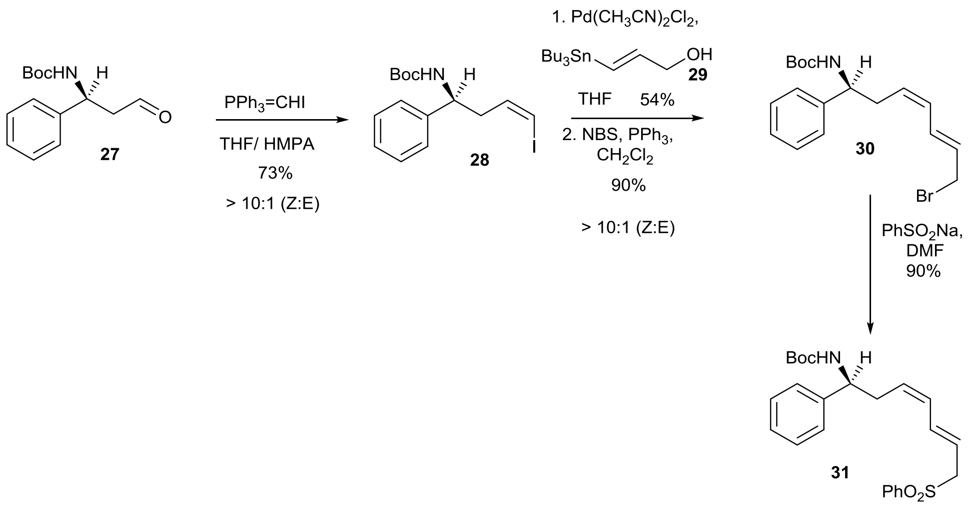

Attempts to build the tetraene using a Julia olefination proved unsuccessful in a closely related model system. This route was put on hold and another investigated.[27] The new route involved construction of the lower tetraene using either Wittig or Horner-Emmons chemistry. Another change was made in the formation of the upper tetraene, where the previously designed alkyne incorporation and reduction was causing concern. Instead, the intention was to undertake direct tetraene formation using a Stille coupling.

In order to make the upper tetraene, trienyl stannane **34** was required. This was made via a Still-Gennari-style phosphonate to afford *cis*-diene **33** with > 20:1 *E*:*Z* ratio. Palladium catalysed cross coupling with distannylethylene gave the desired triene **34** (**Scheme 3**). Coupling of stannane **34** to give the upper tetraene was successful, giving the desired product **36** in quantitative yield (**Scheme 4**). Formation of the lower tetraene to yield the bis-tetraene **38** was then attempted and the bis-tetraene was obtained as a 1:1 mixture of alkene stereoisomers (**Scheme 5**). Unfortunately, attempts at deprotection and ring closure proved unsuccessful.[28]

Scheme 3 Synthesis of triene **34**

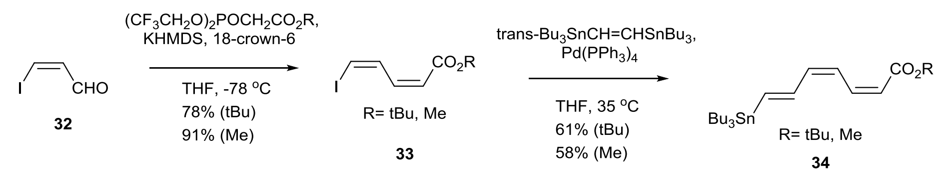

Scheme 4 Synthesis of tetraene **36**

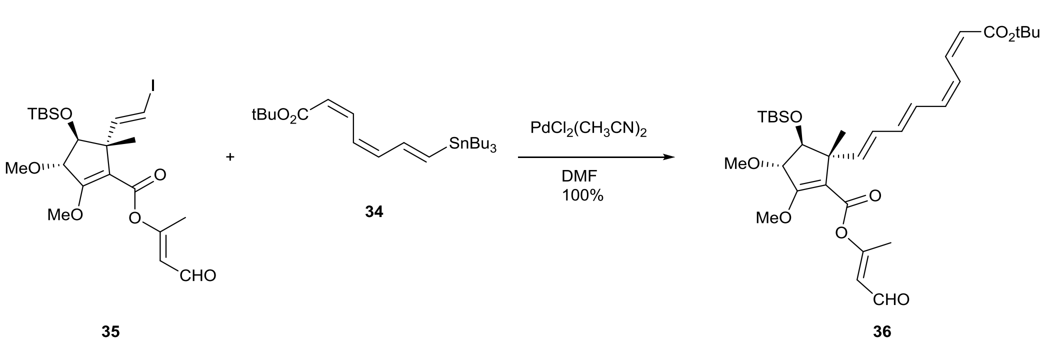

Scheme 5 Synthesis of bis-tetraene **38**

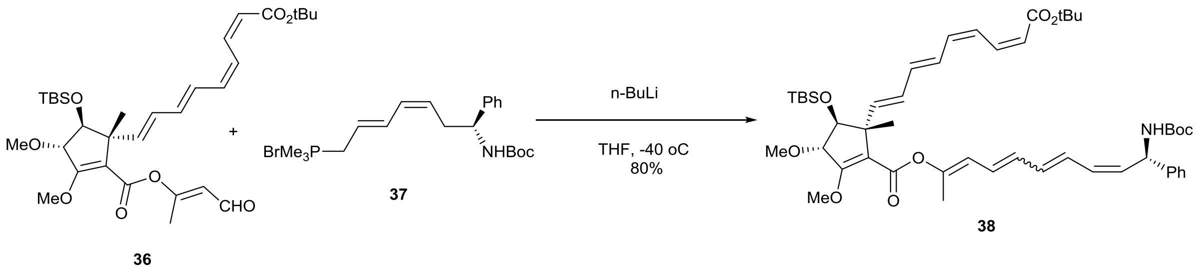

The Whiting group has focussed on Heck-Mizoroki (HM) methodology to build **18**,[29] with the proposed disconnection strategy for viridenomycin shown in **Scheme 6**. A model incorporating benzene rings as *Z*-alkene analogues was also used to identify suitable conditions for the synthesis of the polyene chains. In addition, the northern triene **47** was synthesised using the group's iterative HM/iododeboronation cross-coupling methodology (**Scheme 7**).[30,31] Here, the stereochemistry of the resulting alkenyl iodides could be completely controlled *via* altering the order of addition for the iododeboronation reagents; addition of iodine monochloride first resulted in a *Z* geometry, whereas addition of sodium methoxide first resulted in an *E* geometry.

Scheme 6 Proposed disconnection strategy for **18**

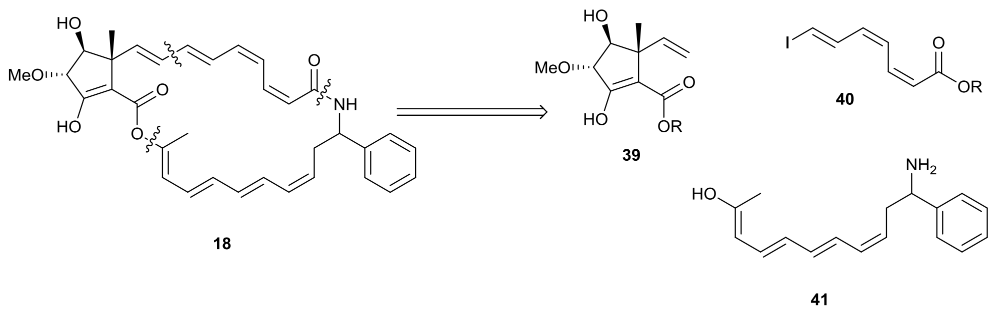

Scheme 7 HM/iododeboronation methodology used in the synthesis of triene **47**

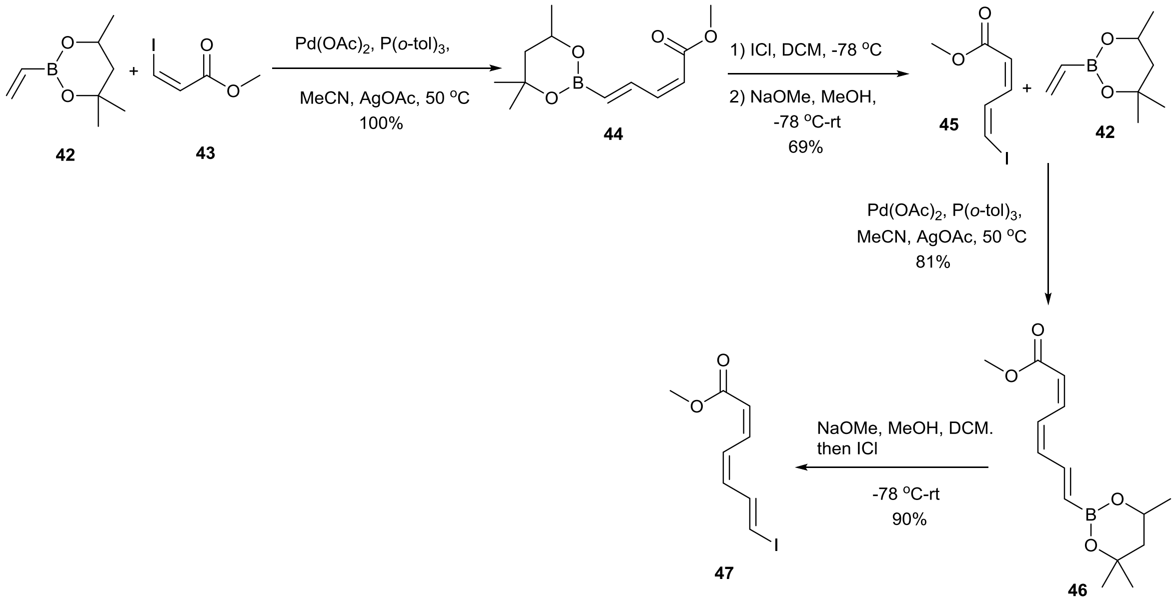

Marinomycins A-C

Marinomycins A-C **19-21** are three polyenic macrodiolides isolated by Fenical *et al.* in 2006 from the saline culture of a new group of marine actinomycetes, *Mannispora* strain CNQ-140. The marinomycins display antitumour and antibiotic activity. Fenical *et al.* showed that marinomycin A **19**, the most abundant and active of the three natural products, was photochemically converted into an equilibrium mixture of marinomycins A **19**, B **20** and C **21** upon exposure to ambient light. As a result, the total synthesis of marinomycin A **19** would also constitute a total synthesis of the two others.[32]

The marinomycins are characterised by a highly complex 44-membered dimeric molecule, with a monomer consisting of a tetraene conjugated with an aromatic unit derived from 2-hydroxybenzoic acid and connected to a pentahydroxylated polyketide chain.[33] The variation between the three different marinomycins lies in the stereochemistry of the two double bonds adjacent to the 2-hydroxybenzoic acid groups.

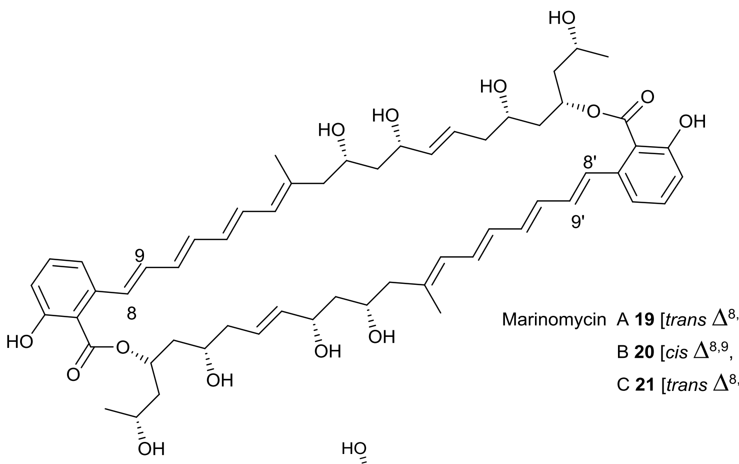

Marinomycin A **19** [*trans* $\Delta^{8,9}$, *trans* $\Delta^{8',9'}$]
B **20** [*cis* $\Delta^{8,9}$, *cis* $\Delta^{8',9'}$]
C **21** [*trans* $\Delta^{8,9}$, *cis* $\Delta^{8',9'}$]

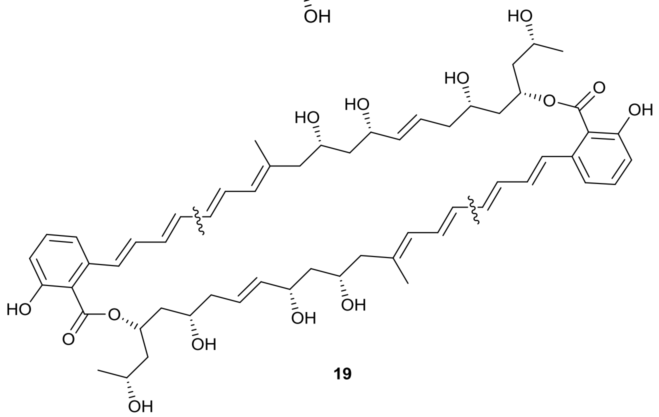

19

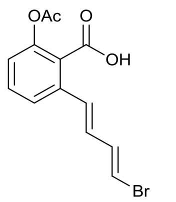

48

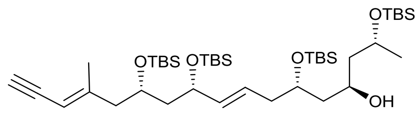

49

Three groups have either attempted or completed the total synthesis of **19**. Nicolaou's group was the first to synthesise **19** and undertake isomerisation studies to form **20** and **21**.[34,35] The retrosynthesis for **19** involved cleavage of the tetraene to give two monomeric counterparts. Two building blocks were synthesised, diene **48** and enyne **49**, which could then be joined together by a palladium catalysed cross coupling. In this synthesis, the tetraenes were built using palladium chemistry, although ylide chemistry was used elsewhere in the synthesis for isolated double bonds. The aryl dienyl bromide **54** was easily made by converting aryl alkyne **50** to the vinyl boronate ester **51**, followed by a Suzuki-Miyaura (SM) reaction with trimethylsilyl vinylbromide **52** and subsequent conversion to the desired bromide (**Scheme 8**). The aryl dienyl iodide was also made, but this compound underwent isomerisation to give the undesired *cis*-isomer.[34,35] A Mitsunobu reaction between the carboxylic acid of aryl diene fragment **48** and the hydroxyl of enyne **49** was used to join the building blocks at one end. The first tetraene formation was then undertaken by conversion of the enyne triple bond to a vinyl boronate ester, and subsequent Suzuki coupling with the aryl dienyl bromide (**Scheme 9**). A further Mitsunobu, followed by another hydroboration/SM sequence was used to close the macrodiolide. The closure was difficult, requiring stoichiometric palladium and 300 equivalents of a thallium base (**Scheme 10**).[34,35] Attempts were also made to improve the yield of the cyclisation, investigating the use of both HM and Stille **c**ouplings as methods of tetraene formation. Unfortunately, none of these routes were successful and the yield was not improved.

The ability to form marinomycins B **20** and C **21** from A **19** was also demonstrated by exposure to ambient light. Marinomycin A underwent photoinduced isomerisation, giving a ratio of roughly 1.1:1:1.5 (A:B:C respectively) after two hours, as analysed by HPLC. [34,35]

The other groups that attempted the synthesis of marinomycin chose to build the tetraene into a building block, rather than form it during a ring closure. Efforts of the Cossy group have yielded the monomeric counterpart of marinomycin A.[33,36] The intention was to form a triene building block, with a palladium catalysed cross coupling envisioned to form the tetraene (**Scheme 11**). Initially, an attempt was made to form the boronate ester variant of the triene **64**. Unfortunately, stereoselectivity problems led to the concept of a tetraene-forming Suzuki coupling being abandoned for a Stille approach (**Scheme 12**). The new approach involved a Stille coupling followed by an olefination to give a trienic vinyl stannane **69** (**Scheme 13**).

Scheme 8 Synthesis of dienyl bromide **54**

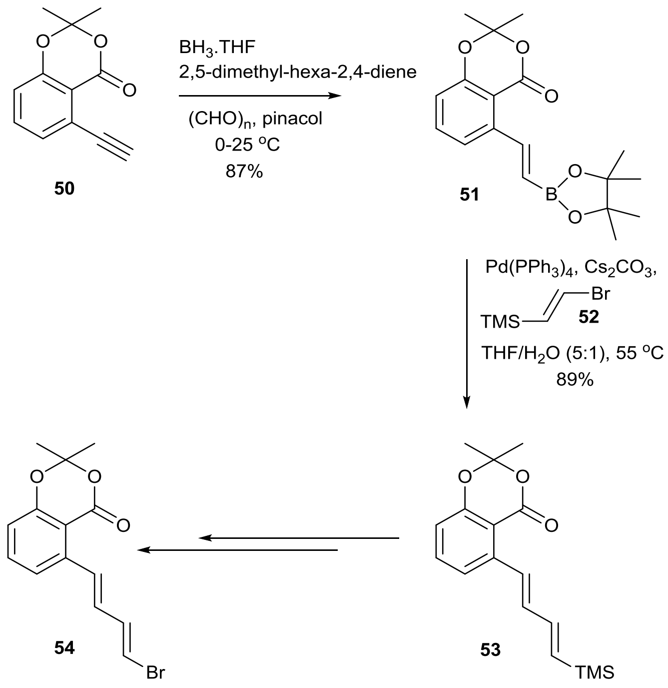

Scheme 9 Construction of tetraene **56**

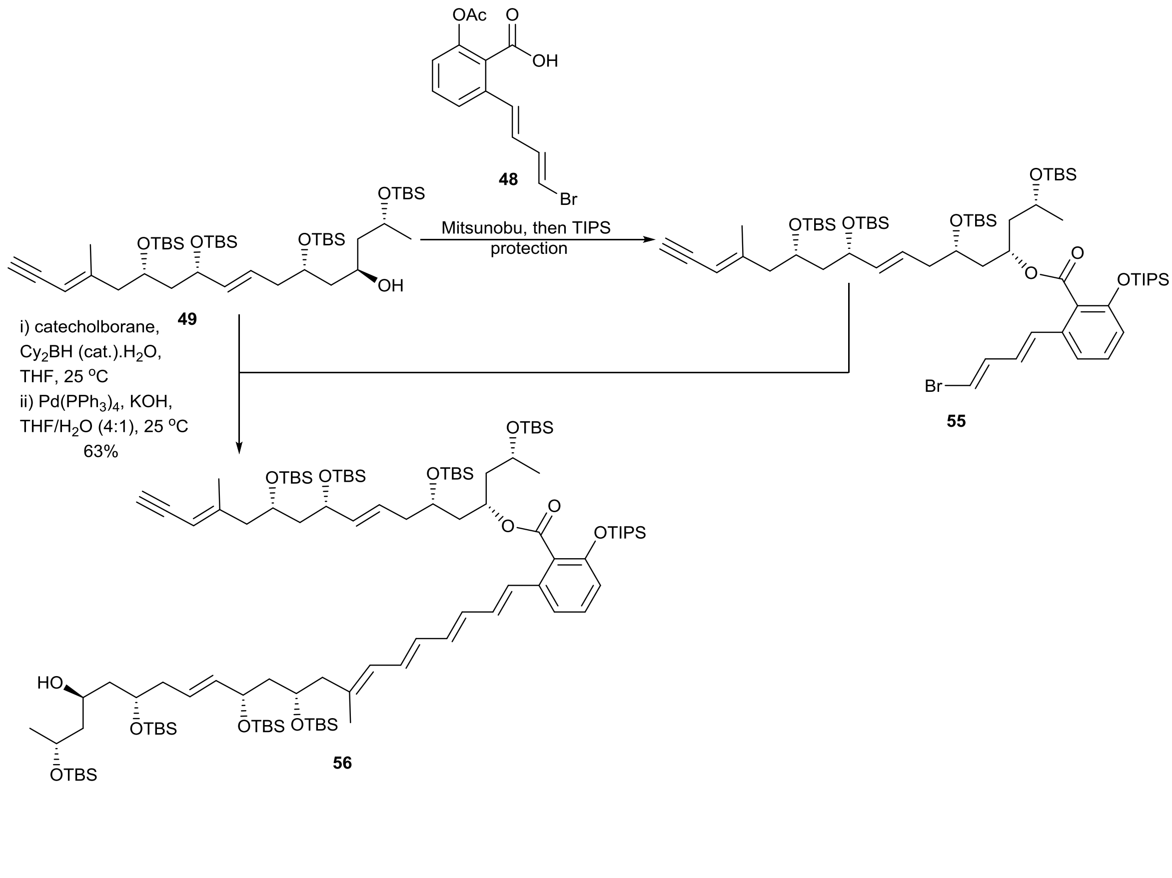

Scheme 10 Completion of the synthesis of **19**

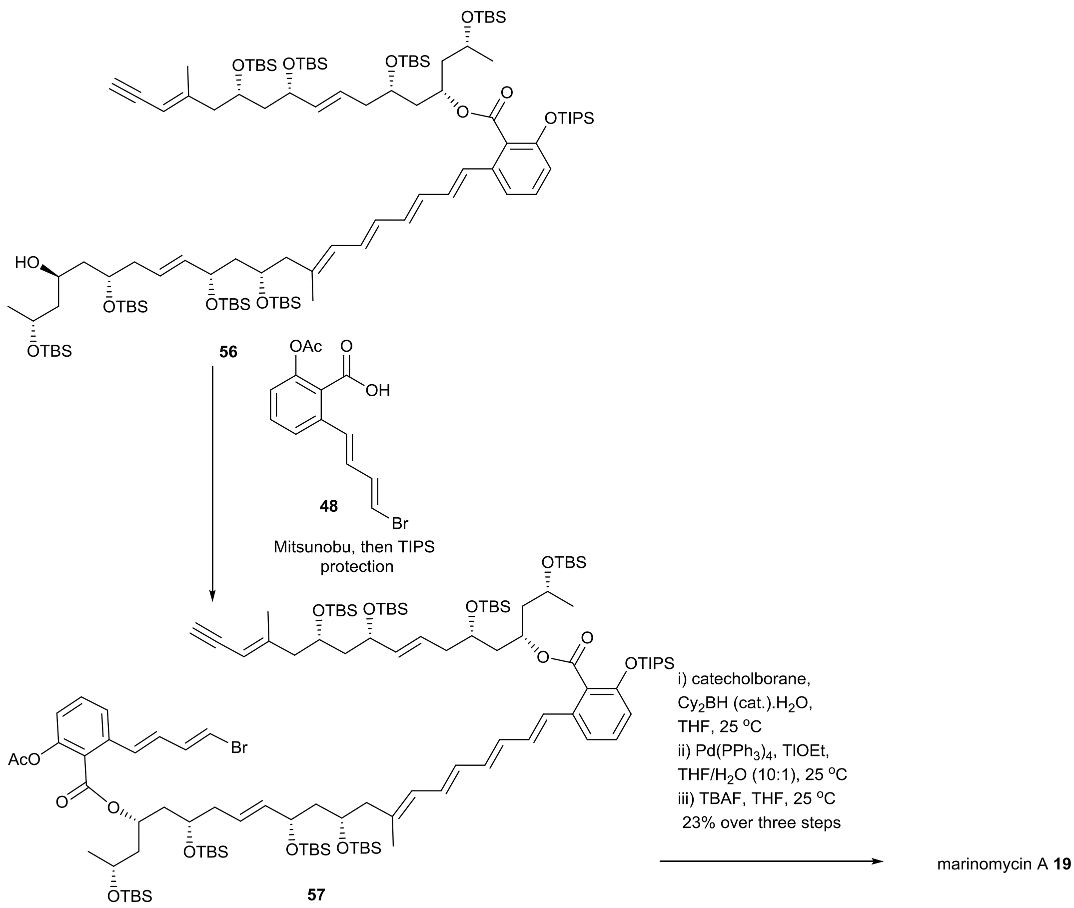

Scheme 11 Envisioned construction of tetraene **60**

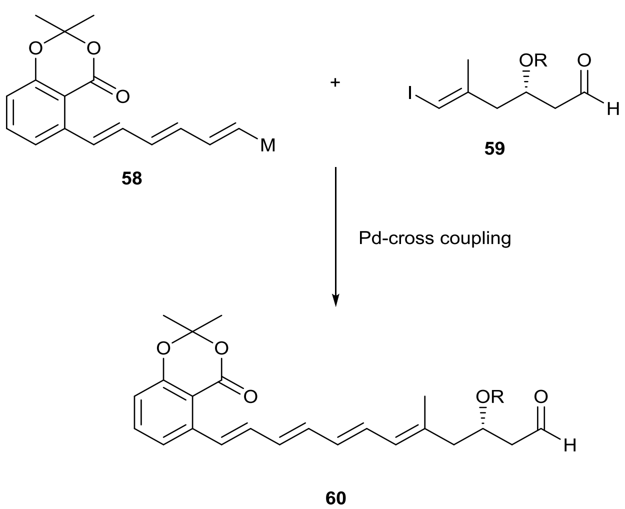

Triene **69** was then used to complete the monomer synthesis *via* a Stille coupling with a penta-alkoxylated alkenyl iodide **70** (**Scheme 14**). Difficulties in deprotection prevented the completion of the total synthesis of marinomycin A **19** using this route.[33,36] In the Evans group, the tetraene was again built before dimerization.[37]

Scheme 12 Attempted route towards **64**

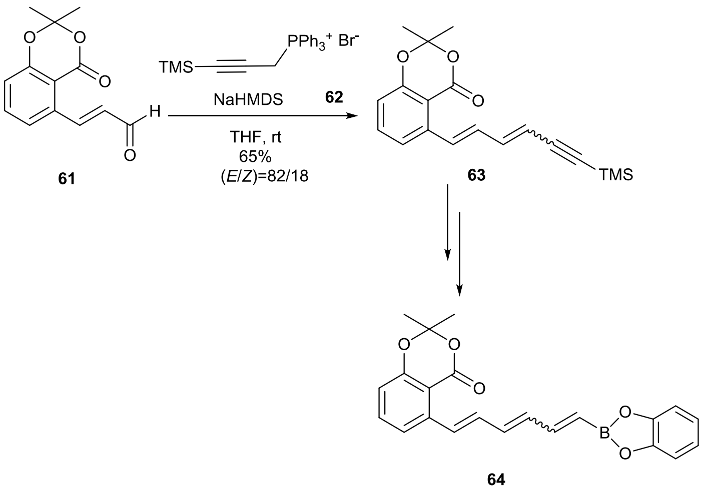

Scheme 13 Synthesis of trienic vinyl stannane **69**

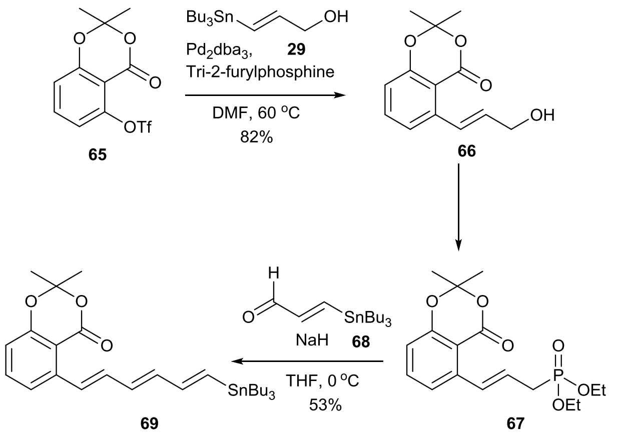

Scheme 14 Stille coupling to form monomer **71**

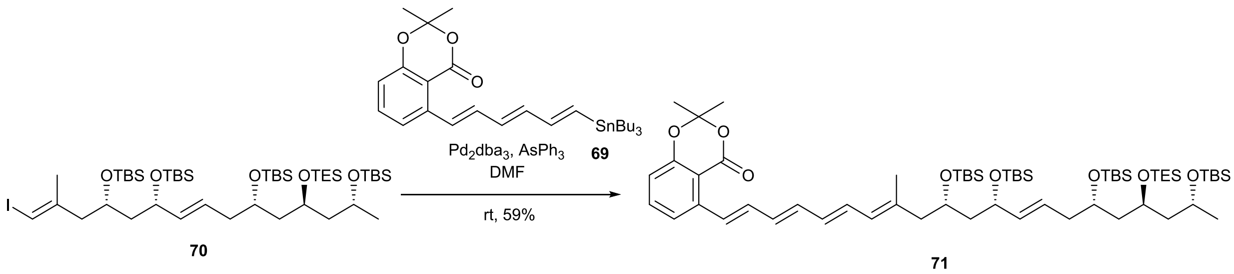

Scheme 15 Synthesis of tetraene **74**

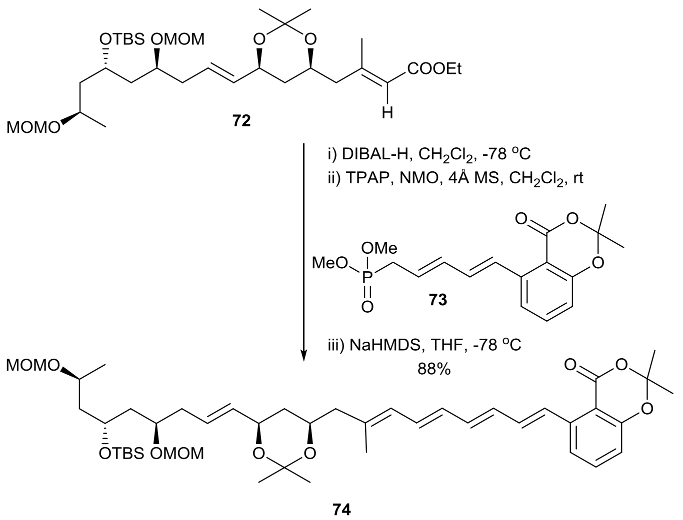

Pentaenes

Macrocyclic pentaenes

Like the tetraene polyene macrolides, there are a number of pentaene containing-compounds with closely related structures. TPU-0043 or chainin **75**, filipin III **76** and fungichromin **77** all possess similar structures, varying in the nature of the aliphatic side-chain and in one substituent on the macrocycle. TPU-0043 **75** is an antifungal compound produced by *Streptomyces* sp. TP-A0625 and *Chainia minutisclerotica.*[38,39,40] Filipin III **76** is another antifungal produced by *S. filipinensis*.[41] It has also been shown to have antimalarial activity.[15] Fungichromin **77** was first isolated from *S. padanus* PMS-702 in 1958[42] and was also shown to be produced by *S. griseus* in 1980.[43] A number of apparently different antifungals were isolated in the 1950s, 60s and 70s, all believed to have the same chemical structure as fungichromin. There were, however, inconsistencies in the analytical data [HPLC, ^{13}C NMR, circular dichroism (CD) and counter-current distribution (CCD)], which the groups reporting these compounds believed to be due to differing stereochemistry in each of the different compounds. The supposed new compounds discovered were named pentamycin, (isolated in 1958 from *S. penticus*)[44] lagosin (isolated in 1964)[45] and cogomycin (isolated in 1975).[46,47] In 1982, it was shown that these compounds were in fact identical and that the previous inconsistencies in the analytical data were due to differing levels of impurities in the isolated samples. This report also listed *S. cellulosae, S. roseoluteus* and *S. fradiae* as the organisms producing fungichromin.[48]

A compound with a similar structure, but a shorter polyol chain is aurenin **78**, an antifungal isolated from *S. aureus*[49] and later from *Actinomyces aureorectus*.[50] Other macrocyclic pentaenes include roflamycoin **79**, RK-397 **80**, roxaticin **81**, mycoticins A **82** and B **83**, marinisporolides A **84** and B **85**, strevertenes A-G **86-92**, eurocidin D **93**, mirabilin **94** and lienomycin **95**. Roflamycoin or flavomycoin **79** is an antifungal isolated from *S. roseoflavus*.[51] RK-397 **80** is another polyene macrolide isolated from a strain of soil bacteria.[52] This compound, along with attempts made at its total synthesis, are discussed later (*vide infra*). Roxaticin **81** is an antifungal isolated from streptomycete X-14994.[53,54] Mycoticins A **82** and B **83** are compounds with broad antimicrobial properties, isolated from *Streptomyces ruber* (ATCC #3348).[55,56]

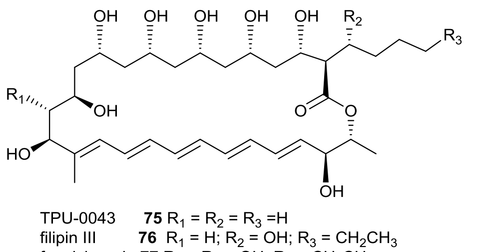

TPU-0043 **75** $R_1 = R_2 = R_3 = H$
filipin III **76** $R_1 = H$; $R_2 = OH$; $R_3 = CH_2CH_3$
fungichromin **77** $R_1 = R_2 = OH$, $R_3 = CH_2CH_3$

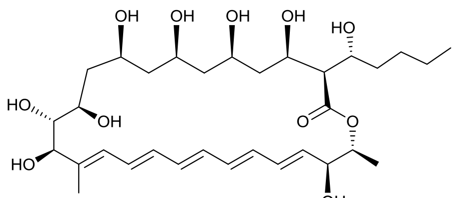

aurenin **78**

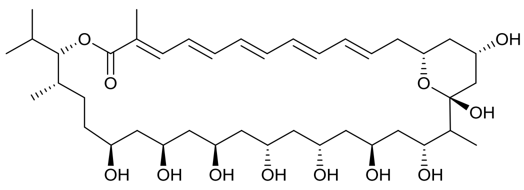

roflamycoin **79**

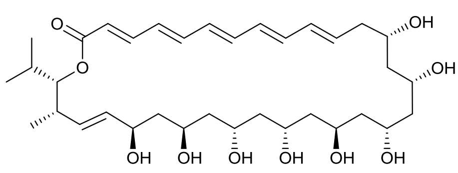

RK-397 **80**

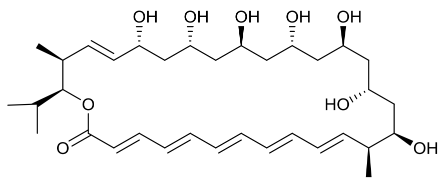

roxaticin **81**

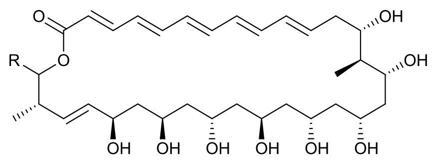

mycoticin A **82** R = *i*-Pr

mycoticin B **83** R = *s*-Bu

Marinosporolides A **84** and B **85** are produced by *Marinispora sp.* and display antifungal activity against *Candida* fungi.[57] Strevertenes A-G **86-92** are a closely related class of polyene macrolides produced by *Streptoverticillium sp.* LL-30F848. They possess antifungal activity against phytopathogenic fungi.[58,59] Eurocidin D **93** is produced by *Streptoverticillium sp.* and displays antifungal activity against *T. vaginalis*.[59]

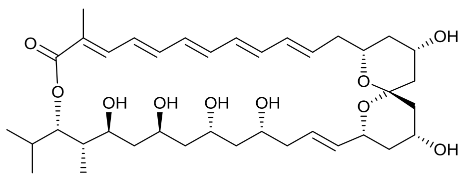

marinisporolide A **84**

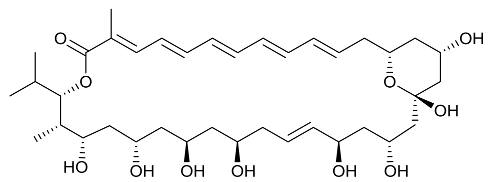

marinisporolide B **85**

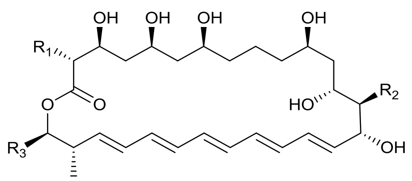

strevertene A **86** R1 = Me, R2 = CO_2H, R3 = Me
B **87** R1 = Et, R2 = CO_2H, R3 = Me
C **88** R1 = Me, R2 = CO_2H, R3 = Et
D **89** R1 = Et, R2 = CO_2H, R3 = Et
E **90** R1 = Me, R2 = CO_2H, R3 = i-Pr
F **91** R1 = Et, R2 = CO_2H, R3 = i-Pr
G **92** R1 = Me, R2 = CH_2OH, R3 = Me

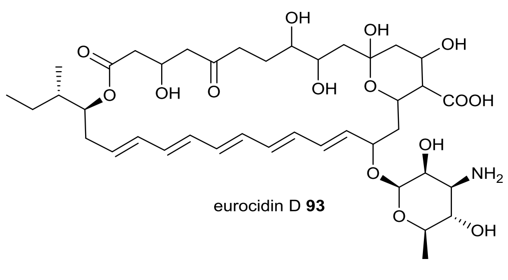

eurocidin D **93**

Mirabilin **94** and lienomycin **95** have more distinct structures from those detailed above. Mirabilin possesses a 6-membered cyclic ether as part of its structure, along with a long side chain containing an amide moiety. Produced by *Siliquariaspongia mirabilis*, **94** displays antitumour activity.[60] Lienomycin is a larger macrocycle and possesses a shorter side-chain, containing a primary amine functionality. Isolated from *Actinomyces diastatochromogenes* var. *lienomycini*, lienomycin **95** possesses antifungal, antibacterial and antitumour activity.[61]

Linear pentaenes

Compounds whose pentaene fragments are not contained within a macrocyclic system include mycolactones A **96** and B **97**, and spirangiens A **98** and B **99**. Mycolactones A and B are produced by *Mycobacterium ulcerans and Mycobacterium marinum.* **96** and **97** are believed to be linked to the Buruli ulcer skin disease.[62] Spirangiens A and B are produced by *Sorangium cellulosum* (strain So ce 90) and are discussed later (*vide infra*).[63]

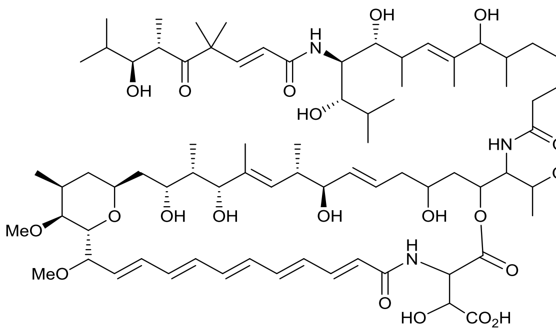

mirabilin **94**

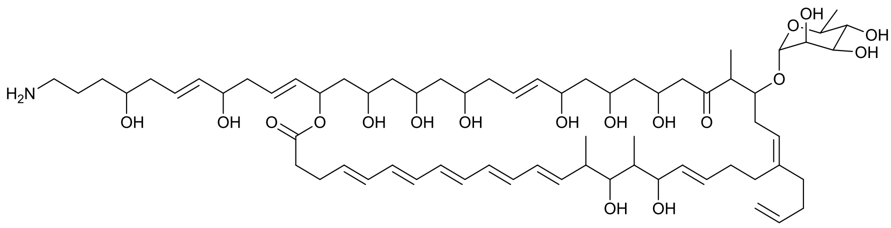

lienomycin **95**

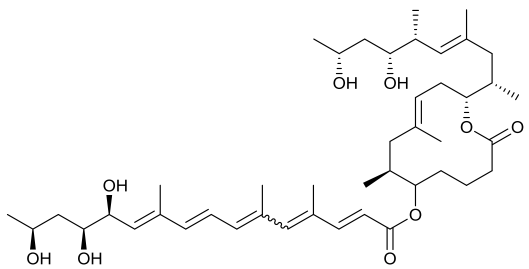

mycolactone A **96**: Δ4',5' = *Z*
mycolactone B **97**: Δ4',5' = *E*

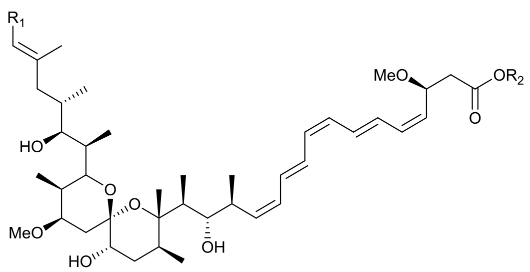

spirangien A **98** R_1= Me, R_2=H
spirangien B **99** R_1= Et, R_2=H

RK-397

RK-397 **80** was isolated from *Streptomyces sp.* in 1993 and displays antifungal activity. In 2009, it was shown to be active against human leukaemia cell lines K-562 and HL-60 at 50 and 25 μg/ mL, respectively.[52]

Five groups have reported efforts towards its total synthesis, but the efforts of the Loh group were towards the polyol chain and are not discussed here.[64] The first total synthesis of **80** was accomplished by Burova and MacDonald in 2004.[65]

This synthesis involved a combination of ylide and palladium chemistry to achieve the synthesis and incorporation of the polyene fragment, involving synthesis of a trienyl building block. This building block was all-*trans*-7-(tributylstannyl)-2,4,6-heptatrien-1-ol **100** and was originally made in the de Lera group[66] using Wittig chemistry and a di*iso*butylaluminium hydride (DIBAL) reduction starting from all-*trans*-5-(tributylstannyl)-2,4-pentadienal **101** (**Scheme 16**). The polyol core **103** had already been synthesised, containing a primary alcohol moiety at one end and a vinyl iodide at the other. Esterification of the primary alcohol with diethylphosphonoacetic acid gave phosphonate ester **104** ready for HWE-type ring closure.

Scheme 16 Synthesis of all-*trans*-7-(tributylstannyl)-2,4,6-heptatrien-1-ol **100**

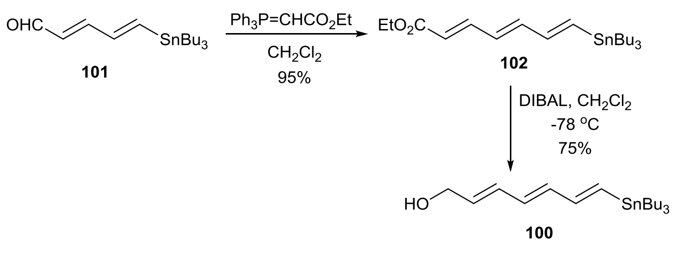

Scheme 17 MacDonald synthesis of **80**

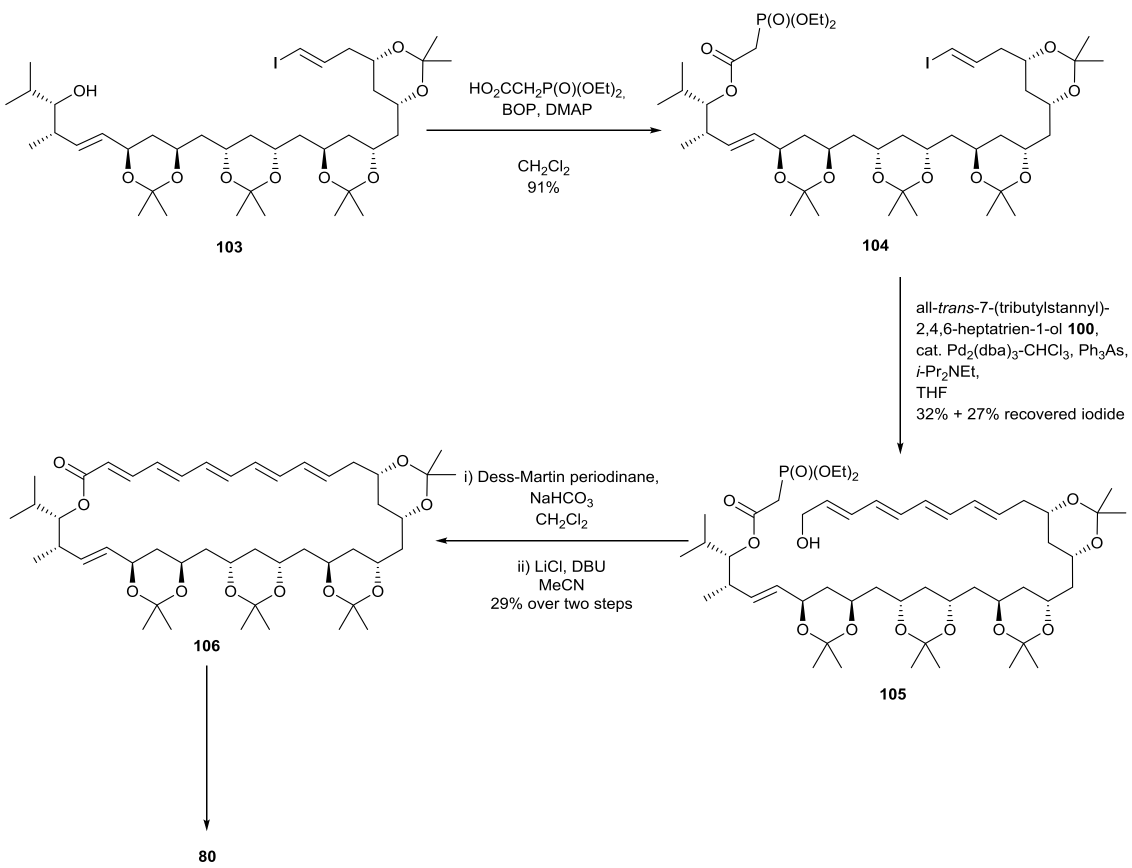

The trienyl building block **100** was then installed into the polyol core using a Stille coupling between the tributylstannyl group on the trienyl fragment and the vinyl iodide group on the polyene core. Oxidation of the primary alcohol of the resulting tetraene **105** to the corresponding aldehyde and then Horner-Emmons macrocyclisation under Masamune-Roush[67] conditions gave the tetraacetonide derivative of the natural product **106**. Deprotection furnished RK-397 **80** (**Scheme 17**).[65] Denmark and co-workers published a total synthesis shortly after MacDonald, in 2005.[68] Here, the polyene fragment was fully installed before macrocyclisation was attempted, palladium chemistry was used to build the key tetraenyl intermediate **107** and ylide chemistry to incorporate the polyene into the rest of the molecule. Synthesis of **107** involved sequential palladium-catalysed cross coupling of 1,4-bis-silyl-1,3-butadiene compound **108**, first with 3-iodo-2-propenol THP ether **109** and then with ethyl (*E*)-3-iodoprenoate **110**. These reactions proceeded with high yields but poor diastereoselectivity, with mixtures of olefins being obtained.

Deprotection and isomerisation to give the all-(*E*)-tetraenoate using iodine, then conversion to the phosphonate ester gave the desired building block **107** (**Scheme 18**). This was installed using standard HWE chemistry, then ring closure and deprotection gave RK-397 **80**.[68]

In 2007, Sammakia *et al.* reported a total synthesis of RK-387 **80**[69] using a trienyl aldehyde **113** which was installed onto the polyol core **114** by olefin-cross metathesis with Grubb's first generation catalyst. HWE yielded the pentaenyl moiety, followed by saponification, Yamaguchi macrolactonisation and global deprotection to yield **80** (**Scheme 19**). O'Doherty *et al.* reported a total synthesis of RK-397 **80** in 2008. The polyene core, however, was installed using the procedure developed in the Denmark group.[68,70]

Spirangien A and B

The spirangiens A **98** and B **99** were isolated from *Sorangium cellulosum* (strain So ce 90) in 2005 by Niggemann *et al.*[63] Aside from their antifungal properties, these compounds have been investigated for either treatment or prevention of IL-8 or IL-6 mediated disorders.[71,72] The spirangiens are linear polyene natural products, with the polyene moiety having a (4*Z*,6*E*,8*Z*,10*E*,12*Z*)-configuration. Three groups have completed the total synthesis of **98** and **99**, but only Paterson reported a synthesis of the polyene fragment;[73] both Rizzacasa and Ley reported formal total syntheses, but utilised the Paterson methodology.[74,75] The total synthesis of spirangens A and B was accomplished by the Paterson group in 2008. A bis-stannylated triene **119** was obtained as the (1*E*,3*Z*,5*E*)-isomer *via* a (*Z*)-selective Julia olefination. A Stille coupling furnished the tetraenyl methyl ester **121**, with a second Stille coupling forming the pentaene and completing the synthesis of the methyl ester of spirangien A **123** (**Scheme 20**).[73]

Scheme 18 Synthesis of tetraene **107**

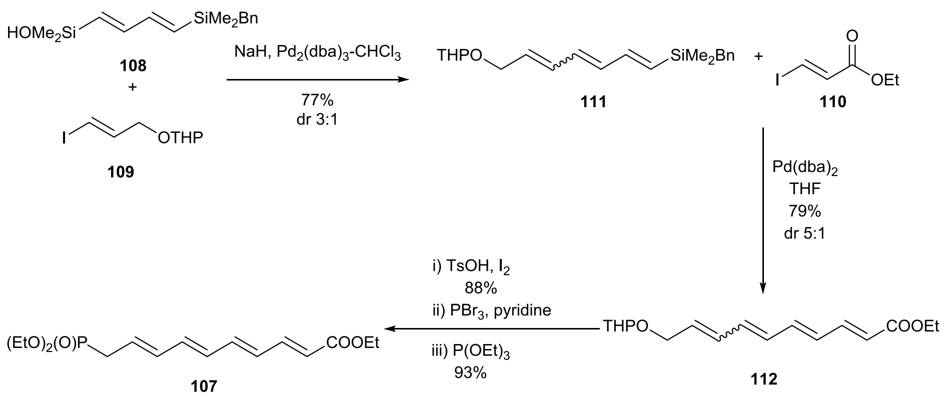

Scheme 19 Sammakia synthesis of **80**

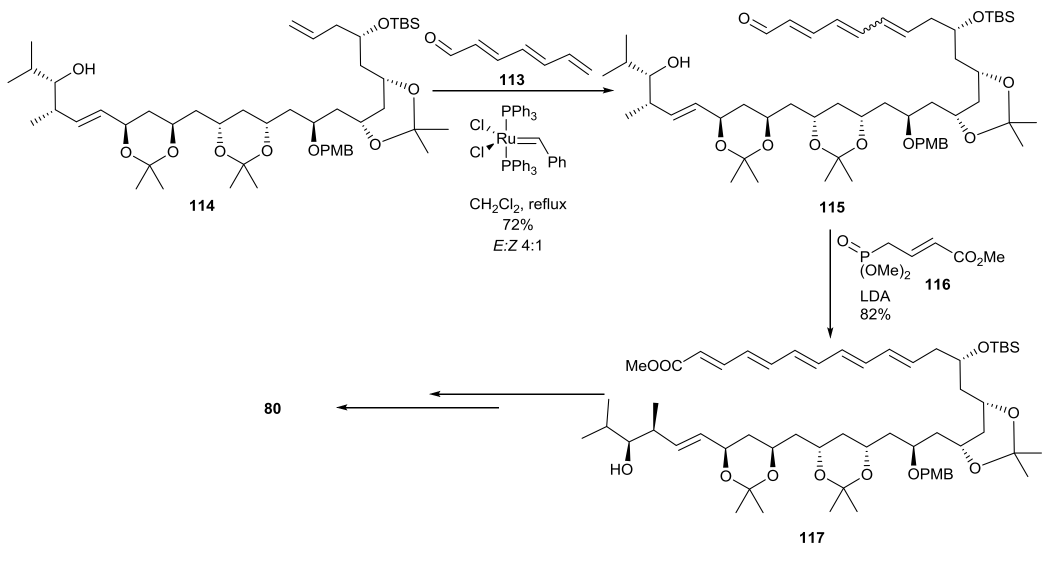

Scheme 20 Paterson route to the synthesis of **123**

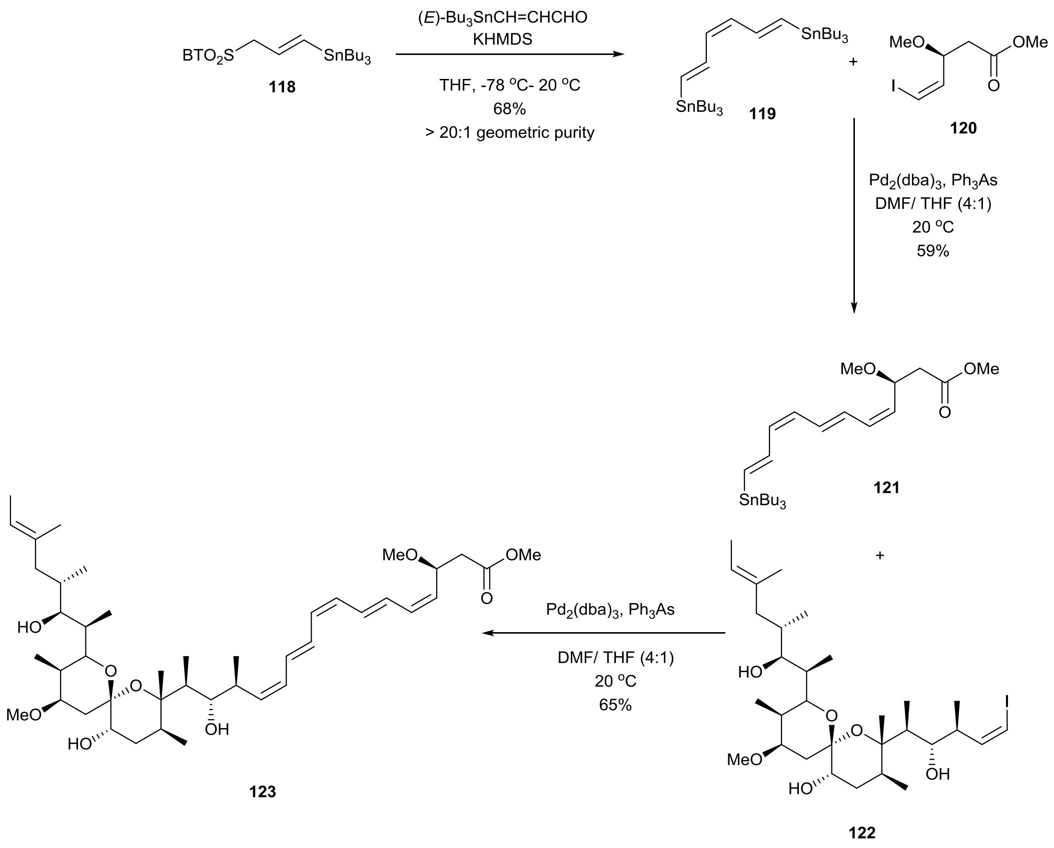

Hexaenes

Cyclic hexaenes

Perhaps the most well-known of the cyclic hexaenes are the polyene macrolides dermostatin A **124** and B **125**, isolated from *S. virdigreseus* Thirum.[76] Their biological activity and synthesis are discussed later (*vide infra*).

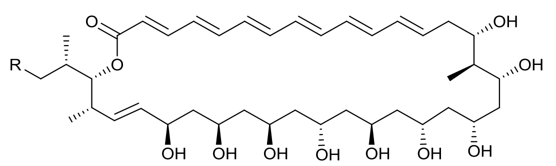

dermostatin A **124** R = H

dermostatin B **125** R = CH_3

Linear hexaenes

The linear hexaenes include the mediomycins A **126** and B **127**, clethramycin **128** and etnangien **129**. The mediomycins and clethramycin are similar in structure. They are all produced by *S. mediocidicus* ATCC23936 and display a broad spectrum of antifungal activity.[77] Etnangien **129** has a different structure, with an unsaturated lactone as part of the compound, isolated from *Sorangium cellulosum*.[78] Its synthesis is discussed later (*vide infra*).

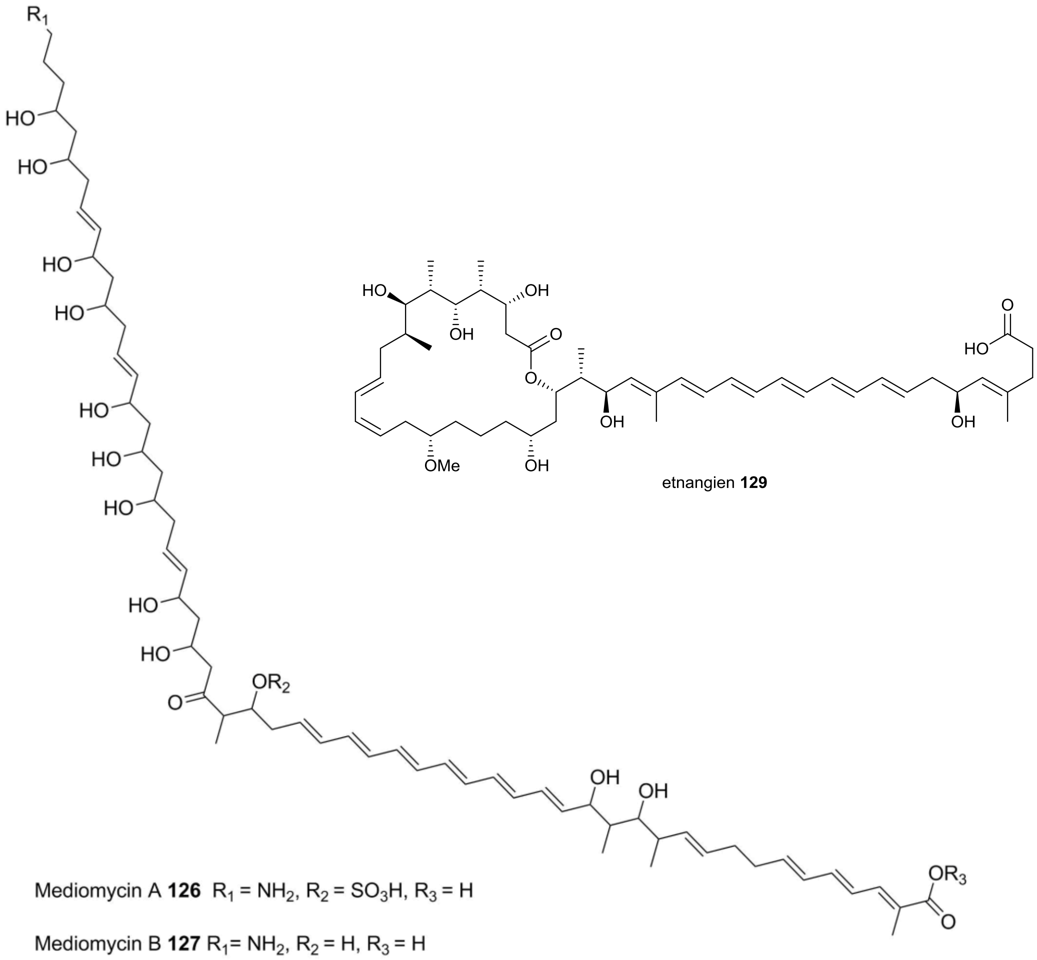

etnangien **129**

Mediomycin A **126** $R_1 = NH_2$, $R_2 = SO_3H$, $R_3 = H$

Mediomycin B **127** $R_1 = NH_2$, $R_2 = H$, $R_3 = H$

Clethramycin **128** R_1 = 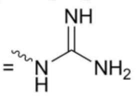

, $R_2 = SO_3H$, $R_3 = H$

Dermostatin A and B

The dermostatins A **124** and B **125** were first isolated from *S. virdigreseus* Thirum. in 1962.[76] These compounds display potent antifungal activity against a number of human pathogens.[79,80] They have also been used clinically as a treatment for deep vein mycoses,[79] and display anti-proliferative activity against human immunodeficiency virus (HIV) in H9 cells.[81] Initially, the dermastatins were thought to be pentene compounds, but their structures were further elucidated and found to contain a hexaene moiety.[82,83] Two groups have completed the total synthesis of dermostatin A **124**. The Rychnovsky group completed a total synthesis of **124** in 2001. This synthesis was analogous to Burova and McDonald's synthesis of RK-397 **80**, utilising the tetraene analogue of all-*trans*-7-(tributylstannyl)-2,4,6-heptatrien-1-ol **100** as reported by de Lera *et al.*,[66] and installing using the same method. The tetraenyl alcohol **130** was attached to the polyol **131** fragment using a Stille coupling. The primary alcohol of the resulting pentaene **132** was then oxidised to give the corresponding aldehyde and the ring closure achieved using the same Horner-Emmons macrocyclisation under Masamune-Roush conditions (**Scheme 21**).[84,85]

Scheme 21 Rychnovsky synthesis of **124**

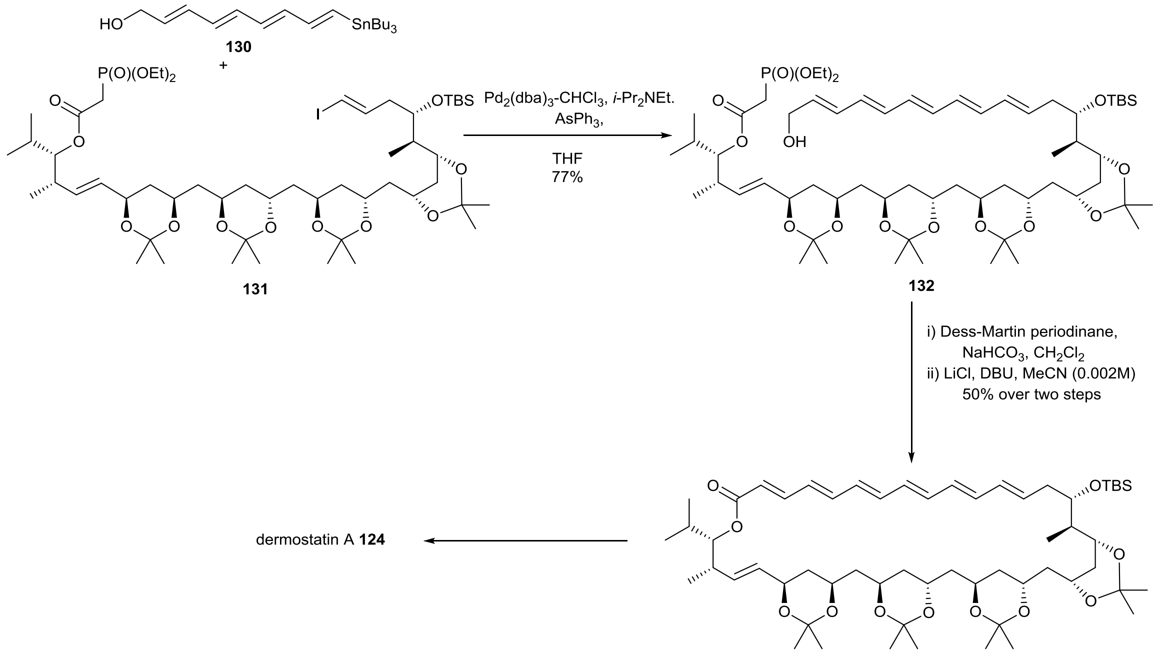

In 2011, the Sammakia group reported a total synthesis, analogous to their synthesis of RK-397 **80**, using ruthenium cross metathesis for incorporation of the polyene into the polyol core.[69,86] Model studies were undertaken to establish the best polyenyl substrate to undertake the olefin cross metathesis with, finding that the same trienyl aldehyde **113** as used in the synthesis of RK-397 was by far the most reactive, and better than the tetraenyl analogue.

Application of the first generation Grubbs catalyst gave the desired triene **135** in an 82% yield as a 4:1 mixture of olefin isomers distal to the aldehyde. HWE with phosphonate ester **136** gave the desired hexaenoate **137** which could be isolated in a geometrically pure form. Hydrolysis, Yamaguchi cyclisation and global deprotection gave dermostatin A **124** (**Scheme 22**).[69,86]

Scheme 22 Sammakia synthesis of **124**

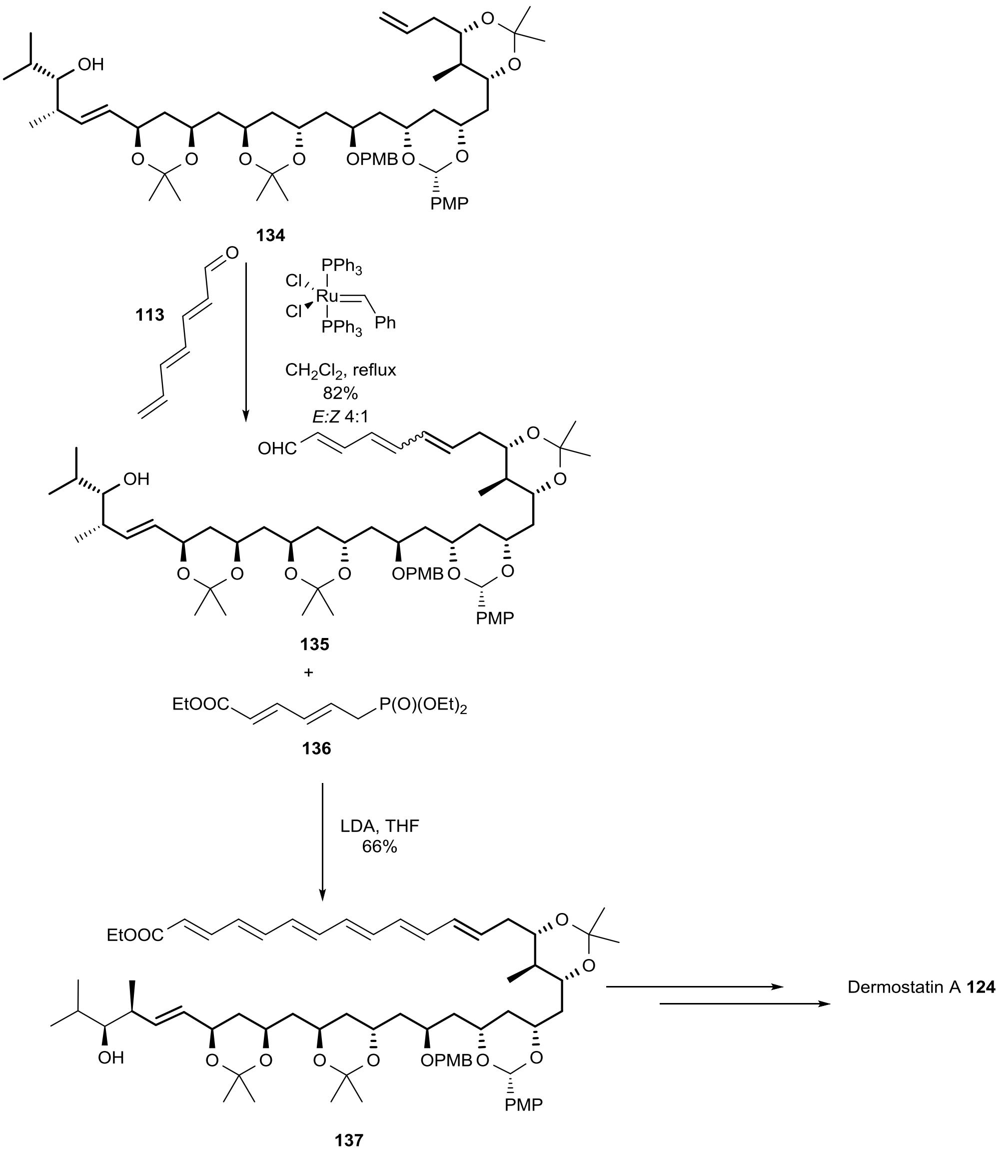

Etnangien

Etnangien **129** was isolated from *Sorangium cellulosum* and found to be active against a range of Gram-positive bacteria.[78] It was also found to inhibit retroviral RNA and DNA polymerases.[87] Etnangien **129** was also reported to have an unstable structure, presumed to be due to the polyene chain. It has only been synthesised by the Menche group,[87,88] which also established the absolute stereochemistry in the process of completing the total synthesis. The synthetic route involved a mixture of ylide and palladium chemistry. The hexaene chain was synthesised from two trienyl building blocks **142** and **148**. Ylide chemistry was used to create diene **140**, then a series of steps were used to form the macrocycle. Selective removal of the primary TBS group and allylic oxidation were followed by a Takai reaction to install the *E*-vinyl iodide **142** (**Scheme 23**). Homologation of alkene **143** by olefin cross-metathesis using the Grubbs (II) catalyst gave the required enal **145**. HWE chemistry furnished the required trienyl stannane **147** and tetrabutylammonium fluoride (TBAF) deprotection gave building block **148**. The side-chain was coupled to the trienyl iodide using a Stille coupling (**Scheme 24**).[87,88]

Scheme 23 Synthesis of iodide **142**

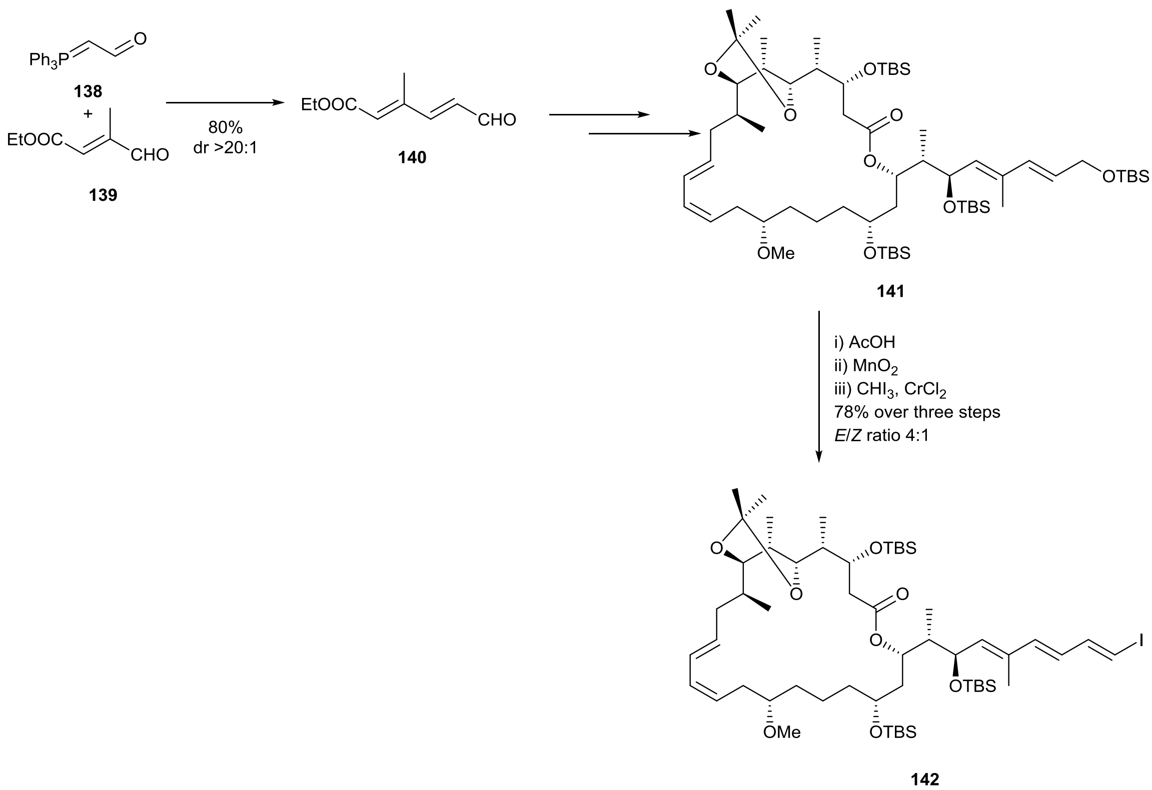

Scheme 24 Completion of the synthesis of **129**

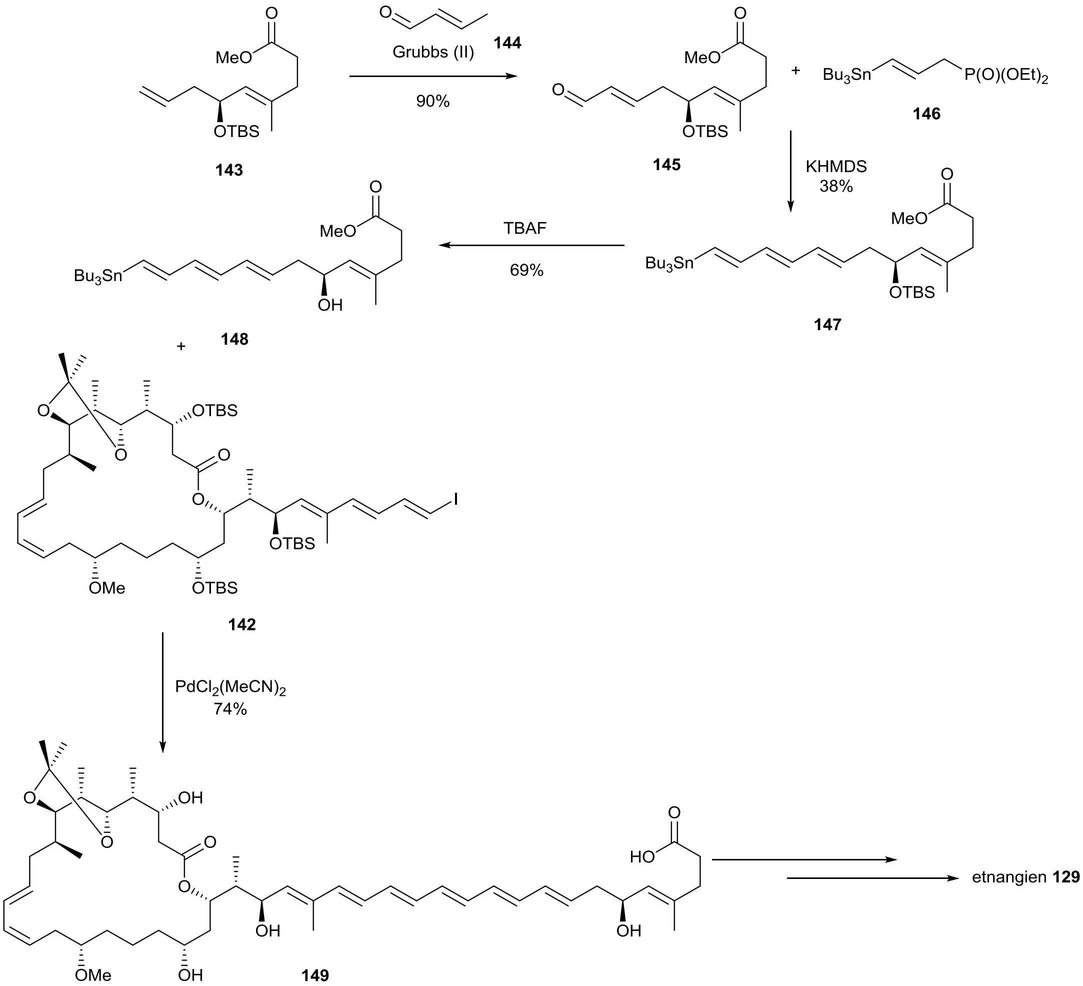

Heptaenes

Cyclic heptaenes

One of the most commonly known and widely used polyene natural products is a member of the heptaene polyene macrolide class of compounds, amphotericin B **150** and its derivatives **151-153**, which are discussed later (*vide infra*). The polyene macrolide candidin **154** has a similar structure to amphotericin B, possessing an extra carbonyl moiety on the polyol fragment. It is an antifungal agent produced by *S. viridoflavus*, and has also been patented as a treatment for mammalian tumours.[89,90] Another very closely related structure is mycoheptin **155**, produced by *Streptoverticillium mycoheptinicum*, which displays antifungal activity and is used in the therapy of coccidioidomycosis, histoplasmosis, cryptococcosis, chromodermycosis, blastomycosis, aspergillosis, sporotrichosis, and candidiasis.[91,92]

Another class of compounds with very similar structures, all containing a side-chain with a *para*-amino phenyl ketone group, are hamycin **156**, levorin A2 **157**, partricin A and B **158-159** and 67-121 A and B **160-161**. Perimycin A **162**, DJ-400 B_1 and B_2 **163-164**, FR-008 **165** and trichomycin A **166** are also similar. Hamycin **156** is produced by *S. pimprina* and displays antimicrobial activity against a number of forms of candidiasis and deep-seated mycoses.[93] Levorin A2 **157**, or candicidin D, is produced by *A. levoris* and *S. griseus* ATCC 3570.

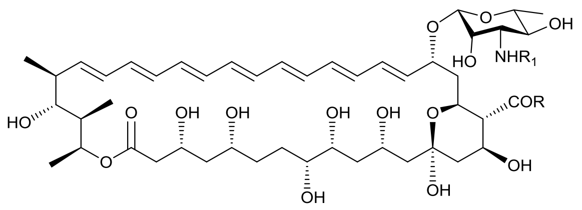

amphotericin B **150** R = OH, R_1 = H

amphotericin B methyl ester **151** R = OMe, R_1 = H

N-Acetylamphotericin B **152** R= OH, R_1 = COMe

N-Acetylamphotericinmethyl ester **153** R = OMe, R_1 = COMe

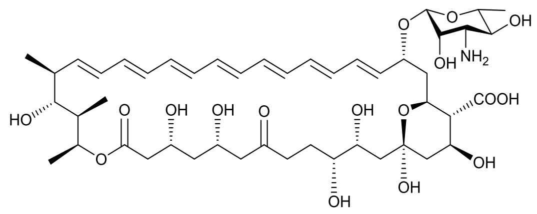

candidin **154**

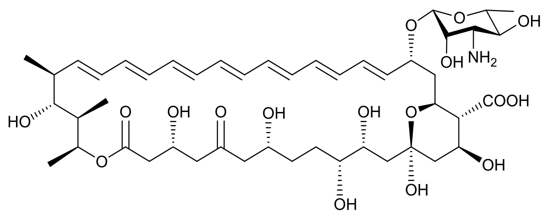

mycoheptin **155**

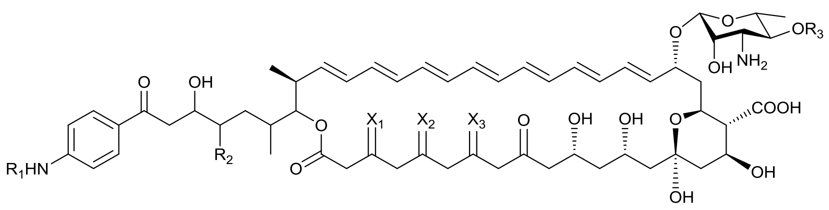

	R_1	R_2	R_3	X_1	X_2	X_3
hamycin **156**	H	H	H	H,OH	H,OH	H,OH
levorin A2 **157**	H	Me	H	=O	H, H	=O
partricin A **158**	Me	H	H	H,OH	=O	H,OH
partricin B **159**	H	H	H	H,OH	=O	H,OH
67-121A **160**	Me	H	H	H,OH	H,OH	H,OH
67-121B **161**	Me	H	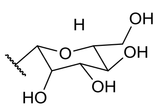	H,OH	H,OH	H,OH

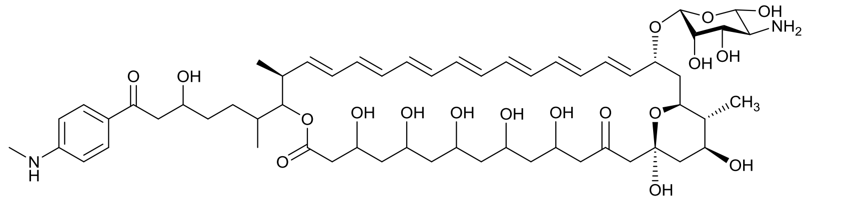

perimycin A **162**

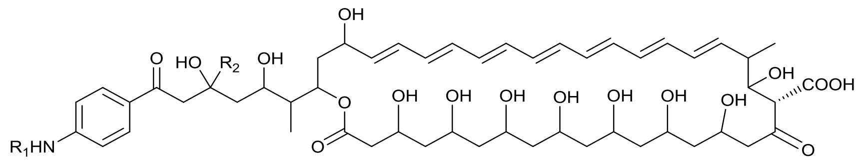

DJ-4OO B_1 **163** R1 = Me, R2 = 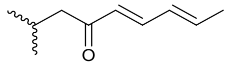

DJ-4OO B_2 **164** R1 = R2 = H

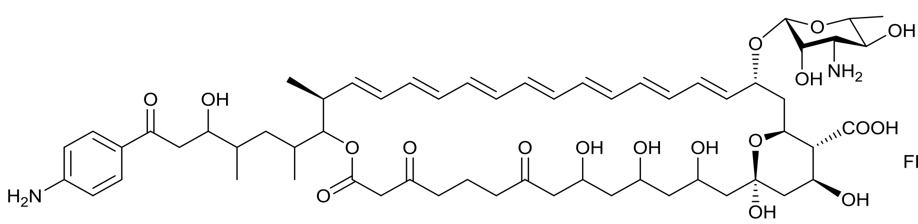

FR-008 **165**

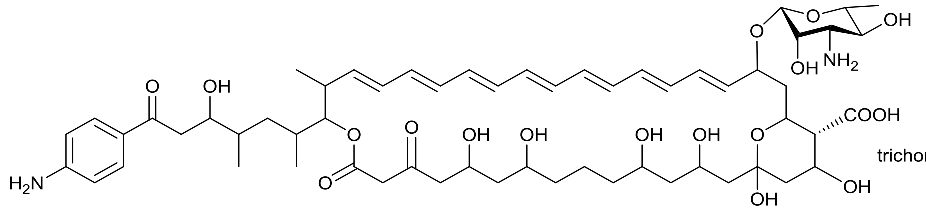

trichomycin A **166**

This compound is an antifungal and possesses the ability to inhibit the growth of adenoma prostate.[94,95] Partricin A and B **158-159** are produced by *S. aureofaciens* and possess high antifungal activity, particularly against *Candida albicans*, and antiprotozoal activity.[96] 67-121 A and B **160-161** are produced by *Actinoplanes caeruleus* and are antifungals.[97,98] Perimycin A **162**, otherwise known as fungimycin, NC-1968 and aminomycin, is an antifungal produced by *S. coelicolor var. aminophilus*.[99] DJ-400 B_1 and B_2 **163-164** is produced by *S. Surinam* and displays antifungal activity.[100,101] FR-008 **165** is also an antifungal produced by *S. griseus*.[102] Trichomycin A **166** is produced by *S. hachijoensis* and is used as a potent clinical drug for the treatment of vaginal infections.[103]

Linear heptaenes

Two interesting linear heptaene structures are peridinin **167** and fucoxanthin **168**, which contain an allene moiety. Peridinin **167** is produced by *Gonyaulax polyedra* and is believed to possess activity against atherosclerosis, rheumatoid arthritis and cancer. In particular, this compound is believed to reduce membrane permeability to reactive oxygen species.[104,105] Fucoxanthin is discussed later (*vide infra*).

Amphotericin B

Amphotericin B **150** and its derivatives **151-153** have a wide range of biological applications. First reported in 1955, amphotericin B is an antifungal antibiotic produced by *S. nodosus*.[106] It was tested as early as in 1957 for activity against *Candida albicans*,[107] and has since been shown to have a number of other biological applications, including activity against deep-seated mycotic infections,[108] activity against intercranial fungal masses,[109] activity against visceral leishmaniasis,[110] potential as a treatment for prion infection treatment,[111] as a malaria treatment in humans and animals,[15] activity against HSV I, HSV II and hepatitis B,[8] and as a treatment for severe mucocutaneous candidal infections in the mouth.[112]

Despite being such an important compound, only the Nicolaou group has completed the total synthesis of amphotericin B **150**.[113,114] The Negishi group has also completed a synthesis of the polyenyl fragment. Completed in 1987, the Nicoloau synthesis used ylide chemistry to build up the polyene fragment. This was achieved *via* a series of HWE reactions using dienyl phosphonate ester **170** as a key building block. Ring closure was also accomplished using a HWE reaction (**Scheme 25**).[113,114]

The Negishi synthesis of the polyene fragment **176** was published in 2013 and utilised HWE, alkyne hydrozirconation, palladium-catalysed Negishi coupling, and HM coupling chemistry.[115]

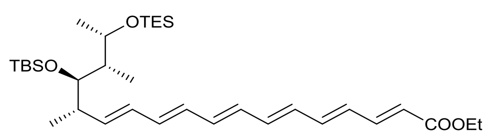

176

Scheme 25 Nicolaou synthesis of **150**

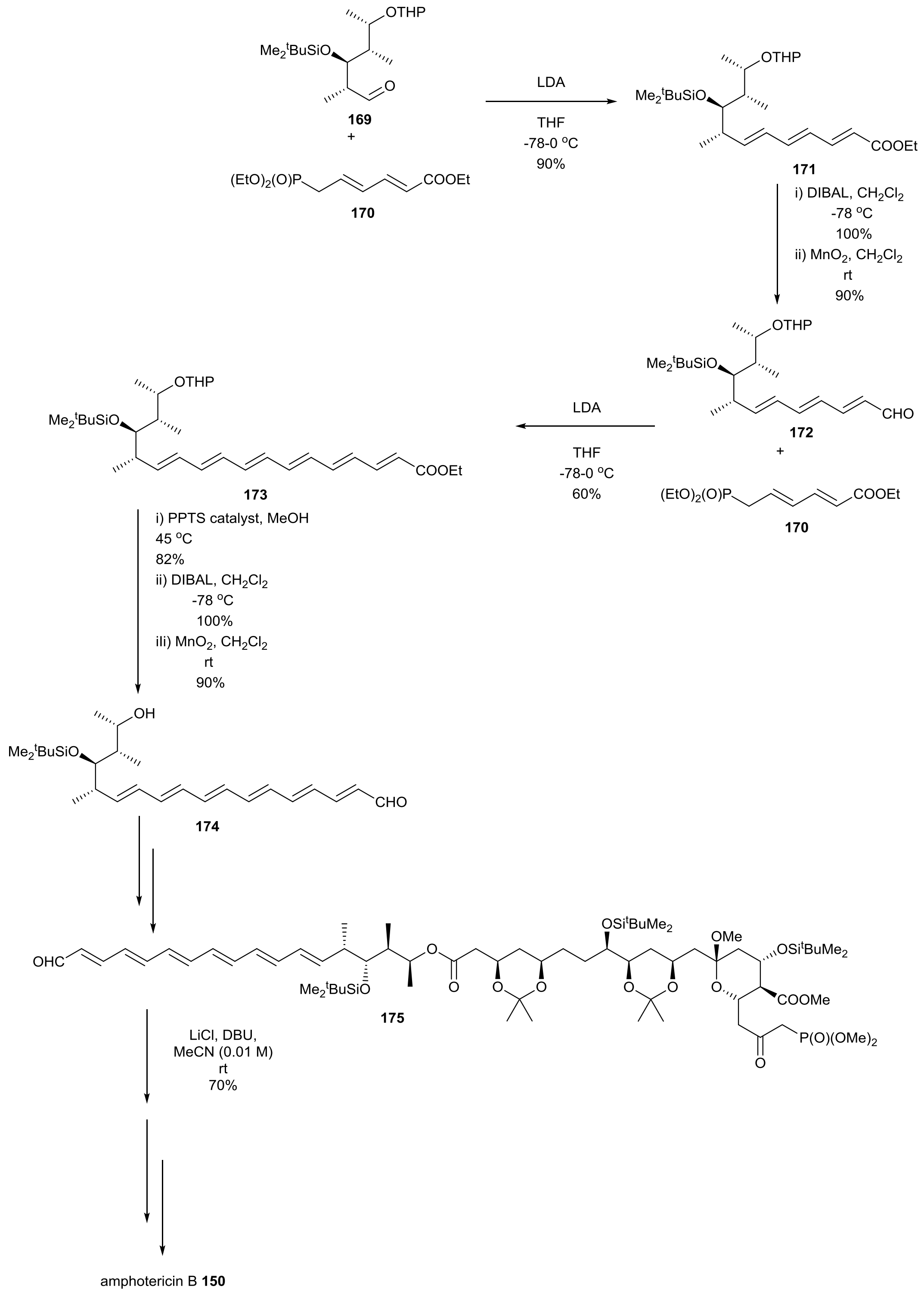

The first building block made was a trienyl phosphonate ester **182**. The first step involved a hydrozirconation of metallated propargyl alcohol **177**, iodinolysis, *in situ* metallation and then Negishi alkenylation. The next step involved hydrozirconation of the metallated enyne **179** and then another Negishi alkenylation to yield trienyl alcohol **181**, which was then converted to the phosphonate ester **182** (**Scheme 26**). A HM reaction was then used to form dienyl ester **184**, which was then reduced and used in a HWE reaction with trienyl phosphonate ester **182** to complete the hexaene fragment **176** (**Scheme 27**).[115]

Fucoxanthin

Fucoxanthin **168** is an allenic compound found in brown algae. Its isolation, along with a number of other brown pigments, was reported in the early 1900s.[116–118] Fucoxanthin **168** is a pigment associated with a range of biological activities,[119,120] including potential as a treatment for diabetes and obesity,[121] as an anti-inflammatory agent,[122] in neutrophil modulation,[123] in inhibition of cancer metastasis,[124] and the ability to protect against UV-B induced cell damage.[125]

The synthesis of **168** was first completed by the Ito group in 1994. Construction of the polyene fragment was achieved solely by ylide chemistry, but was hampered by poor selectivity and low yields. This can be seen in the synthesis of building blocks **192** and **195**, where diastereomeric ratios of 1:1 or less were achieved (**Scheme 28**).[126,127]

Another synthesis was completed by the Katsumara group in 2012.[128] Again, de Lera group chemistry was used in the construction of a key building block.[66] A modified version of the de Lera procedure was used to create trienyl iodide **199**, which was then coupled with an alkyne to install the epoxycyclohexane group. This was then converted to allenyl building block **203** (**Scheme 29**). [129,130,131,132]

A second benzothiazolylsulfone building block **208** was synthesised and the two building blocks coupled using a Julia olefination which gave a mixture of isomers at the connected olefin, predominantly Z. Deprotection and oxidation of **207** yielded fucoxanthin **168** (**Scheme 30**).[128,129,130,131,132]

Scheme 26 Synthesis of phosphonate ester **182**

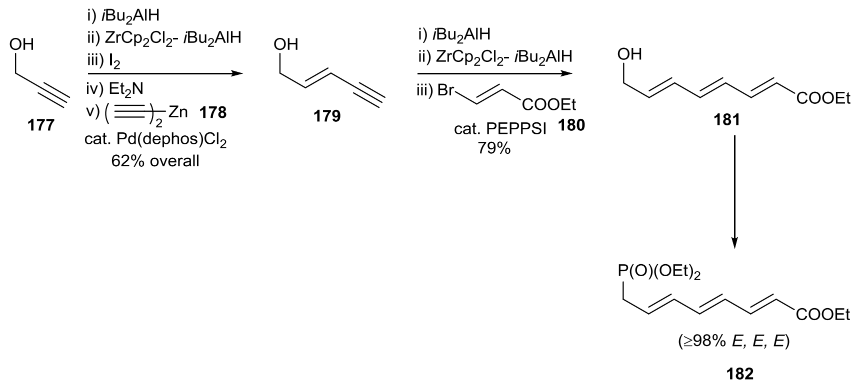

Scheme 27 Synthesis of hexaene **176**

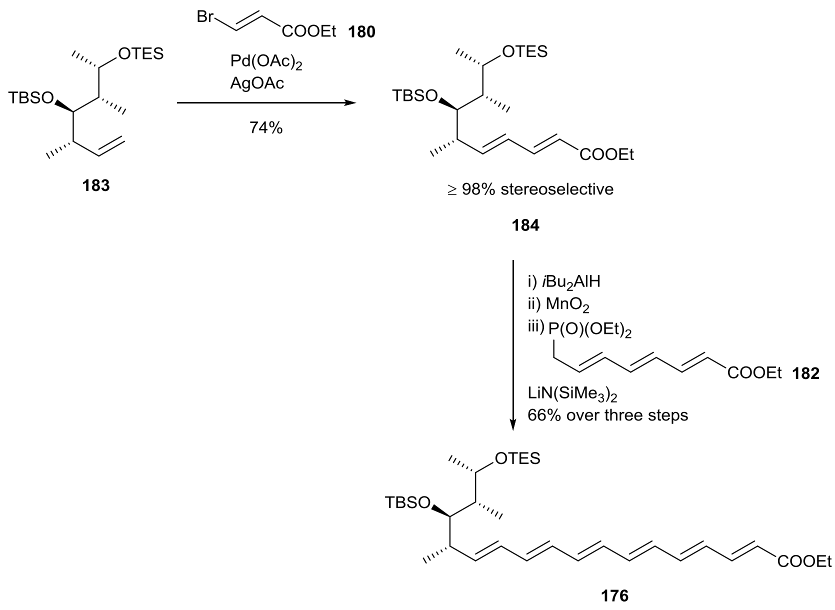

Scheme 28 Ito synthesis of **168**

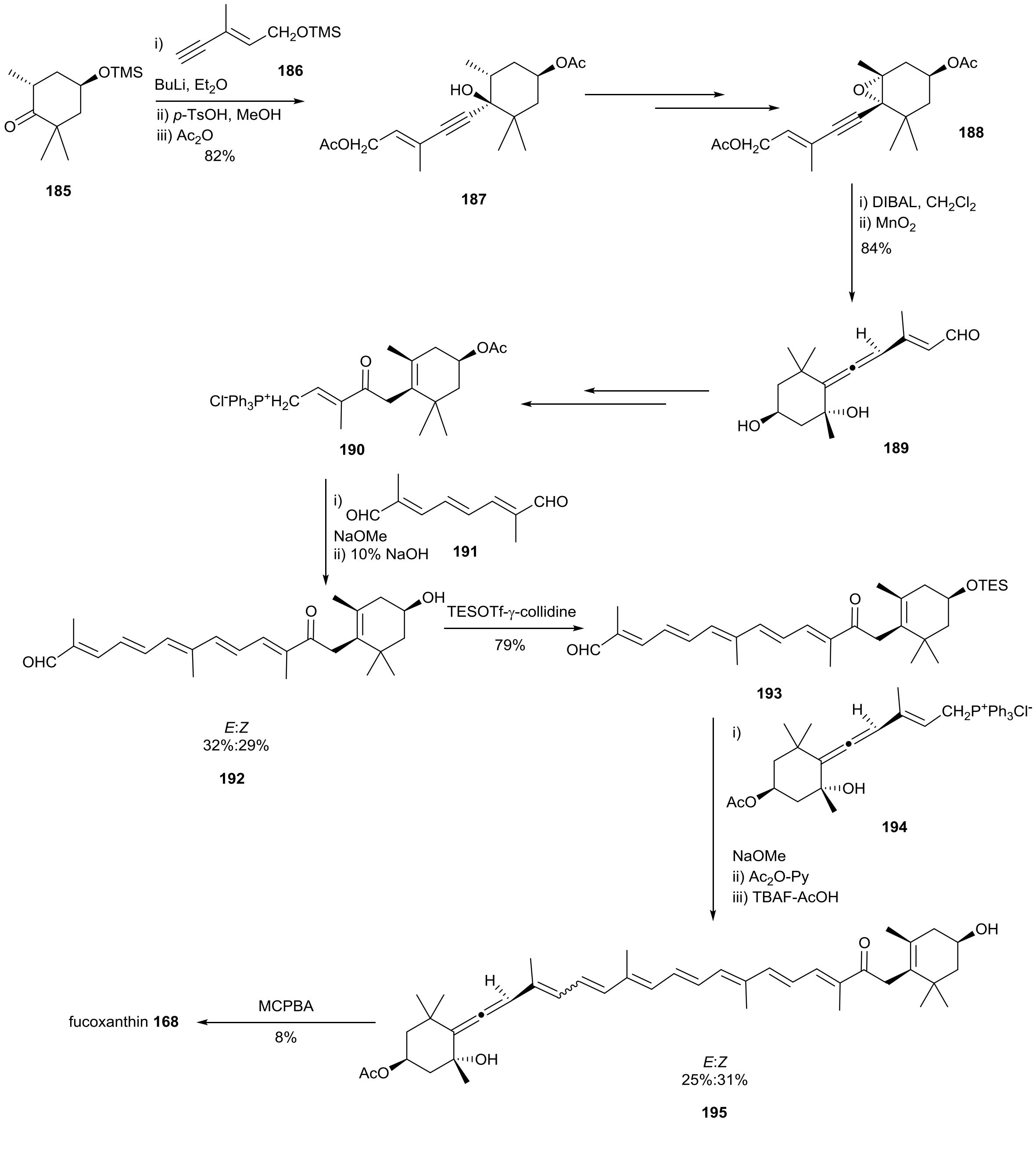

Scheme 29 Synthesis of building block **203**

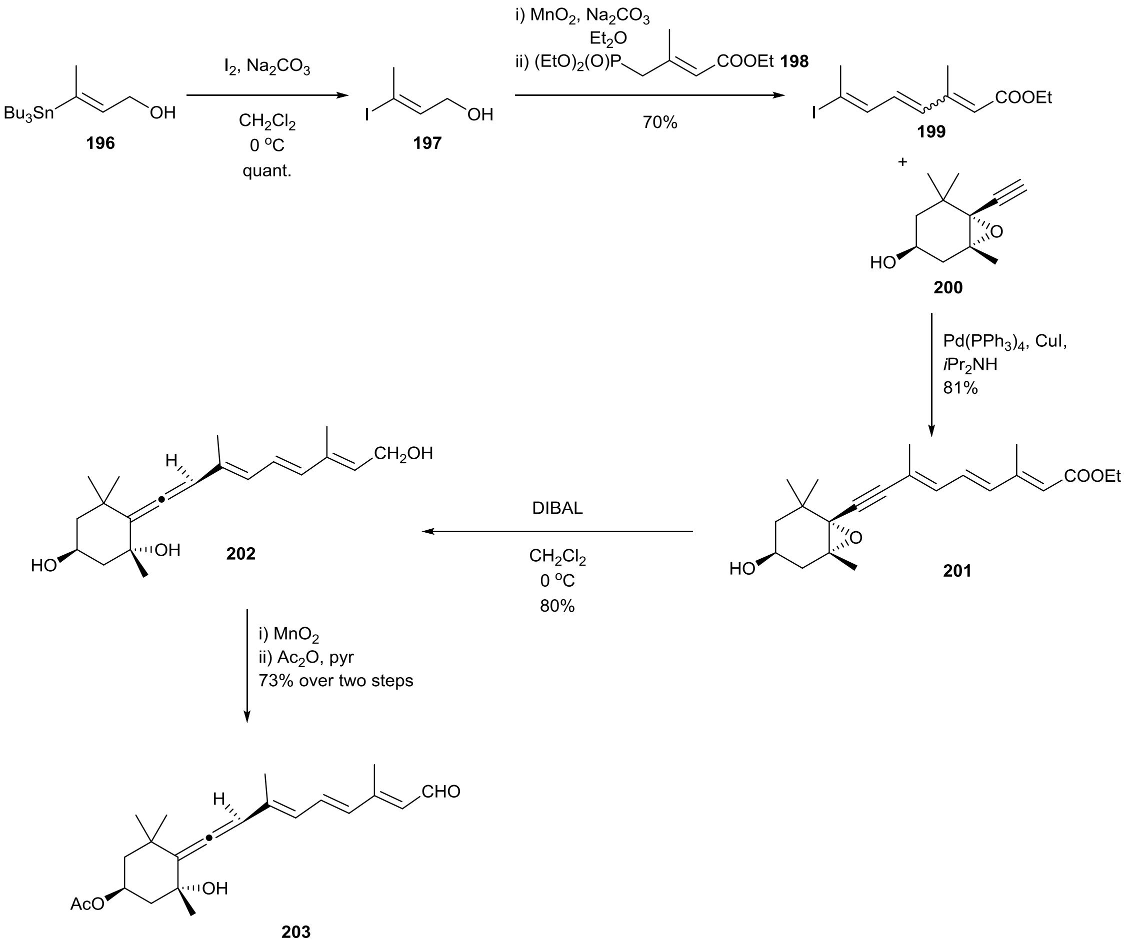

Scheme 30 Completion of the Katsumara synthesis of **168**

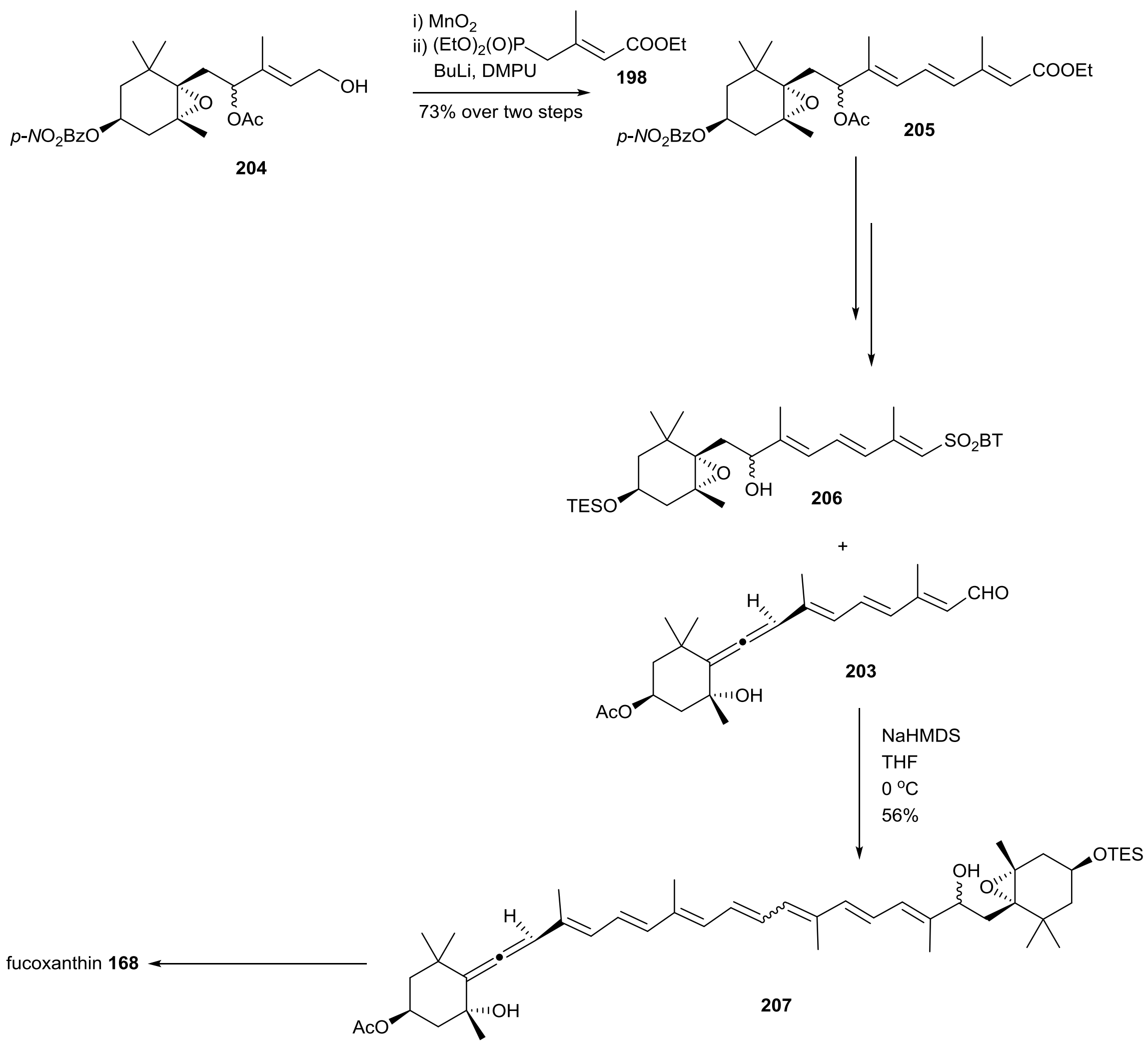

Octaenes and above

Those natural products possessing a polyene chain of eight or more conjugated double bonds are dominated by linear structures. To the best of our knowledge, no polyene macrolide structures containing an octaene polyene fragment have been elucidated, nor have any structures for polyene macrocycles containing more than eight conjugated double bonds. Two of these linear polyenes are xanthomonadin **208** and granadaene **209**. Xanthomonadin **208** is an octaene bacterial pigment isolated from *Xanthomonas juglandis*. Its structure was elucidated in 1976[133] and was later shown to protect against photodamage.[134] It was also isolated from

Xanthomonas oryzae pv. oryzae in 1997.[135] Granadaene **209** is a dodecaene red pigment characteristic of *Streptococcus agalactiae*, isolated in 2006.[136,137]

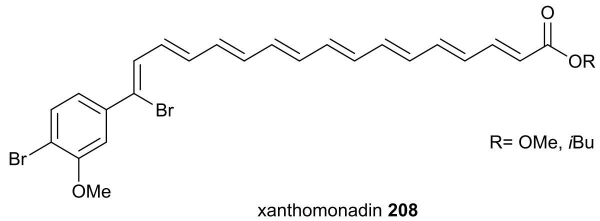

xanthomonadin **208**

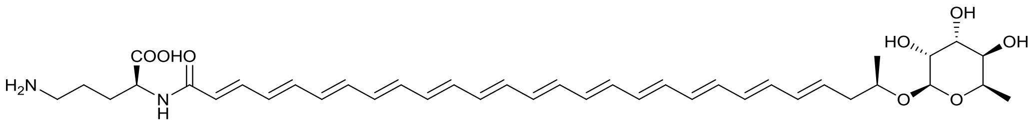

granadaene **209**

Correlation between polyene chemical structure and biological activity

There has been surprisingly little reported in the literature about the correlation between polyene chemical structure and biological activity. Some work has been done to compare the activity of various polyene macrolides. In a review published by Hamilton-Miller in 1973, it was stated that the biological activity of the polyene macrolides increases with the number of conjugated double bonds.[100] Several natural product tetraene macrolides, namely pimaricin **8**, AB-400 **9**, rimocidins A-C **10-12** and CE-108s A-C **13-15,** were compared with the heptaene macrolide amphotericin B **150** to assess their biological activities on *Trypanosoma cruzi*. These tetraene compounds were found to be less effective, but also less toxic.[19] Kotler-Brajtburg *et al.* attempted to correlate the chemical structures of polyenes and their biological properties by investigating their ability to cause K^+ leakage and cell death.[138] The work hypothesised that the polyene macrolides could be categorised into two functionally different groups. Amongst the polyenes in group I was the tetraene pimaricin **8**, pentaenes (chainin **75** and filipin **76**) and the hexaene (dermostatin A **124**), while group II included the heptaenes (amphotericin B **150**, amphotericin B methyl ester **151**, N-acetylamphotericin B **152**, hamycin **154** and candicidin **156**) and one tetraene, nyastatin **17**. Group I antibiotics caused potassium ion leakage and cell death or hemolysis at the same concentrations of added polyene, while group II caused considerable potassium ion leakage at low concentrations and cell death or hemolysis at high concentrations.[138]

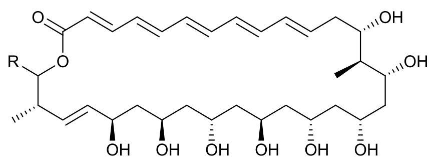

mycoticin A **82** R = *i*-Pr

mycoticin B **83** R = *s*-Bu

Work undertaken by Akiyama *et al.* supported the above theory. Polyene antibiotics were classified according to their synergistic effect on fungi into two groups: a non-heptaene group including pimaricin **8** and filipin **76**, and a heptaene group including amphotericin B **150**.[139]

A study into the difference between the linear polyenes and the macrocyclic polyenes does not seem to have been undertaken. It appears that in general, the longer chain linear polyenes possess a more diverse range of biological activities, additional to antimicrobial properties, for example fucoxanthin **168**, xanthomonadin **208** and granadaene **209**, all of which have polyene chains of seven double bonds or greater. As discussed in previous sections (*vide supra*), these compounds have properties such as antioxidant and anti-inflammatory activities and an ability to inhibit cancer metastasis.

The link between polyene structure and cancer activity in particular is interesting. Seemingly small changes in structure can impart a significant increase in biological activity. An example of this is the difference in biological activity between RK-397 **80** and the mycoticins A and B **82** and **83**. RK-397 displays anti-leukaemic activity, whereas the mycoticins only possess antimicrobial activity. The structures are exceptionally similar, differing only in the stereochemistry of the polyol chain and in the absence of a methyl group in the RK-397 structure.

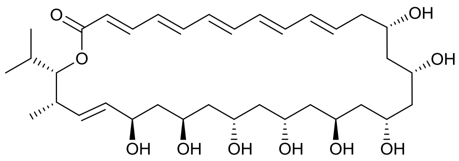

RK-397 **80**

Conclusion

The polyene natural products include a wide variety of different structures with a range of biological activities. Total syntheses of a number of interesting compounds have been accomplished using a mixture of ylide chemistry, palladium cross coupling and cross-metathesis. Whilst ylide chemistry was used effectively in a number of total syntheses, there are a number of examples where poor stereoselectivity was a clear issue, for example in the 1994 synthesis of fucoxanthin **168**. Palladium chemistry, on the other hand, has given consistently better stereoselectivity in the total syntheses reported. The examples where olefin cross-metathesis was used highlight its potential as an efficient and selective method of polyene synthesis. Despite all the research that has been undertaken in this area of polyene natural product synthesis, there is not yet a standout method for the highly stereoselective formation of polyene chains that has completely general application in synthesis, though some methods have clear advantages over others.

In addition, relatively little is understood about the correlation between chemical structure and biological activity as a general phenomenon. Establishment of the structural features which contribute to the activity of the polyene natural products is necessary for a better understanding of this interesting class of compounds.

Section 1

Synthesis of polyene natural products

Section 1.1 Synthesis of Xanthomonas pigments- introduction and proposed targets

Section 1.1.1 Xanthomonas pigments

Members of the genus *Xanthomonas* are the cause of a number of plant diseases e.g. *Xanthomonas oryzae pv. oryzae*, rice blight; *Xanthomonas campestris pv. campestris*, black rot of crucifers. These bacteria form characteristic yellow colonies due to the yellow, membrane-bound pigments they produce.[135,140–150]

Andrewes and Starr pioneered the investigations into these yellow pigments, first proposing arylated, polyenic, halogenated structures in 1973.[151] Andrewes then reported the total synthesis of one of the proposed structures later in that year, although the characteristics of this compound did not match any of the isolated pigments.[152] The first of these pigments, *iso*butyl xanthomonadin **208**, was successfully isolated and characterised from *Xanthomonas juglandis* strain XJ103 in 1976, then the micro- and Raman resonance spectroscopy characteristics obtained by Sharma *et al.* in 2012.[133,153]

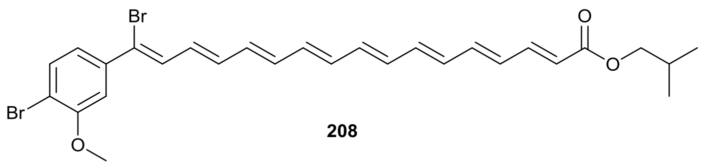

208

Their initial investigations in 1973 suggested four different pigments.[151] In 1977, this work was extended further, with the pigments of a range of different *Xanthomonas* species isolated as the *iso*butyl esters and analysed.[154] The two most common pigments were found to be xanthomonadin **208** and the putative monobrominated analogue **210**. Starr later went on to try to establish the biological function of **208** in 1982, providing the first evidence that the pigment may protect bacteria from photodamage.[155]

Br somewhere along the polyene

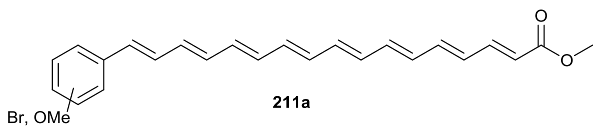

211a

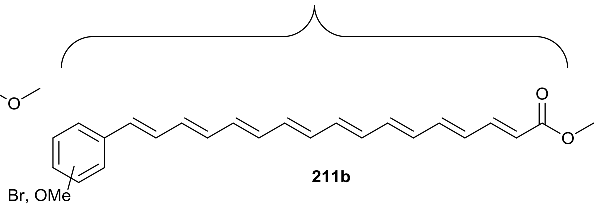

211b

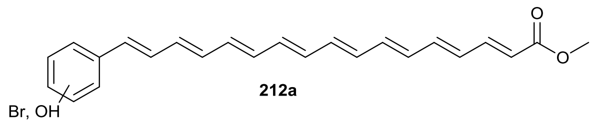

212a

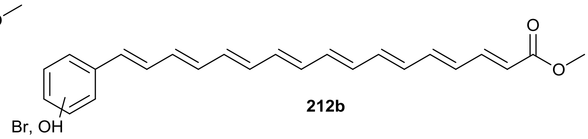

212b

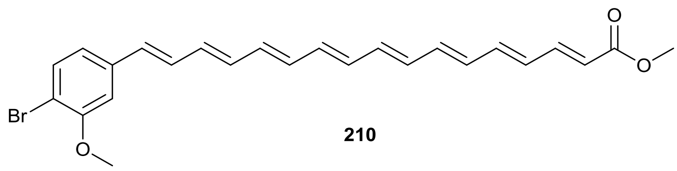

210

Starr observed the *Xanthomonas* pigments' similarity to the carotenoids and postulated that their biological role may be to protect the bacteria from photodamage. Xanthomonadin **208** was tested and shown to protect *Xanthomonas juglandis* strain XJ103 from photodamage, but whether or not the pigment protected the bacterium from oxygen-related killing was not determined.[155] The Sonti group showed that **208** does indeed display antioxidant properties in *Xanthomonas oryzae pv. oryzae* in 1997.[135] In particular, they showed that it protects membrane lipids from peroxidation. The Poplawsky group has pioneered much of the investigation into the mechanism of bacterial survival for the Xanthomonas genus. [135,140–150] In 2000, they investigated the role of **208** in *Xanthomonas campestris pv. campestris*. They concluded that it is unlikely that the xanthomonadin pigments offer protection against direct UV damage and that they were more likely to offer protection when a photosensitiser was present. They also showed that a diffusible factor is needed for xanthomonadin production *via* quorum sensing. In addition, they showed that the pigB transcriptional unit was vital for bacterial survival. [141,146]

The group's research has gone into greater detail about the mechanisms behind xanthomonadin production, identifying the diffusible factor as 3-hydroxybenzoic acid and also implicating 4-hydroxybenzoic acid in the pathogenesis of *Xanthomonas oryzae* pv. *oryzae*.[150] The group also proposed that a novel type II polyketide synthase pathway is responsible for xanthomonadin synthesis, a hypothesis that has been supported by other groups.[4,20,21]

A number of other pigments have been identified or proposed in the literature, and some are detailed below.[155,158,159] A common feature amongst the non-brominated analogues below is that they all possess a phenolic OH. Studies of these pigments have provided an insight into the synthesis of the xanthomonadins, in particular the installation of the bromines on the scaffold. The pigment **213** made by *Lysobacter enzymogenes* is unbrominated and the bacterium does not possess a halogenase enzyme, suggesting that the bromine functionalities may be incorporated into the xanthomonadins by halogenases.[158]

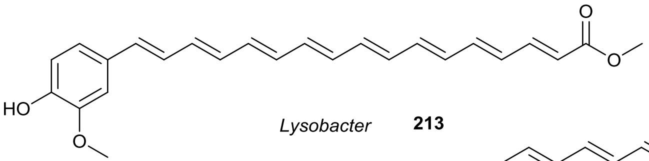

Lysobacter **213**

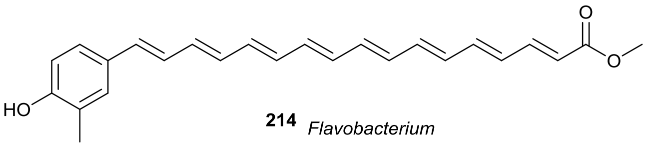

214 *Flavobacterium*

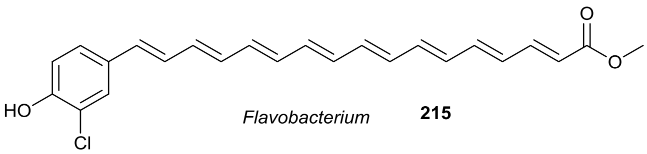

Flavobacterium **215**

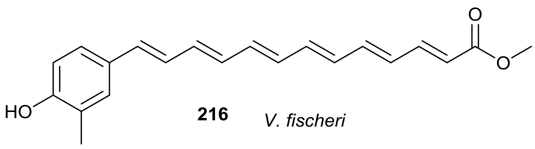

216 *V. fischeri*

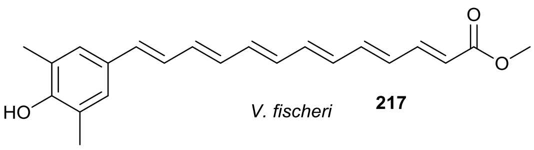

V. fischeri **217**

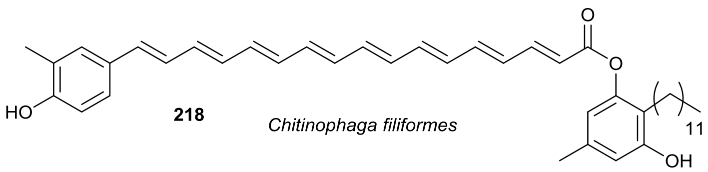

218 *Chitinophaga filiformes*

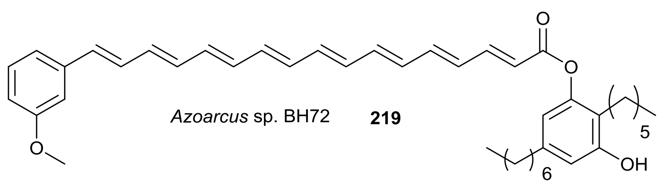

Azoarcus sp. BH72 **219**

Starr proposed that the main pigment produced by *Xanthomonas populi* **220** is in fact a nonbrominated aryl heptaene, not fitting with the traditionally accepted halogenated octaene model associated with the xanthomonadins. Mass spectrometric analysis of this pigment gave a molecular weight of 376, which was consistent with the formula $C_{25}H_{28}O_3$. No structure was given but a proposed compound fitting these data is shown below.

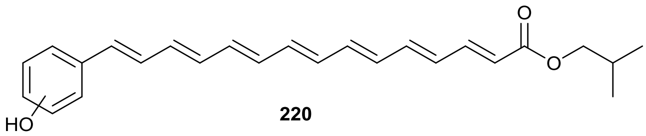

220

Section 1.1.2 Characterisation of *Xanthomonas* pigments

Xanthomonadin **208** is the only pigment to have been extensively characterised, with mass spectrometric, 40 MHz ^{1}H NMR, IR, X-ray crystallographic and UV-Vis data obtained by Andrewes and Starr when it was first isolated in 1976.[133] The X-ray crystallographic data was reported to be of poor quality. Other pigments have been characterised by mass spectrometry, and the UV-Vis properties of mixtures of pigments have been measured, but none of the other pigments have been fully isolated and characterised.

Section 1.1.3 Summary

Xanthomonas pigments have garnered interest amongst the scientific community due to their contribution to the survival of a number of prolific agricultural diseases. It has been proposed that these pigments are non-carotenoid, polyenyl structures, with one pigment, xanthomonadin **208**, successfully isolated. Structures for other pigments have been proposed in the literature, with the most common pigments postulated to be octaenes. These pigments are believed to be membrane-bound, protecting membrane lipids from peroxidation, but the exact conditions under which these pigments protect the bacterium from photodamage are not known; there is some evidence to suggest that the pigments only offer protection in the presence of a leaf-made photosensitiser compound. Similar compounds are produced by other bacteria, with a considerable about of variation in the structures of these polyenes, raising questions about exactly which functionalities are required for photoprotection.

Section 1.1.4 Previous work done within the group

The original retrosynthesis of methyl xanthomonadin **208** involved utilising the group's iterative cross-coupling methodology to build two tetraenes and then join them together using a Suzuki-Miyaura cross-coupling (**Scheme 31**).[160–167]

Scheme 31 Original retrosynthesis of xanthomonadin **208**

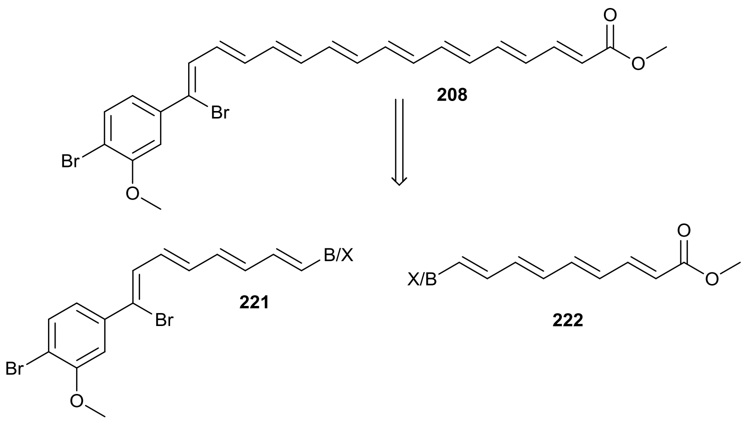

Progress had already been made towards the synthesis of xanthomonadin **208** on starting this project, with a route towards aryl intermediate **228** determined (**Scheme 32**).[168] The deprotection step in the route was poor yielding at 36%, yielding the aryl in an overall 23% yield, with an average of 75% per step. In addition, the group's iterative cross-coupling methodology had been used to access trienyl iodide **230**,[169] and the methodology further applied to give pentaenyl boronate on a small scale, in an overall 3% yield (**Scheme 33**).[170] In all of these routes there was obvious room for development, in particular for the iterative cross-coupling methodology, where the low yields obtained would make accessing the heptaene difficult.

Scheme 32 Previously established route towards aryl **228**

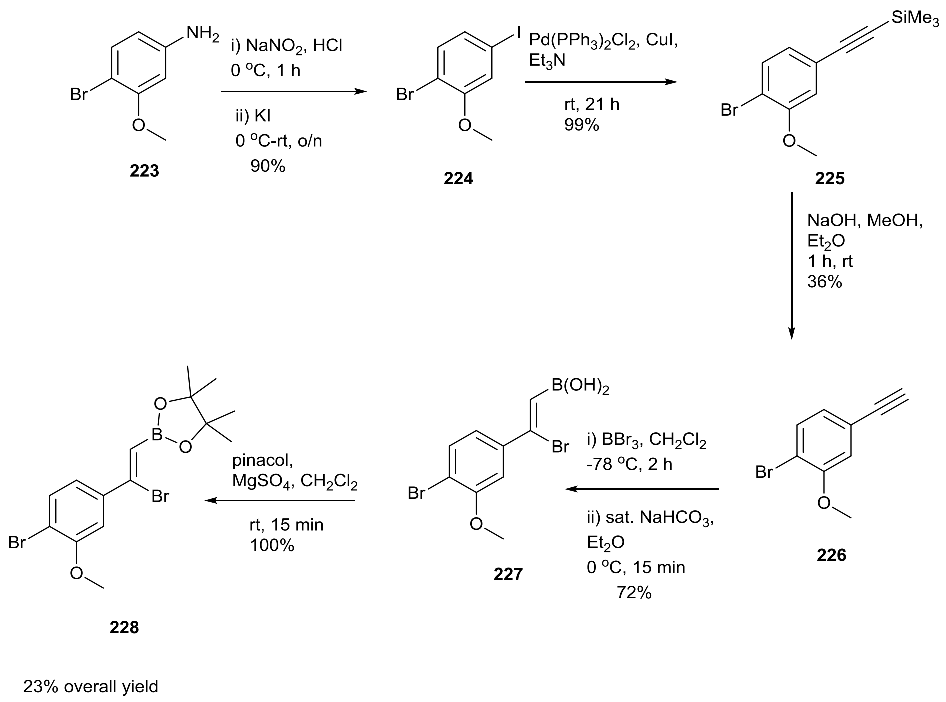

Scheme 33 Previous applications of the iterative cross–coupling methodology.

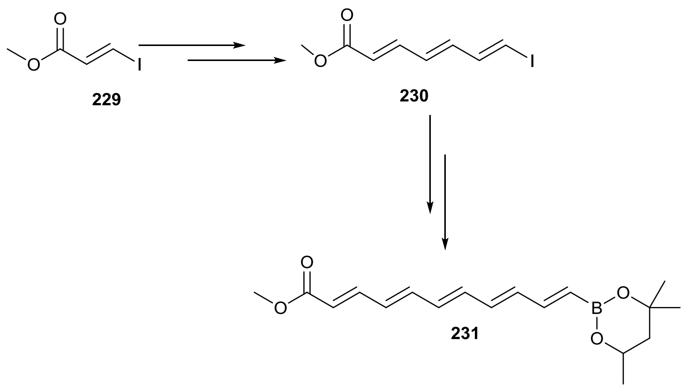

Section 1.1.5 Project aims and objectives

The only target within the group at this time had been xanthomonadin **208** itself. Following consideration of the literature on commencing this project, a number of key questions were identified:

1) Do the compounds proposed in the literature offer protection for bacteria against photodamage?
2) What is the mechanism of this protection?
3) What structural moieties are required to impart this protection?
4) What is the function of the polyenic bromine in xanthomonadin **208**?
5) Are these pigments lipid-bound?

In response to this, the project was expanded to include 6 target compounds in total, where compounds **208** and **210** were the natural products, xanthomonadin and the proposed monobrominated xanthomonadin not previously targeted in the group. The alkyne moiety in analogue **232** was chosen not only in the hope that it will impart some stability to the compound, but also to investigate the effect of the non-natural group on the activity of the pigment. The shorter chain analogues **233-235** were chosen in order to investigate the required polyene chain length for photoprotective activity, as well as providing good models for development of the iterative cross coupling methodology. The shortest polyene chain identified in the literature search was a hexaene, and therefore a pentaene was chosen to see if this could still impart any photoprotective activity.

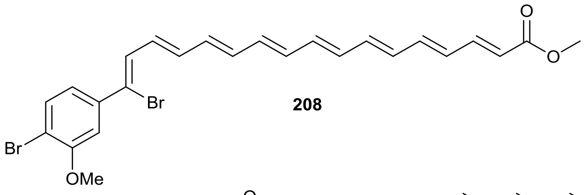

208

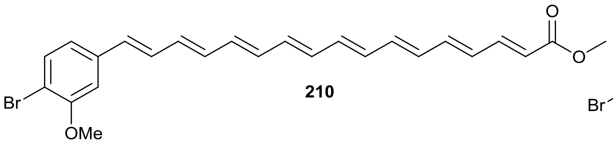

210

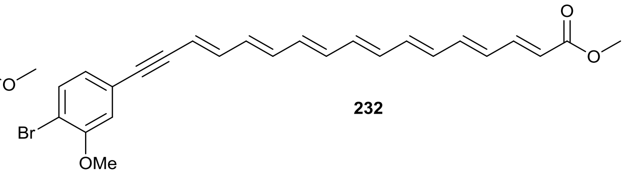

232

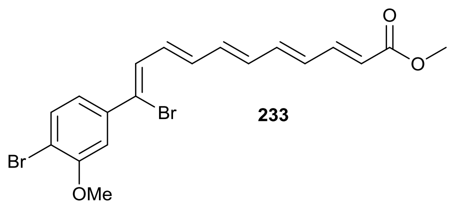

233

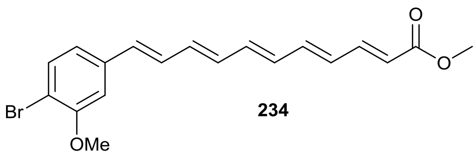

234

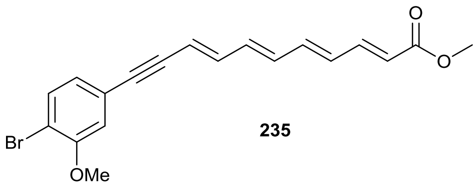

235

In order to synthesise these compounds in the most efficient way possible, it was envisaged that a polyenyl intermediate would be used to couple with different aryl building blocks.

Section 1.2 Synthesis of Xanthomonas pigments- construction of key aryl building blocks and selection of cross coupling reactions

Section 1.2.1 Synthesis of a range of aryl building blocks

In the design of key aryl building blocks, flexibility was the primary focus, as the final cross-coupling to connect the polyenyl chain and aryl had not been identified for the pigments and their analogues. One of the coupling partners would have to be an iodide and the key consideration would be one of stability. Attention was first turned to improving the route to brominated boronate ester **228**, where use of TBAF in the deprotection of trimethylsilane **225** gave a large increase in the yield of the deprotection step (**Scheme 34**).

Scheme 34 Improved route to brominated boronate ester **228**

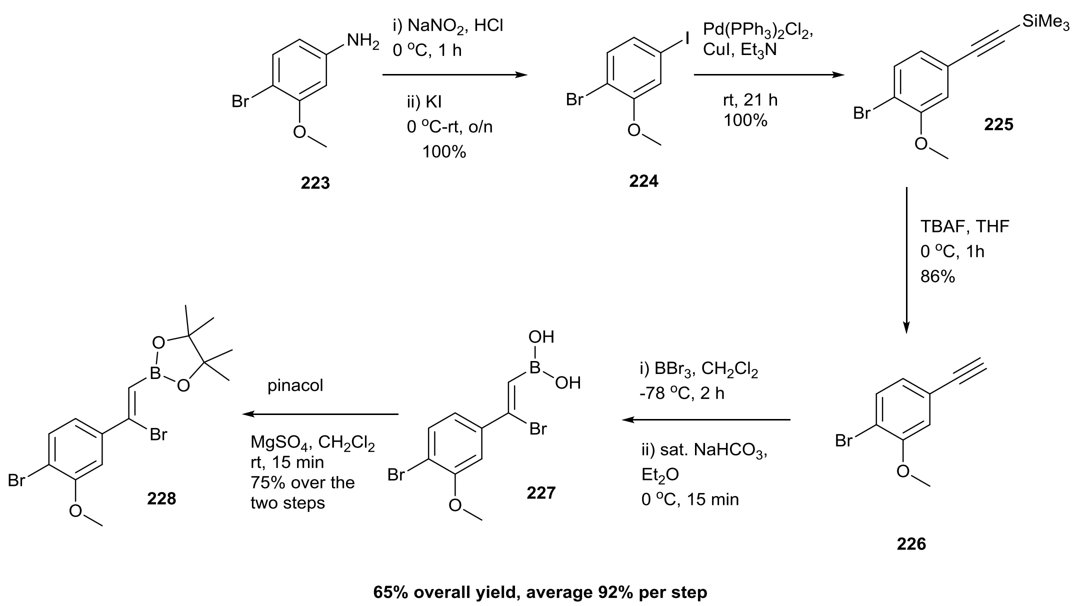

The most challenging step in this synthesis proved to be the reliable formation of boronic acid **227**. It was found that all samples of boronic acid **227** contained between 10 and 20 per cent of a side product. This product gave characteristic signals in the ^{1}H NMR spectrum, i.e. two doublets at 5.80 and 6.12 ppm (**Figure 1**). These corresponded to the proton signals of unsubstituted geminal alkene **236 (Equation 1**). Initially it was thought that this product was formed due to protodeboronation by excess base, but it was later shown that addition of more base to the reaction mixture did not affect the proportion of unsubstituted alkene. It is now believed that formation of this product was due to reaction with hydrogen bromide present in the boron tribromide reagent. It was eventually found that this could be minimised, although not eliminated, by using fresh boron tribromide. Boronic acid **227** was found to be unstable over time, and so was taken straight through to the ester formation.

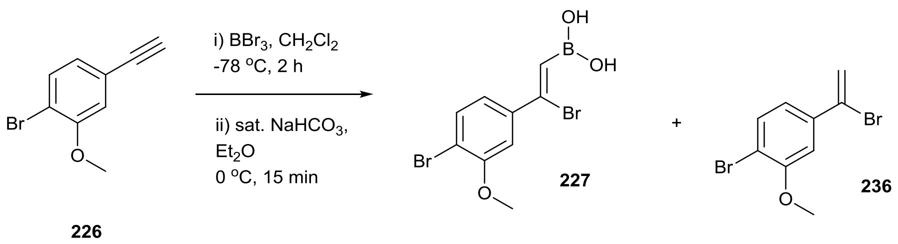

(1)

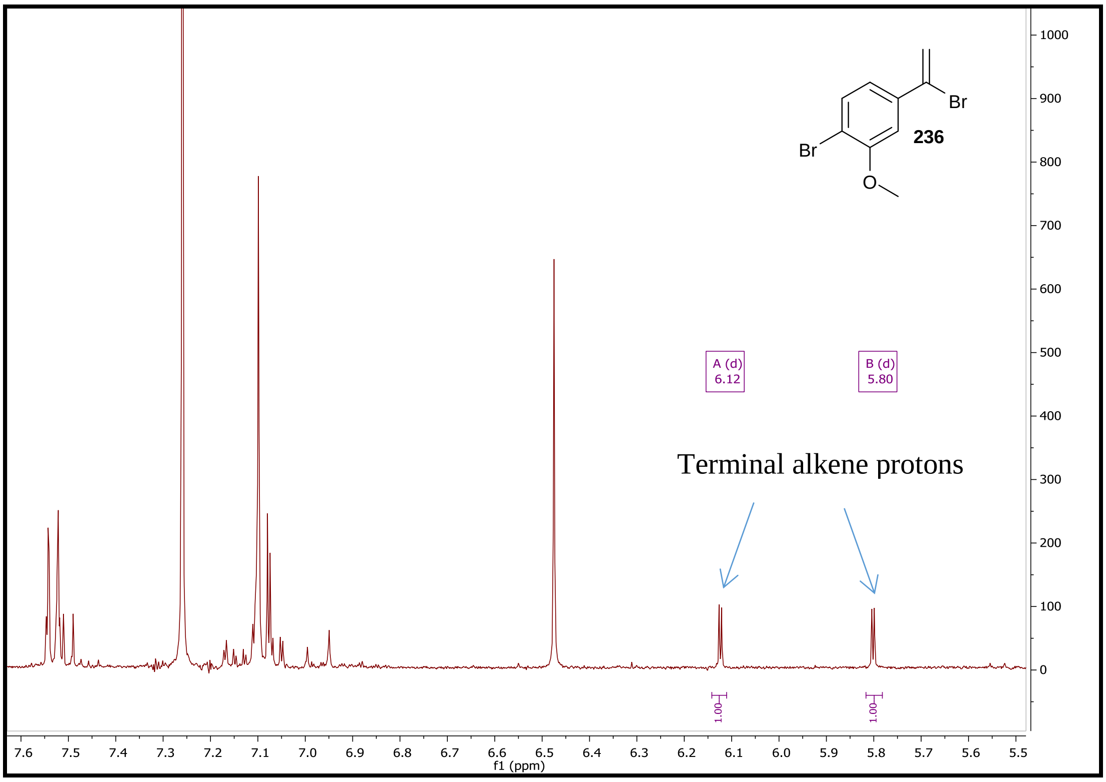

Figure 1 ^{1}H NMR spectrum of boronic acid **227**, showing the characteristic peaks of side product **236**

Attention was then turned to the conversion of the pinacolate ester to an iodide, to provide another coupling partner for the final cross-coupling. Iododeboronation methodology had been previously applied to boronate ester **228**, but with limited success.[170] A literature procedure was found which could effect the conversion of boronic acids to halides using *N*-halidesuccinimides at room temperature in acetonitrile.[171] Initially, this was attempted using *N*-iodosuccinimide (NIS) **237** on pinacol ester **228** (**Equation 2**), due to concerns over the stability of boronic acid **227**. None of the desired iodide was isolated, but the ^{1}H NMR spectrum of the product obtained from the column showed a singlet at 3.14 ppm, corresponding to the alkyne hydrogen for compound **226**, formed by an elimination reaction.

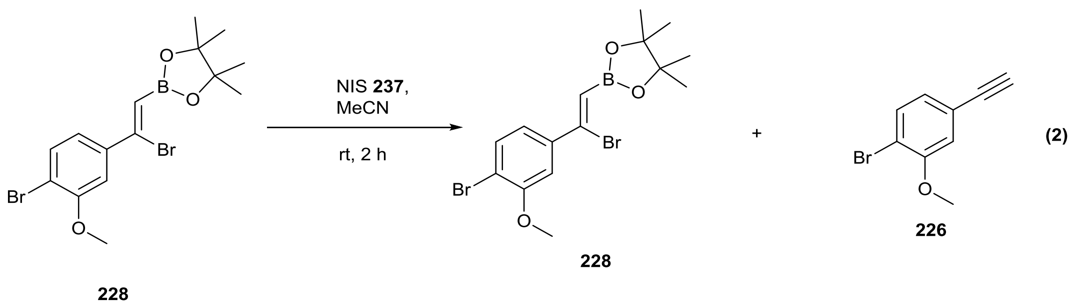

Due to the fact that this reaction used acetonitrile as the solvent, the same solvent used for the HM couplings, formation of the iodide was attempted again. Instead of subjecting the reaction mixture to work up, the product was transferred directly into a Heck-Mizoroki (HM) coupling to see if the iodide was forming *in situ* (**Scheme 35**). After stirring for one day, no polyene-like peaks were observed in the ^{1}H NMR spectrum and so it was concluded that the iodide had not been formed.

Scheme 35 Attempted one-pot formation of iodide **238** and HM coupling.

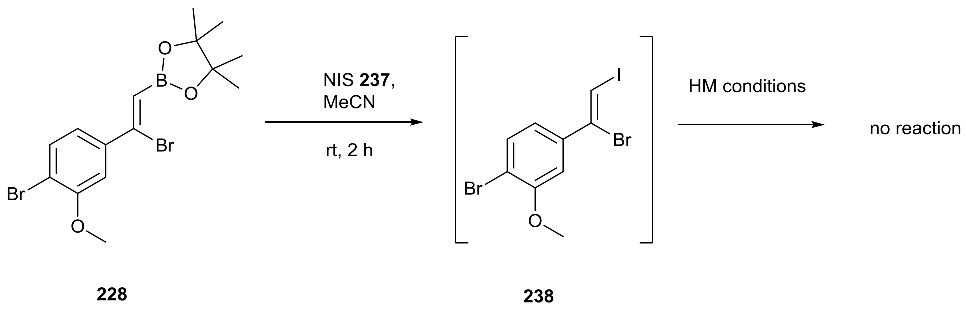

The mechanism for the iodide-forming reaction given in the literature reference first involves coordination of an NIS carbonyl to the boron, forming a boronate anion. This is then able to leave and the bond between the carbon and boron used to form a new bond with the electropositive iodine atom in a concerted step

(**Scheme 36**).[171] The formation of alkyne product **226** indicated successful coordination, but unsuccessful substitution of the boronate anion for an iodine. Two possible mechanisms are given below. The first is an E_{1cb}-like loss of the boronate to give an alkenyl anion, followed by loss of the bromide and triple bond formation. The second is a more concerted, *pseudo* E_{1cb}-like loss of both groups in the same step (**Scheme 37**). The conclusion made was that the steric hinderance of the boronate ester had prevented successful iodine substitution. As a result, the same reaction was attempted on styrenyl boronic acid **227**, giving styrenyl iodide **238** in a 78% yield as a white solid (**Equation 3**). Iodide **238** proved to be quite stable, perhaps surprisingly so given the dihalogenated alkene and the continual observation within the group that alkenyl iodides can be very unstable, and could be stored successfully for months at -18 °C under argon and in the dark.

Scheme 36 Mechanism proposed in the literature for conversion of a boronic acid moiety to an iodine atom with NIS[171]

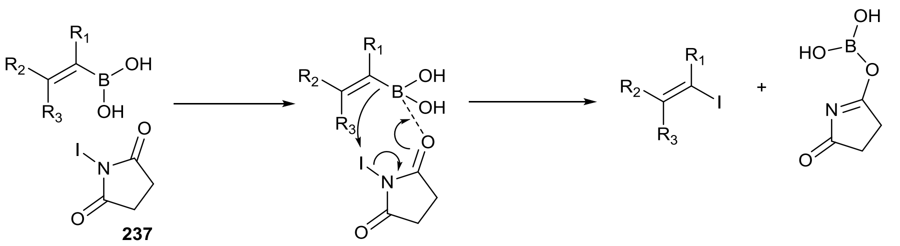

Scheme 37 Proposed mechanisms for elimination of pinacol boronate ester group and bromide ion to give alkyne **226**

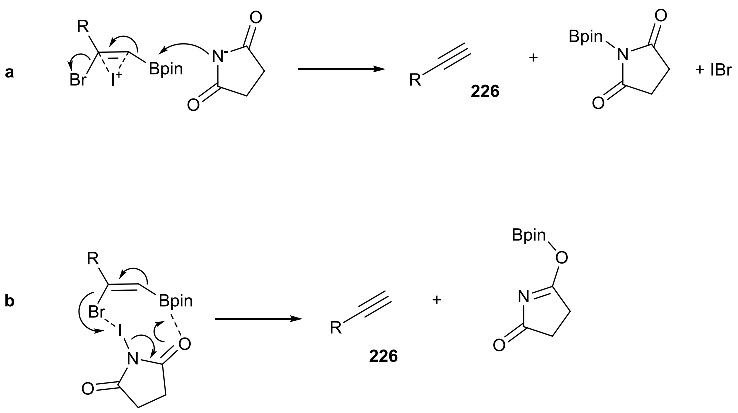

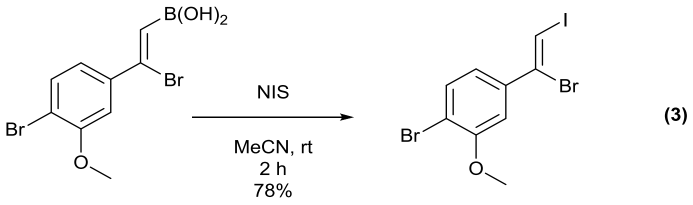

227

238

An attempt was made to make iodide **238** directly from alkyne **226** in a one-pot procedure *via* dibromoboron intermediate **239**, circumventing the isolation of the unstable boronic acid **227**. Unfortunately, a 50:50 mixture of boronic acid **227** and geminal by-product product **236** was obtained (**Scheme 38**).

Scheme 38 Attempted one-pot formation of styrenyl iodide **238**, resulting in formation of boronic acid **227** and geminal by-product compound **236**

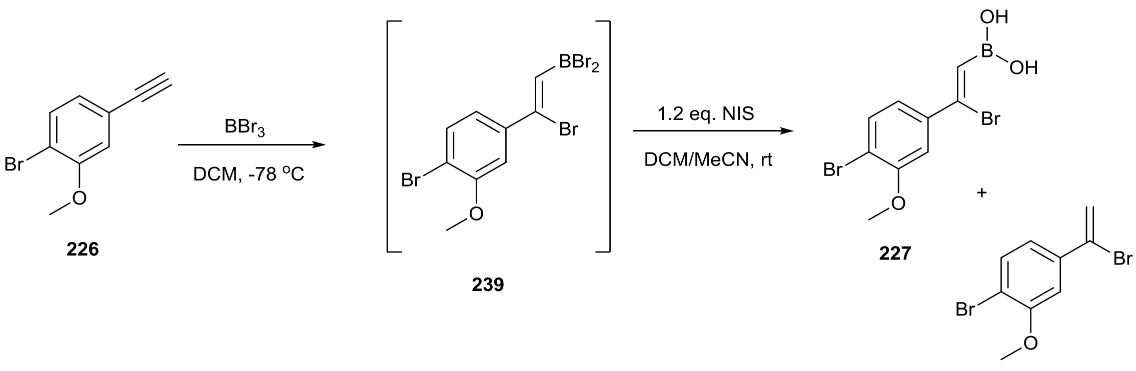

226

239

227

236

For the monobrominated analogues of xanthomonadin, the de-brominated analogue of pinacolate ester **228**, compound **240** was required. It was envisaged that this could be easily synthesised by hydroboration of alkyne **226**. Copper-catalysed borylation of **226** was attempted using copper chloride, xantphos, sodium *tert*-butoxide and 4,4,5,5-tetramethyl-2-(tetramethyl-1,3,2-dioxaborolan-2-yl)-1,3,2-dioxaborolane in THF and methanol (**Equation 4**). Gratifyingly, this approach was successful and, with some optimisation of the purification conditions, styrenyl pinacolate ester **240** was isolated in a 79% yield.

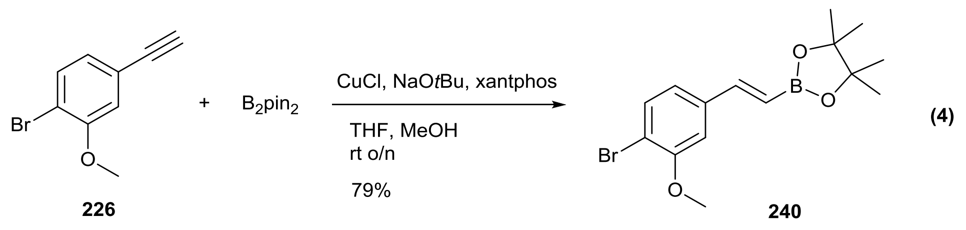

As a result, three key building blocks could be accessed in a highly efficient manner, with both pinacolate esters accessed *via* either a bromoboration or hydroboration protocol from key alkynyl building block **226** (**Scheme 39**).

Scheme 39 Current route to key aryl intermediates **226**, **228** and **240**

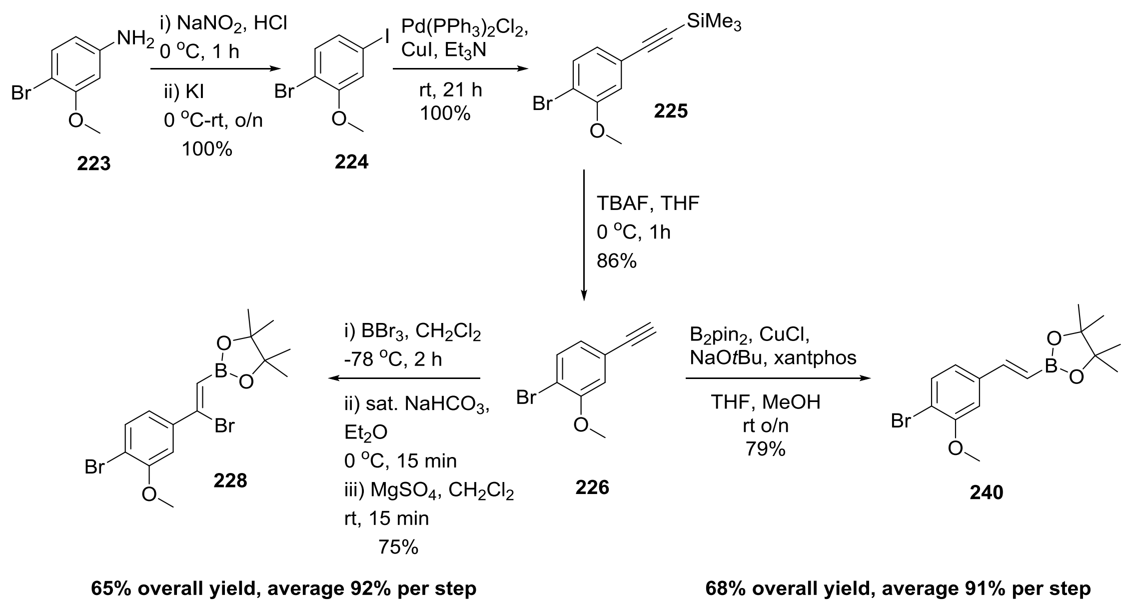

Section 1.2.2 Selection of cross-coupling reactions to form *Xanthomonas* pigment and their analogues

With a range of potential building blocks successfully obtained, potential cross-coupling reactions were evaluated. At this stage it was envisioned that HM coupling onto styrenyl iodide **238** would be the route to building an aryl polyenyl building block, and that SM couplings onto boronates **228** and **240** would also be useful. For the alkynyl target analogues, a Sonogashira coupling onto terminal alkyne **226** was required. Hence, work was undertaken on establishing the reactivity of the above mentioned building blocks to the desired cross-coupling reactions.

Section 1.2.2.1 HM couplings

A HM coupling was attempted on styrenyl iodide **238** (**Equation 5**), using the standard HM conditions developed within the group and detailed in the Introduction for the partial synthesis of viridenomycin. After stirring for 24 hours, the ^{1}H NMR spectrum showed a number of compounds, which were difficult to identify. It was not easy to tell if the desired diene had been made. The crude mixture was subjected to work up and silica gel chromatography in an attempt to identify the products.

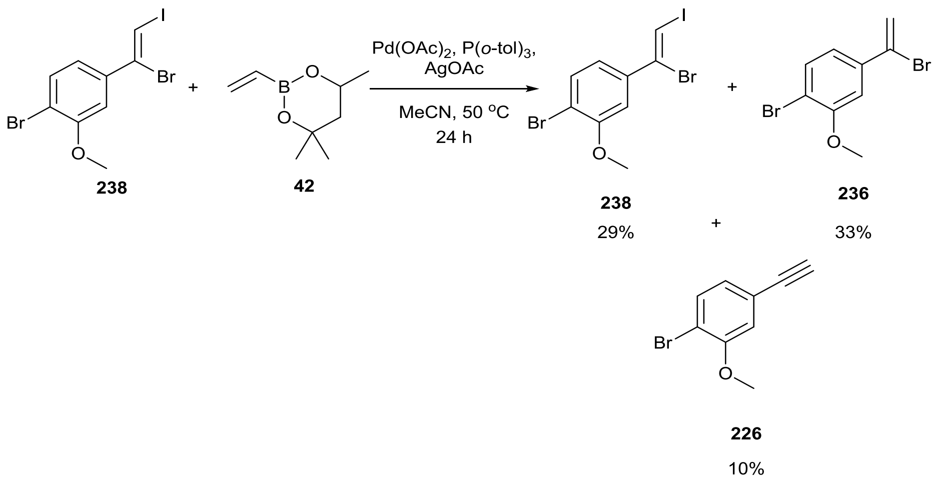

(5)

The sample of iodide **238** used to attempt this reaction contained 17% of the unsubstituted geminal impurity **236**. The products isolated from the column included 33% **236**, 29% unreacted styrenyl iodide **238** and 10% alkyne **226**. This corresponded to an increase in the impurity **236**, suggesting that it was a side-product in this attempted HM coupling. Formation of **236** and **226** could be attributed to protodehalogenation and elimination reactions on the palladium, respectively. The isolation of these compounds indicates that oxidative addition of styrenyl iodide **238** was occurring, but that there was a problem with catalyst turnover after this point. This is not unexpected due to the hindered nature of the styrenyl iodide, with a bromine atom on the α-carbon, the large pentanediol ester on the vinyl boronate acceptor **42** and the steric bulk of the tri-(*o*-tolyl)phosphine ligand. It may be that the palladium intermediate is too crowded for effective ligand exchange and migratory insertion.

It was found that drying of boronic acid **227** on the high vacuum line overnight resulted in considerable decomposition of the product, and increased proportions of the unwanted geminal by-product **236** (**Scheme 40**). The geminal by-product **236** was isolated from the mixture in a 13% yield and a HM coupling attempted on it. A potential alkene signal was observed at δ 5.58 ppm with an integral of 17% with respect to that of the geminal species **236**, but no other signals corresponding to the other alkenyl or aryl peaks could be easily identified from the complex signals observed (**Scheme 40**).

Scheme 40 Formation of geminal by-product **236** from alkyne **226** and its attempted HM coupling

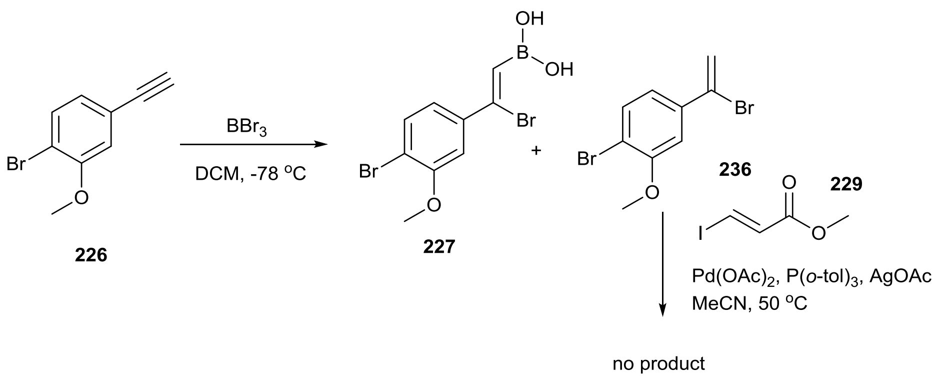

Section 1.2.2.1 Initial SM couplings

Suzuki-Miyaura (SM) coupling of all of the brominated aryl intermediates was investigated, with boronic acid **227** investigated first, using $Pd(PPh_3)_4$ and THF. A range of bases were tried, but unfortunately in all of these cases, no product was observed (**Table 1**, **Equation 6**). In the cases of potassium acetate and sodium hydroxide, complete decomposition of boronic acid **227** was seen with no obvious product formed. With sodium methoxide and barium hydroxide, conversion of boronic acid **227** to geminal by-product product **236** and alkyne **226** was observed in differing amounts (sodium methoxide gave 16% alkyne, whereas barium hydroxide gave 28%). With the carbonate bases, decomposition of boronic acid **227** was observed, along with some conversion to geminal by-product **236**. Additionally, at this temperature, loss of all of the THF from the reaction mixture was observed over the 3 days.

Table 1 Table showing the effect of base on the attempted SM coupling of boronic acid **227**

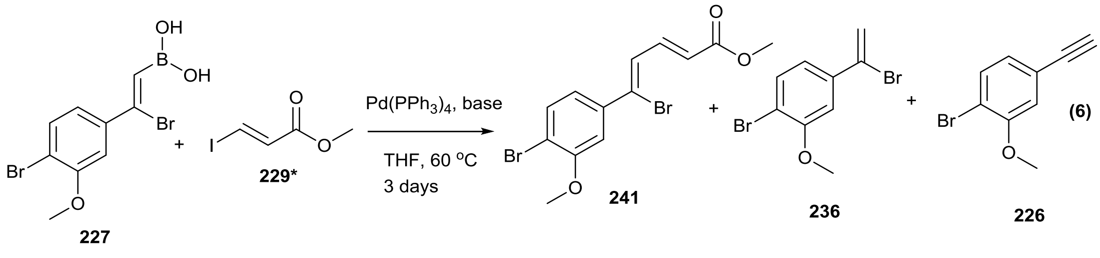

Entry	Base	Effect on boronic acid **227** after 3 day stir
1	KOAc	Decomposition
2	NaOH	Decomposition
3	NaOMe	Conversion to geminal by-product **236**, 16% alkyne **226**
4	$Ba(OH)_2$	Conversion to geminal by-product **236**, 28% alkyne **226**
5	Cs_2CO_3	Decomposition and some conversion to geminal by-product **236**
6	Na_2CO_3	Decomposition and some conversion to geminal by-product **236**

The reasons for this pattern of reactivity are unclear. Geminal by-product product **236** is likely a product of protodeboronation, whereas alkyne **226** is likely formed by elimination of the boronic acid and bromine atom. Both of these can occur due to base, and both could result from complexation with palladium (for proposed mechanisms, see **Scheme 41**). In all cases, the first step could be the quaternisation of the boron by the alkoxide ion of the base. The following step could be either elimination of the boron-'ate' anion and bromide ion or abstraction of a proton, presumably from another boronic acid group present in solution to effect protodeboronation. This can either take place straightaway, or following transmetallation onto the palladium.

Instead of attempting to achieve some level of reactivity on this unstable intermediate, focus turned to potential SM couplings on the more stable pinacolate ester **228** and styrenyl iodide **238**.

Scheme 41 Proposed mechanisms for the different routes by which boronic acid **227** can undergo elimination and protodeboronation

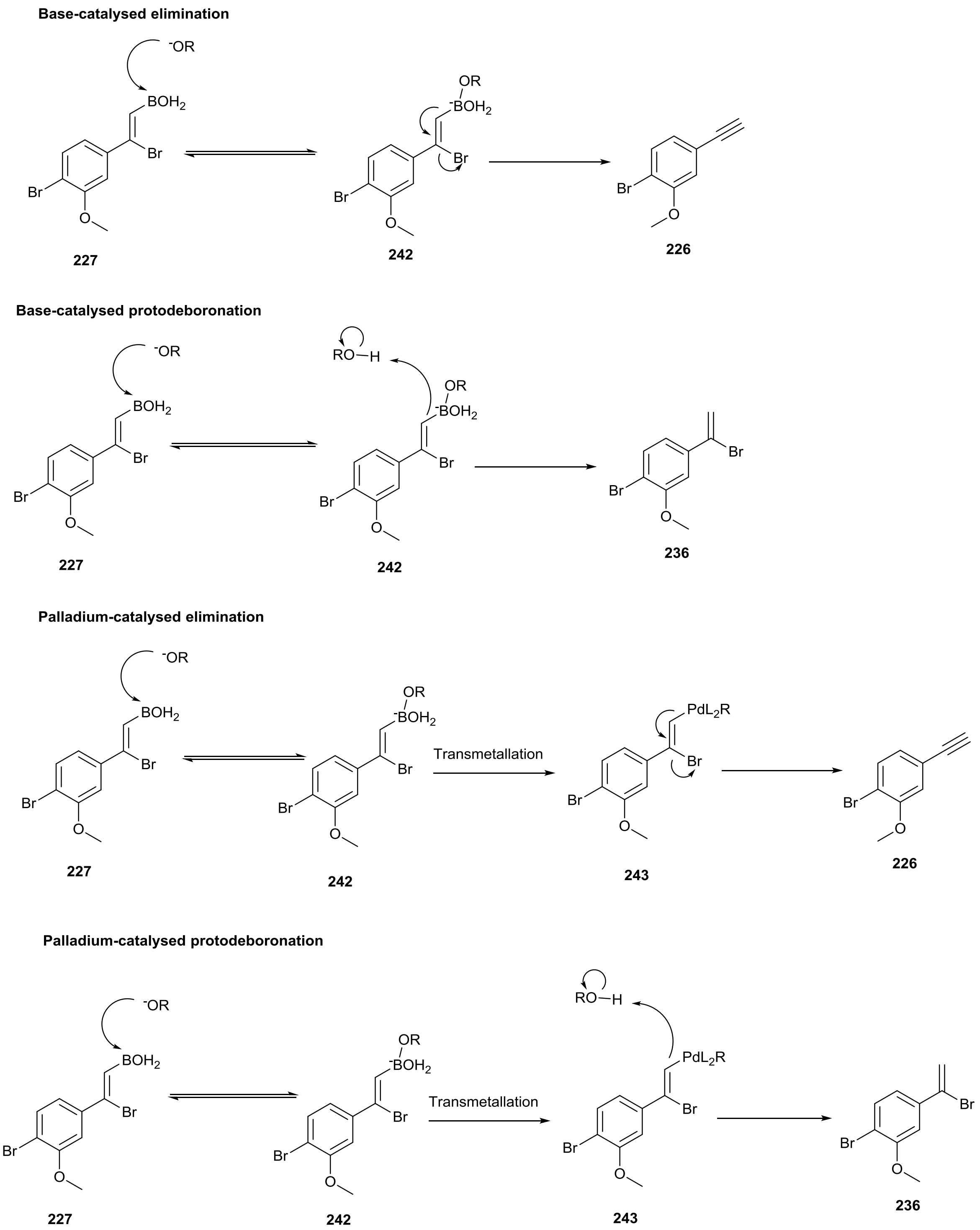

In a similar manner to the SM screen undertaken for boronic acid **227**, conditions for the potential SM coupling of iodide **238** were investigated. The same bases were used for this screen as were for the screen on boronic acid **227**, with the addition of silver(I) oxide (**Table 2**, **Entry 7**)., in the hope that it would help prevent elimination of the alkenyl iodides in the cross-coupling reactions. $Pd(PPh_3)_4$ was used as the catalyst, as before, but the solvent was changed to 1,2-dimethoxyethane (DME) in order to circumvent issues with solvent loss. The results of this screen show quite a profound effect of base on the stability of iodide **238** (**Table 2**, **Equation 7**).

Table 2 Table showing the effect of base on the attempted SM coupling of styrenyl iodide **238**

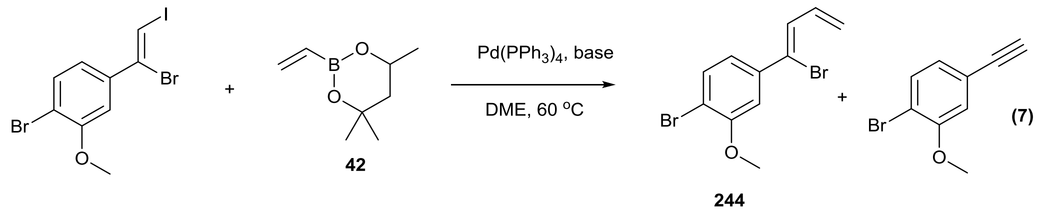

238 42 244 226

Entry	Base	Effect on iodide **238** after 3 day stir
1	KOAc	Iodide intact, no alkyne **226** formation
2	NaOH	Only alkyne **226** present
3	NaOMe	73% alkyne **226** present
4	$Ba(OH)_2$	8% alkyne **226** present
5	Cs_2CO_3	Only alkyne **226** present
6	Na_2CO_3	7% alkyne **226** present
7	Ag_2O	Complete decomposition of iodide, no alkyne **226** formation

In all cases, no SM product **244** was seen, and the only identifiable product was alkyne **226**, presumably formed by an E_1-type elimination, post-oxidative addition of the iodide onto the palladium (**Scheme 42**) *via* complex **245**. No protodehalogenation to give geminal by-product **236** was observed for any of the reactions, indicating that this E_1-type elimination is very facile. The level of elimination varied between bases, with only potassium acetate leaving iodide **238** intact. In the cases of sodium hydroxide and cesium carbonate (**Table 2**, **Entries 2** and **5**), complete conversion to alkyne **226** was seen. Sodium methoxide effected a 73% conversion of iodide **238** to alkyne **226** (**Table 2**, **Entry 3**), where barium hydroxide and sodium carbonate resulted in minimal alkyne formation (**Table 2**, **Entries 4** and **6**). Silver(I) oxide (**Table 2**, **Entry 7**), although employed in an attempt to counteract any elimination, resulted in complete decomposition of iodide **238**, with no obvious identifiable product.

Scheme 42 Proposed mechanism for elimination of iodide **238** to give alkyne **226**

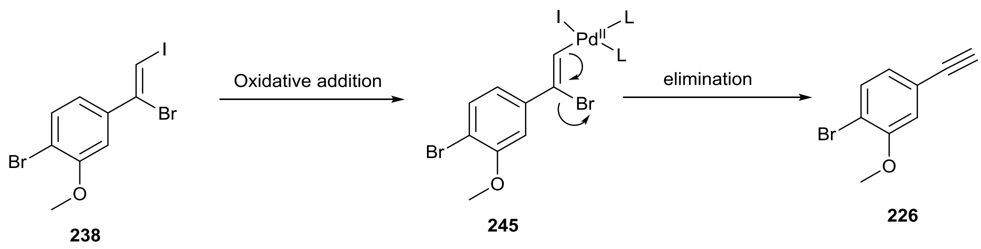

There was no obvious pattern in the results (**Table 2**) relating to either alkoxide nature or cation size. Indeed, both strong and weak bases, as well as large and small cations were able to effect the complete conversion of iodide **238** to alkyne **226**. This is clearly seen in the contrast between sodium hydroxide and barium hydroxide, and cesium carbonate and sodium carbonate (**Table 2**, **Entries 2**,**4**,**5** and **6**). The nature of the alkoxide ion can influence the rate of ligand exchange post oxidative addition, in a successful cycle enabling better transmetallation of the acceptor onto the palladium species. In that case, it would be suspected that a more nucleophilic alkoxide would facilitate the regeneration of the palladium(0) complex, and therefore speed up the rate of reductive elimination. Both hydroxide and carbonate, were observed to effect complete conversion of the iodide **238**. It was observed that complete conversion occurred when a strong base was paired with a small cation (sodium hydroxide, **Table 2**, **Entry 2**) and when a weaker base was paired with a large cation (cesium carbonate, **Table 2**, **Entry 5**). Nevertheless, it would be expected with such hindered systems that a strong base paired with large cation would facilitate the coupling, as has previously been detailed in the literature.[172]

A model system was therefore investigated in the hope of finding conditions to successfully couple onto the iodide analogue (**Table 3**, **Equation 8**). It was found that the combination of $Pd(OAc)_2$ with potassium acetate gave no conversion at all (**Table 3**, **Entry 2**), with the other conditions giving good conversions (**Table 3**, **Entries 1**, **3** and **4**).

Table 3 Table showing the conditions attempted to optimise SM coupling onto model iodide **246**

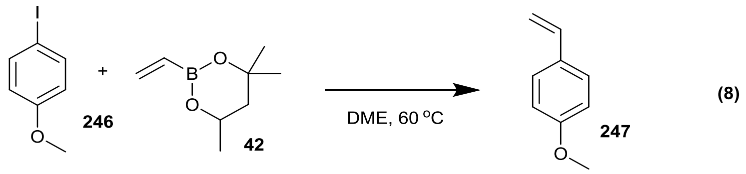

Entry	Catalyst	Base	Conversion/ %
1	$Pd(PPh_3)_4$	$Ba(OH)_2$	67
2	$Pd(OAc)_2$	KOAc	0
3	$Pd(PPh_3)_4$	*t*-BuOK	81
4	$Pd(PPh_3)_2Cl_2$	Cs_2CO_3	77

Despite **Entry 3** giving the highest conversion, concerns over the ability of potassium *tert*-butoxide to potentially facilitate elimination of iodide **238** led to the conditions in **Entry 4** being chosen to attempt SM coupling onto **238**.

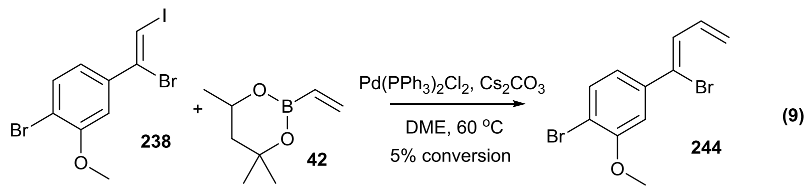

Unfortunately these conditions were not met with any success, with elimination of the iodide and 5% of the desired product observed (**Equation 9**). Buchwald's G2 XPhos precatalyst was tested, both using aqueous and anhydrous conditions (**Scheme 43**). No elimination was observed, but no coupling was observed either.

Scheme 43 Attempted SM coupling onto iodide **238**, using XPhos G2 precatalyst and both aqueous and anhydrous conditions

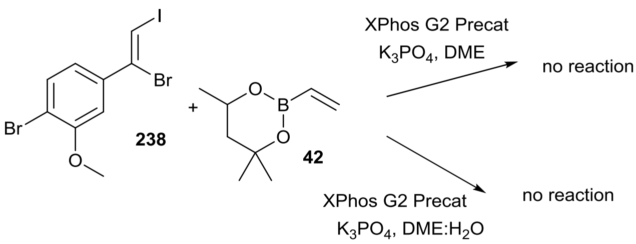

Section 1.2.2.2 Other cross-couplings

Following the unsuccessful attempts at SM couplings onto boronic acid **227** and iodide **238**, and HM couplings onto iodide **238** (see **Equations 5**, **6**, **7** and **9**), other types of cross coupling were considered. Both Stille and Sonogashira couplings were considered, as the conditions used for these are commonly milder than those generally used in SM and HM couplings.

The Stille coupling was attempted on iodide **238** with vinyl stannane **248** (**Equation 10**). Conditions without a base were deliberately employed in the hope of avoiding the elimination of iodide **238** before it could react. Initially the reaction was undertaken at room temperature, and ^{1}H NMR analysis after 16 hours was inconclusive, not displaying the expected multiplicity for the desired product **244**.

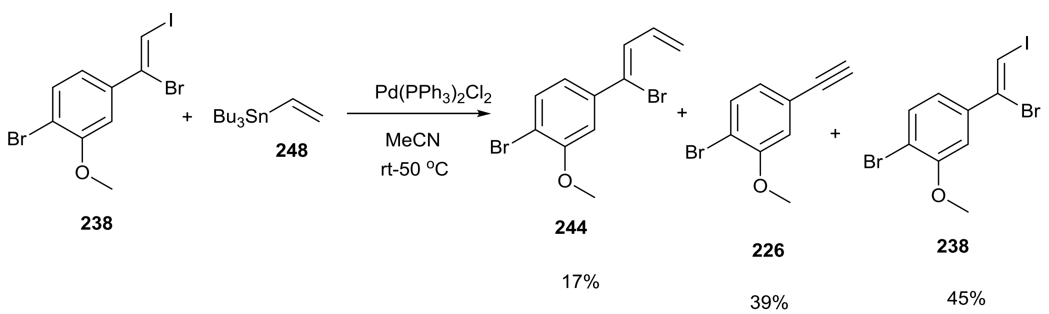

(10)

TLC analysis was also inconclusive, so the temperature was increased to 50 ^{o}C and the reaction stirred for a further 2 days to see the effect. At this point, a series of smaller signals were observed with the expected multiplicity for **244**, showing approximately 25% conversion. An attempt was made to isolate this compound by silica gel chromatography, but it was isolated as a mixture together with unreacted iodide **238**, alkyne **226** and tin by-products in an approximate 17% yield. The presence of compound **244** was confirmed by accurate mass spectrometry.

With the successful isolation of a cross coupling product (albeit not pure), attempts were made to optimise this reaction to obtain a higher conversion (**Table 4**, **Equation 11**). Addition of 1.2 equivalents of LiCl was attempted, in the hope that this would promote the reaction (**Table 4**, **Entry 2**). After stirring at 50 ^{o}C for 24 hours, only 7% product was observed, and the iodide **238** had converted to the alkyne. The proportion of catalyst was increased to 20 mol% and the reaction undertaken in the microwave at 105 ^{o}C (**Table 4**, **Entry 3**). Conversion to the alkyne was again seen. A copper catalysed coupling was attempted using copper(I) thiocarboxylate, a procedure which could be undertaken at 0 ^{o}C, in the hope this this would preserve iodide **238** (**Table 4**, **Entry 4**). Unfortunately, no reaction between iodide **238** and stannane **248** was observed, even after allowing the reaction mixture to warm to room temperature. The reaction was then stirred at 50 ^{o}C overnight. After this, full consumption of the vinyl stannane was seen, but the ^{1}H NMR did not show any peaks corresponding to product **244**. Stirring the reaction mixture with no additives at 50 °C resulted in no conversion, only giving the undesired elimination and homocoupling products **226** and **249** (**Table 4**, **Entry 5**).

It was also found that stirring the tin acceptor with the catalyst in an 'activation' period before adding the iodide resulted in some improvement (**Table 4**, **Entry 6**). On larger scale, however, the successful coupling could not be repeated (**Table 4**, **Entry 8**). The preactivation period was, however, much shorter (3 hours *vs* overnight). Addition of silver(I) oxide also improved the conversion further (**Table 4**, **Entry 9**), giving the best conversion of 50%. This benefit was only observed when a prestir was used in the procedure, giving no conversion without this step (**Table 4**, **Entry 7**). Success in this coupling appeared to be a fine balance between the heat required to facilitate the desired Stille coupling and the temperature at which the competitive elimination takes place.

Table 4 Table showing the conditions attempted to effect Stille coupling onto styrenyl iodide **238**

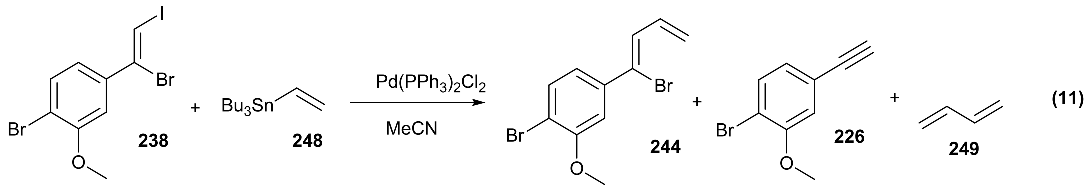

Entry	Conditions	Result
1	rt, o/n, then 50 °C	<10%, then 25% conversion
2	LiCl addn, 50 °C	7%, Elimination of iodide
3	20 mol% cat., microwave 105 °C	Elimination of iodide
4	CuOTc, NMP, 0 °C	No reaction
5	50 °C	Elimination of iodide and butadiene formation
6	o/n rt, no iodide, then warm to 50 °C and add iodide	34% conversion
7	50 °C, Ag_2O as additive	No product formation, minimal butadiene
8	o/n rt, no iodide, then warm to 50 °C and add iodide (10x scale)	Solely elimination and butadiene formation
9	o/n rt, no iodide, then warm to 50 °C and add iodide (10x scale), Ag_2O as additive	~50% conversion, butadiene formation, small amount of iodide elimination

In light of these promising results (**Table 4**), a new polyenyl building block incorporating a stannane and boronate ester at each end was considered (see **Section 1.3**), but synthesis of this building block consistently proved challenging and attention turned away from the Stille as a potential cross-coupling.

A Sonogashira coupling was attempted on styrenyl iodide **238** (**Equation 12**). After stirring for three days at room temperature, consumption of the iodide was seen, along with a change in shift for the singlet proton on the brominated alkene. The reaction was worked up and subjected to silica gel chromatography in the hope of isolating this product. A mixture of compounds was obtained, but the Sonogashira product **251** was identified by mass spectrometry and and seen to be the major component in the mixture by ^{1}H NMR, opening up the potential to deprotect the alkyne and complete the polyene chain, reducing down the alkyne to the desired alkene. Notably, in this coupling, no elimination product was observed. Unfortunately, the isolated yield in this reaction was disappointingly low.

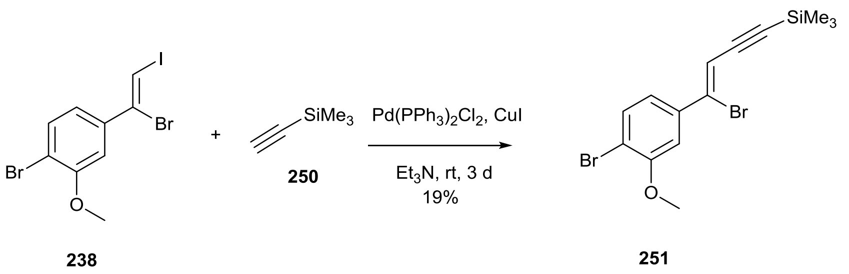

(12)

A Sonogashira coupling was attempted on alkyne **226** to establish whether it would be reactive to coupling (**Equation 13**). This was successful, giving the resulting product **252** in an 89% yield.

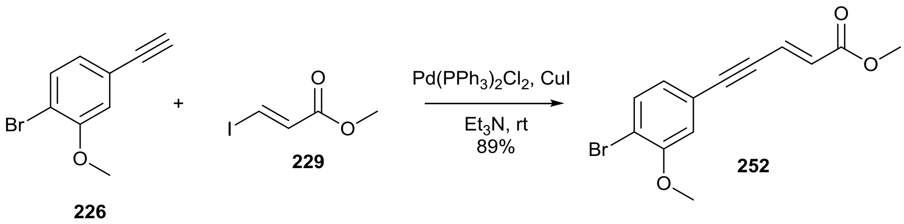

(13)

Following the success of this reaction (**Equation 13**), an attempt was made to form the brominated alkene **244**. It seemed prudent to avoid the use of HBr in aqueous solution due to the ester and alkene, so this reaction was attempted by generating HBr *in situ* using ethanol and acetyl bromide (**Equation 14**), in the hope of accessing **244**. Unfortunately, no reaction at the alkyne was observed.

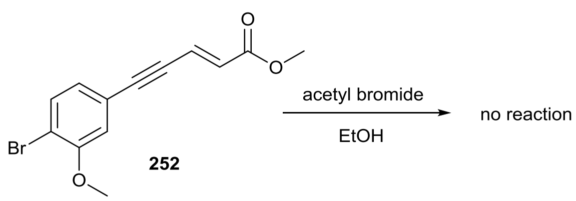

(14)

Section 1.2.2.3 Revisiting the SM couplings

Attention was turned back to the SM cross coupling, focussing now on the seemingly more stable brominated pinacol ester **228**. Initally this was unsuccessful, as was coupling onto the non-brominated styrenyl pinacol ester **240**. It was noted that the boronate esters were not decomposing during the course of the reaction, but the alkenyl/ polyenyl iodide coupling partners employed were decomposing. To that end, coupling onto both the pinacolate analogues was attempted using silver(I) oxide as the base in an attempt to prevent elimination. The desired SM product could be identified in both of the crude products by accurate mass. It became apparent that the temperature being used in the cross-coupling could well be a cause of the decomposition of the iodides and so lower temperature SM conditions needed to be identified if at all possible. Previous SMs were revisited, and new conditions were tested for the SM between monobrominated pinacol ester **240** and iodoacrylate **229**, in order to try to optimise this cross-coupling (**Table 5**, **Equation 15**). Isolation of diene **253** proved difficult in the past due to the diene's tendency to polymerise, so the crude mixtures were not subjected to chromatography. ^{1}H NMR data could be attributed to the desired diene and this, in combination with the accurate mass analysis previously obtained, provided evidence that the desired diene was being formed. The aryl and alkenyl sections of the ^{1}H NMR data were very complex, but the characteristic doublet at δ 5.96 ppm for the diene was easily identifiable, as was the characteristic doublet for pinacolate ester **240**.

The SM did tolerate lower temperatures, but benefitted from an increase in catalyst in order to improve the reaction rate (**Table 5**, **Entries 2** and **3**). Doubling the $Pd(PPh_3)_4$ loading from 5 to 10 mol % at 40 ^oC increased the conversion from 69 to 92%.

Equivalent conversion was also seen at 30 ^oC (**Table 5**, **Entry 4**), but dropping to room temperature resulted in a drop in yield to 78% (**Table 5**, **Entry 5**). However, room temperature coupling using *in situ* generated $Pd(PPh_3)_4$ from $Pd(OAc)_2$ and PPh_3, along with Ag_2CO_3 as the base and MeCN as the solvent gave an increased yield comparable with those seen at 30 and 40 ^oC (**Table 5**, **Entry 6**).

A minor side-product **254** was observed, with ^{1}H NMR signals at δ 6.12 (1H, d, J=18.3 Hz), 6.55-6.60 (1H, m) and 7.90 (1H, dd, J=12.4, 7.8 Hz) *inter alia*. This side product was not isolated. When *t*BuOK was used as the base, this side-product was observed as the major product, suggesting that the unwanted product could be an elimination product.

Table 5 Conditions screen for the Suzuki-Miyaura coupling of styrenyl Bpin **240** with iodoacrylate **229**

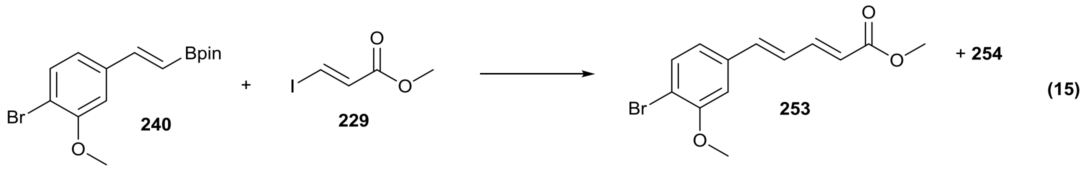

Entry	Catalyst	Catalyst loading/ mol%	Base	Eq. base	Temperature / ^{o}C	Solvent	Product conversion after 24 h/ %
1	$Pd(PPh_3)_2Cl_2$	5	Ag_2O	1.2	60	DME	35[a]
2	$Pd(PPh_3)_4$	5	Ag_2O	1.2	40	DME	69
3	$Pd(PPh_3)_4$	10	Ag_2O	1.2	40	DME	92
4	$Pd(PPh_3)_4$	10	Ag_2O	1.2	30	DME	90

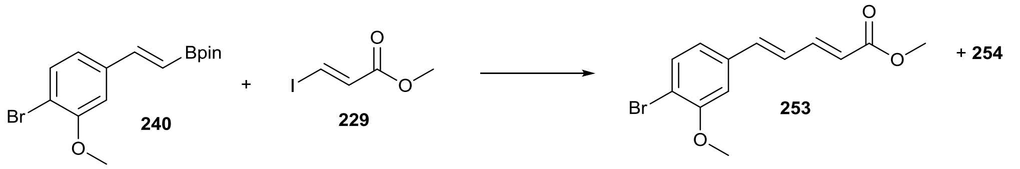

(15)

Entry	Catalyst	Catalyst loading/ mol%	Base	Eq. base	Temperature / ^{o}C	Solvent	Product conversion after 24 h/ %
5	$Pd(PPh_3)_4$	10	Ag_2O	1.2	rt	DME	78
6	$Pd(OAc)_2$/ PPh_3 (3 eq.)	10	Ag_2CO_3	2	rt	MeCN	89
7	$Pd(PPh_3)_4$	10	^{t}BuOK	2	40	DME	42[b,c]

[a] Multiple side-products observed. [b] Major product was the minor side-product observed in all other reactions. [c] Conversion after 14.5 h

Following the success of this screen, a similar optimisation was attempted with brominated styrenyl Bpin **228** (**Table 6**, **Equation 16**). In this case, the ^{1}H NMR spectra were much more difficult to analyse, with multiple alkenyl products observed. For some of the cleaner spectra, it was observed that ^{1}H NMR for the presumed dienyl product was lacking a proton signal (**Figure 2**).

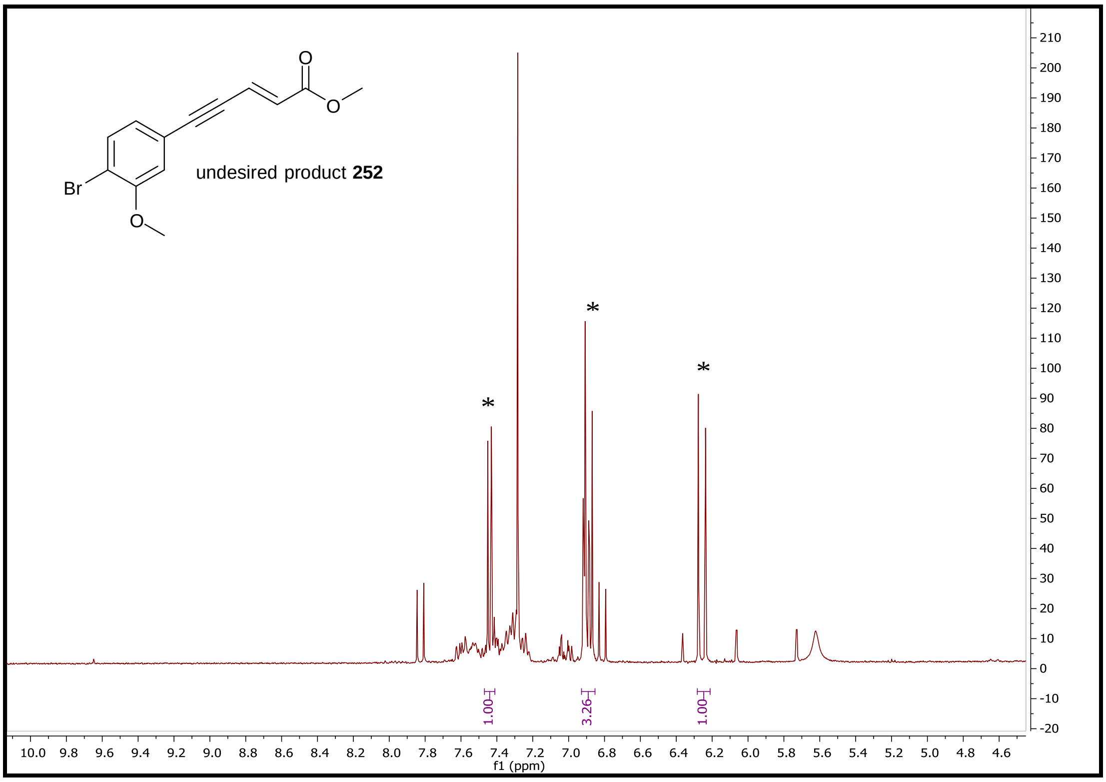

Figure 2 ^{1}H NMR spectrum of undesired product **252** formed by subjecting brominated styrenyl Bpin **228** and iodoacrylate **229** to SM conditions, showing that not enough proton signals are present.

The product was isolated from one of the reaction mixtures and found to be alkynyl dienyl analogue **252**, rather than the desired brominated alkene **241** (**Figure 2**). Mass spectrometry of the crude reaction mixture in **Entry 4** showed that the mass ions for both the desired brominated diene **241** and the alkynyl analogue **252** were present. As was the case for the monobrominated diene **253**, identification of the brominated diene **241** was difficult due to the complexity of the spectra. Again, ^{1}H NMR peaks could be attributed to the desired diene, with a characteristic alkenyl signal at δ 6.12 ppm, which could be used to approximate the conversion in the cross-couplings. These NMR data were corroborated by accurated mass analysis of a crude reaction mixture, providing confidence that the desired brominated diene had been formed. A number of different conditions were attempted in the hope of obtaining the desired alkenyl product **241** (**Table 6**, **Equation 16**). Another non-isolated side-product **255** was formed in some cases (indicated by a doublet observed in the ^{1}H NMR spectrum at δ 8.24, J=12.6 Hz), along with the brominated diene **241** and the undesired (presumed) Sonogashira product **252**. Desired product **241** was seen when 5 mol% of either $Pd(PPh_3)_4$ or $Pd(OAc)_2$ was used at 60 ^oC (**Table 6**, **Entries 4** and **5**). Use of $Pd(PPh_3)_2Cl_2$ at 60 ^oC with Ag_2O gave a moderate amount of brominated diene **241**, but changing the base to Cs_2CO_3 gave exclusively the alkynyl dienyl product **252** (**Table 6**, **Entries 1** and **3**). The one attempt to perform this coupling at 40 ^oC lead exclusively to alkynyl dienyl product **252** (**Table 6**, **Entry 2**), giving rise to concerns as to whether a low-temperature SM would be possible.

Table 6 Attempted Suzuki-Miyaura couplings onto brominated styrenyl pinacolate ester **228**

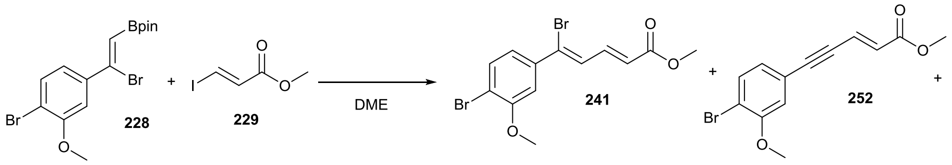

(16)

Entry	Catalyst	Catalyst loading/ mol%	Base	Temperature/ °C	Conversion after 24 h/ %		
					241	**252**	**255**
1	$Pd(PPh_3)_2Cl_2$	5	Cs_2CO_3	60	0	43	0
2	$Pd(PPh_3)_4$	10	Ag_2O	40	0	72	0[a]
3	$Pd(PPh_3)_2Cl_2$	5	Ag_2O	60	38	62	0
4	$Pd(PPh_3)_4$	5	Ag_2O	60	37	61	2
5	$Pd(OAc)_2$	5	Ag_2O	60	0	48	52
6	$Pd(dppf)Cl_2$	5	Ag_2O	60	34	66	0

[a] Conversion after 14.5 h

In order to shed some light on why this coupling was proving so unsuccessful, the two starting materials **228** and **229** were exposed to the reaction conditions separately (**Scheme 44**). They were first exposed to the silver base, and then to $Pd(PPh_3)_4$ after stirring overnight at 40 °C. Iodoacrylate **229** was stable to both additions, but brominated styrenyl Bpin **228** was deboronated immediately to give the geminal by-product compound **236** on addition of base.

Scheme 44 Effect of SM reaction conditions on brominated styrenyl Bpin **228** and iodoacrylate **229** separately

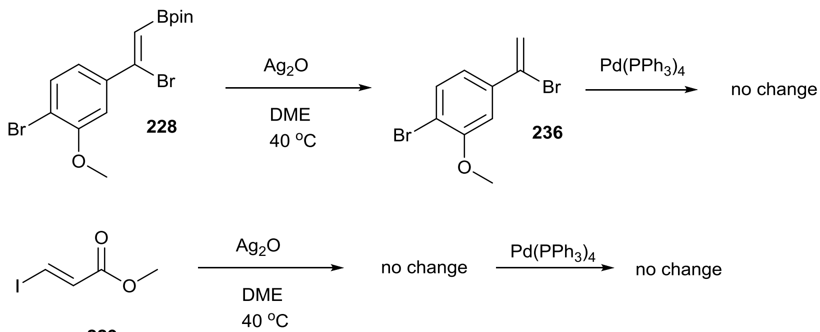

Whilst ideal Suzuki-Miyaura conditions had not been identified, enough progress had been made to select a Suzuki-Miyaura coupling for both mono- and di-brominated xanthomonadins and their truncated analogues, and a Sonogashira coupling for preparation of the alkynyl analogues.

Section 1.2.3 Summary

A number of different aryl building blocks **226**, **228**, **238** and **240** were made and evaluated as partners for key cross-coupling reactions to complete the synthesis of the target pigment molecules. The brominated styrenyl building blocks **228** and **238** suffered from a tendency to undergo undesired side reactions under cross-coupling conditions, particularly elimination and protode-boron/halogen-ation. After investigating a number of different couplings, it was decided that the most promising cross-coupling was the SM coupling, where the brominated styrenyl pinacol boronate ester **228** seemed to be the most amenable to optimisation. The debrominated styrenyl pinacol boronate ester **240** was much more amenable to cross-coupling, where SM conditions were more readily optimised, and fewer side-products were observed.

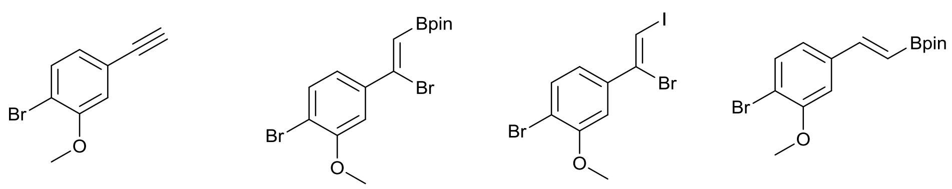

226 228 238 240

Section 1.3 Synthesis of Xanthomonas pigments - synthesis of polyene chains using the Heck-Mizoroki/iododeboronation iterative cross coupling methodology

As was discussed in **Section 1.1**, some progress had been made towards the construction of the all *trans*-heptaene moiety of xanthomonadin *via* the iterative Heck-Mizoroki (HM)/ iododeboronation (IDB) methodology previously developed within the group, with the synthesis of (2*E*,4*E*,6*E*)-7-iodo-hepta-2,4,6-trienoic acid methyl ester **230**, *via* iodoacrylate **229**, and its subsequent conversion to pentaenyl boronate **231** on a small scale.[169,170] In order to access the all-*trans* heptaene, the methodology required considerable optimization. In addition, there was no indication of how stable the longer chain analogues would be.

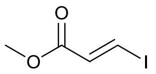
229

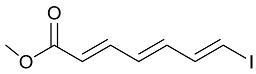
230

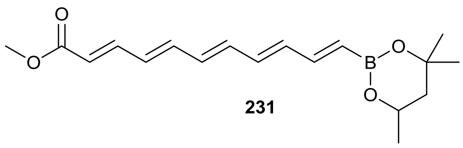
231

Work was undertaken to improve the efficiency of the routes already determined to key iodoacrylate building block **229**. The original synthesis of **229** involved sodium iodide addition to methyl propiolate **256** to form the (*Z*)-analogue **43**, followed by an isomerization reaction using hydrogen iodide to give the desired (2*E*)-3-iodoprop-2-enoate **229** (**Scheme 45**) in a 70% yield over the two steps**.**[169] Because the (*Z*)-analogue was not to be required during the synthesis of xanthomonadin **208**, an alternative route which did not require an isomerisation reaction seemed desirable to avoid the need to purify a mixture of isomers. As a result, an alternative pathway to **229** was investigated (**Scheme 46**). This route involved the addition of hydroiodic acid across the alkyne bond of propiolic acid **257**, and then the subsequent methylation of the acid **258** to give **229**. This route was successful, affording **229** in a higher overall yield than the previous route (86% cf. 70% with previous method). The geometry of the double bond was confirmed by performing X-ray crystallography on a sample of the crude (*E*)-3-iodoprenoic acid **258** (**Figure 3**). Iodoacrylate **229** was found to be stable for over a year if kept at 4 °C, in the dark and under argon.

Scheme 45 Original route for synthesis of **229**[169]

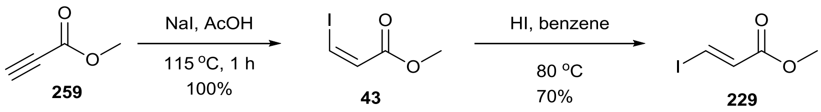

Scheme 46 New route for synthesis of **229**

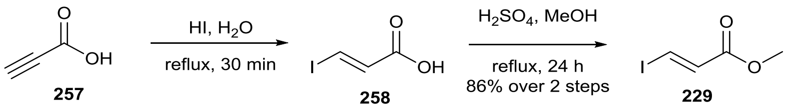

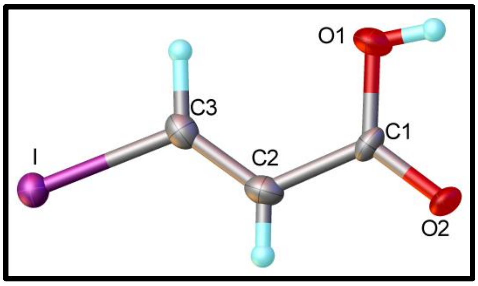

Figure 3 Crystal structure confirming the (*E*)-geometry of the double bond of (*E*)-3-iodoprenoic acid **258**

Section 1.3.1 Propagation of polyene chains from iodoacrylate 1, using HM/IDB ICC methodology

Due to the photosensitivity of the polyenes, and particularly the polyenyl iodides, all reactions, work ups and purifications were performed in the dark. Iodoacrylate **229** was subjected to the previously developed HM conditions to afford dienyl boronate **259** (**Scheme 47**); 100% conversion of iodoacrylate **229** was observed, with approximately 10% of this being converted to the Suzuki-Miyaura (SM) product, but only 78% was recovered after silica gel chromatography. A range of different eluent systems was tried, but streaking of the boronate compound was consistently observed, and this was presumed to be the cause of the lower mass recovery on purification. Dienyl boronate **259** was cleanly converted to dienyl iodide **260** using an IDB approach, adding sodium methoxide before the iodine monochloride to preserve the *trans* geometry. Silica gel chromatography of iodide **260** was performed using eluents cooled to 0 °C, with the separation being much better than for dienyl boronate **259**, and with no streaking. This was then converted to trienyl boronate **261** *via* another HM coupling. Purification of the trienyl boronate was particularly troublesome, proving to be very low yielding despite 100% conversion being observed in the coupling reaction itself (**Scheme 47**).

Scheme 47 Initially obtained yields for synthesis of trienyl boronate **261**

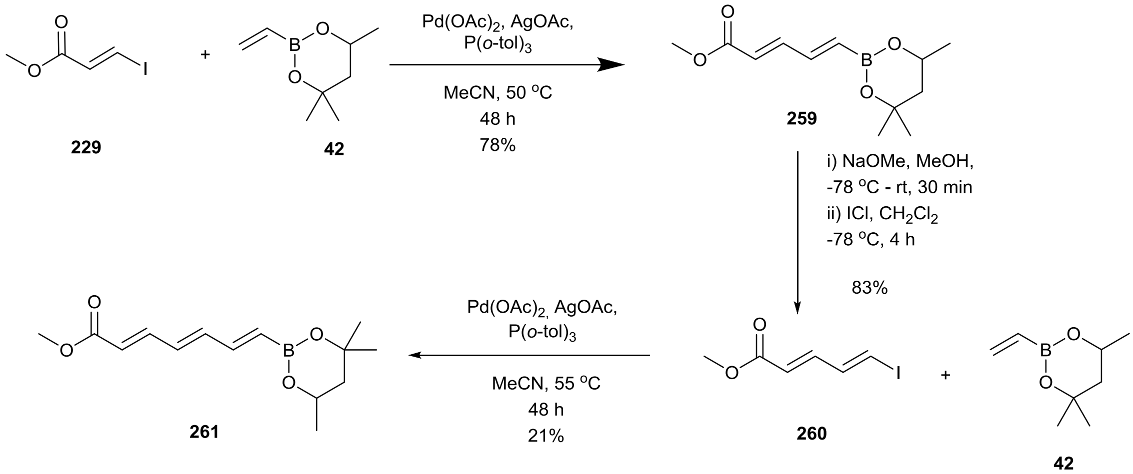

In order to try and minimise the loss of yield during the polyene synthesis, telescoping the crude dienyl boronate **259** into the IDB step directly was attempted, using only a filtration through a short Celite/silica plug to remove silver and palladium residues. This was attempted on a month-old sample of crude dienyl boronate **259**, giving a 56% yield of clean dienyl iodide **260** over the two steps (**Equation 17**). Complete conversion of the dienyl boronate intermediate **259** to iodide was observed, indicating that nothing present in the crude HM product was interfering with the desired iododeboronation.

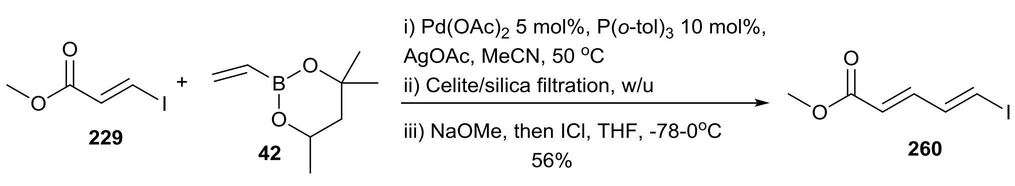

(17)

Whilst the yield was not as high for the two steps (**Equation 17**) as had been obtained by doing the steps discreetly (**Scheme 47**), it seemed that telescoping the polyenyl boronates through into the IDB step was a viable course of action. The stability of the polyenyl iodides (particularly those longer chain iodides) was still a cause of concern and therefore an HM/IDB ICC cycle where all intermediates were telescoped through without the need for silica gel chromatography would be preferable. Dienyl iodide **260** was therefore subjected to HM coupling conditions to give crude trienyl boronate **261**, which was then telescoped into the IDB step to give crude trienyl iodide **230**. This was then telescoped into the next HM coupling, to give crude tetraenyl boronate **262** (**Scheme 48**).

Scheme 48 Attempted synthesis of xanthomonadin **208** by sequential telescoped HM/IDB steps

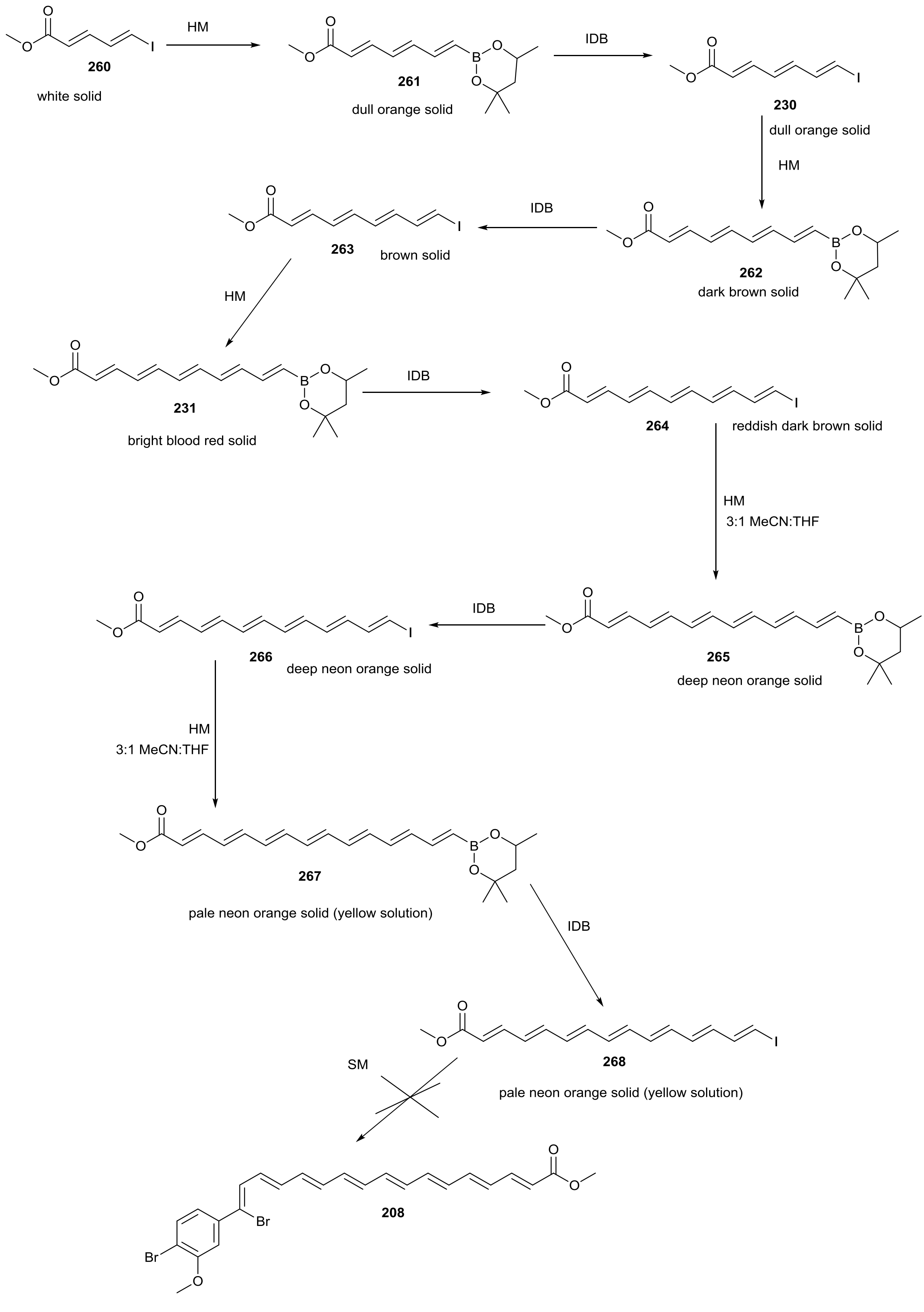

It was noted that the ^{1}H NMR spectrum for tetraenyl boronate **262** looked remarkably clean, with the main impurites being residual borate from the IDB and a build-up of phosphine ligand (**Figure 4**).

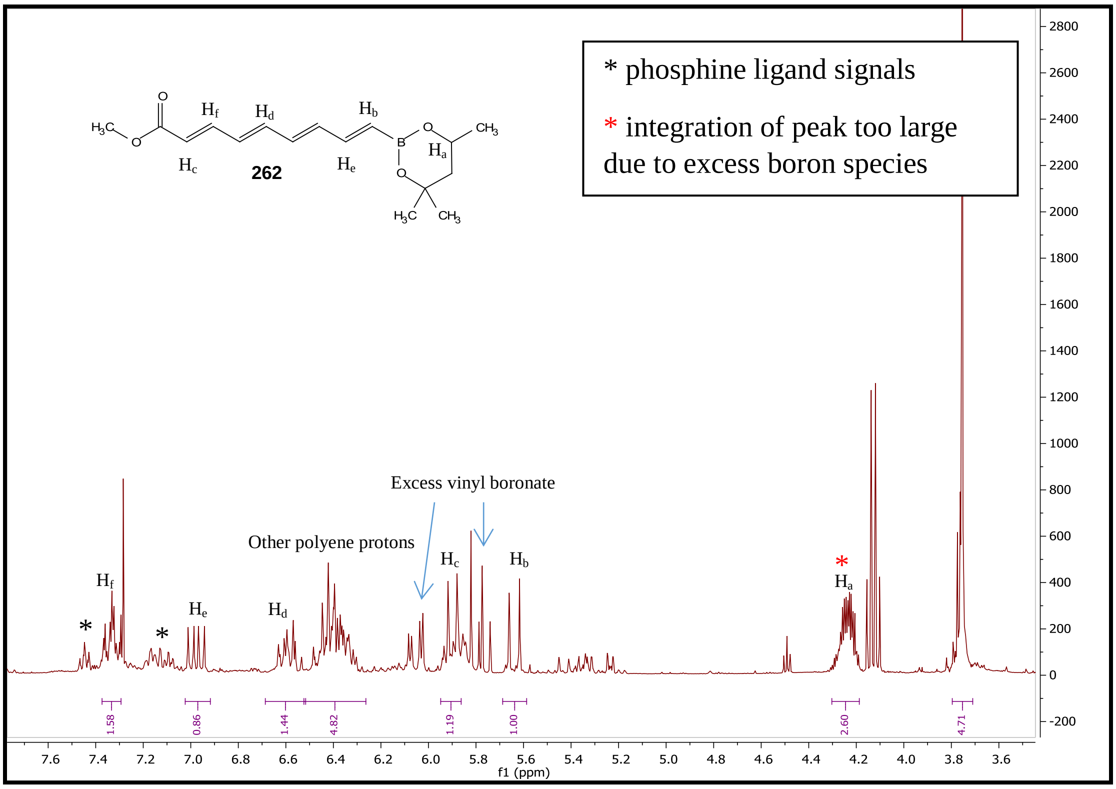

Figure 4 ^{1}H NMR spectrum for crude tetraenyl boronate **262**

Crude tetraenyl boronate **262** was consequently telescoped through further IDB/HM sequences to yield tetraenyl iodide **263**, pentaenyl boronate **231** (a small amount of this was isolated to confirm presence of product as at this stage in the route there was a considerable amount of borate present), pentaenyl iodide **264**, hexaenyl boronate **265** (presence confirmed by MS) and hexaenyl iodide **266** (**Scheme 48**). It was noted that there was a distinct colour change as the double bonds were added, even though the excess iodine species in the crude mixture added brown colour. The colour became more and more vivid with each addition changing from brown in the shorter chain polyenes to neon orange-dark neon yellow in the longer chain polyenes. This is consistent with the increased conjugation of the longer polyene chains.

It became much more difficult to calculate the correct amount of reagents for the IDB step as the polyene chain became longer, due to large amounts of borate present, as well as accumulating amounts of ligand. Excess vinyl boronate **42** left in the crude polyenyl boronates could be removed by using the right amount of ICl and NaOMe, such that the vinyl boronate **42** was converted to vinyl iodide **269**, which was then removed *in vacuo*. Iodides were not fully characterised, due to their inherent instability. Instead, successful synthesis of the subsequent polyenyl species was used to confirm presence of desired iodide.

It was found that, as predicted, the solubility of the polyenyl iodides in MeCN decreased with increasing chain length, presumably due to the increasing hydrophobicity of the growing chain. From pentaenyl iodide **264** onwards, it was necessary to perform HM couplings in a 3:1 mixture of MeCN:tetrahydrofuran (THF), dissolving the iodide in THF before adding it to the MeCN (**Scheme 48**). From the hexaenyl iodide onwards, the ^{1}H NMR was far too complex to identify peaks corresponding to product. The final HM/IDB ICC cycle was performed in an attempt to make heptaenyl iodide **268**. However, no real change in the ^{1}H NMR from the hexaenyl derivatives was observed and the large amount of borate present made it next to impossible to determine if the desired iodide **268** was present. The crude iodide was taken on into an attempted SM coupling with boronic acid **227**, but unfortunately the boronic acid decomposed to the alkyne **226** under SM conditions and xanthomonadin **208** was not formed (**Scheme 48**). It was suspected that the heptaene was in fact not made, due to a possible over calculation of the amount of ICl for IDB and therefore decomposition of the polyene.

Nevertheless, the principle of telescoping the products through multiple HM/IDB ICC cycles was proven. Synthesis of the polyene chain was recommenced, with more attention paid to when purification was necessary. It was found that drying the crude boronates on under high vacuum removed excess vinyl boronate **42** and other borate species, giving a much cleaner product. Trienyl boronate **261** was exceptionally clean (**Figure 5a**), as was tetraenyl boronate **262** (**Figure 5b**). However, tetraenyl boronate **262** started to show a build-up of phosphine ligand and small amounts of borate. Using this method, tetraenyl boronate **262** was produced from iodoacrylate **229** in an estimated 26% yield over the five steps. This was a considerable improvement, where previously the three steps involving columns from iodoacrylate **229** to trienyl boronate **261** were accomplished in only a 14% yield. There was still a considerable loss of yield observed, which was attributed to the iododeboronation steps.

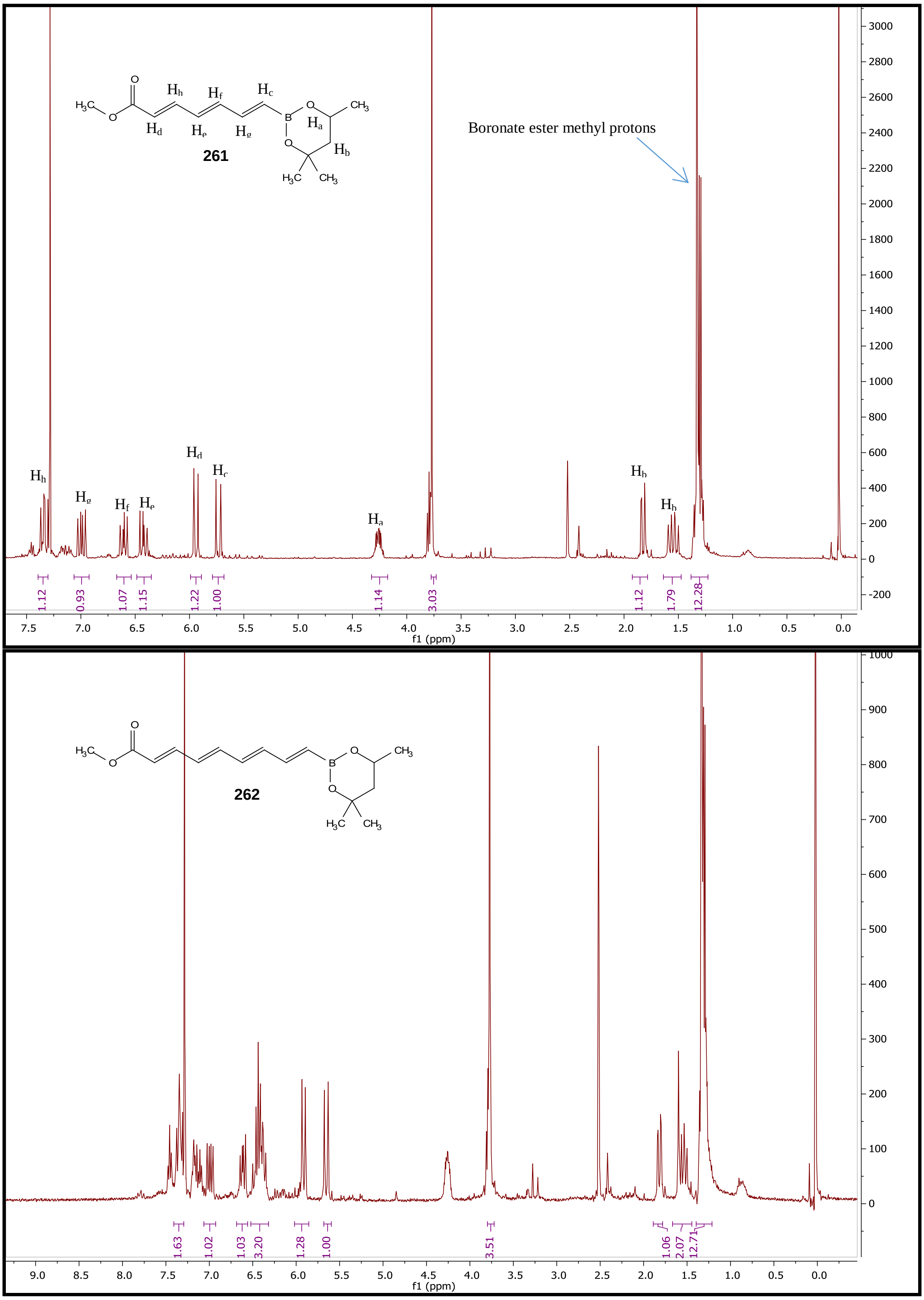

Figure 5 ^{1}H NMR spectrum for **a)** crude trienyl boronate **261** and **b)** crude tetraenyl boronate **262** (see **Figure 4** for assigments)

Upon repeating this sequence of reactions, the overall yield to tetraenyl boronate **262** improved to 47% over the 5 steps (**Scheme 49**).

Scheme 49 Improved yields for the HM/IDB ICC methodology, yielding tetraenyl boronate **262**

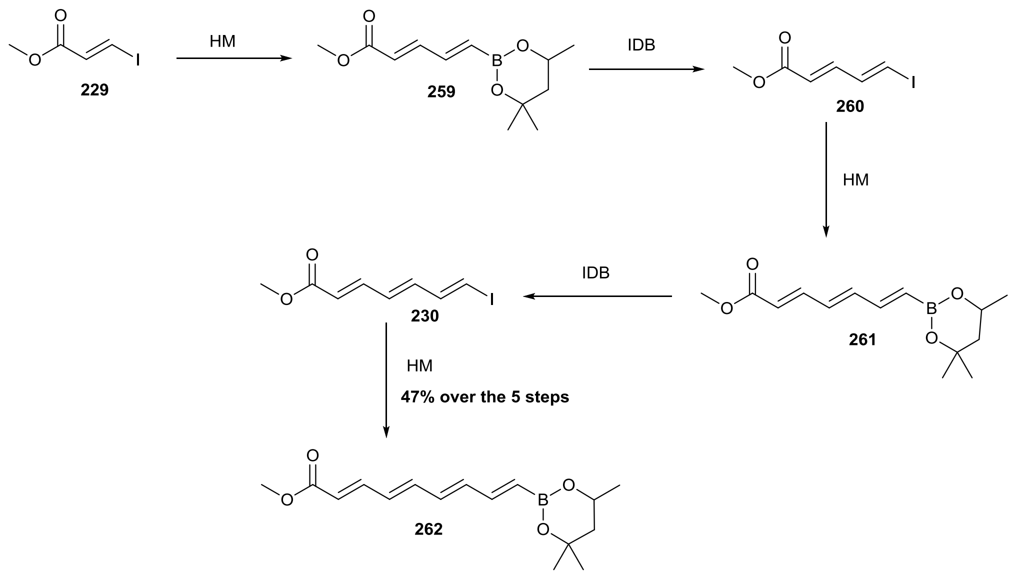

Throughout the different attempts to apply the HM/IDB ICC methodology, it was observed that the stability of the polyenes reduce considerably with increasing chain length. It also appeared that chains with an odd number of alkenes were much less stable than those with an even number of chains.

It was found that tetraenyl iodide **263** could be purified by silica gel chromatography. A considerable amount of yield was lost upon purification, with the overall yield from the starting acrylate being 20% (76% per step). However, this intermediate proved remarkably stable and could be stored successfully for up to 8 weeks at -18 °C, in the dark, under argon. As a result, it was chosen as a likely building block for the construction of the different polyene-containing target molecules.

Section 1.3.2 Propagation from the aryl end using the HM/IDB ICC methodology

As discussed in **Section 1.2**, it was envisaged that the xanthomonadins would be completed with a final Suzuki-Miyaura coupling between polyenyl intermediates. The lack of reactivity of the brominated styrenyl iodide **238** to HM coupling meant that a the ester polyenyl intermediate would have to be a heptaene, but the reactivity of the de-brominated styrenyl pinacol boronate **240** towards the HM/IDB ICC methodology was yet to be established.

De-brominated styrenyl pinacol boronate **240** was subjected to IDB and HM steps in an attempted to make the aryl dienyl boronate **270** (**Scheme 50**). This was successful, with the product characterised by ^{1}H NMR and accurate mass. The dienyl boronate was then taken through two more HM/IDB cycles to give the aryl tetraenyl boronate **272**, with the boronate characterised after each cycle by accurate mass to make sure it was there. In all cases, complete conversion was observed. The overall estimated yield was very low, only 5% over the 6 steps, but this was attributed to the small scale these reactions were performed on, where temperature control was very difficult in the IDB steps.

Scheme 50 Initial investigations into the reactivity of aryl boronate **240** towards HM/IDB ICC methodology

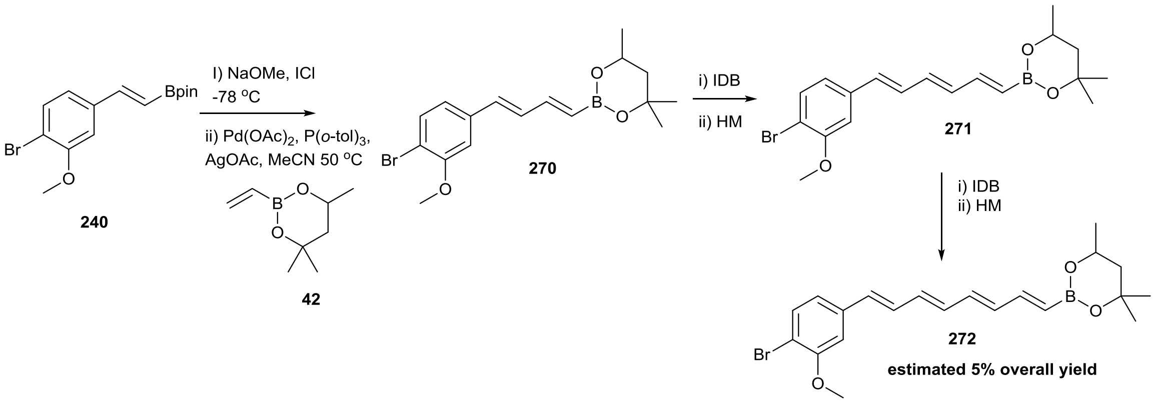

This sequence was attempted again, with boronates subjected to silica gel chromatography to observe their stability upon purification (**Scheme 51**). The polyenyl iodides were not subjected to any purification after work up. The boronates proved to be stable to silica gel chromatography and purifying them improved the iododeboronation step as it was easier to calculate the right amount of ICl to add. It had been previously assumed that all intermediates would become brown on iododeboronation, but in this sequence addition of precisely the right amount of ICl allowed this brown colour to be removed on work up, regardless of how many steps in the sequence had been performed. Streaking of the polyenyl boronates was still observed during silica gel chromatography, but even with columns, the overall yield was improved from 5% to 9%, increasing to an average of 67% per step. The yields did appear to drop off as the length of the polyene chain increased, with this trend particularly obvious in the HM steps (**Scheme 51**). It was noted that, whilst the polyenyl boronates appeared more stable and easier to handle than the ester polyenyl boronates in **Section 1.3.1**, the polyenyl iodides were considerably less stable that those in **Section 1.3.1**. Aryl trienyl iodide **275** proved to be unstable even at room temperature in the dark, where the colour changed from bright yellow to murky brown within two hours.

Scheme 51 Improved yields for the construction of aryl tetraenyl boronate **272**

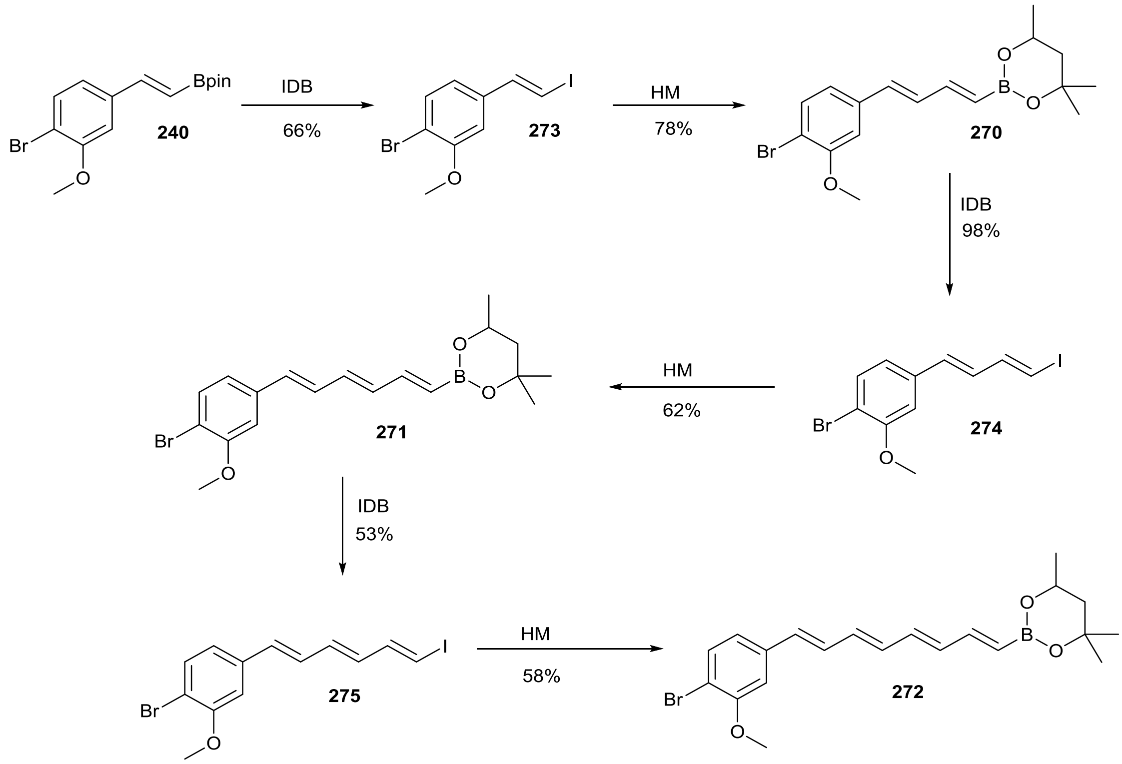

Section 1.3.3 Application of the HM/IDB ICC methodology to give a trienyl building block

With the recurring trend of decreasing stability with increasing polyene chain length, it seemed appropriate to adopt a more convergent approach to the construction of pigment molecules. Terminal trienyl iodide **279** was proposed as a possible building block for synthesis of both *Xanthomonas* pigments, with the yields obtained for the construction of the building block and its proposed use in the synthesis of xanthomonadin **208** shown in **Scheme 52**.

Scheme 52 Route to terminal trienyl building block **279**, and its proposed use in the synthesis of xanthomonadin **208**

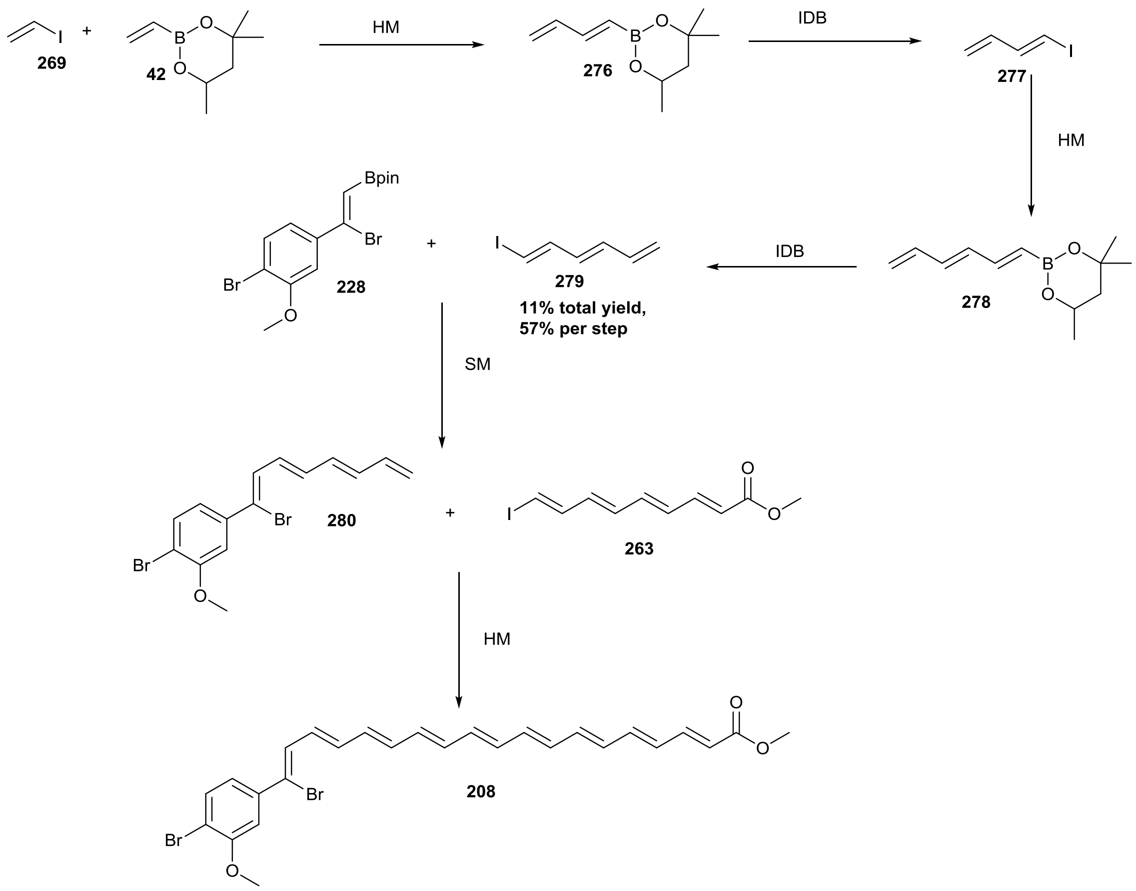

The sequence commenced with the formation of terminal dienyl boronate **276**, using vinyl iodide **269** as a HM donor. The optimisation of these conditions is discussed in **Section 2.1**.[173] During optimisation of this methodology, it was found that any unreacted vinyl boronate could not be separated from dienyl boronate **276** by silica gel chromatography and this, combined with concerns over stability of the terminal polyene, meant that chromatography was not attempted as a means of purification. The dienyl boronate was also shown to be highly susceptible to polymerisation (see **Section 2.1**), so distillation was not viewed as a viable purification method either. Unfortunately, the high volatility of all intermediates meant that crude products could not be purified using vacuum. It was found that dienyl boronate **276** could be successfully iododeboronated to give dienyl iodide **277**. Dienyl iodide **277** was successfully converted to trienyl boronate **278** *via* another HM coupling, obtained as a mixture with excess vinyl boronate **42**. Trienyl boronate **278** was then subjected to IDB conditions to give trienyl iodide **279** in an

11% yield over the 4 steps, giving an average of 57% per step (**Scheme 52**) which, given the volatility of the compounds, was considered an acceptable yield.

Section 1.3.4 Attempted construction of a bismetallated building block

Similar to the reasoning behind the construction of terminal trienyl iodide **279** in **Section 1.3.3**, and in light of the promising results obtained for attempted Stille couplings onto the brominated styrenyl iodide, a trienyl stannane building block was targeted to help with convergent construction of the pigment molecules.

Trienyl distannane building block **281** was originally envisaged to complete the synthesis, but concerns over potential selectivity issues led to bismetallated building block **282** being considered.

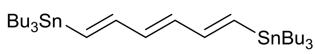

281

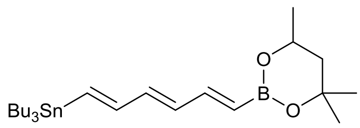

282

This building block had been synthesised in the Menche group, and successfully used in the synthesis of polyene natural product analogues.[174,175] Alcohol **285** had been made in the Goldring group starting from iodoacrylate **229**.[176] This provided an excellent opportunity to use this building block twice. The route towards bismetallated triene **282** is detailed in **Scheme 53**.

Scheme 53 Route towards the synthesis of bismetallated building block **282**[174–176]

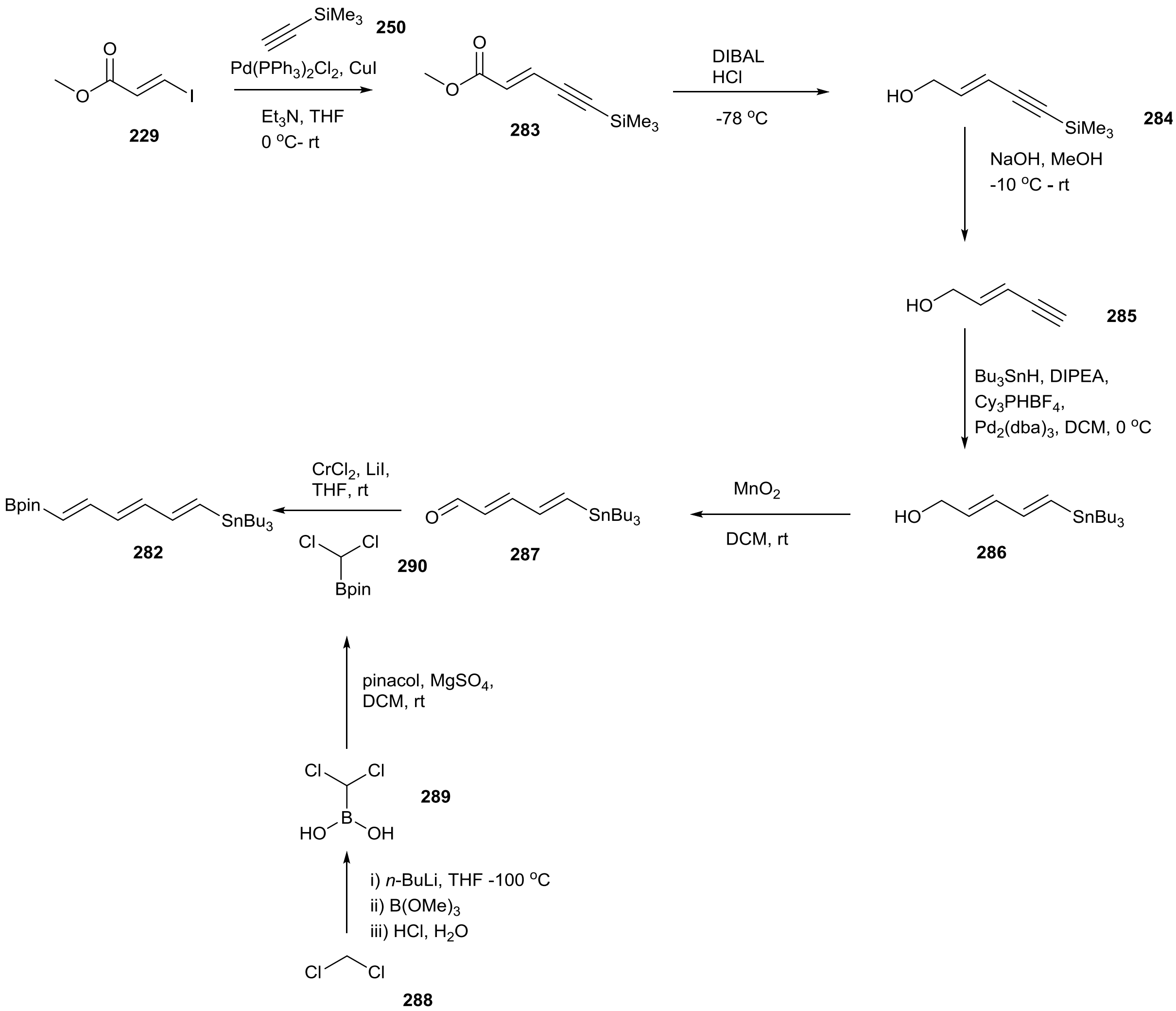

Initial yields for this route were disappointing, with the volatility of the intermediates presenting a real challenge on work up and purification. Despite 100% conversion for the Sonogashira coupling to give alkyne **283**, a poor initial yield of 38% was obtained after silica gel chromatography. Unprotected alcohol **285** was particularly volatile, and a 44% isolated yield was obtained for this step. With some optimisation, the yields of all steps were improved to become more in line with the literature yields, and improved in the case of the DIBAL reduction to alcohol **284** (**Scheme 54**).[174–176] However, the final Takai oxidation proved consistently problematic, with the crude mixture showing the desired triene, but showing a changed ^{1}H NMR spectrum on attempts to purify it. The product obtained from purification was subjected on a number of occasions to Stille conditions, but no coupling was observed, indicating that the desired stannane had not been formed.

Scheme 54 Progress made towards the synthesis of bismetallated building block **282**

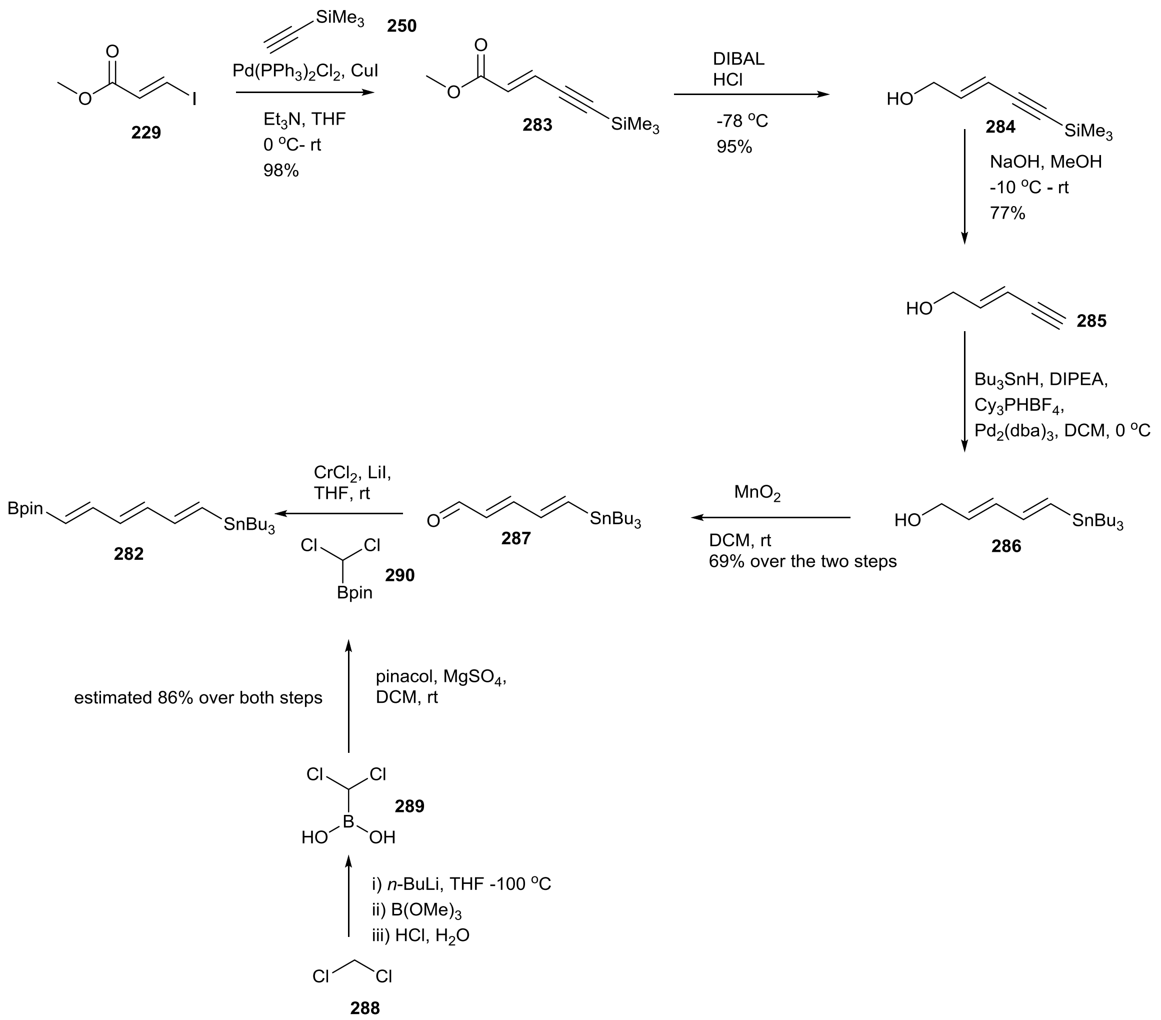

At this point Suzuki-Miyaura cross-coupling started to show more promise as a potential option for the final cross-coupling and so this building block was abandoned, since it was taking too long to optimise.

Section 1.3.5 Temperature studies and reoptimisation of the HM methodology

It was mentioned in **Section 1.2** that reoptimisation of the SM conditions to operate at a lower temperature was required, due to the tendency for the temperatures used to cause decomposition of the polyenyl iodides used. It seemed appropriate, therefore, to investigate the currently used temperatures in the HM/IDB methodology for their effect on the polyenyl iodides. Given the considerable drop off in yields past the tetraene, tetraenyl iodide **263** was chosen. Tetraenyl iodide **263** was dissolved in degassed d_3-MeCN. An initial ^{1}H NMR was run and then the NMR tube was held in the dark at the required temperature for 2 hours. Another NMR was then run and the spectra compared (**Table 7**).

Table 7 Table showing the effect of heat on tetraenyl iodide **263**, comparing the relative integral of a signal possibly corresponding to a decomposition product with a signal corresponding to tetraenyl iodide **263**

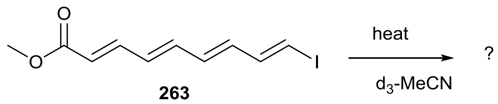

Entry	Temperature/ ^{o}C	Relative integral of signal at 9.65 ppm- initial	Colour change over 2 hours	Relative integral of signal at 9.65 ppm after 2 hours
1	rt	0.01	none	0.03
2	30	0.01	none	0.04
3	40	0.01	none	0.10
4	50	0.02	none	0.11
5	60	0.02	Yellow-pink-dark brown	0.16, plus d at 9.72 (0.08), plus t at 9.20 (0.43)

It was observed that, during the course of heating, a particular dd at 9.65 increased in intensity. This was present in very small amounts in the initial spectra. The proportion by which this increased became larger as the temperature increased, increasing by small amounts at room temperature and 30 °C, but becoming more significant above this. Upon heating to 60 ^{o}C a large change was noticed, with multiple new peaks appearing. This indicated that there was a possibility that some of the unexplained loss of product through the ICC sequence could be due to decomposition of iodide intermediates in HM reaction conditions, particularly for the longer chain iodides.

In response to this, a temperature screen was undertaken, to establish whether the HM coupling could be performed at lower temperatures (**Table 8**, **Equation 18**). The reaction was highly tolerant of lower temperatures, achieving 100% conversion at all temperatures, and requiring no increase in catalyst loading.

Table 8 Temperature screen for the HM coupling of iodoacrylate **229** and vinyl boronate **42**, showing HM vs competing SM ratios.

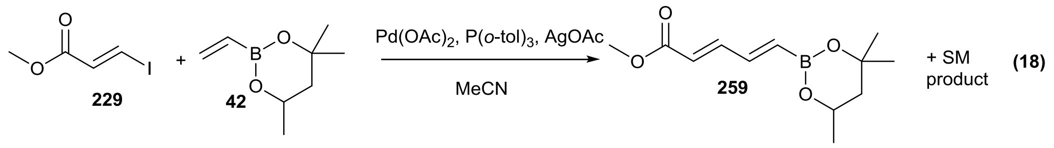

Entry	Catalyst loading/ mol%	Temperature / ^{o}C	Conversion after 24 h/ %	HM: SM ratio
1	5	50	100	90:10 to 97:3
2	5	40	100	87:13
3	10	40	100	80:20
4	5	30	100	87:13
5	10	30	100	85:15
6	5	rt	100	72:28
7	10	rt	100	68:32

It was observed that in the room temperature reactions a considerable amount of SM product was being formed, hence all ^{1}H NMRs were analysed to see how much was being formed. Some SM product was formed in the original conditions (**Table 8**, **Entry 1**). Decreasing the temperature to 40 and 30 °C had a minimal impact (**Table 8**, **Entries 2** and **4**), but operating the HM coupling at room temperature resulted in a deterioration of the HM:SM ratio. It was decided that 30 °C could be a viable operating temperature for the HM coupling, and so was trialled in the synthesis of two of the polyenyl intermediates.

The synthesis of tetraenyl iodide **263** was attempted first. As suggested by the temperature screen, the quantity of SM side product did seem higher throughout route, but was at a tolerable level and so the route was continued. None of the polyenes required an increase in catalyst loading, nor an increased reaction time to achieve completion, with intermediates proving to be easily coupled at this lower temperature. It was immediately noted that the reaction mixtures were much paler in colour throughout the synthesis, and crude mass recovery was good all the way through. Unfortunately, due to the increased amount of crude tetraenyl iodide **263**, purification became problematic. Chromatography took several hours, and required two attempts, resulting in the loss of a huge amount of material. Material that was obtained has decomposed considerably. However, the yield even with the problems in purification was comparable to the route performed at 50 ^{o}C, with an estimated yield at the tetraenyl boronate **13** stage of 49%, working out at average 87% per step (**Scheme 55**).

Scheme 55 ICC methodology to access tetraenyl iodide **263**, with HMs performed at 30 $^{\circ}$C

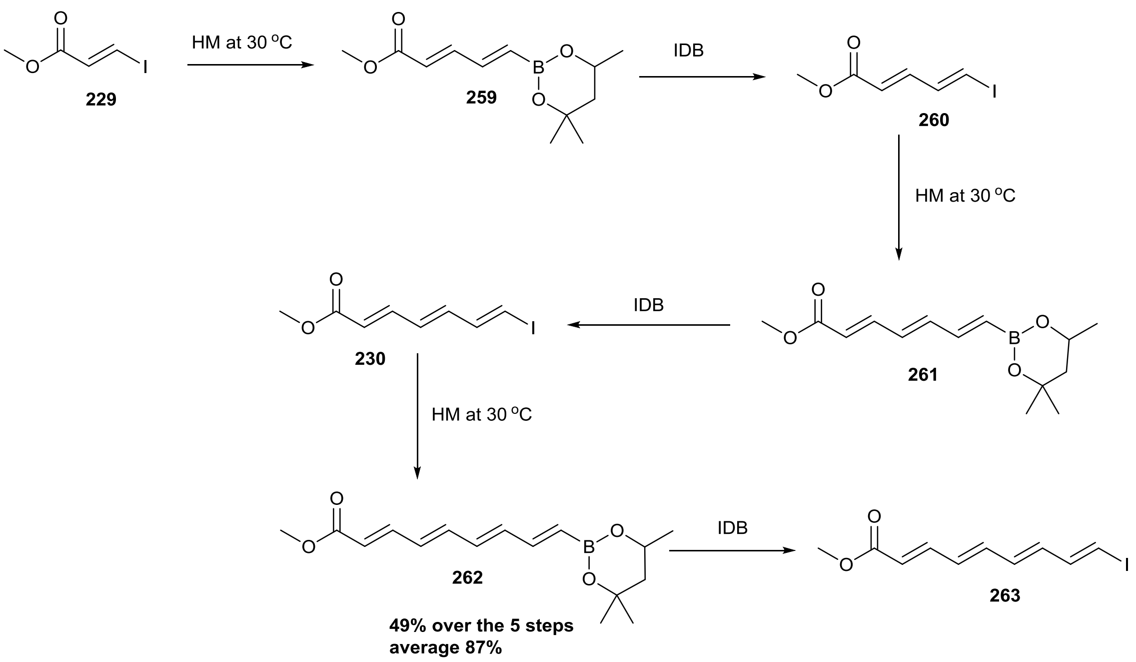

The lower temperature methodology was then applied to the synthesis of aryl tetraenyl boronate **272**, with intermediates again proving to be reactive at lower temperatures (**Scheme 56**). In this case, the benefit was much more obvious, with the overall yield doubling for this route. This is not surprising, given the instability of the iodides that had been observed previously.

Scheme 56 ICC methodology to access aryl tetraenyl boronate **272**, with HMs performed at 30 °C

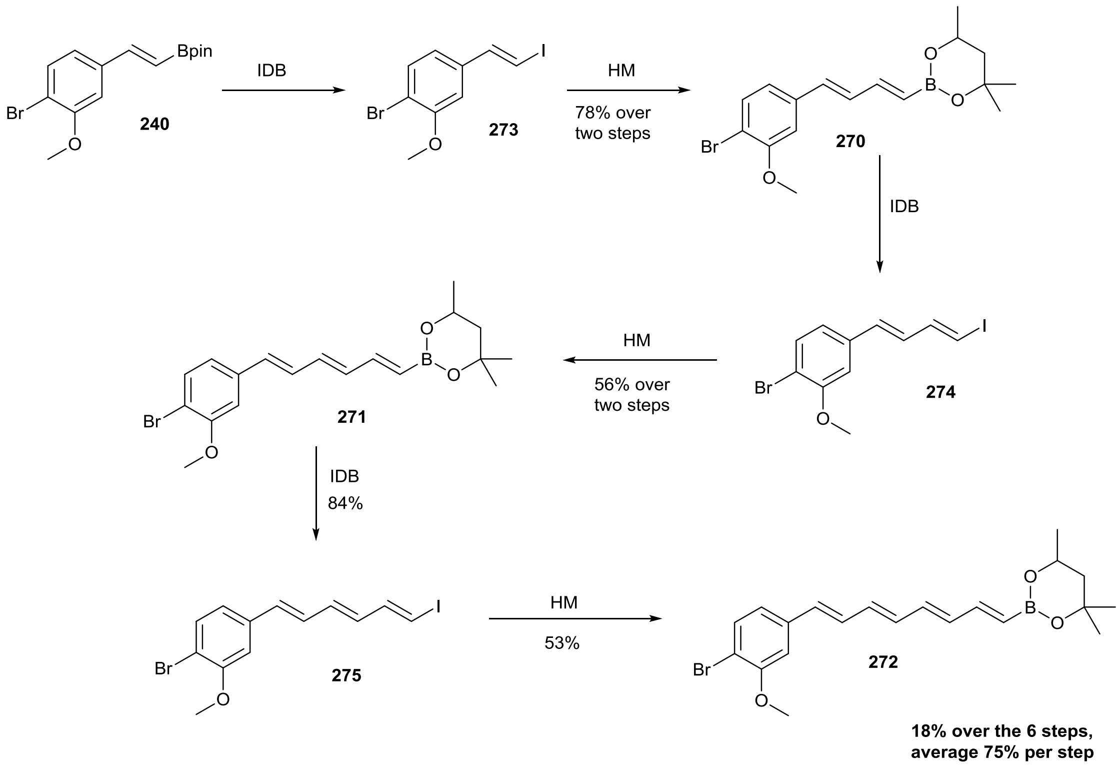

This methodology was further optimised to operate at room temperature, with these results discussed in **Section 2.1**.

Section 1.3.6 Summary

The group's stereoselective ICC methodology was applied to the synthesis of a number of polyene building blocks. The methodology required reoptimisation to reflect the increased instability observed with increasing chain length. Issues with stability above the tetraene length led to only two key tetraenyl building blocks **263** and **272** being selected for further use, along with a terminal trienyl iodide **279**.

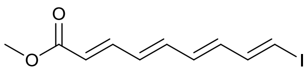

263

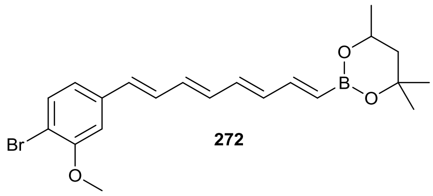

272

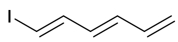

279

Section 1.4 Synthesis of *Xanthomonas* pigments - new retrosynthetic routes to access mono- and di-brominated xanthomonadin, along with truncated analogues

Section 1.4.1 Attempts to access xanthomonadin *via* a heptaenyl iodide

Initial attempts to make xanthomonadin **208** focussed on application of the HM/IDB methodology to the synthesis of key heptaenyl iodide (see **Section 1.3**). The final SM was attempted on **268** in an attempt to make xanthomonadin **208** (**Scheme 57**). Unfortunately, the reaction to make boronic acid **227** was problematic due to a lot of HBr present in the BBr_3 used and so most of crude **227** was in fact the undesired geminal product. Some boronic acid was present, therefore this was coupled with **268**. The mixture was subjected to silica gel chromatography and all spots isolated, but no trace of desired natural product **208** was found. The crude ^{1}H NMR showed loss of all peaks corresponding to a longer chain polyene, and also loss of the boronic acid peaks. Some alkyne was observed, indicating that decomposition of both the polyenyl and aryl intermediates had taken place. The loss of the boronic acid was unsurprising, due to the instability it had previously shown on storage.

Scheme 57 Attempted synthesis of xanthomonadin **208** by sequential telescoped HM/iododeboronation

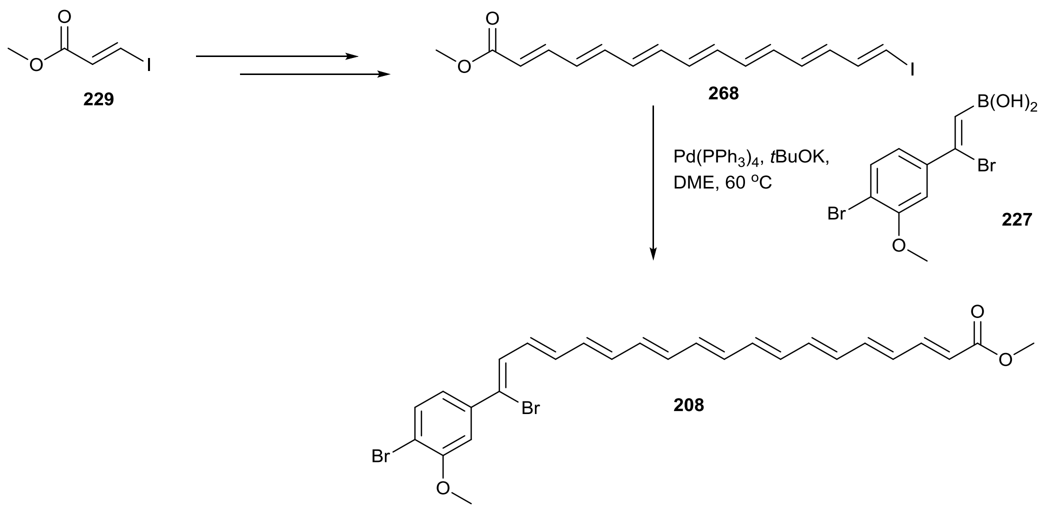

In response to this, another attempt was made at forming xanthomonadin **208** (**Scheme 58**), with a focus on acquiring a purer sample of the heptaenyl iodide to use, but also using the more stable pinacol boronate ester aryl building block **228**. As previously observed (**Section 1.3.1**), mass recovery during the HM/IDB sequence was good until formation of the pentaene. The pentaenyl boronate was in fact isolated during this sequence to see if cleaning up the crude polyene would help with the latter stages of chain extension. Unfortunately, drop offs in mass recovery became progressively worse with each subsequent step. An attempted coupling between the crude heptaenyl iodide **268** and brominated styrenyl Bpin **228** was performed, but xanthomonadin **208** could not be identified from the crude mixture by mass spectrometry. The crude ^{1}H NMR showed no clear peaks corresponding to either of the starting materials, suggesting that yet again they had not survived the reaction conditions.

Scheme 58 Attempted synthesis of xanthomonadin **208** using brominated boronate ester **228**

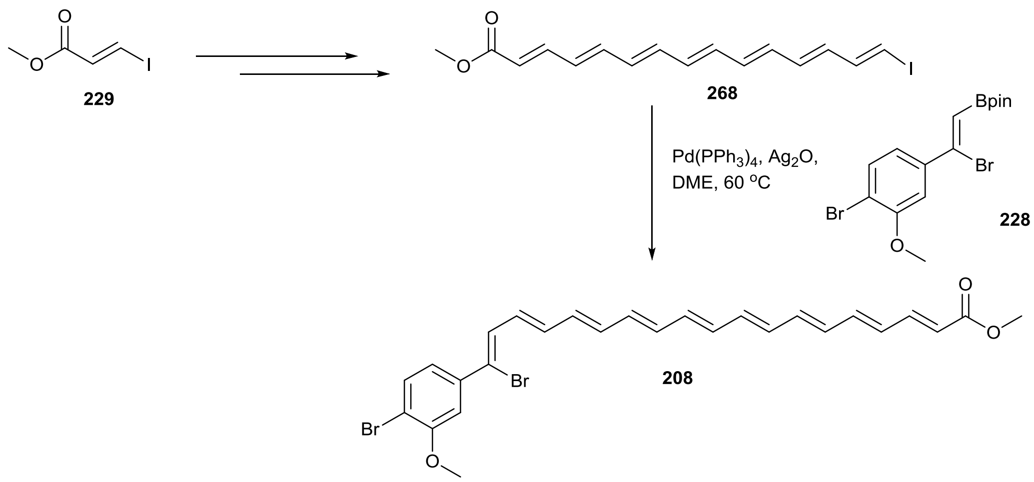

These attempts highlighted the issues with the final SM cross-coupling conditions and were a cause of the investigations undertaken in **Section 1.2**. They also led to the strong suspicion that the stability of the heptaenyl iodide was a real issue in the final cross-coupling reaction. It was apparent that a different approach needed to be adopted towards the synthesis of these pigment molecules, particularly avoiding the use of such unstable polyenyl iodides.

Section 1.4.2 Redesigning the retrosynthetic route

After the initial attempts to access xanthomonadin, it became obvious that the previously envisaged route, where different aryl building blocks were all reacted with one heptaenyl intermediate to give the desired octaenes, was unlikely to be successful. It seemed prudent to develop a 'toolbox' of polyenyl building blocks in order to impart some flexibility into the way the pigments were accessed, with the synthesis of these discussed in detail in **Section 1.3**. The key focus was on the construction of building blocks that could be connected *via* palladium cross-coupling. Terminal trienyl iodide **279** was proposed as a possible building block, with the potential to act as a donor in a range of palladium cross-coupling reactions at the iodide moiety and then as a HM acceptor at the terminal alkene (**Scheme 59**). A SM coupling was attempted between the iodide and aryl pinacol boronate ester, in the hope that it would be more stable than heptaenyl iodide **268** to the conditions (**Scheme 59**, **Equation 19**).

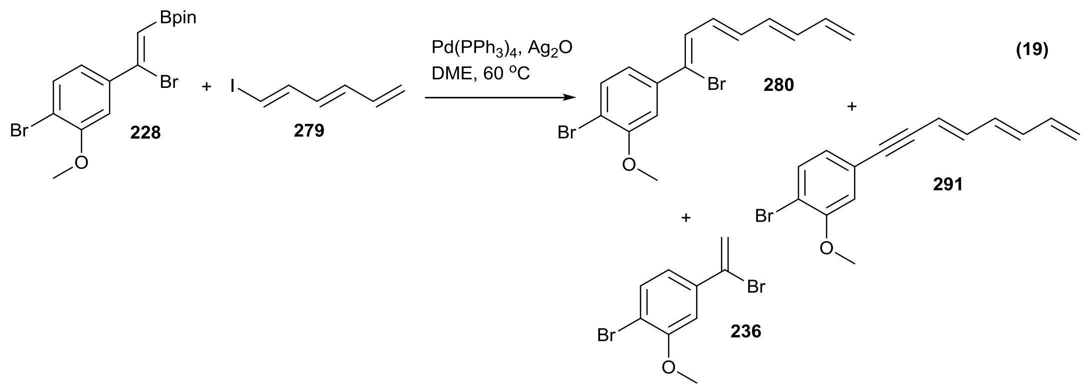

TLC analysis of the reaction mixture showed a number of highly conjugated species. The crude ^{1}H NMR looked promising, with two key peaks at δ 5.22 (1H, dd, J=7.8, 2.5 Hz) and 5.33 (1H, d, J=15.1 Hz). These fitted the pattern observed for previous compounds of the *cis* and *trans* terminal alkenyl protons, giving some confidence that a coupling had taken place. Other peaks seemed consistent with a conjugated terminal arylated tetraene, with signals observed at δ 3.96 (s corresponding to aryl methoxy group) and multiplets at δ 6.40, 6.73, 6.95, 7.10 and 7.52. Furthermore, the signals observed were consistent with those we had seen previously in other related compounds, where inter chain alkenyl signals typically come together in a large multiplet at δ 6.40 ppm, and the aryl signals typically come at ~ δ 7 ppm and between δ 7.4 and 7.5 ppm. The mixture of conjugated polyenyl species proved difficult to separate by silica chromatography, with considerable decomposition of the presumed product observed. Accurate mass analysis did identify the desired brominated aryl tetraene, giving confidence in the previously identified NMR data. Initially it was thought that the isolated solid contained a mixture of the desired brominated tetraene and a large amount of the protodeboronated aryl, but later analysis of the mass spectrum also showed alkynyl species **291**. This mixture was then subjected to HM conditions with tetraenyl iodide **263** in an attempt to make xanthomonadin **208**. The crude ^{1}H NMR showed polyenyl peaks that could correspond to the natural product, at an approximate 7% yield. The mass spectrum did not clearly show the molecular ion for xanthomonadin **208**, but it did show the fragment ions found by Andrewes *et al.* when they isolated xanthomonadin **208** were visible (501 and 473 for loss of methoxy and carbomethoxy fragments, **Figure 6**).[1] A potential mass ion for alkynyl pigment analogue **232** was observed with low abundance.

Scheme 59 Attempted synthesis of xanthomonadin **208** *via* terminal trienyl iodide **279**

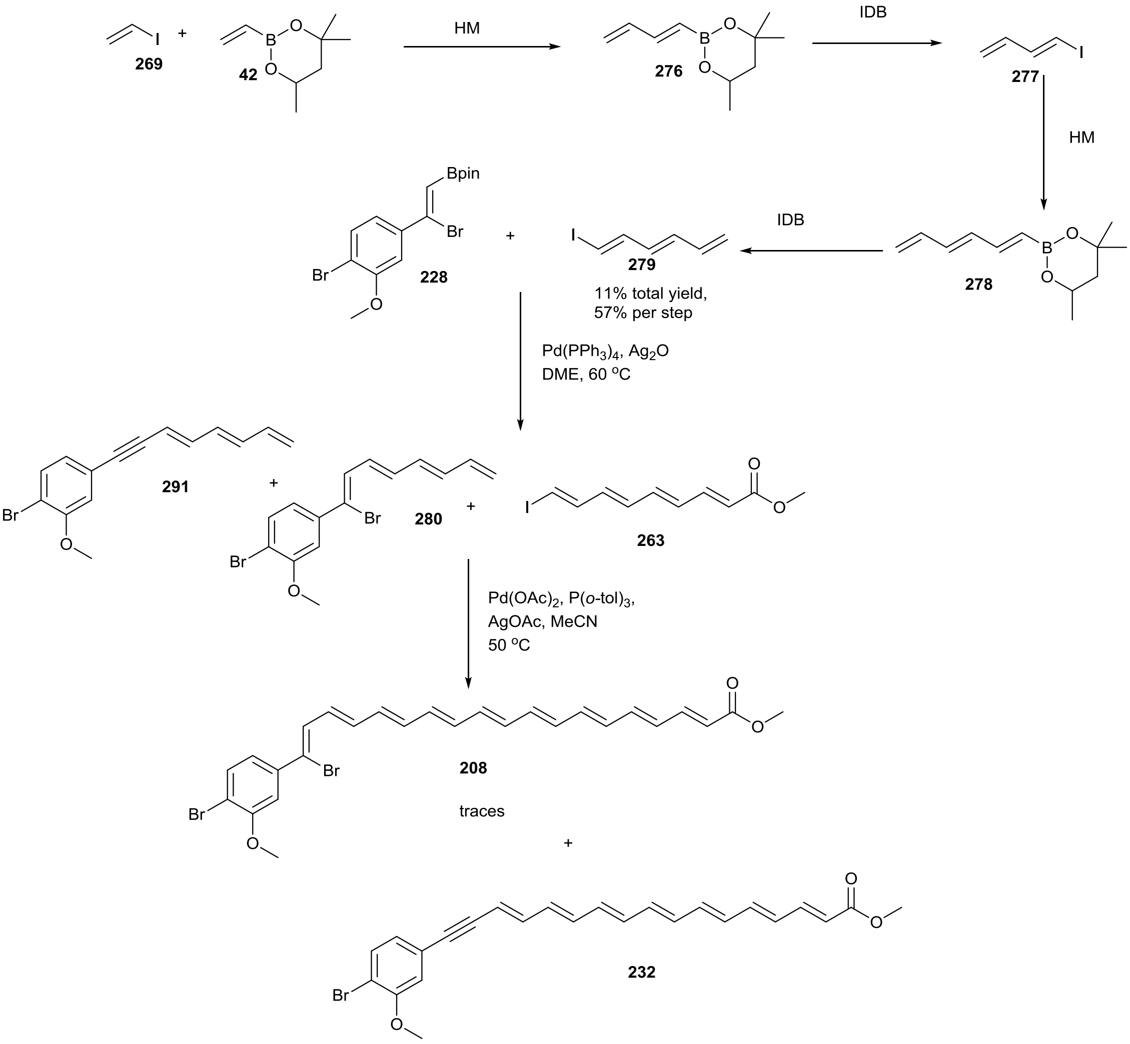

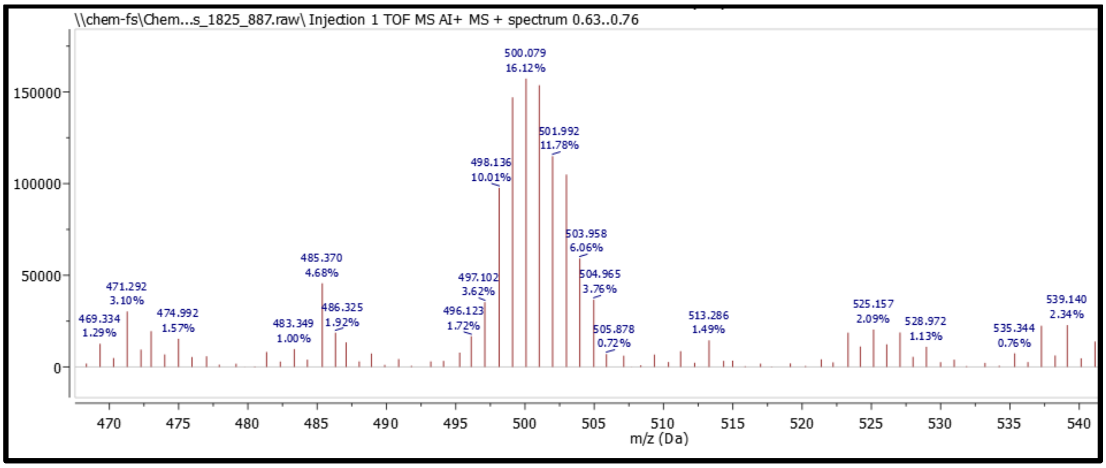

Figure 6 ASAP MS chromatogram showing fragment ions comparable to those found by Andrewes *et al.* for xanthomonadin **208** (501 and 473 for loss of methoxy and carbomethoxy fragments)

The crude reaction mixture was subjected to silica gel chromatography in the hope of isolating xanthomonadin **208**. Unfortunately, the compound giving rise to this mass could not be isolated cleanly, so whether or not the HM reaction was successful was inconclusive.

Terminal trienyl iodide **269** was also coupled with monobrominated styrenyl Bpin **240** to give terminal aryl tetraene **292**. This compound was susceptible to polymerisation and degraded before the final HM could be attempted (**Equation 20**). The desired tetraene was, however, characterised by accurate mass, and also displayed two key signals in the crude ^{1}H NMR spectrum that were indicative of a terminal alkenyl species; δ 5.13 (1H, d, J=8.4 Hz), 5.26 (1H, dd, J=16.7, 1.6 Hz).

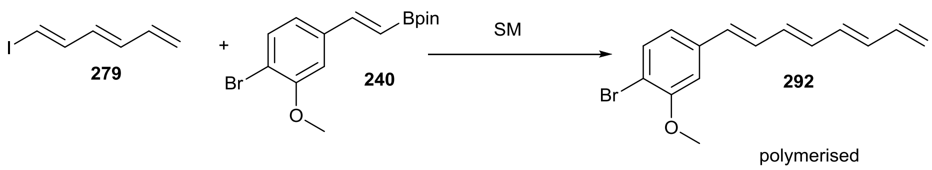

(20)

In light of the above reactions, where the heptaenyl iodide was proving challenging to access and the HM to close up the two tetraenes did not seem facile, focus turned away from xanthomonadin **208** to the synthesis of debrominated xanthomonadin **210** and the truncated analogues. Here the heptaene seemed not to be required, as the aryl boronate ester had proven amenable to the HM/IDB methodology and the tetraene **272** had been successfully made (see **Section 1.3**).

Section 1.4.3 Sonogashira couplings to give alkynyl analogues

Having already successfully performed a Sonogashira coupling onto the alkyne building block **226** (see **Section 1.2**), another Sonogashira coupling was attempted using tetraenyl iodide **263** (**Equations 21** and **22**). This reaction proved extremely facile. Silica gel chromatography again proved difficult, with a number of fractions discarded for the sake of purity. Nevertheless, desired truncated analogue **235** was synthesised in a 56% yield as a bright yellow solid.

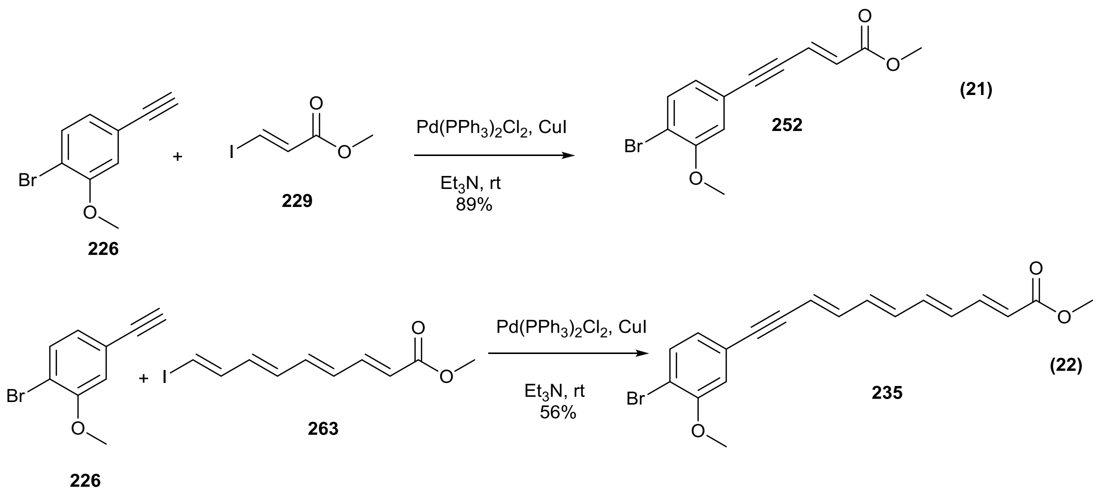

With the success of this reaction, it was considered that xanthomonadin might be accessible *via* the alkyne analogue **232**. An attempt was also made to add HBr across alkyne **235**, with a view to giving truncated xanthomonadin analogue **233**. This was done using HBr in AcOH (33% by weight). Accurate mass did show presence of desired product, but the ^{1}H NMR was extremely complex. Given the difficultly that had already been experienced in separating the crude mixtures of polyenyl compounds, this was not considered to be a viable route.

Crystals of alkynyl dienyl analogue **252** were successfully obtained and analysed by X-ray crystallography. The structure showed a degree of planarity between the alkyne and the aryl, seeming also to extend through to the alkene, but with the ester group lying out of the plane (**Figure 7a**). The molecules packed by alternating orientations, with the alternating aryl and ester groups interacting with each other, hydrogen bonds forming between the ester and the aryl bromine atom. A further interaction was presumed between the aryl methoxy group and the ester carbonyl oxygen (**Figure 7b-d**). The molecules alternately stack together, held together by π-π stacking interactions and weak hydrogen bonds.

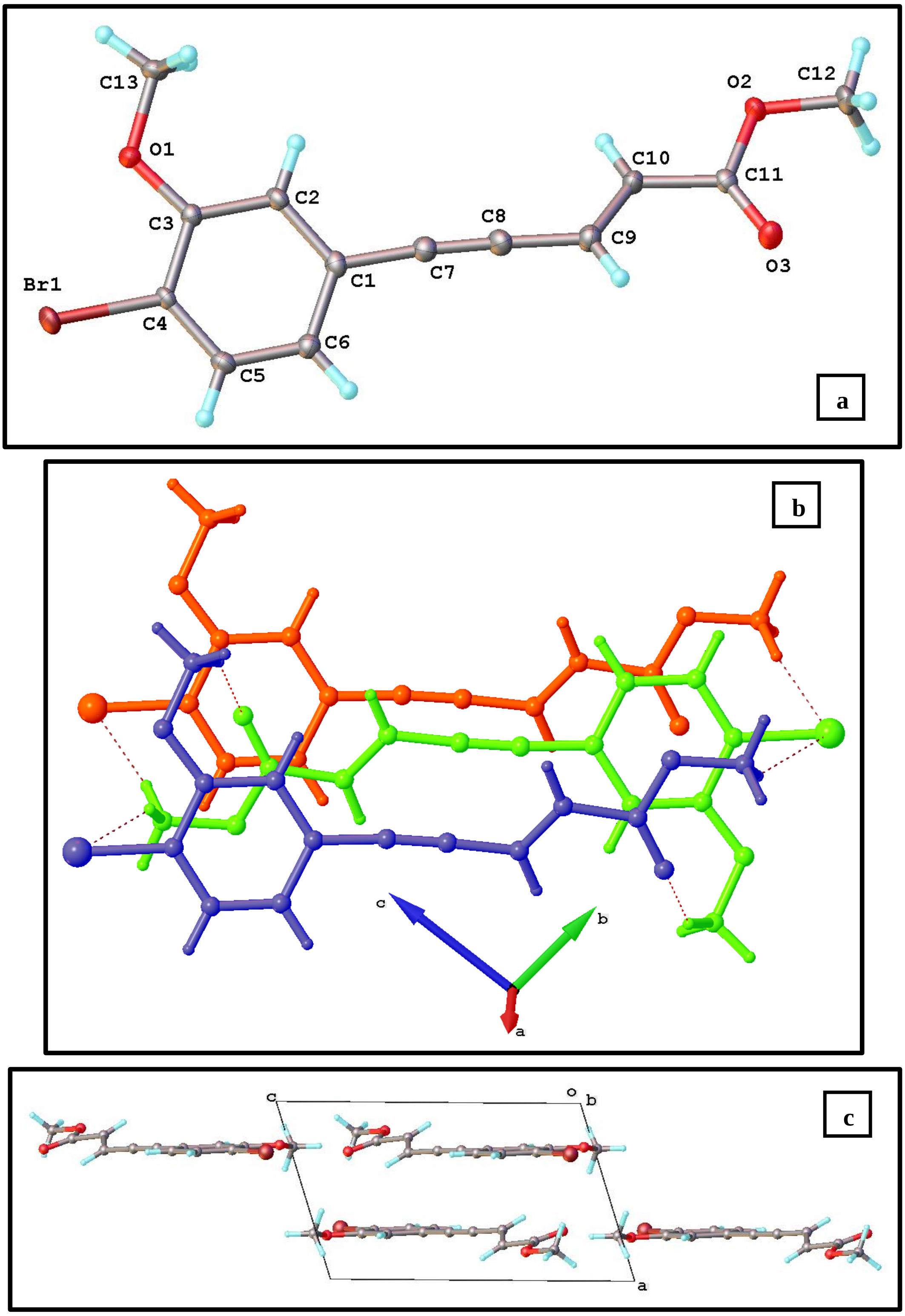

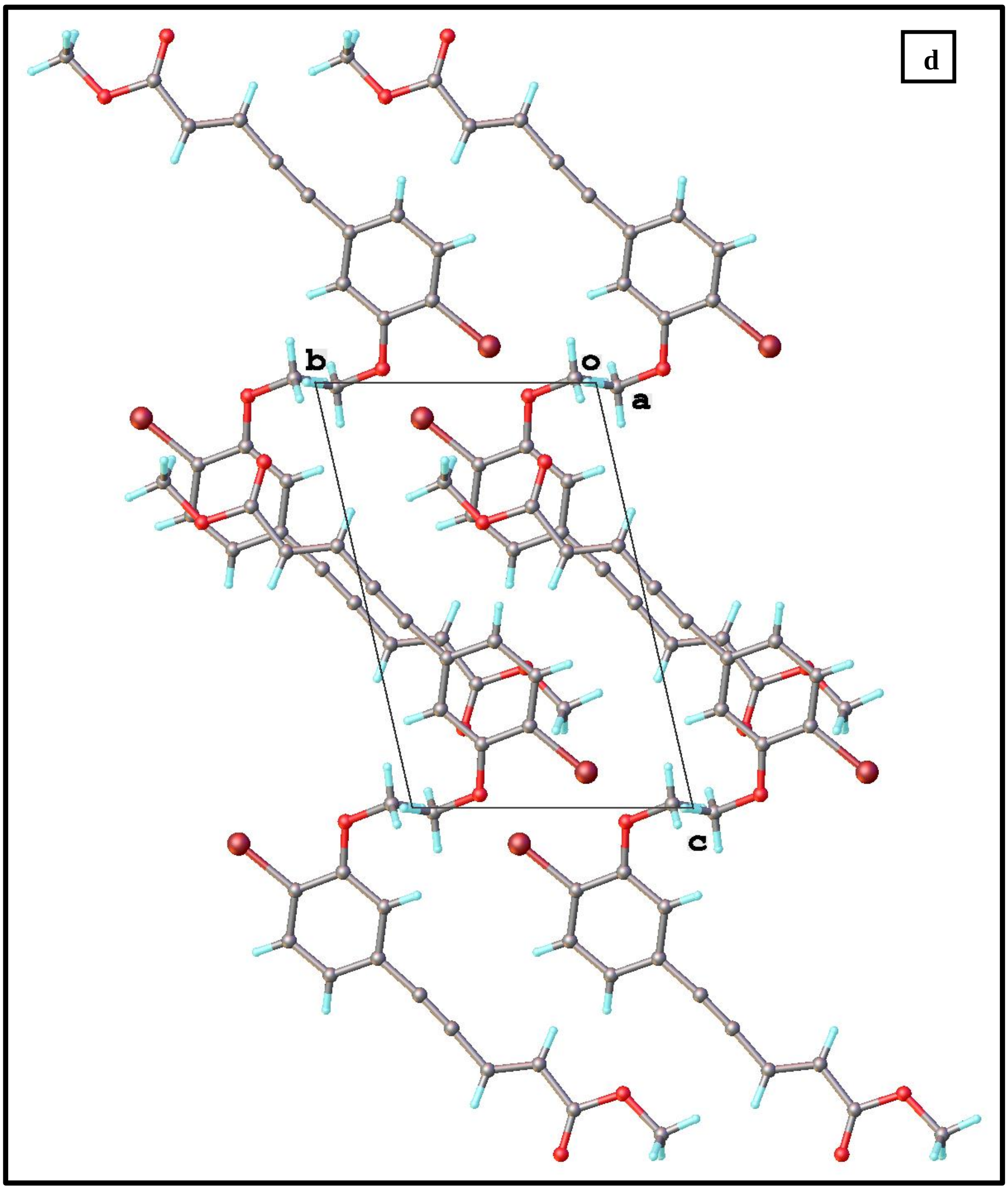

Figure 7 Pictures obtained from X-ray crystallography on analogue **252**

Section 1.4.4 Returning to SM couplings

An initial attempt was made to form monobrominated pentaenyl analogue **234**, using the best conditions to come out of the first screens undertaken to optimise the key SM couplings (**Equation 23**). Unfortunately, no peaks that could be ascribed to product were observed by ^{1}H NMR during the course of the reaction. On closer analysis, it was observed that the polyene was decomposing in the reaction mixture.

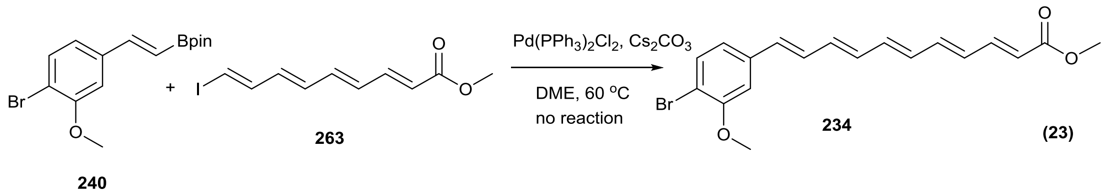

Simultaneously to the optimisation of the required SM conditions, the coupling reaction to produce analogue **234** was attempted again, this time using silver(I) oxide as the base in an attempt to minimise degradation of the polyene (**Equation 24**). A number of polyenyl products were formed, most of which could not be separated in order to identify them, but desired compound **234** was isolated. During the purification process, compound **234** could be seen as one clear, fluorescent spot on TLC, but as will be discussed in **Section 1.5**, the NMR spectra were rather complicated.

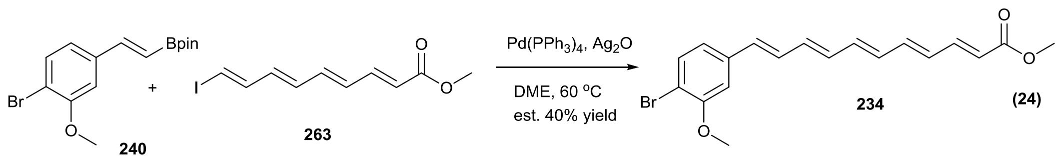

Synthesis of pentaenyl xanthomonadin analogue **233** was also attempted using the Pd(PPh$_3$)$_4$/silver(I) oxide conditions (**Equation 25**). NMR and accurate mass analysis was performed on the purified product, where a lot of mass loss was due to poor separation. Mass spectrometry clearly identified the desired compound, which looked exceptionally clean with only two major mass ions, one being the desired product and an m/z corresponding to [M-HBr]. Originally this ion was thought to have originated during the mass experiment, but it was later realised that this was in fact due to the alkynyl product, formed during the attempted SM itself in an approximate 2:1 ratio of alkyne to desired pentaene. Again, the mixture obtained ran as one fluorescent spot on TLC.

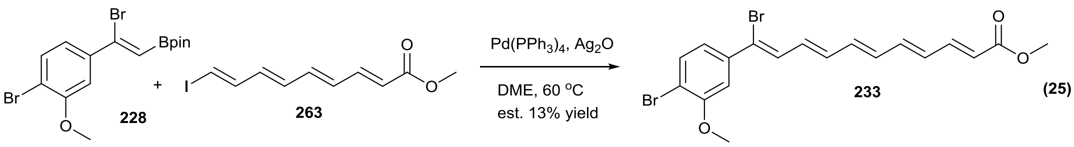

A series of NMR experiments were used to evaluate the nature of these mixtures, showing that there was likely a mix of some isomers and some other polyenyl products (see **Section 1.5** for this discussion). The potential to make these analogues was demonstrated, however, and the need for a new purification system was highlighted.

As detailed in **Section 1.3**, styrenyl boronate **240** was successfully converted to aryl tetraenyl boronate **272** through repeated HM/IDB ICC cycles, telescoping each intermediate through and performing the final cross coupling on the crude tetraene (**Scheme 60**).

Scheme 60 Initial synthesis of aryl tetraenyl boronate **272**

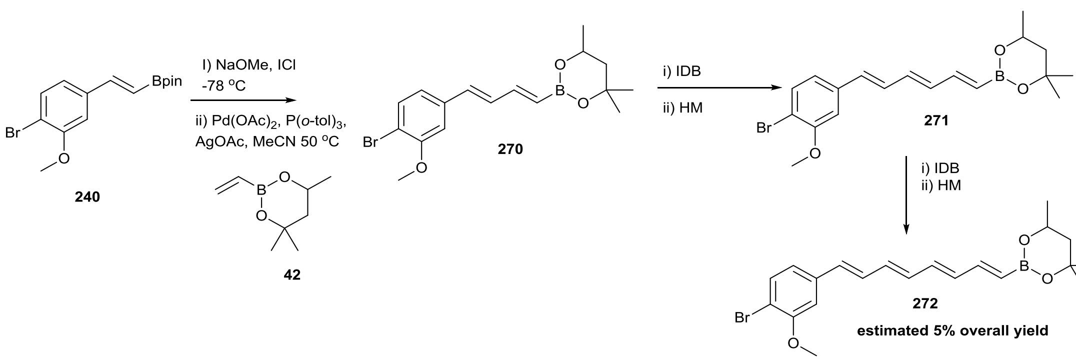

Aryl tetraenyl boronate **272** and tetraenyl iodide **263** were subjected to the SM conditions used to make pentaenyl analogue **234** in an attempt to make monobrominated xanthomonadin **210** (**Equation 26**). The ^{1}H NMR spectrum after stirring overnight showed consumption of boronate and iodide, giving rise to new polyenyl peaks, particularly a large complex multiplet at around δ 6.31. Mass analysis of the crude mixture showed a weak signal in the ASAP corresponding to [M-2H] at 450.084, for which the exact mass is 450.083, along with the ^{81}Br isotope at 452.082 (**Figure 8**).

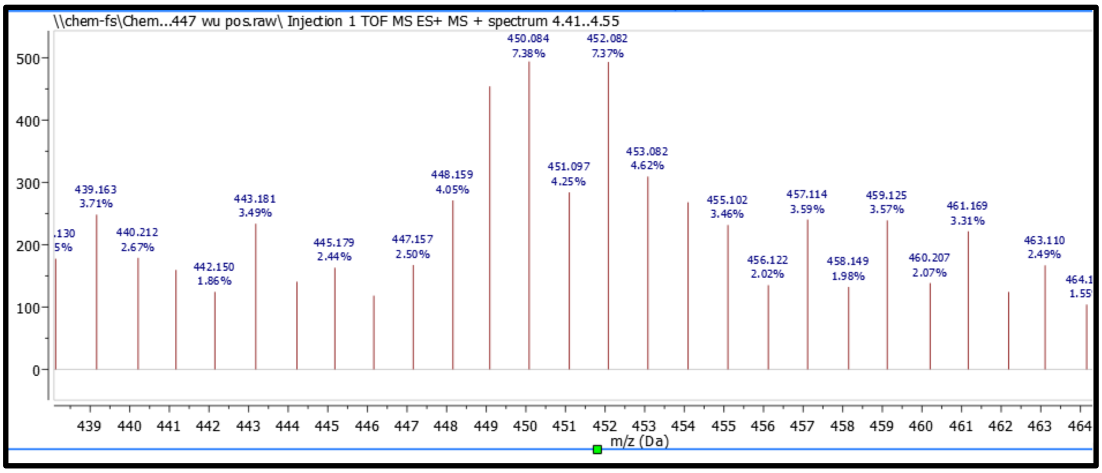

Figure 8 ASAP mass spectrum of the crude residue from the attempted formation of debrominated xanthomonadin **210**

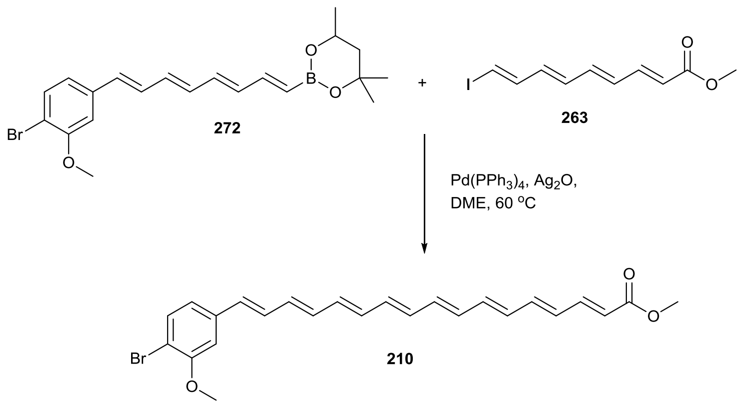

(26)

The crude mixture was subjected to silica gel chromatography in an attempt to isolate the compound **210**. One of the isolated spots was very impure, but contained a series of peaks which integrated to give the correct number of protons, including a complex multiplet at δ 6.24-6.47 containing the vast majority of the polyene protons, as well as the signals for the two methoxy groups and the characteristic low and high shifted multiplets for the more distal polyene protons (**Figure 10**). This fraction also showed a mass ion in the ASAP for [M-H] at 451.093 (exact mass 451.092) and at 453.094 for the ^{81}Br isotope (**Figure 9**).

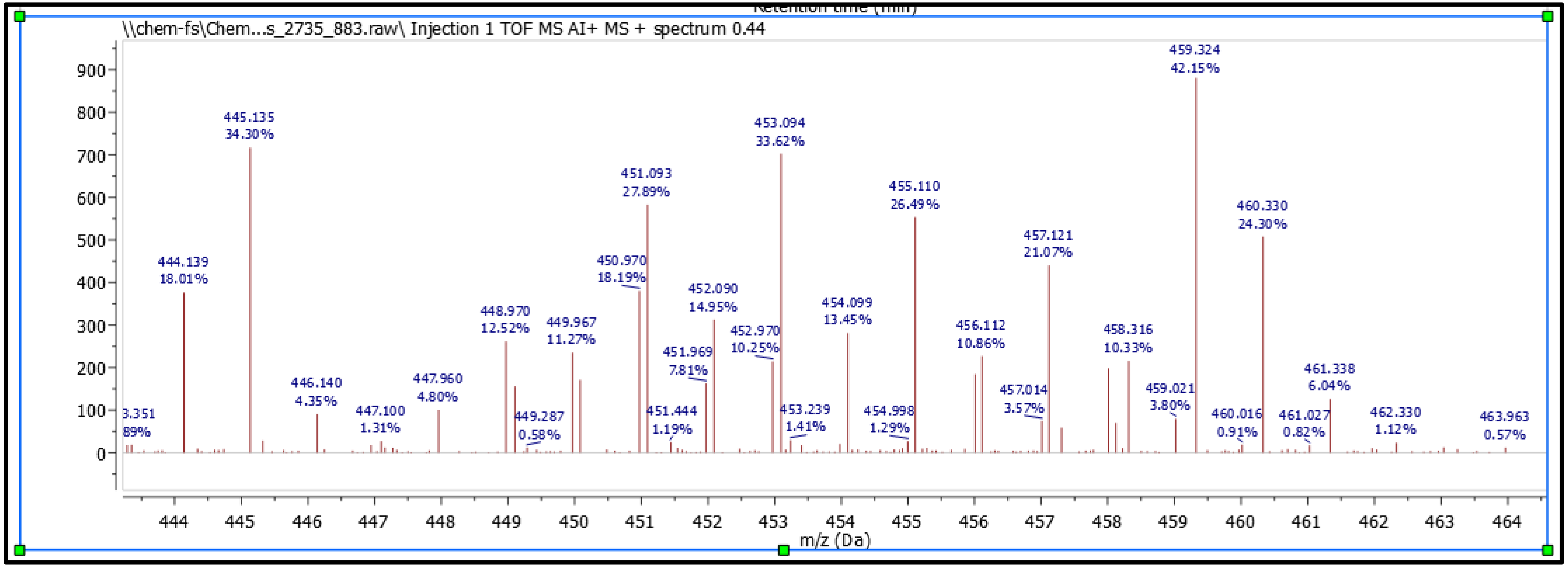

Figure 9 ASAP mass spectrum of isolated fraction presumed to contain monobrominated xanthomonadin **210**

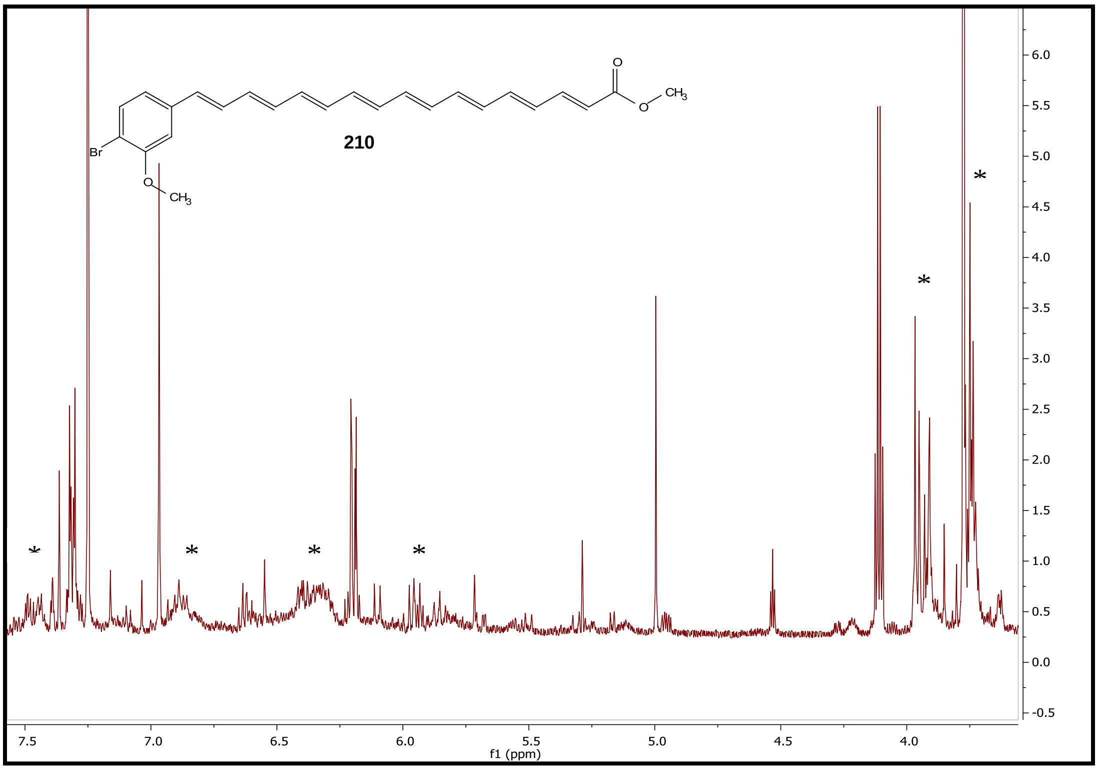

Figure 10 [1]H NMR spectrum showing the presence of monobrominated xanthomonadin **210**

A yield for the reaction could not be accurately estimated from the ^{1}H NMR spectrum due to lack of purity, but this, combined with the mass spectrum, provided the first real evidence for the presence of monobrominated xanthomonadin. There were clearly, however, still problems with the SM conditions which needed to be remedied if more than trace amounts of the natural product were to be detected. It was assumed that the high temperatures were causing at least some degradation of the tetraenyl iodide, but whether either the tetraenyl boronate or indeed the product itself was decomposing was still unknown.

In order to shed some light on the reason for such low reactivity, the synthesis of aryl tetraenyl boronate **272** was attempted again, this time performing silica gel chromatography on each of the boronate intermediates, but still leaving the iodides crude (**Scheme 61**). The boronate intermediates proved stable to silica gel chromatography, and their purification resulted in improved iododeboronation. Despite this, the boronates were still prone to streaking, and yield was still lost. Even with columns, the overall yield was improved from 5% to 9%, increasing to an average of 67% per step.

Scheme 61 Improved yields to aryl tetraenyl boronate **272**

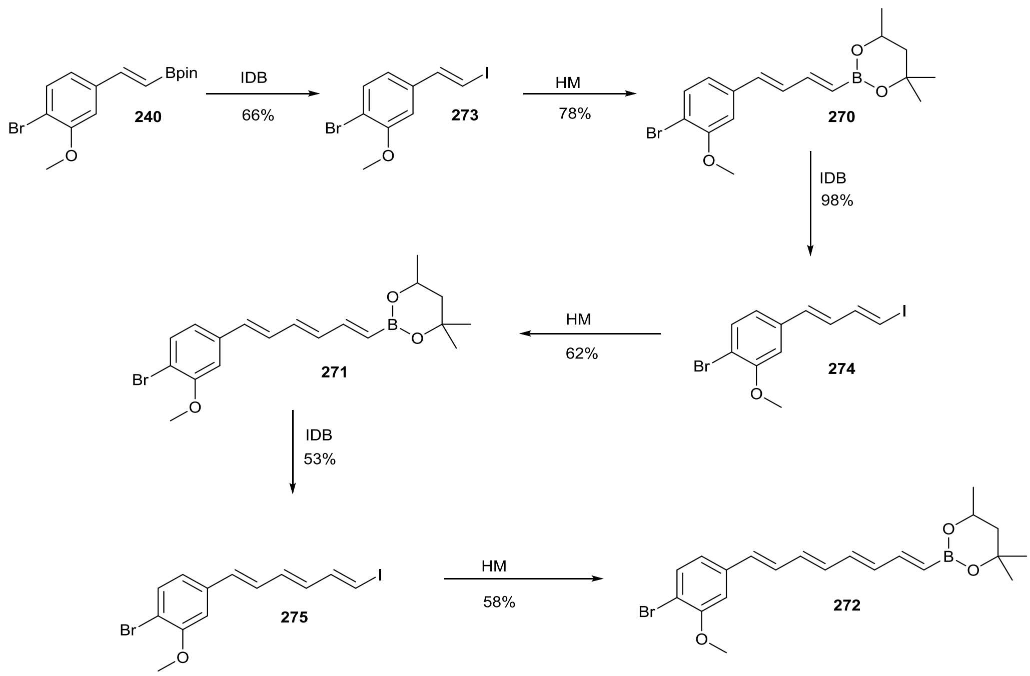

It was noted that the yields appeared to drop off as the length of the polyene chain increased. Aryl trienyl iodide **274** appeared unstable even at room temperature in the dark, where the colour changed from bright yellow to murky brown within two hours. The final SM was attempted again on a larger scale than done previously (**Equation 27**).

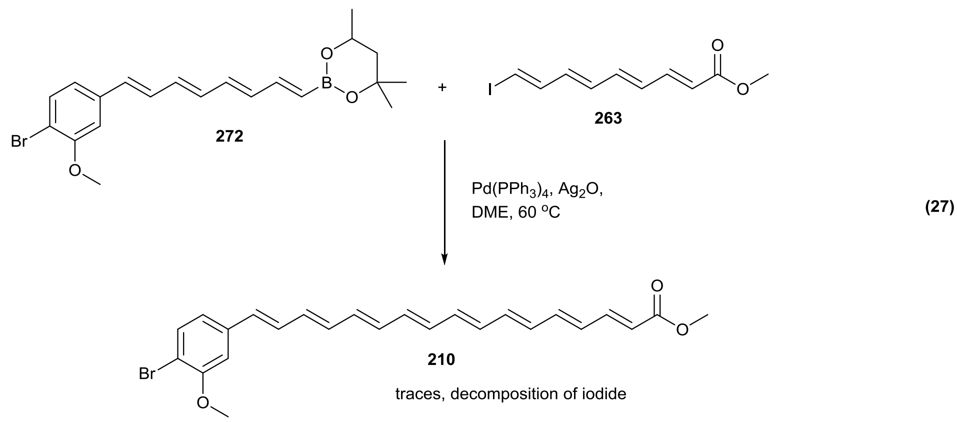

This was the first time that 'clean' building blocks had been used in this final SM coupling. Following on from the suspicion that the temperature in this reaction was too high for natural product **210**, the reaction was closely monitored for consumption of starting material. It was noted that the reaction mixture turned dark brown almost instantly on heating. After 2 hours it appeared that tetraenyl iodide **263** had all been consumed. The crude ASAP spectrum showed a peak at the correct mass, but the sample was too weak in intensity to obtain accurate mass.

^{1}H NMR analysis of the crude reaction mixture did not show quantifiable amounts of MB xanthomonadin **210**. It did, however, show complete consumption of tetraenyl iodide **263**, with a large amount of unreacted aryl tetraenyl boronate **272**. It seemed at this point that the heat was causing decomposition of the iodide and, as a result, reoptimisation of the final SM coupling (and HM couplings) was undertaken as detailed in **Sections 1.2** and **1.3**. Alongside this, a small amount of aryl tetraenyl boronate **272** was recovered from the crude reaction mixture and this was put into a test reaction at a lower temperature of 40 ^{o}C overnight (**Equation 28**). ^{1}H NMR analysis showed peaks in the same places as observed previously, when low resolution mass spectrometry indicated potential formation of the natural product. The TLC of the crude reaction mixture was complicated; several spots were observed, with more than one spot both showing activity under long wave UV and also having a yellow colour.

The original isolation of xanthomonadin **208** involved its precipitation from chloroform with petroleum ether, and it was decided to attempt this method of purification from the crude reaction mixture.[151] In addition, purification of pigment mixtures was undertaken using benzene as the eluent for silica gel chromatography. TLC performed on the crude mixture showed a greatly improved separation, better than had been seen before with any other solvent system. Precipitation from $CDCl_3$ with 40-60 °C petroleum ether at 0 °C gave a red solid which only gave two spots under UV, one very bright under long wave UV and colourless, and another less strong, but bright yellow. ^{1}H NMR analysis of this solid showed that the vast majority of this solid was $Pd(PPh_3)_4$, but a small proportion was a highly conjugated polyenyl product, with was confirmed by accurate mass to be monobrominated xanthomonadin. The yield was estimated to be extremely low, at around 2%.

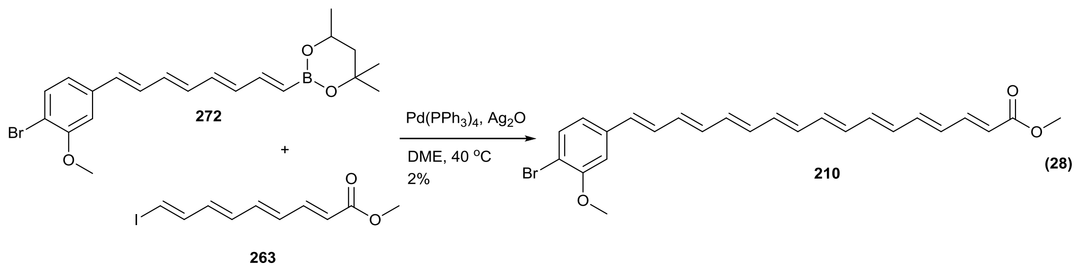

The synthesis of aryl tetraenyl boronate **272** was scaled up and a much larger scale cross coupling was attempted to access monobrominated xanthomonadin **210**. Unfortunately no obvious reactivity was seen, with both iodide **263** and boronate **272** remaining untouched in the reaction mixture. Heating to 50 ^{o}C resulted in the expected decomposition of some of the tetraenyl iodide **263**, but again no obvious increase in reactivity. Addition of more catalyst did not result in any increased reactivity either.

What tetraenyl boronate **272** could be salvaged was recovered by chromatography and two small scale reactions put on in an attempt to increase the proportion of natural product formed, one using the same conditions as before and one using the same conditions, but with a 3:1 ratio of DME to water. An increased peak at δ 5.1 ppm was seen in the ^{1}H NMR spectrum for the reaction containing water, but nothing could be easily concluded from the reactions.

Pentaenyl analogue **234** was synthesised in a 42% yield, at a lower temperature of 40 ^{o}C (**Equation 29**). Reactivity was better than this, going to completion, but yield was sacrificed in trying to obtain purer product.

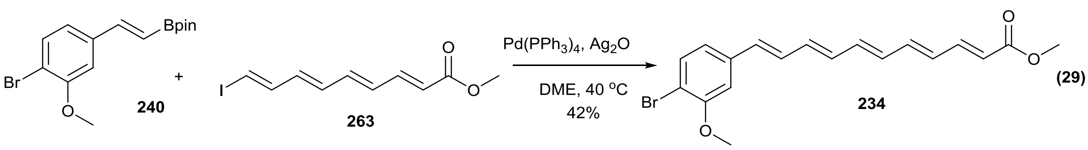

A SM reaction was also attempted using the room temperature conditions identified in **Section 1.2**, using palladium(II) acetate, triphenyl phosphine and silver(I) carbonate in acetonitrile (**Equation 30**). This reaction also went to completion, with pure product being obtained after silica gel chromatography with benzene (81% estimated yield from ^{1}H NMR).

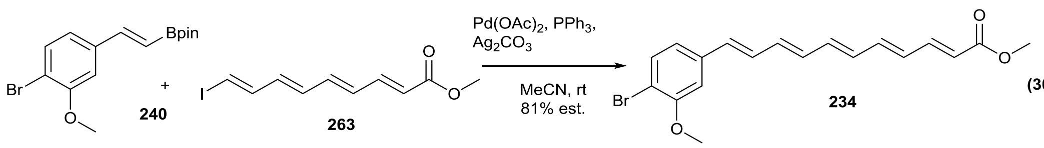

(30)

In light of this, the synthesis of monobrominated xanthomonadin **210** was attempted again, using the same room temperature conditions. Peaks corresponding to product **210** could be observed in the ^{1}H NMR spectrum. Neutral alumina was selected for column chromatography following TLC trials on the crude mixture. A mixture of polyenyl products was obtained, amongst which a bright orange spot was observed under long wave UV. This appeared most easily separated by silica gel chromatography on TLC, so purification was attempted again. Unfortunately, the desired product could not be isolated from the column, suggesting that it had decomposed during purification.

Scheme 62 below shows the routes used in an attempt to synthesise the mono- and di-brominated xanthomonadins. It would appear that the biggest obstacle to the synthesis of these natural products lies in their purification. 2D TLC analysis indicates decomposition of the polyene over time.

Scheme 62 Current routes to **a)** MB xanthomonadin **210** and **b)** xanthomonadin **208**

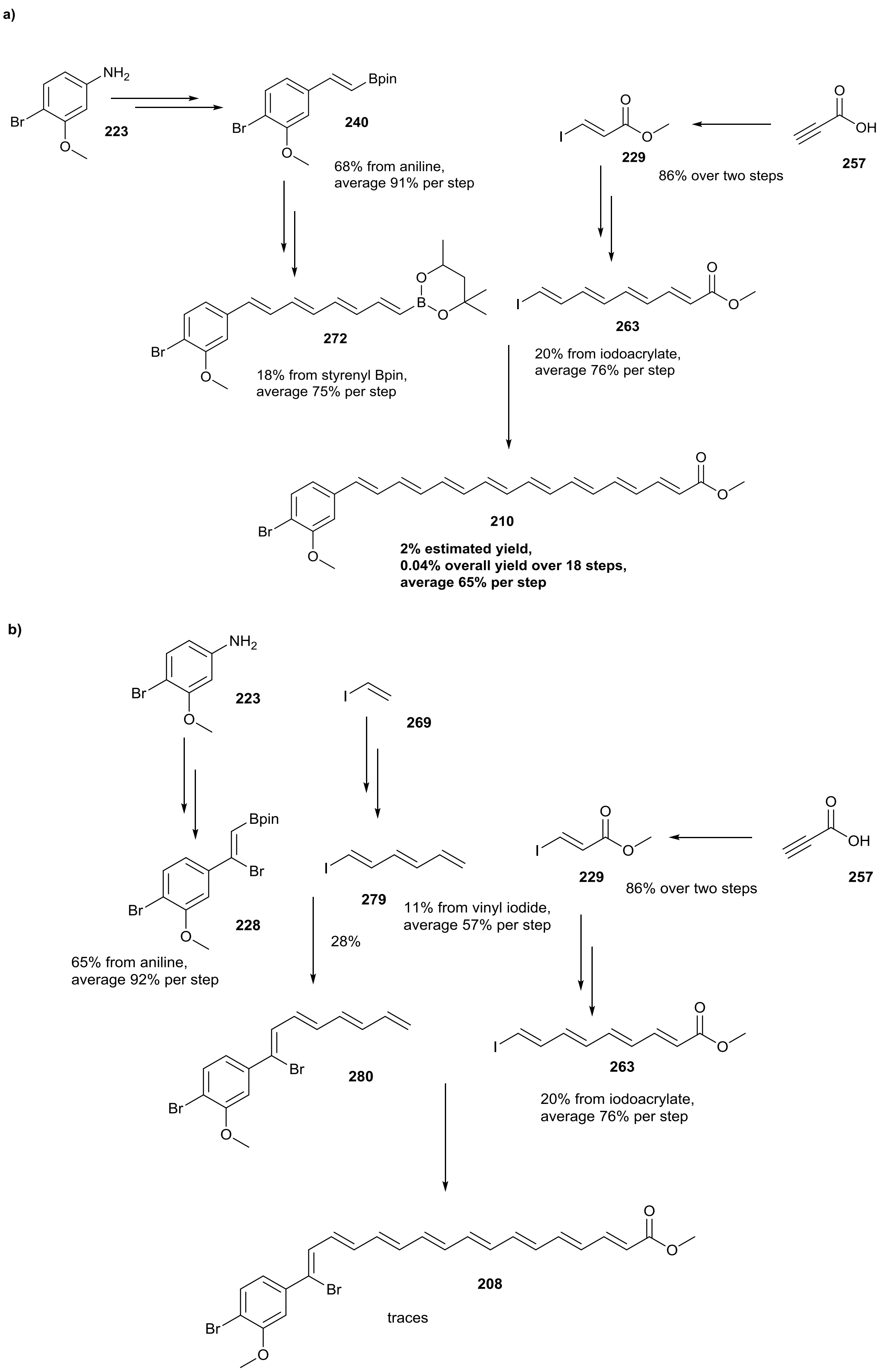

Section 1.4.5 Summary

Two truncated pigment analogues **234** and **235** have been successfully isolated, with the truncated pentaenyl xanthomonadin analogue **233** also made, but proving difficult to separate from the alkyne **235**, formed during the final SM coupling. Several attempts have been made to synthesise both xanthomonadin **208** and debrominated xanthomonadin **210**, with accurate mass spectrometry indicating successful formation of debrominated xanthomonadin **210**. Unfortunately, the octaenes have proven extremely unstable and their successful isolation has been elusive.

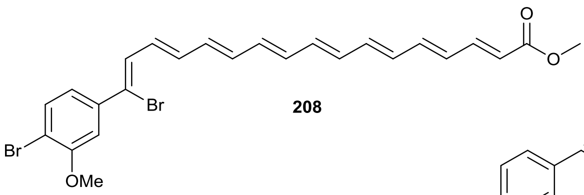

208

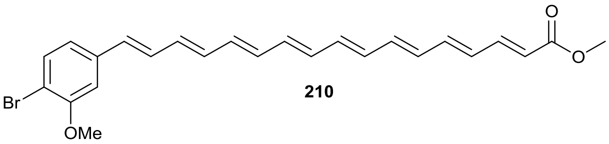

210

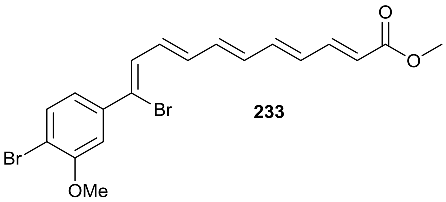

233

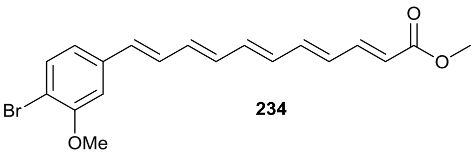

234

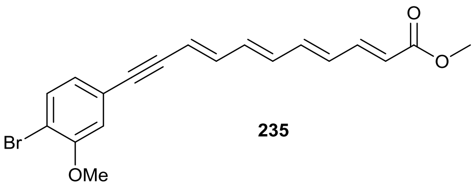

235

Section 1.5 Synthesis of Xanthomonas pigments- spectroscopic properties

Section 1.5.1 NMR observations and studies

Following on from the synthesis of various polyenyl analogues and intermediates, the next challenge lay in their spectroscopic analysis. In their isolation of the *Xanthomonas* pigments, Andrewes *et al.* obtained mass spectrometry, some infrared and some UV-Vis analysis, but high resolution ^{1}H NMR data was not available, nor any ^{13}C data (see **Figure 11** for the only NMR data reported). There were also no NMR spectra available for any of the pigments isolated.[133,151,154] X-ray crystallography data was reported to be poor. As a result, there was not a great deal of spectroscopic data to use as a benchmark.

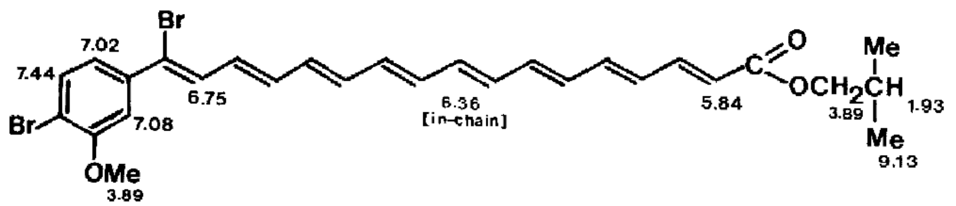

ISOBUTYL XANTHOMONADIN I (1)

Figure 11 ^{1}H NMR data as reported by Andrewes *et al.* for isobutyl xanthomonadin **208**[133]. Reprinted from Tetrahedron Letters, volume 17, Andrewes *et al.*, Structure of xanthomonadin I, a novel dibrominated aryl-polyene pigment produced by the bacterium *Xanthomonas juglandis*, 4023-4024, 1976, with permission from Elsevier

Nevertheless, the ^{1}H NMR peaks reported by Andrewes *et al.* provided a good indication of the types of shifts likely to be present for our polyenyl compounds.[133] Some NMR spectra were available for a series of hexaenyl pigments analogous to the xanthomonadins, reported by Fischbach *et al.*, but again ^{13}C NMR spectra were not given.[159] These spectra did, however, confirm what we had begun to observe for our own compounds; that the NMR data was very complex for these polyenyl structures.

Dehydro-tetraen-yne xanthomonadin **235** had been successfully made in a 56% yield previously (**Equation 31**), but good ^{13}C NMR data had not been acquired, so assignment of ^{1}H NMR signals had not been possible. The NMR sample was left exposed to normal light and was not degassed, to see what the effect would be (**Figure 12**). It was observed that the solution changed from bright yellow to bright orange and over time it was also noted that a new set of signals was visible in the ^{1}H NMR spectrum after 1 week, at around 6% intensity. This ratio seemed essentially unchanged after 2 weeks. There were other signals that overlapped with those of the original alkynyl compound **235**, but some were separate and identifiable. These new signals had lower coupling constants than some of the desired dehydro-tetraen-yne xanthomonadin **235**, suggesting isomerisation of at least one of the alkenes in the structure. The data is tabulated in **Table 9**, showing the new identifiable signals and their coupling constants.

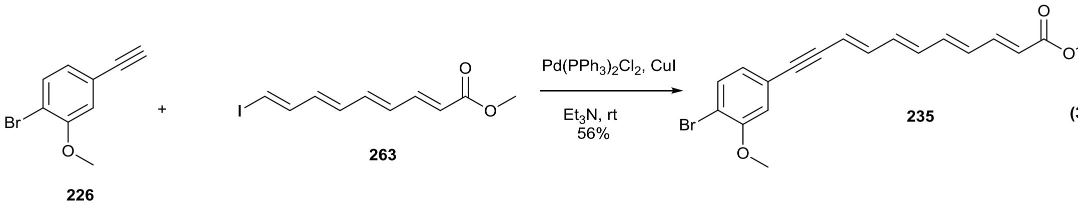

(31)

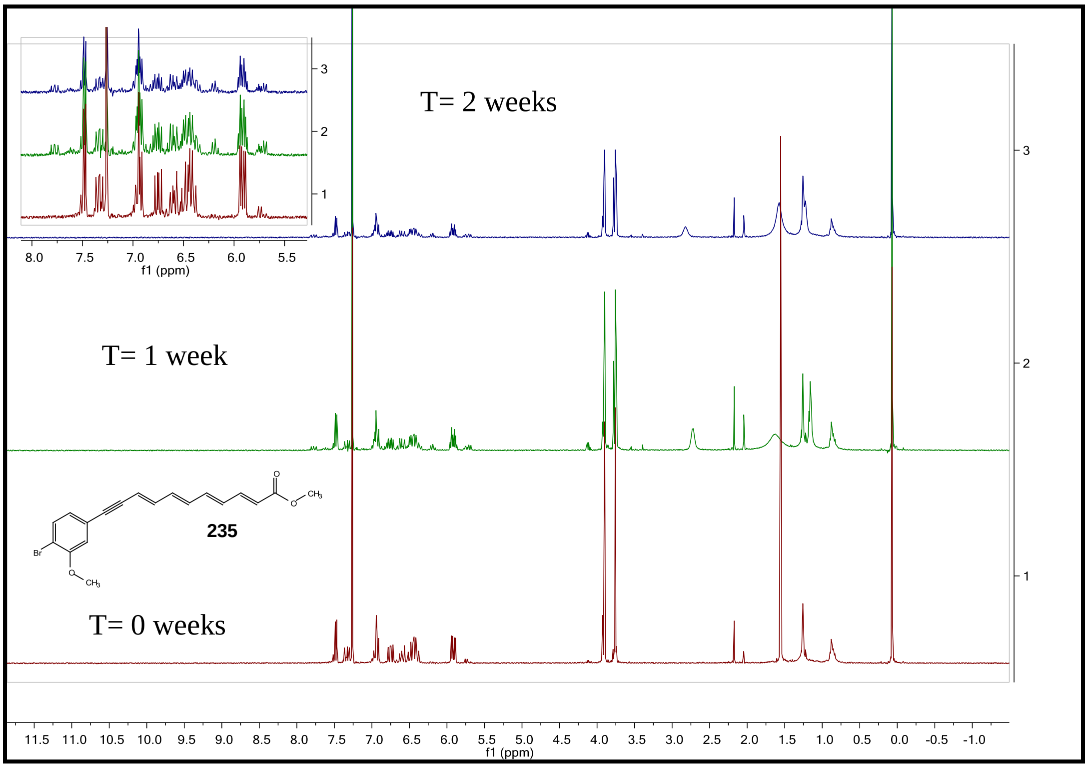

Figure 12 ^{1}H NMR spectra showing the change in dehydro tetraen-yne xanthomonadin **235** over a period of 2 weeks.

Table 9 ^{1}H NMR signals and coupling constants for dehydro-tetraen-yne xanthomonadin **235** and minor compound **293**

Pentaenyl analogue **235**			Minor component **293** (~5%), new identifiable signals	
Entry	δ_H	J/ Hz	δ_H	J/ Hz
1	-	-	5.72 (1H, d)	11.2
2	-	-	5.74-5.79 (1H, m)	-
3	5.91 (2H, dd)	15.3, 6.1	-	-
4	-	-	6.21 (1H, t)	11.5
5	6.29-6.54 (3H, m)	-	-	-
6	6.60 (1H, dd)	14.8, 10.5	-	-
7	6.75 (1H, dd)	15.4, 10.4	-	-
8	6.89-6.99 (2H, m)	-	-	-
9	7.28-7.39 (1H, m)	-	-	-
10	7.49 (1H, dd)	11.4, 8.3	-	-
11	-	-	7.78 (1H, d)	12.4
12	-	-	7.82 (1H, d)	12.0

In order to shed more light on which bonds might be isomerising, another sample was made in order to obtain ^{13}C NMR and 2D NMR data, so that the carbons and protons in the molecule could be assigned. The ^{1}H NMR spectrum possessed a number of complex multiplets, so the coupling constants for all of the protons could not be easily determined. The signals have, however, been assigned below. This information, combined with that in **Table 9** above, suggests that the bond isomerising is most likely to be the one adjacent to the ester, or that adjacent to the alkyne.

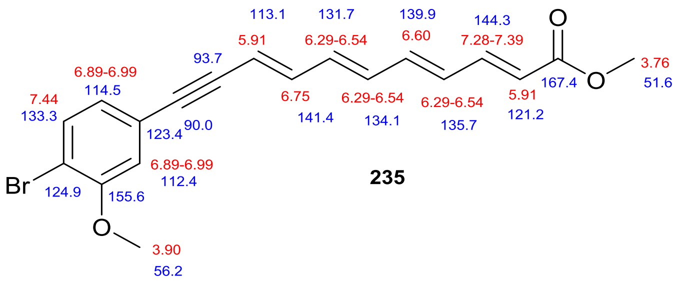

235

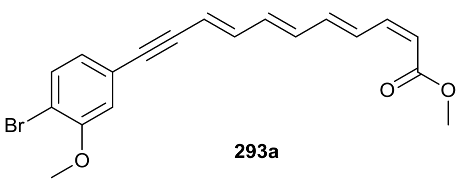

293a

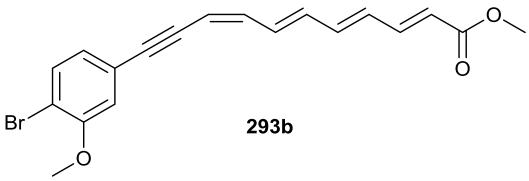

293b

Synthesis of pentaenyl xanthomonadin **233** was attempted using the $Pd(PPh_3)_4$/ silver(I) oxide conditions previously determined (**Equation 32**). NMR and accurate mass analysis was performed on the purified product. Mass spectrometry clearly identified the desired compound, which looked exceptionally clean with only two major mass ions (one for the dibrominated pentaene **233**, and one for the loss of bromine).

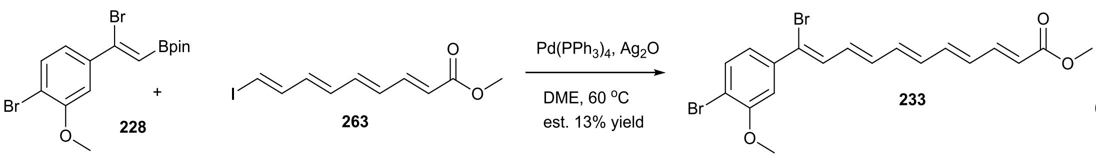

(32)

However, the NMR data was more complicated (**Figure 13**). The sample contained two major products; the desired pentaenyl xanthomonadin **233** (27%) and dehydro-tetraen-yne xanthomonadin **235** (69%), accounting for the two mass ion peaks observed. The ^{1}H NMR spectrum also showed signals similar to those found for dehydro-tetraen-yne xanthomonadin **235** after a week of exposure to light (4%) (**Figure 13a**). There were several singlets in the regions corresponding to the methyl ester and aryl methoxy groups, suggesting the presence of a number of compounds possessing these groups. The ^{13}C NMR spectrum showed a large number of signals, forming clusters at different shifts (**Figure 13b**). The HSQC looked fairly simple, but again the HMBC was complicated, showing that a number of different compounds were present, despite being one spot on TLC and having a clean mass spectrum (**Figure 13c and d**). At this point it was not clear whether this complexity arose from impurities in the sample, or from isomers of the natural product analogue, as the clustering of methyl peaks in the ^{1}H NMR spectrum and of the signals in the ^{13}C NMR spectrum indicated that a number of the compounds were similar. DOSY NMR analysis was undertaken to try to correlate the signals with a diffusion coefficient (**Figure 13e**).

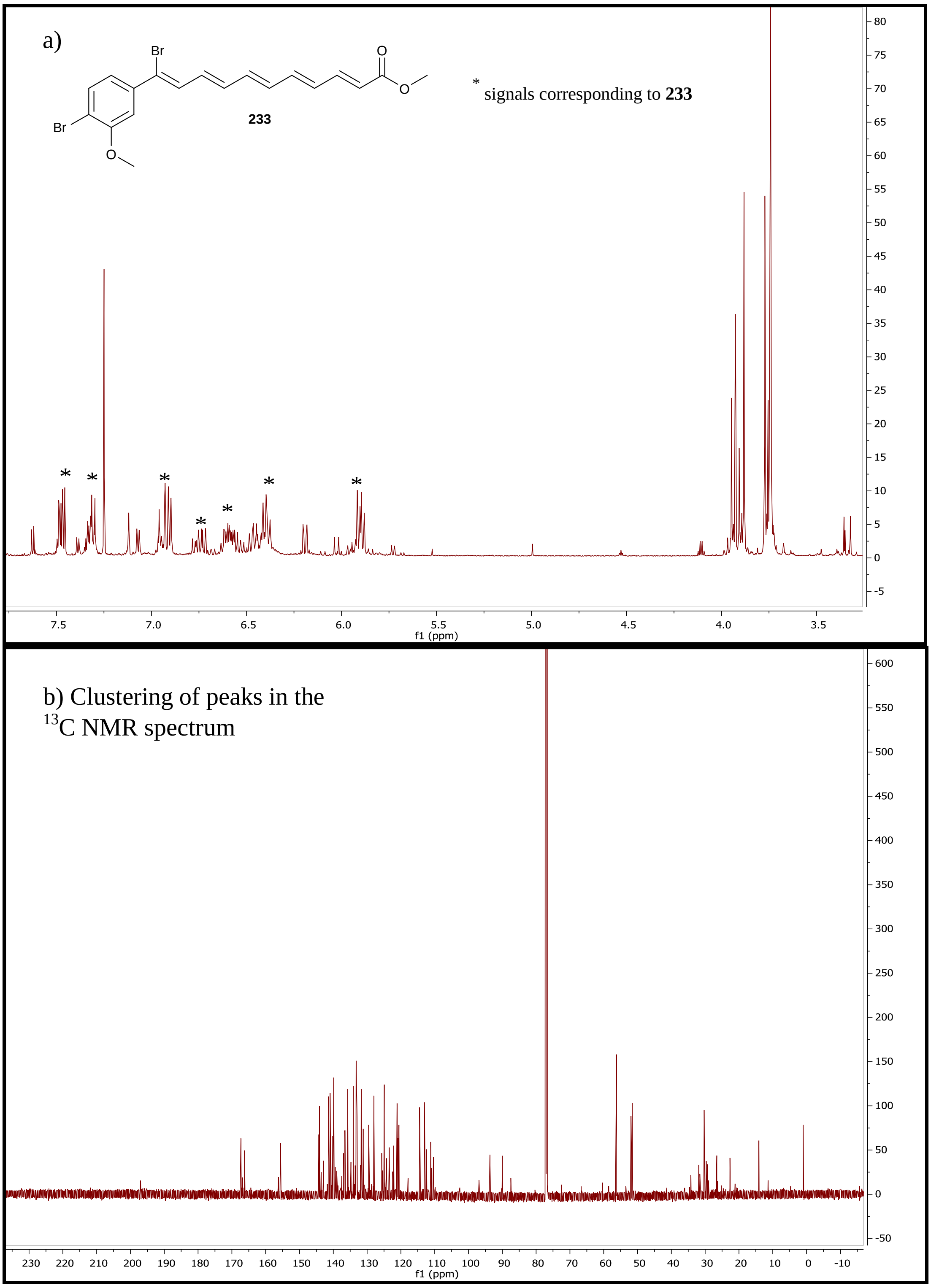
a)
Br
Br
O
O
O
233
* signals corresponding to 233
f1 (ppm)
b) Clustering of peaks in the
13C NMR spectrum
f1 (ppm)

c) Complex HMBC spectrum

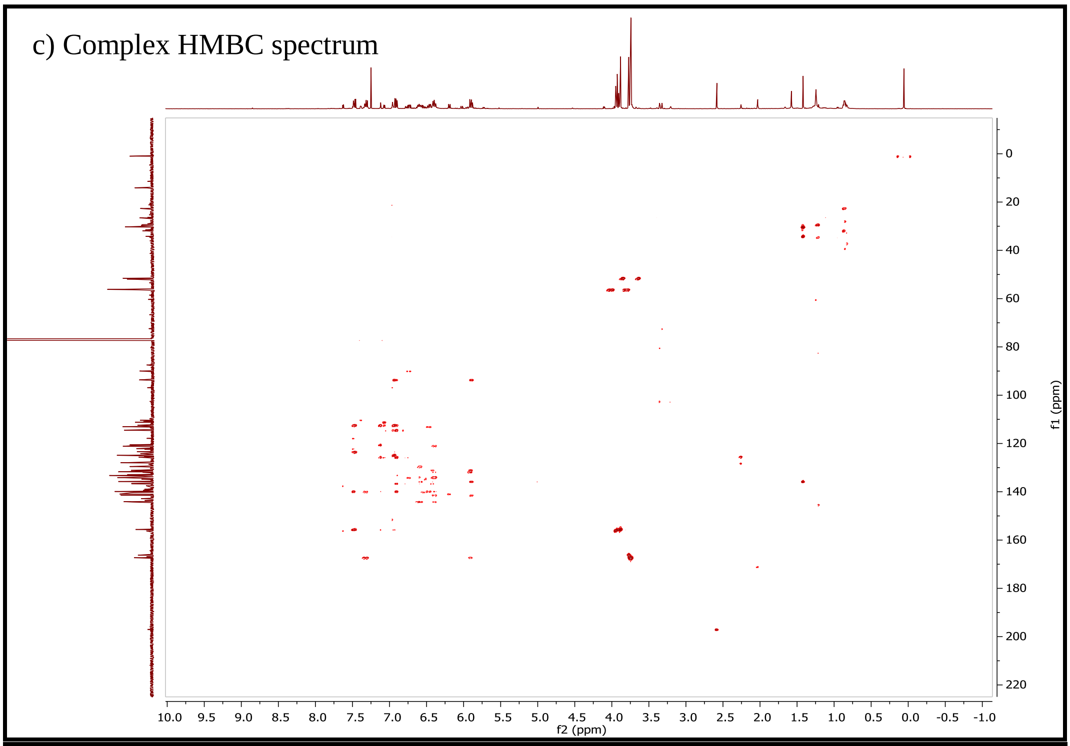

d) Less complex HSQC spectrum

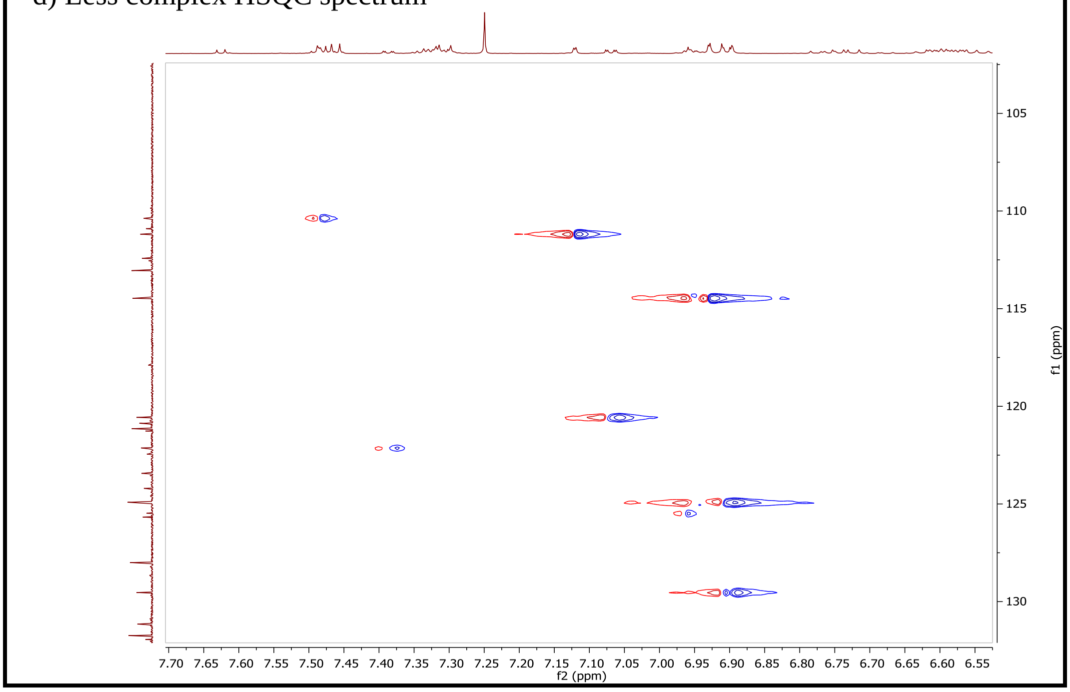

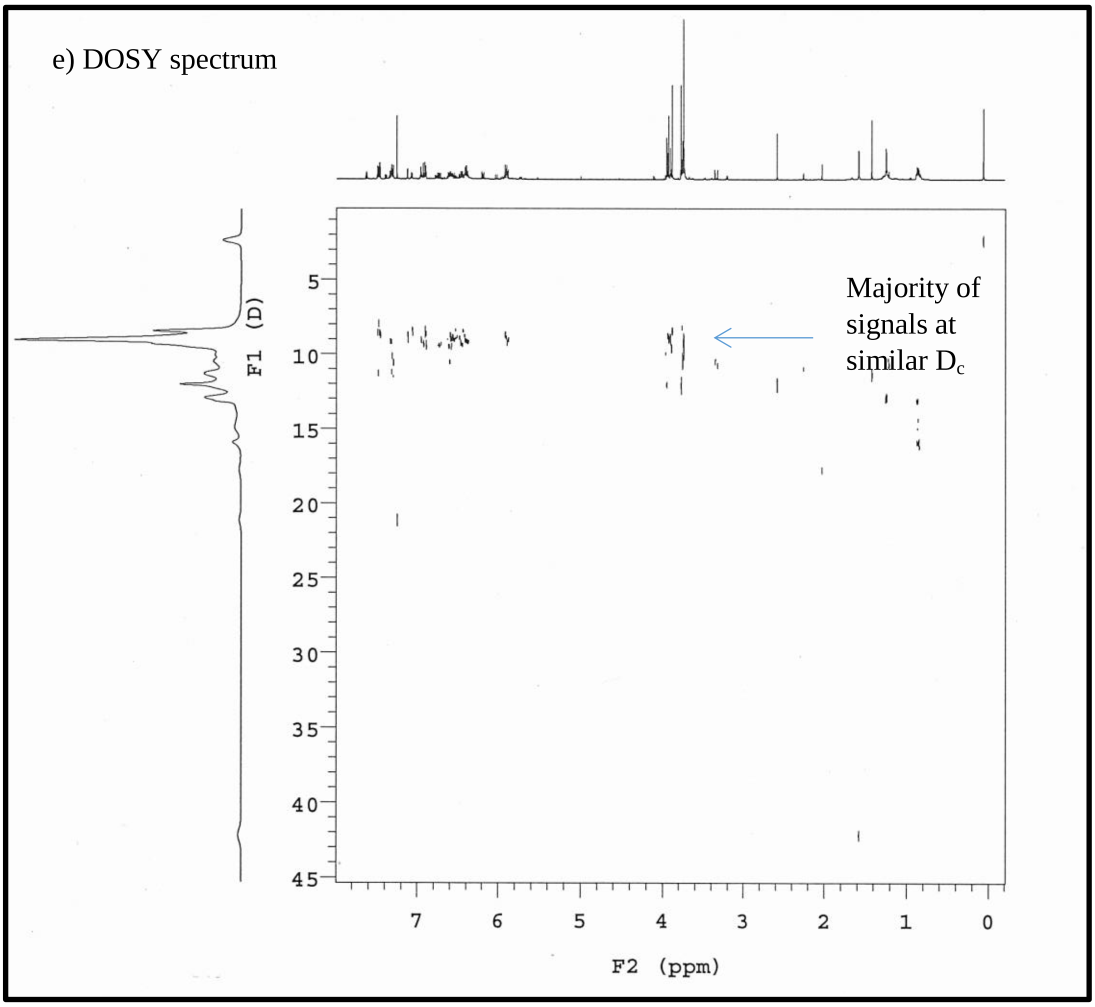

Figure 13a) ^1H NMR, **b)** ^{13}C NMR, **c)** HMBC 2D NMR, **d)** HSQC 2D NMR and **e)** DOSY NMR spectra for dibrominated pentaenyl analogue **233**

The DOSY NMR spectrum showed that the majority of alkenyl signals formed a cluster at a similar diffusion coefficient, which was consistent with the mass spectrum in suggesting that many of the different signals corresponded to compounds of a high level of structural similarity. There were also, a number of signals that did not correlate with this diffusion coefficient, indicating that some of the polyenyl species present were not isomers of the desired natural product analogue. The ^1H NMR data is shown in **Table 9**, showing that the signals for the most identifiable minor component(s) differed in a similar way to those of dehydro-tetraen-yne xanthomonadin **235**, with the most shifted signals displaying *cis*-type J couplings of the order of 8-10.5 Hz.

Table 10 ^{1}H NMR signals and coupling constants for pentaenyl analogue **233** and minor compound(s)

Pentaenyl xanthomonadin **233**			Minor component(s) (~4% total mixture, 15% compared to pentaenyl xanthomonadin **233**), new identifiable signals	
Entry	δ_H	J/ Hz	δ_H	J/ Hz
1	-	-	5.74 (1H, d)	10.5
2	5.91 (2H, dd)	15.4, 10.4	-	-
3	-	-	6.04 (1H, dd)	15.5, 10.0
4	6.35-6.50 (3H, m)	-	-	-
5	6.56-6.67 (2H, m)	-	-	-
6	6.70-6.77 (1H, m)	-	-	-
7	6.87-6.98 (2H, m)	-	-	-
8	7.03-7.15 (1H, m)	-	-	-
9	-	-	7.40 (1H, dd)	8.1, 1.9
10	7.44-7.51 (1H, dd)	-	-	-
11	-	-	7.64 (1H, d)	8.1

The same thing was observed for debrominated pentaenyl xanthomonadin **234**, where the compound was also one spot on TLC, displayed a clean mass spectrum and yet had complex NMR spectra (**Figure 14, Equation 33**). Unfortunately, the multiplets for this compound were not as well resolved, so it was harder to make a comparison. Some less easy to identify peaks are omitted from the table, but it is still possible to see *cis* alkenyl couplings in similar places as observed for dibrominated pentaenyl analogue **233**, again of the order of 8-10.5 Hz (**Table 11**).

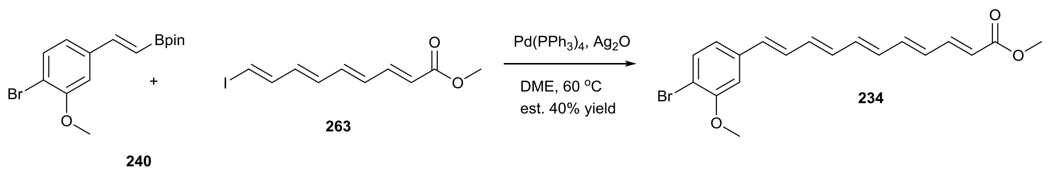

240 263 234 (33)

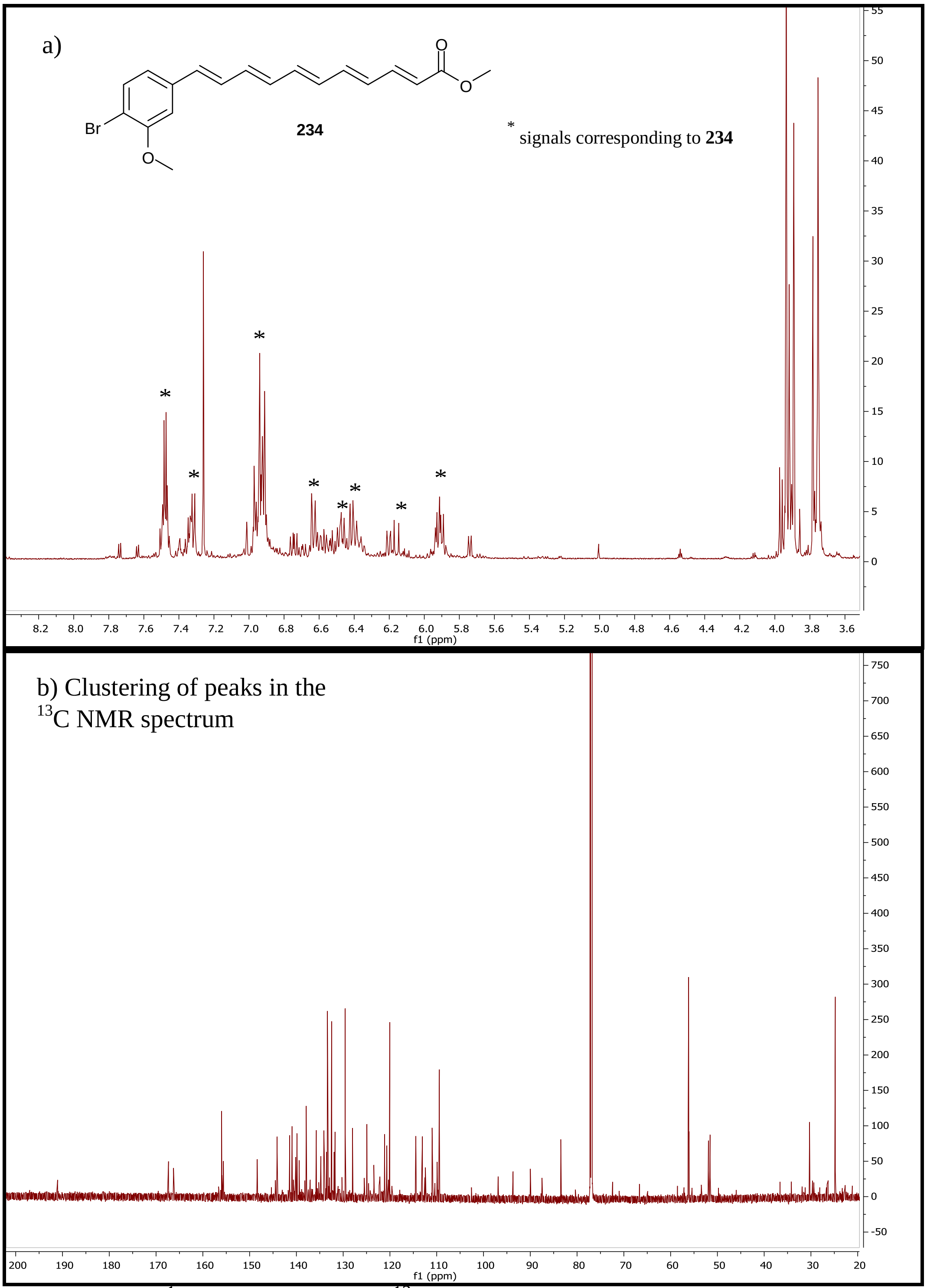

Figure 14a) ^{1}H NMR and **b)** ^{13}C NMR spectra for debrominated pentaenyl xanthomonadin **234**

Table 11 ^{1}H NMR signals and coupling constants for debrominated pentaenyl xanthomonadin **234** and minor compound(s)

Debrominated pentaenyl xanthomonadin **234**			Minor component(s) (~11%), new identifiable signals	
Entry	δ_H	J/ Hz	δ_H	J/ Hz
1	-	-	5.74 (1H, d)	10.5
2	5.97-5.97 (2H, m)	15.4, 10.4	-	-
3	6.35-6.53 (3H, m)	-	-	-
4	6.63 (1H, dd)	11.8, 2.7	-	-
5	6.87-6.94 (4H, m)	-	-	-
6	7.29-7.35 (1H, m)	-	-	-
7	7.44-7.51 (2H, m)	-	-	-
8	-	-	7.64 (1H, d)	8.1
9	-	-	7.74 (1H, d)	7.9

The lack of stability for debrominated pentaenyl xanthomonadin **234** was of particular note. When illuminated by long wave UV, a spot on TLC corresponding to product shone bright orange, being clearly visible and fluorescent. This spot visibly faded, to the point of no longer being visible after around 15 minutes on the TLC plates.

The new signals for both the mono- and dibrominated pentaenes showed a good deal of similarity and, if the shifts for the pentaenes are analogous to those of the alkynyl derivative, suggesting that the bond isomerising in the most identifiable minor component could be the one next to the ester.

Whilst these NMR studies provided evidence that many of the complex signals observed corresponded to isomers, it could be seen from the DOSY NMR in particular that there were indeed some signals corresponding to polyenes of a different molecular weight, indicating that the current purification conditions were not effectively separating mixtures of polyenes. This proved a key discovery, and led to the use of benzene as a column chromatography solvent (see **Section 1.4**).

Polyenyl intermediates also displayed complex NMR spectra. The ^{1}H NMR spectrum for tetraenyl iodide **263** after column chromatography showed a number of peaks in the area corresponding to the methyl ester, as were observed for the natural product analogues. In this case, there were two distinct spots visible on the TLC, both visible in the long wave UV. One spot was, however, blue whilst another was white. Previously, extensive NMR analysis was not undertaken due to the presumed instability of the compound at room temperature. In light of the NMR studies undertaken on the natural products, it was decided to run a number of NMR experiments to study the compound's behaviour over time. ^{1}H NMR experiments were run in between the longer 2D and ^{13}C experiments to observe any changes in the signals over these few hours (**Figure 15a**). An increasing level of complexity was visible over time, with some signals increasing and others changing in multiplicity. In **Section 1.3**, a study was performed on tetraenyl iodide **263** to ascertain the effect of temperature on its stability. The peaks observed due to decomposition were different to those observed to be increasing or changing in this case. It was not possible to quantify all of the peaks due to the complexity of the spectrum, but two signals were observed to be clearly increasing at δ 6.64 and 6.80 ppm. The integrations of these were compared to the integration of a peak corresponding to tetraenyl iodide **263** that did not change over time (**Table 12**). In the space of a few hours, the relative integration of these peaks quadrupled, eventually being observed at an equivalent integration to the tetraenyl iodide itself. The ^{13}C NMR also showed clustering, as was observed before for the truncated pentaenyl analogues (**Figure 15a**). 2D HSQC and HMBC experiments were done to try to correlate the clusters with specific proton signals. This showed that they are indeed clusters corresponding to individual multiplets. DOSY analysis was not undertaken for this sample, so these signals were not correlated to a particular diffusion coefficient.

Table 12 Table showing the change in selected signals for a possible isomer of tetraenyl iodide **263** over a period of a few hours through ^{1}H NMR spectra run at intervals

Entry	Relative ^{1}H NMR integral to δ 6.29 ppm (m @ 6.64 ppm)	Relative ^{1}H NMR integral to δ 6.29 ppm (m @ 6.80 ppm)
1	0.25	0.29
2	0.23	0.28
3	0.58	0.56
4	1.00	0.99
5	1.01	1.01
6	0.99	0.99

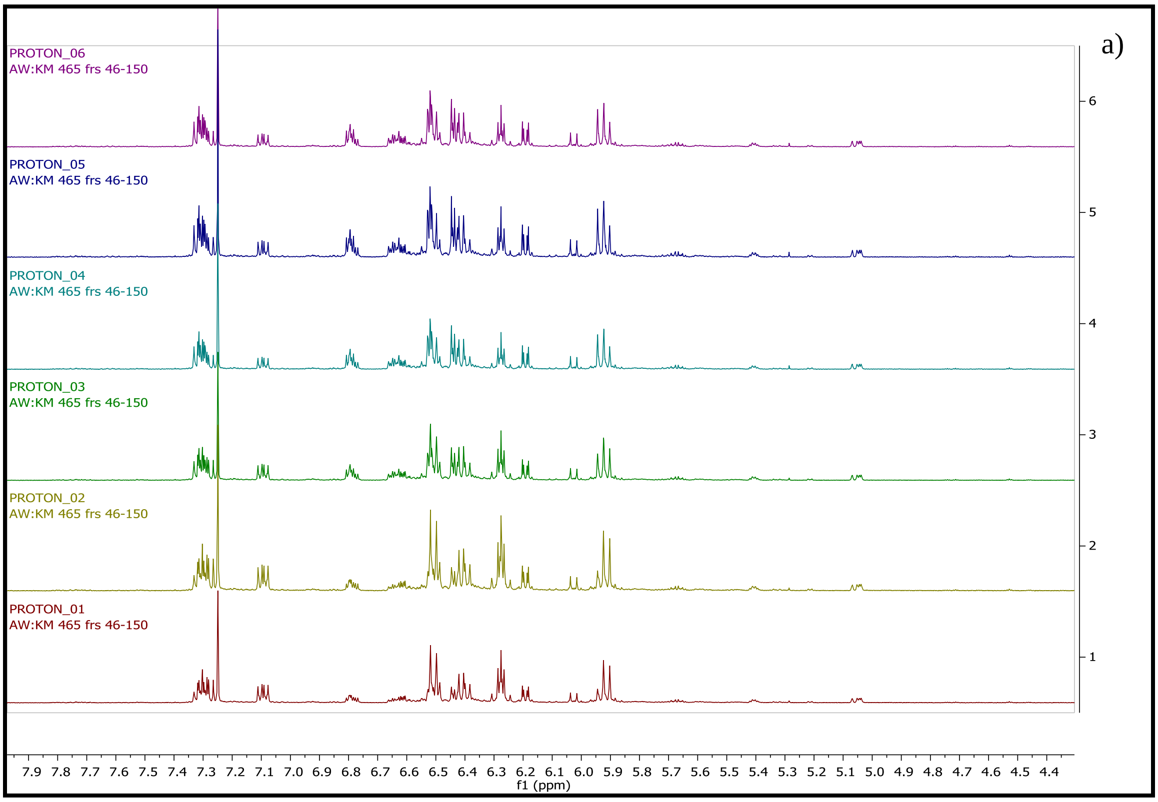

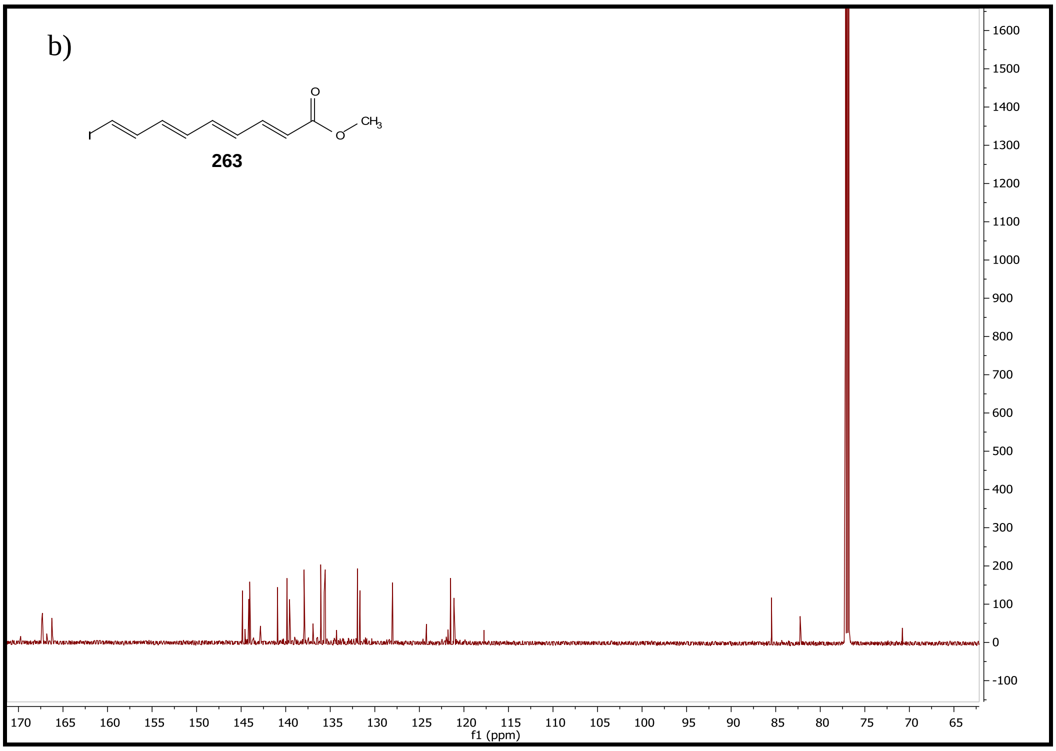

Figure 15a) Stacked ^{1}H NMR spectra for tetraenyl iodide **263**, showing change over time and **b)** ^{13}C NMR spectrum for tetraenyl iodide **263**

After storing all three pentaenyl natural product analogues **233-235** for two months, ^{1}H NMR spectra were compared (**Figure16-Figure 18**). The compounds were stored in the dark, under argon, and at -18 ^{o}C.

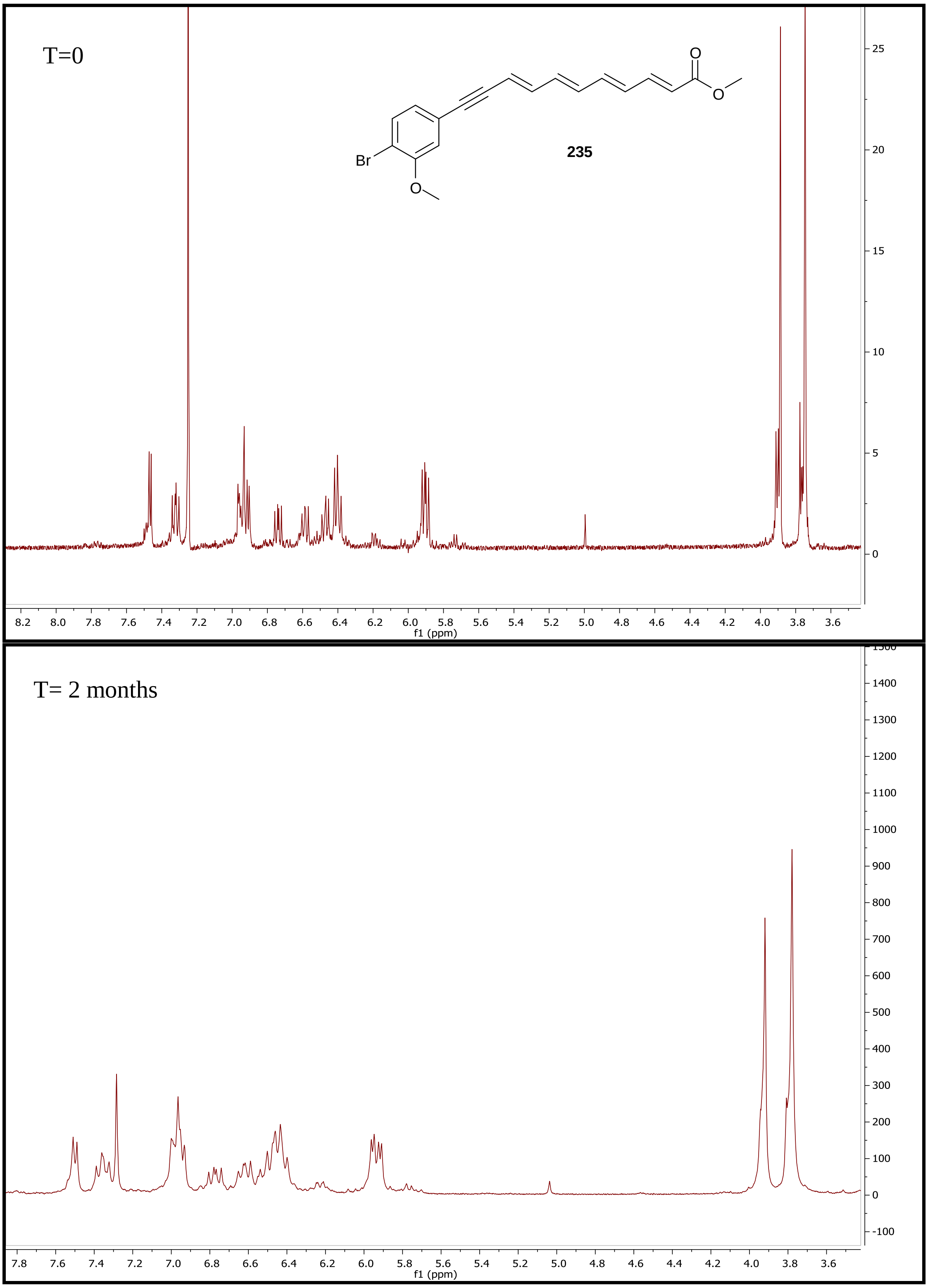

Figure 16 ^{1}H NMR spectra for dehydro-tetraen-yne xanthomonadin **235**, indicating stability over 2 months

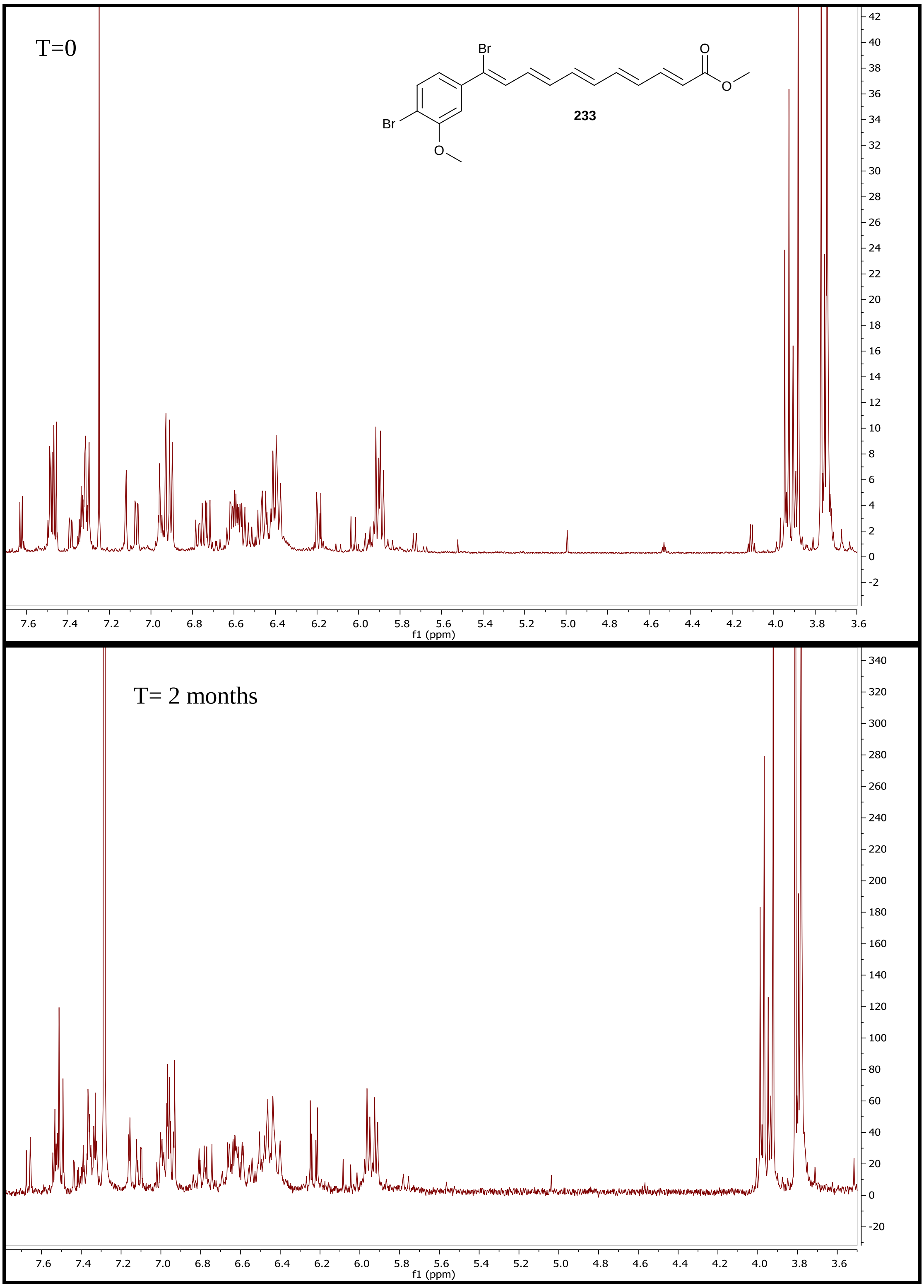

Figure 17 ¹H NMR spectra for dibrominated pentaenyl analogue **233**, indicating stability over 2 months

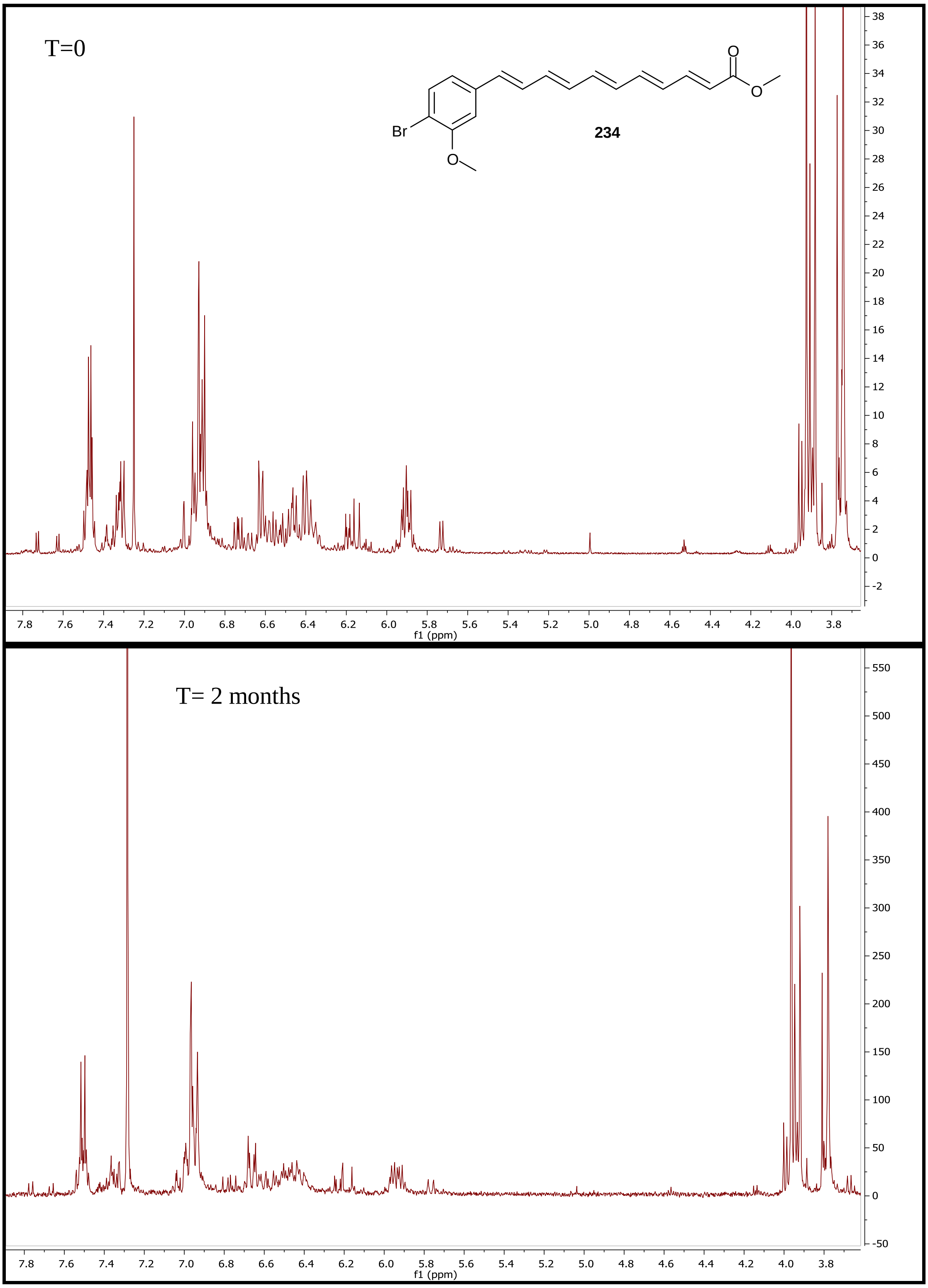

Figure 18 ^{1}H NMR spectrum for debrominated pentaenyl xanthomonadin **234**, indicating stability over 2 months

Debrominated pentaenyl xanthomonadin **234** appeared to be the least stable, with the most changes visible on comparison of the spectra. There were some small differences between the spectra for brominated analogue **233**, but this analogue did appear to be more stable than **234**, suggesting an explanation for dibrominated xanthomonadin being the most observed pigment in *Xanthomonas* bacteria. The resolution was poor for the ^{1}H NMR spectrum obtained for dehydro tetraen-yne xanthomonadin **235** after two months, but it can be seen that the two spectra are very similar (**Figure 16**).

Debrominated pentaenyl xanthomonadin **234** was re-isolated as a bright yellow solid that clearly fluoresced under normal lighting, using new conditions for column chromatography. Using benzene as an eluent proved highly successful, with debrominated pentaenyl xanthomonadin **234** observed as a single spot that shone brine orange under long wave UV. Dehydro tetraen-yne xanthomonadin **235** slowly turned from custard yellow to orange over time at room temperature (particularly if dissolved and then concentrated again *in vacuo*), but no colour change was observed for debrominated pentaenyl xanthomonadin **234**.

The behaviour of debrominated pentaenyl xanthomonadin **234** in solution was investigated in the same way as for tetraenyl iodide **263**, with ^{1}H NMR spectra run periodically in between 2D experiments overnight. No change in the sample was observed in this time, as shown by **Figure 19** and **Table 13**.

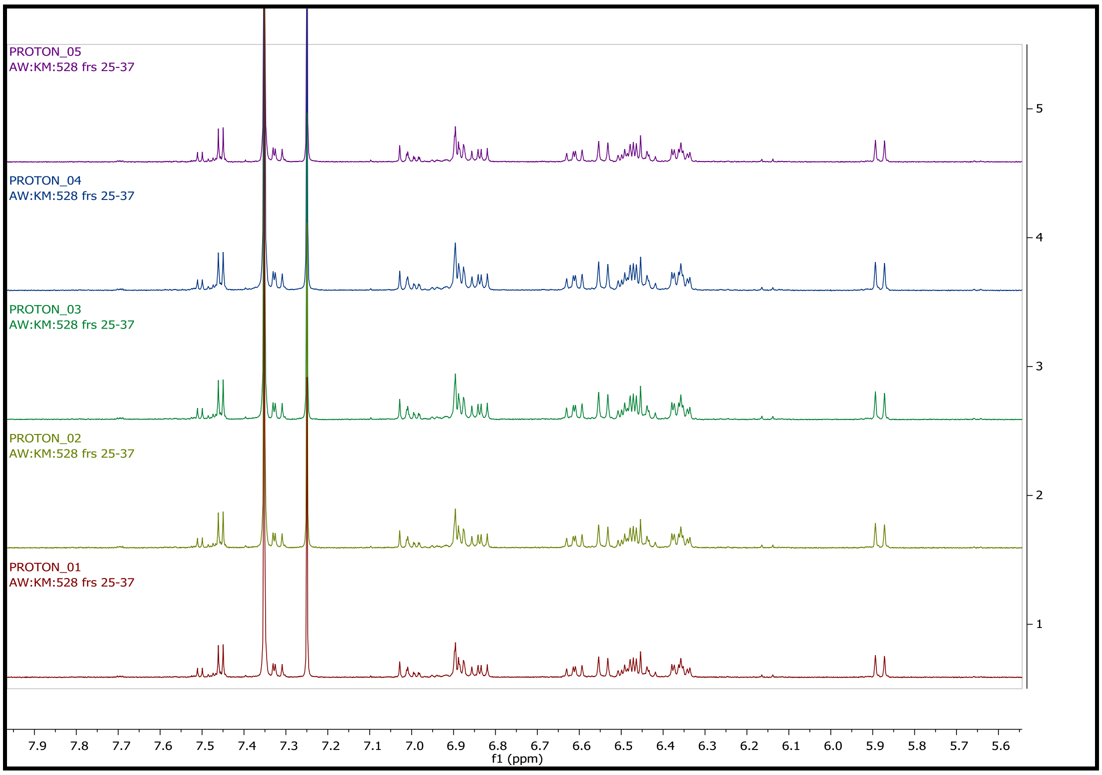

Figure 19 Stacked ^{1}H NMR spectra for debrominated pentaenyl xanthomonadin **234**, showing stability overnight.

Table 13 Table showing the change in selected signals for a possible isomer of debrominated pentaenyl xanthomonadin **234** over a period of a few hours through ^{1}H NMR spectra run at intervals

Entry	Relative ^{1}H NMR integral to δ 5.88 ppm (m @ 7.51 ppm)
1	0.26
2	0.30
3	0.26
4	0.27
5	0.26

It was immediately noticeable that all of the NMR spectra were much less complex than those obtained previously for debrominated pentaenyl xanthomonadin **234** (**Figure 20**, c.f. **Figure 14**). The HMBC still displayed considerable complexity, and smaller peaks corresponding to a potential isomer were visible in the ^{1}H NMR.

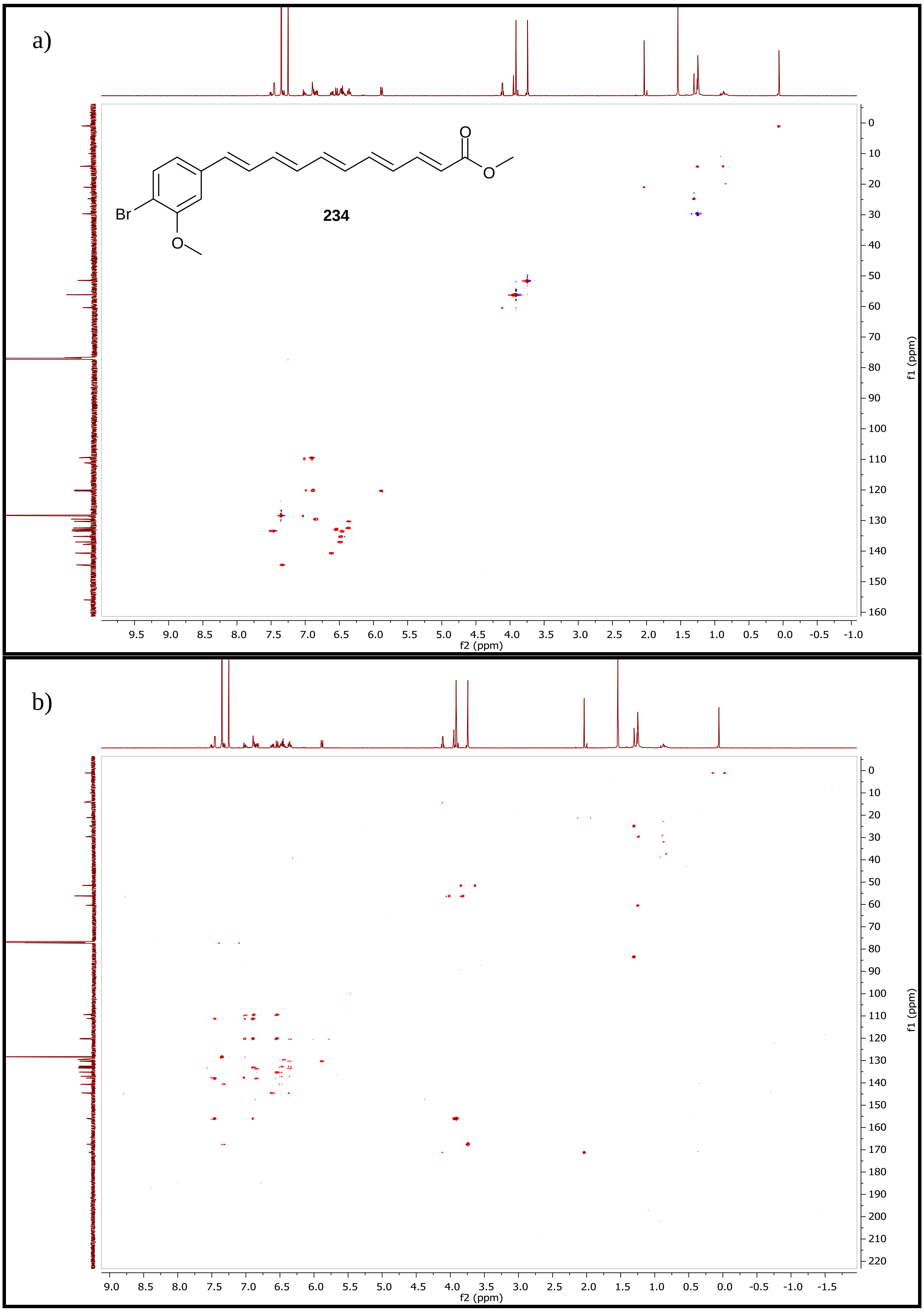
a)
Br
O
O
O
234
f2 (ppm)
f1 (ppm)
b)
f2 (ppm)
f1 (ppm)

c)

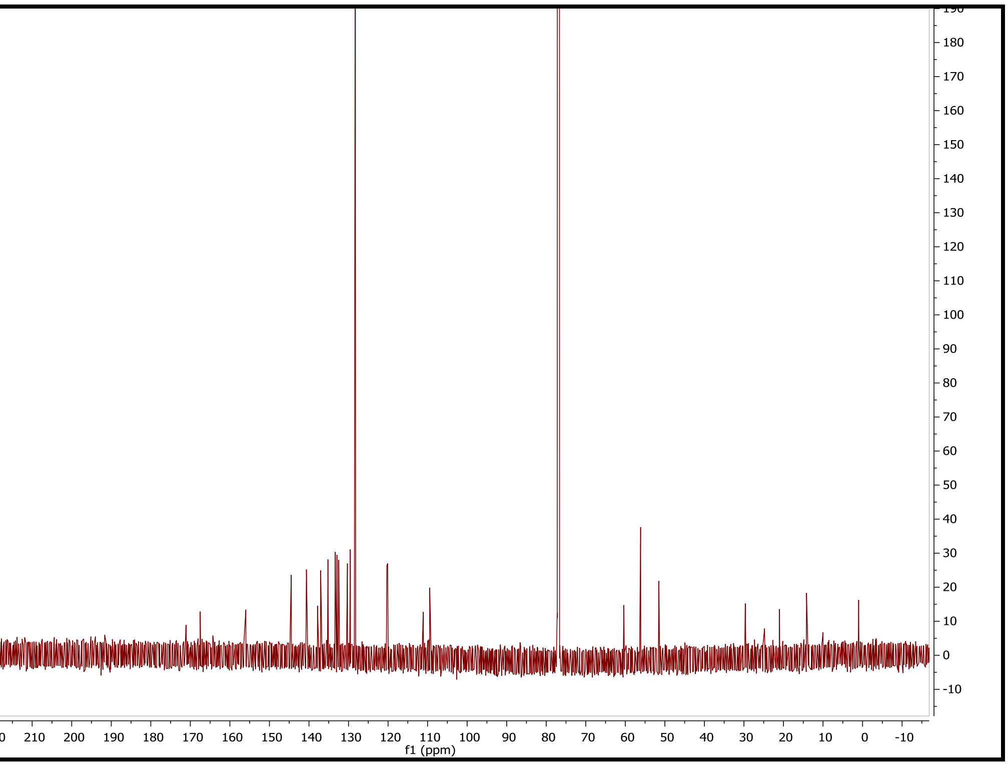

Figure 20a) HSQC 2D NMR **b)** HMBC 2D NMR and **c)** ^{13}C NMR spectra for a sample of debrominated pentaenyl xanthomonadin **234**, isolated using benzene

Unfortunately, not enough sample was obtained to ascertain the stability of compound **234** over a longer period, as was investigated for dehydro-tetraen-yne xanthomonadin **235** (**Figure 12**). However, these data indicated that benzene was a much more effective solvent for purification of these pigment analogues, as well as showing that there is still a considerable degree of complexity for the pure compounds.

Section 1.5.2 UV-Vis and fluorescence data

Andrewes *et al*. reported both UV-Vis data for mixtures of pigments that they initially isolated from *Xanthomonas* bacteria, and also data from their isolated sample of isobutyl xanthomonadin **208**, with the the values for isobutyl xanthomonadin **208** given in **Table 14**.[151] No fluorescence data was reported.

UV-Vis and fluorescence data was obtained for both dehydro tetraen-yne xanthomonadin **235** and the debrominated pentaenyl xanthomonadin **234**, and their UV-Vis values compared to that of isobutyl xanthomonadin **208** (**Table 14**). The shapes of the UV-Vis curves were comparable to those reported by Andrewes *et al.*, as shown in **Figure 21**.[151]

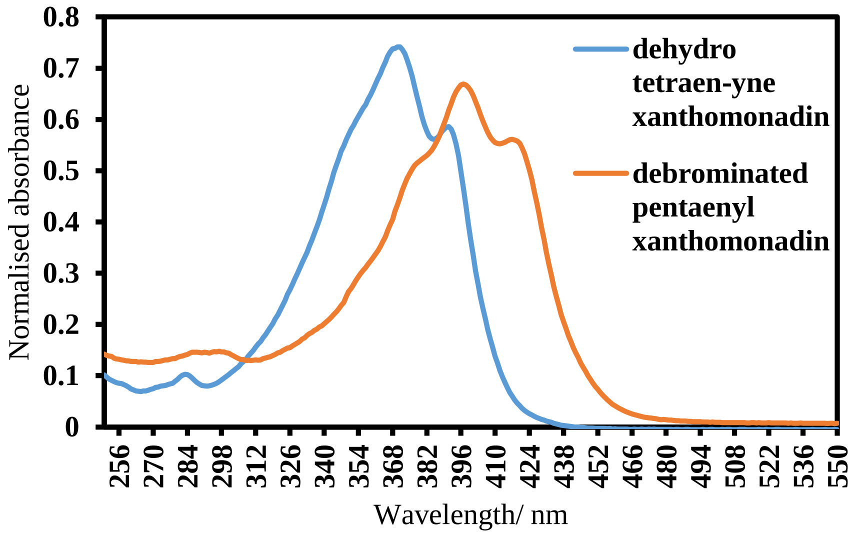

Figure 21 UV-Vis spectra obtained for dehydro tetraen-yne xanthomonadin **235** and debrominated pentaenyl xanthomonadin **234**

Table 14 UV-Vis and fluorescence data for isobutyl xanthomonadin **208**, along with dehydro-tetraen-yne xanthomonadin **235** and debrominated pentaenyl xanthomonadin **234**

Compound	UV-Vis absorption/ nm	Emission/ nm
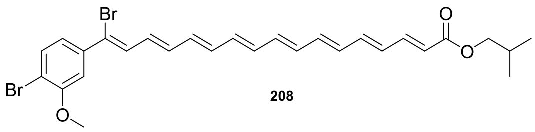 **208**	453, 482[a]	-
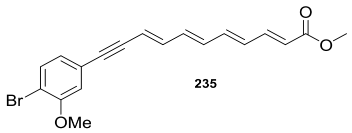 **235**	370, 391[b]	440, 468, 494[b]
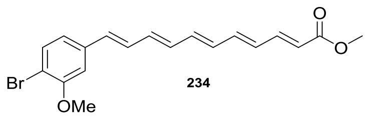 **234**	397, 417[b]	498,527, 566, 594[b]

[a]Data reported by Andrewes *et al.*[151]

[b]This work

The UV-Vis absorption maxima for the two truncated analogues were lower than those of isobutyl xanthomonadin, appearing to be consistent with lower conjugation. Debrominated pentaenyl xanthomonadin **234** showed a noticeable red shift when compared to dehydro-tetraen-yne xanthomonadin **235**, again seeming to be consistent with the increased conjugation of the pentaene. Debrominated pentaenyl xanthomonadin **234** also showed an increased Stokes-shift when compared to dehydro-tetraen-yne xanthomonadin **235**. In order to establish the trend in UV-Vis absorption maxima more definitively, the expected λ_{max} values for dehydro tetraen-yne xanthomonadin **235** and debrominated pentaenyl xanthomonadin **234** were calculated using the polyene specific Fieser-Kuhn rules,[177] following **Equation 34**, with the results shown in **Table 15**. The expected λ_{max} value for xanthomonadin was also calculated.

$$\lambda_{max} = 114 + 5M + n(48.0 - 1.7n) - 16.5R_{endo} - 10R_{exo} \qquad \textbf{(34)}$$

Where n = the number of conjugated double bonds

M = the number of alkyl or alkyl-like substituents

R_{endo} = the number of rings with endocyclic double bonds

R_{exo} = the number of rings with exocyclic double bonds

The solvent was also corrected for, subtracting 7 nm for diethyl ether and 1 nm for chloroform, to allow for a direct comparison.[177]

Table 15 Calculated and observed values of λ_{max}, for isobutyl xanthomonadin, dehydro-tetraen-yne xanthomonadin **235** and debrominated pentaenyl xanthomonadin **234**

Compound	λ_{max}^{calc}/ nm	λ_{max}^{obs}/ nm
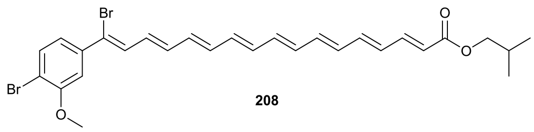 **208**	459.2	453 (chloroform)[151]
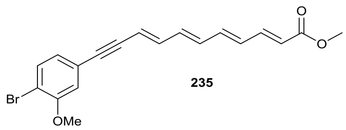 **235**	392.2	391 (diethyl ether)
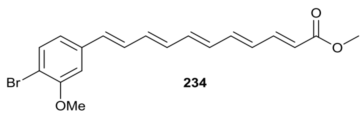 **234**	417.3	417 (chloroform)

It can be seen in **Table 15** that the calculated λ_{max} values for dehydro tetraen-yne xanthomonadin **235** and debrominated pentaenyl xanthomonadin **234** correspond almost identically to the highest energy λ_{max} observed for each of these two molecules, providing further evidence of the successful construction of these polyenes. They also corroborate the ^{1}H NMR data, due to the presence of a lower energy λ_{max} that could be explained by a *cis-trans* isomerisation of one of the alkenes in the structures. It would be expected that the *cis* isomer would also display a lower absorption coefficient, which is not observed here. It could well be the case that majority of molecules in solution during the UV-Vis experiments are in fact the *cis* isomerised molecules. The calculated λ_{max} value for isobutyl xanthomonadin corresponds with the lower energy λ_{max} value observed by Andrewes and Starr,[151] though with a larger discrepancy between the values of 6.2 nm. Molecular distortion is known to have an effect on the value of λ_{max}.[177] The crystal structure obtained for brominated styrenyl Bpin does show a considerable distortion of the mo1ecule due to the alkenyl bromine atom, removing the planarity.

Calculation of the expected λ_{max} value for dehydro tetraen-yne xanthomonadin **235** gave an interesting insight into the contribution of the alkyne group to the overall photochemical behaviour of the molecule. Within the group, we have previously assumed that an alkyne moiety will contribute directly to the λ_{max} value for a given compound, increasing the value in a similar way to a conjugated double bond. However, treating the alkyne as a conjugated double bond and allowing it to be accounted for in the value of n (see **Equation 34**), gave a value of 411.3 nm for diethyl ether, which is higher than the observed value. Assuming that the alkyne does not contribute at all, and treating the arene and tetraene ester as separate functionalities on the molecule would mean that the highest number of conjugated double bonds is 5, which gives a value of 314.5 nm for λ_{max}; a value that is far too low. Making the assumption that the alkyne does not contribute directly to λ_{max}, but does allow the conjugation to continue throughout the molecule, gives the much more accurate value seen in **Table 15**.

Section 1.5.3 Summary

There was limited spectroscopic data in the literature for xanthomonadin **208**, with particularly poor NMR data available. There was also little reported on the behaviour of isolated *Xanthomonas* pigments. A series of NMR experiments provided evidence of another isomer formed by *cis-trans* isomerisation, with assignment of the NMR signals providing some insight into which alkene along the polyene structure might the one isomerising. The ^{1}H NMR signals also correlate well with those reported for isobutyl xanthomonadin **208** by Andrewes *et al.*, with the characteristic peaks at δ ~ 5.9 and 6.8 ppm observed, along with the remainder of the polyenyl signals occuring between δ 6.3 and 7 ppm.[133]

In addition UV-Vis data has shown good correlation both with the data measured by Andrewes *et al.* for a mixture of xanthomonadin **208** and debrominated xanthomonadin **210**, but also with the calculated values for their principal λ_{max} according to the Fieser-Kuhn rules.[151,177] A second λ_{max} at a lower wavelength provides evidence of a *cis-trans* isomerisation. In addition, some insight into the contribution of an alkyne functional group to the photochemical behaviour of a molecule has been gained.

These data collectively provide sound evidence that the data obtained by Andrewes *et al.* is accurate, that the compounds made are in fact conjugated pigment natural product analogues, and that they form one major isomer *via cis-trans* isomerisation.[133,151]

Section 2

Novel methods of polyene synthesis

Section 2.1 Use of vinyl iodide as a Heck-Mizoroki coupling partner

Whilst there are strategies by which polyenes can be synthesised,[178–182] new, robust and reliable protocols, which deliver both high yields and stereocontrol are still required. Terminal, unsubstituted polyenes have been accessed by hydrazone formation, elimination and metal-mediated couplings,[183–189] however, such methods are limited by substrate scope and stereoselectivity. The current methodology used within the group to effect formation of polyenes utilises an iterative HM/iododeboronation sequence, with vinylboronic acid pentanediol ester **42** as the alkene donor (**Scheme 63**).[30,31,160–162,164–166] Such methodology is topical in the literature, with variations on both the type of palladium reaction and on the functional group converted to yield the vinyl iodide being reported.[190]

Scheme 63 HM/iododeboronation methodology used within the group.

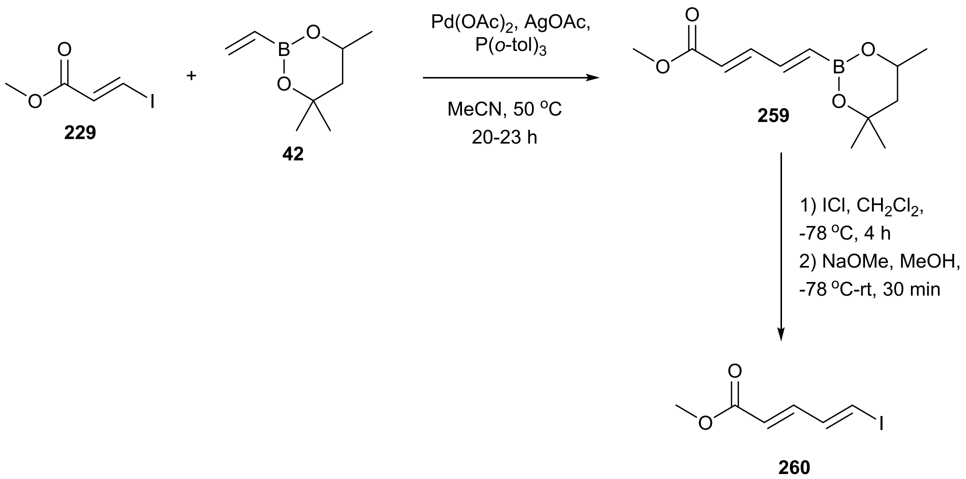

A method to facilitate the elongation of a polyene chain in one step using a palladium catalyst seems not to have been described. It was considered that if the reactivity was in effect switched round, with the growing polyene chain used as the alkene donor and the alkene acceptor being simply vinyl iodide **269**, then polyene homologation in this manner could be achieved (**Equation 35**). In addition, the need to isolate an unstable vinyl iodide compound would be removed.

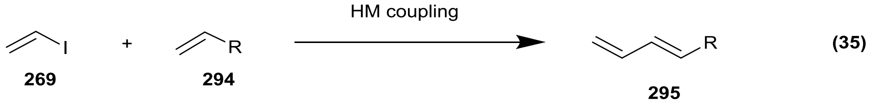

The use of vinyl iodide as a Heck-Mizoroki coupling partner seems to have been overlooked, with only one use of it disclosed in the literature by Heck, where the reaction between vinyl iodide and methyl acrylate using 1 mol% $Pd(OAc)_2$, 2 mol% PPh_3 and Et_3N at 100 °C resulted in a Diels-Alder product instead of the desired diene.[191] Due to the possiblility of extensive applications of these types of polyene boronate species, the initial reactions undertaken to establish the success of vinyl iodide **269** as a HM coupling partner were performed using vinyl boronate ester **42**.

Section 2.1.1 Optimisation of Heck-Mizoroki coupling to form 2-[(1E)-buta-1,3-dien-1-yl]-4,4,6-trimethyl-1,3,2-dioxaborinane

The first attempt at diene formation used 50 mol% of palladium(II) acetate with no ligand or base and three equivalents of boronate **42** with respect to vinyl iodide **269**, using acetonitrile as the solvent (**Equation 36**). After 2 days 2-[(1*E*)-buta-1,3-dien-1-yl]-4,4,6-trimethyl-1,3,2-dioxaborinane **276** was isolated in a 78% yield with approximately 90% purity, giving an approximate 68% yield.

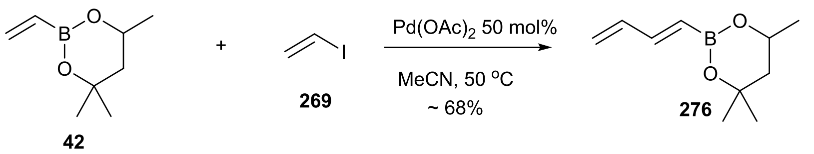

(36)

Diene **276** formation was attempted again, using 5 mol% of palladium(II) acetate and 1.3 equivalents of boronate **42**. All other conditions remained the same as the previous reaction (**Equation 37**). A low crude mass recovery of 73% was obtained after work up, with less than 5% product formation evident from the crude ^{1}H NMR. These conditions were also used in an attempt to form the triene from a sample of diene **276** already isolated. No signals that could be ascribed to product could be observed in the ^{1}H NMR spectrum.

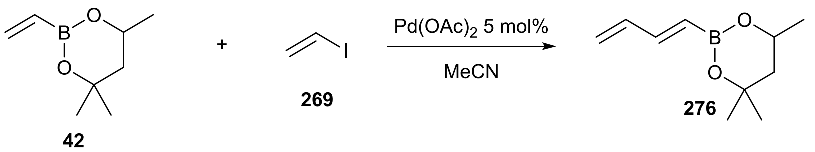

(37)

This result raised the question as to how the reaction is progressing, be it stoichiometrically or catalytically. In order to investigate the possibility of obtaining a successful catalytic reaction, it was decided to screen for appropriate ligands and bases, in the hope that a combination could be found that could yield a satisfactory yield of diene **276**, especially at low catalyst loadings. A slightly higher, though still catalytic, loading of 10 mol% palladium(II) acetate was chosen, along with generic conditions of 1.3 equivalents boronate **42**, 1.2 equivalents base and 1 equivalent bidentate ligand or 2 equivalents monodentate ligand with respect to catalyst. Two bases were chosen i.e silver acetate (this base was currently used within the group to achieve HM couplings) and triethylamine (an example of a standard amine base). The three ligands chosen were triphenylphosphine, tri(*o*-tolyl)phosphine (these ligands were currently used within the group) and the bidentate 1,1'-bis(diphenylphosphino)ferrocene (dppf). Naphthalene (0.1 equivalents) with respect to vinyl iodide **269** was also added as an internal reference to allow calculation of conversion from ^{1}H NMR spectra. The reactions were stirred vigorously at 50 °C for 3 days and investigated by ^{1}H NMR (**Table 16, Equation 38**).

The best conditions were clearly identifiable as those involving silver(I) acetate as the base (**Table 16**, **Entries 5-8**), with the highest conversion of 52% seen where tri(*o*-tolyl)phosphine was used as the ligand (**Table 16**, **Entry 7**). Use of triethylamine (**Table 16**, **Entries 9-12**) yielded no product, and minimal product formation occurred where there was no base (**Table 16**, **Entries 1-4**). Use of the dppf ligand (**Table 16**, **Entries 4** and **8**) seemed to result in lower product conversions. Further analysis of the spectra revealed that the starting materials were not being exclusively converted to product. It seemed that a large amount of the vinyl iodide **5** was being consumed in another side-reaction in addition to the desired HM coupling. This is evident from the crude ^{1}H NMR spectrum of **Entry 7**, where complete vinyl iodide consumption had occurred despite only 52% conversion to diene **276** (**Figure 22**).

Table 16 Determining optimal reaction conditions for formation of diene **276**

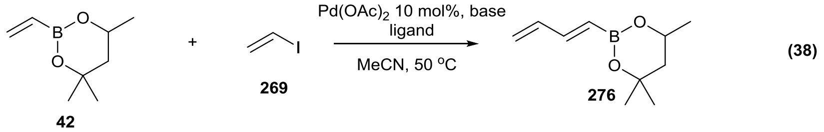

Entry	Base	Ligand	Approx. conversion/ %
1	-	-	4
2	-	PPh_3	2
3	-	P(*o*-tol)$_3$	1
4	-	dppf	<1
5	AgOAc	-	42
6	AgOAc	PPh_3	30[a]
7	AgOAc	P(*o*-tol)$_3$	52
8	AgOAc	dppf	20[a]
9	Et_3N	-	-
10	Et_3N	PPh_3	-
11	Et_3N	P(*o*-tol)$_3$	-[b]
12	Et_3N	dppf	-[c]

[a] Complex ^{1}H NMR spectra may have rendered these estimates less accurate due to overlapping peaks.

[b] ^{1}H NMR too complex to accurately estimate product conversion.

[c] ^{1}H NMR highly complex, but no product signals present.

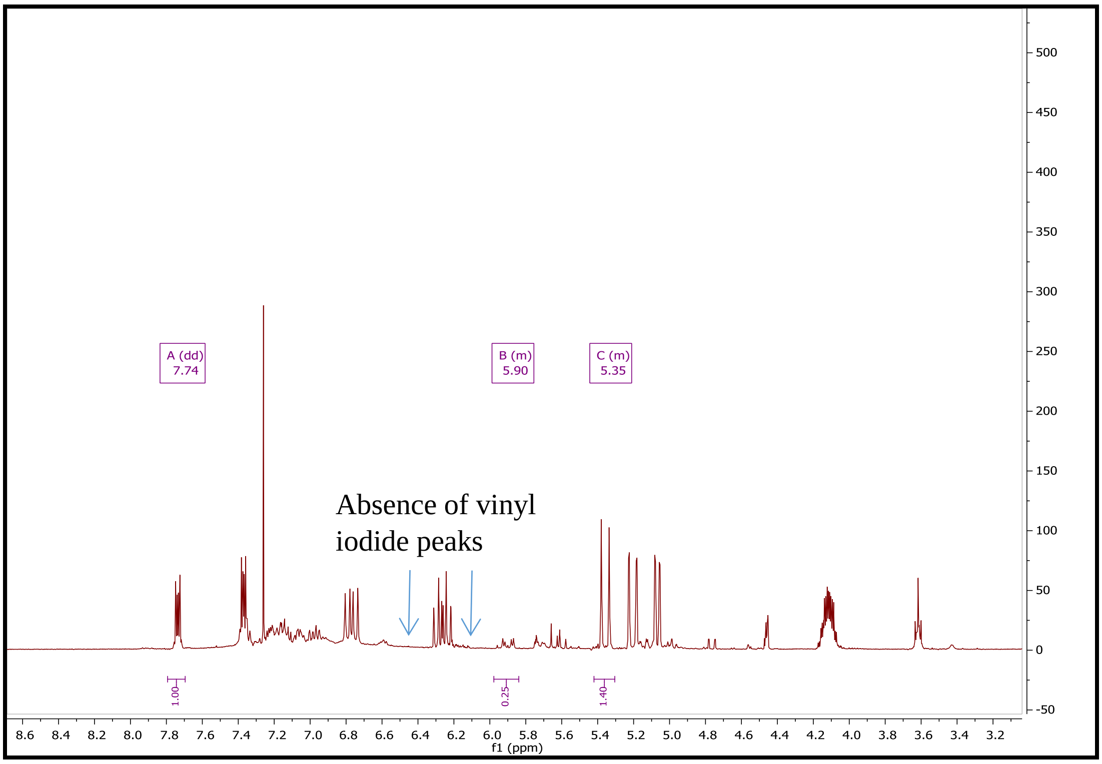

Figure 22 Crude ^{1}H NMR spectrum (**Table 16**, **Entry 7**) highlighting the consumption of vinyl iodide **269**. Vinyl iodide gives signals of a doublet of doublets at δ 6.22 ppm and a multiplet between δ 6.43 and 6.58 ppm.

Our attention was then turned to the optimization of the conditions identified above. In order to determine whether or not the reaction was stalling, the reaction was repeated and monitored by gas chromatography (GC) to analyse its progression, with the results summarised in **Figure 23**. This indicated that the reaction initially progresses rapidly and then stalls. Addition of one further equivalent vinyl iodide at 22 hours, along with a further 5 mol% palladium(II) acetate addition at 27 hours did not seem to make much difference to the reaction, which continued to progress slowly.

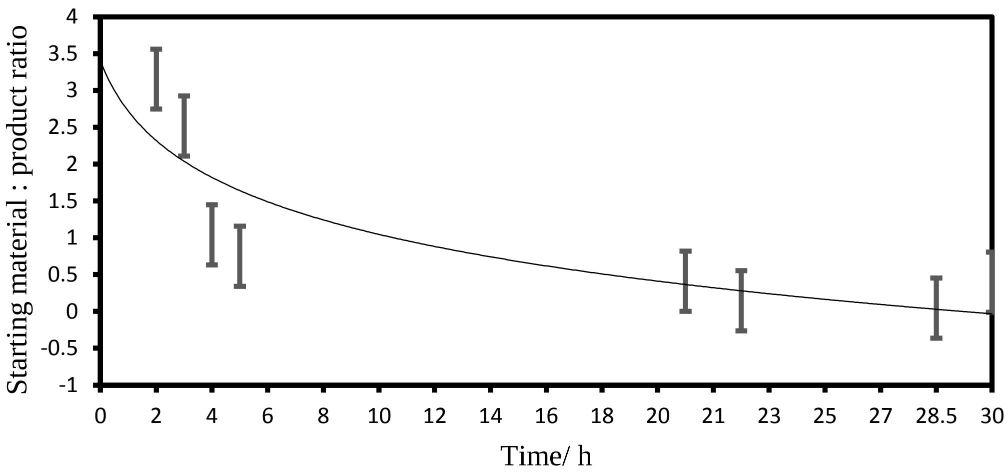

Figure 23 Graph showing diene **276**:vinyl boronate **42** ratio over time.

The lower ratios at 22 and 28.5 hours suggest that the reaction almost reached completion, but these appear to be anomalous as the final ratio of 0.39 agrees with the crude ^{1}H HMR obtained after 30.5 hours. When combined with the crude ^{1}H HMR data, the GC data suggest that the reaction stalled at between 60 and 70% completion, with addition of further catalyst and vinyl iodide having no effect. A number of theories to explain why the reaction tended to stall were investigated (e.g. loss of vinyl iodide, catalyst turnover, base equivalents etc.). The loss of vinyl iodide **269** during the course of the reaction needed to be addressed, although **Figure 22** shows that addition of vinyl iodide at 22 hours did not increase product formation. Vinyl iodide **269** was stirred at room temperature with silver(I) acetate for several days to ascertain whether it was reacting with the base, but no reaction was observed. In order to establish whether or not vinyl iodide **269** was capable of undergoing a HM coupling with itself, a HM coupling using the 5 mol% $Pd(OAc)_2$, 10 mol% P(*o*-tol)$_3$, 1.2 equivalents AgOAc and only vinyl iodide **269** was set up. Crude ^{1}H NMR analysis showed small peaks, which had been previously observed for the previous HM couplings, but not with a larger integral to those previously observed. The doublets of doublets at δ 4.50, 4.80 and 7.17 were identified as vinyl acetate. The vinyl iodide remained largely untouched and no dienyl signals were observed (**Figure 24**).

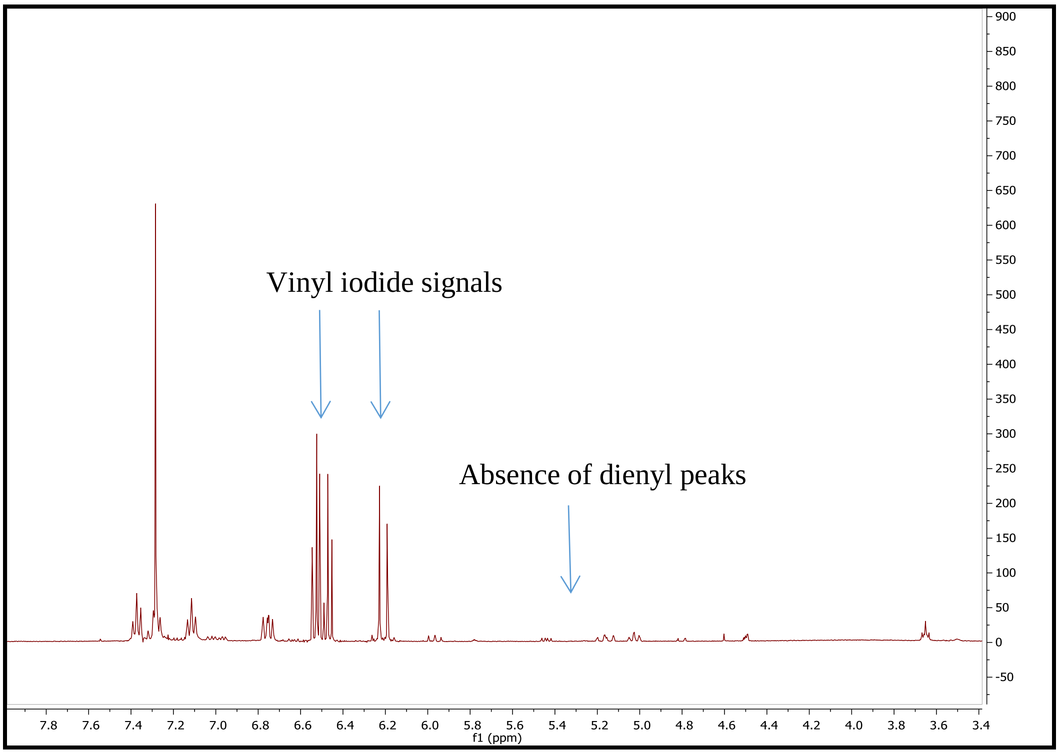

Figure 24 Crude ^{1}H NMR spectrum, showing the unreactivity of vinyl iodide **269** towards itself under HM conditions.

It was later noted that the suba seal placed into the top of the Schlenk flask expanded considerably during the course of these reactions, suggesting that the cause of vinyl iodide disappearance was its absorption by this seal.

A number of screens were undertaken in an attempt to optimise the reaction to form diene **276**. The optimal ratio of vinyl boronate **42** to vinyl iodide **269** was investigated (**Table 17**). Use of 1.2 equivalents of **42** resulted in a significant increase in conversion (**Table 17**, **Entry 4**) from 43 to 69%. The reaction, however, did not go to completion. Purification of diene **276** to this point had proven difficult, with complete removal of the vinyl boronate starting material **42** and ligand having not been achieved. Furthermore, diene **276** proved susceptible to polymerization on silica. This resulted in a considerable loss of yield in cases where extra care had to be taken in an attempt to remove as many of the unwanted compounds from diene **276** as possible. Vinyl boronate **42** proved by far the most difficult to remove, being extremely similar in polarity, and thus optimizing the reaction conditions to give 100% consumption of vinyl boronate seemed essential. This meant that conditions needed to be found that achieved 100% conversion, with a 1:1 ratio of vinyl boronate **42** to vinyl iodide **269**.

Table 17 Determining optimal starting material ratios for formation of diene **276**

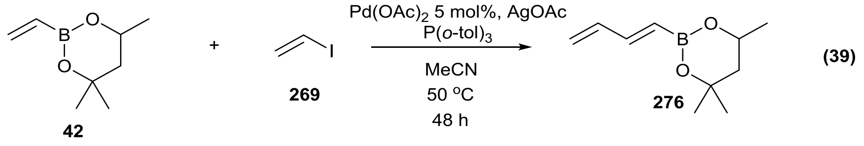

Entry	Equivalents **42** added wrt vinyl iodide **269**	Approx. conversion / %
1	0.8	44
2	1	43
3	1.1	50
4	1.2	69

Product formation monitored by ^{1}H NMR. Ratios estimated using integrals from crude ^{1}H NMR spectra.

A catalyst screen was then undertaken (**Table 18**, **Equation 40**). None of the catalysts investigated resulted in an increased yield. It was noted that palladium(II) chloride and palladium(II) bromide gave comparable yields, and also resulted in less vinyl acetate formation as determined by ^{1}H NMR (**Table 18**, **Entries 5** and **6**).

Table 18 Results of catalyst screen for the reaction of iodide **269** and boronate **42**

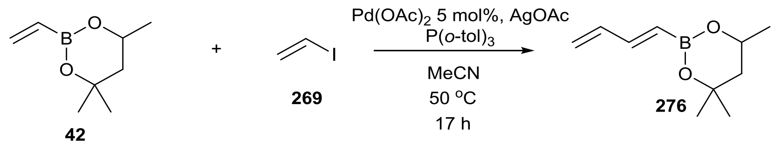

(40)

Entry	Catalyst used	Conversion to **276** after 17 h/ %
1	$Pd(OAc)_2$	55
2	$Pd(dba)_2$	35
3	$Pd(dppf)Cl_2$	47
4	$Pd(PPh_3)_2Cl_2$	25
5	$PdCl_2$	50
6	$PdBr_2$	50
7	PdI_2	40

Product formation monitored by GC, using naphthalene as internal standard.

The effect of base loading on the rate of reaction was then investigated (**Table 19**, **Equation 41**). The relationship between base loading and both the mmol concentrations of vinyl boronate **42** and desired diene **276** is shown in **Figure 25**. It shows that an increase in base concentration resulted in an increase in diene formation, beginning to plateau out after 1.5 equivalents of silver(I) acetate. Formation of diene **276** reached a peak at 1.8 equivalents of base. The concentration of vinyl boronate **42** showed a dramatic drop at this loading. This result was corroborated by the crude ^{1}H NMR spectrum, but was presumed to be due to an error in vinyl boronate addition. The HM reaction mixtures were not clear solutions, but a grey suspension due to the poor solubility of silver(I) acetate in acetonitrile. Previous work done in this group suggested that competitive HI elimination from olefinic iodides could be a competing issue in palladium cross-coupling reactions with alkenyl and polyenyl iodides.[192] Being highly iodophilic, the silver cation is presumed to strip the palladium complex of chelated iodine, helping cycle turnover and therefore facilitating cross-coupling before elimination can take place. This suggests that the improvement in reactivity could be due to either an increase in accessibility to either the silver, or the acetate, or both. In order to establish whether the increase in diene formation was due to an increase in silver cations or due to an increase in acetate anions, a HM coupling was undertaken using 1 equivalent of silver(I) acetate and 0.8 equivalents of a more organic-soluble acetate source, tetrabutylammonium acetate. The crude ^{1}H NMR after 17 hours indicates the presence of numerous compounds, but not diene **276**. It was therefore concluded that the increase in reaction as observed in the base loading screen (**Table 19**, **Figure 25**) was due to the increase in accessible silver cation concentration as opposed to acetate anion concentration.

Table 19 The effect of base loading on the reaction between **42** and **269**

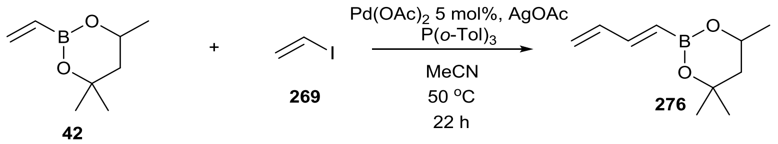

(41)

Entry	Equivalents base used	Diene **276** concentration after 24 h/ mmol	Vinyl boronate **42** concentration after 24 h/ mmol
1	1	0.268	0.496
2	1.2	0.336	0.298
3	1.5	0.458	0.309
4	1.8	0.513	0.096
5	2	0.510	0.252

Product formation monitored by GC, using naphthalene as internal standard.

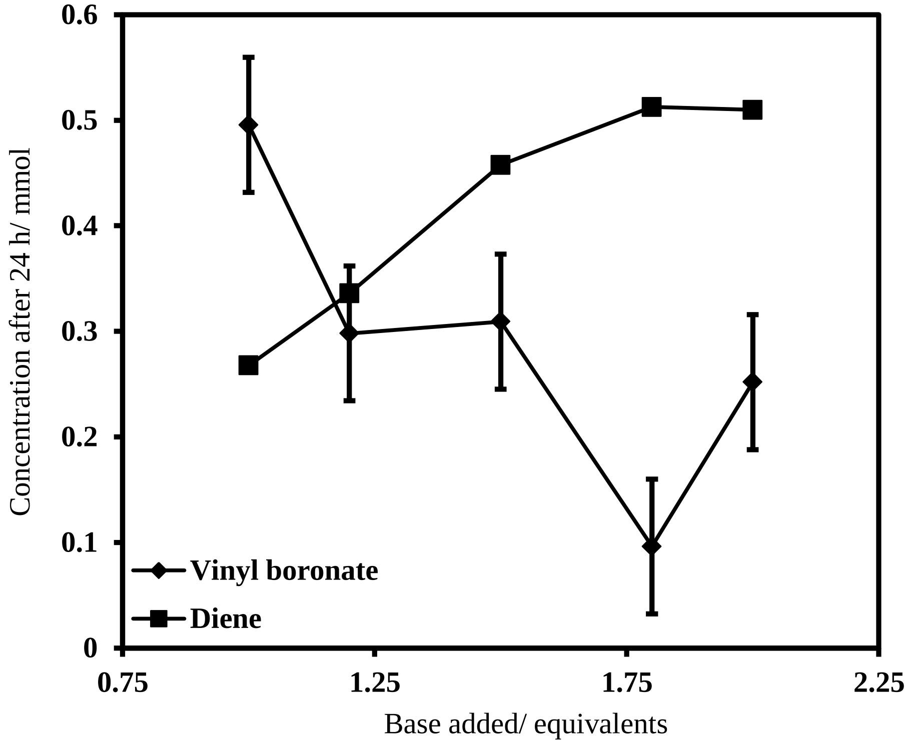

Figure 25 Graph showing the effect of base loading on the mmol concentration of vinyl boronate **42** and diene **276**

A number of different dilutions were tried to see if this would have an effect on the amount of silver accessible for reaction. None of these had any measurable effect on product formation. The reaction was attempted at reflux and under these conditions, the reaction still stalled, only at a faster rate. It was eventually found that undertaking the reaction in a round bottom flask gave a dramatically increased completion of 85% after 24 hours. This is a result that was repeated consistently and is presumed to be due to the more vigorous stirring that could be achieved when using a round bottomed flask. Diene **276** has since been isolated in yields of up to 73%, which has been assessed as an adequate yield to progress on with despite the need for further optimisation. To mitigate the tendency of **276** to polymerise on purification, *ca.* 3 ppm of 2,6-di-*tert*-butyl-4-methyl phenol (BHT) was employed in eluents. Also, prolonged air exposure of the dienes resulted in polymerisation, hence, storage under argon at approx. 4 °C was required with 20 ppm BHT.

Section 2.1.2 Expanding substrate scope

Vinyl iodide **269** was also investigated as an HM coupling partner for a number of other alkenyl substrates (**Table 20**, **Equation 42**).[173] It was originally believed that electron deficient alkenes would react most effectively based on the assumption that this HM coupling was progressing *via* an electron-rich Michael-type palladium intermediate (**Scheme 64**).[193] This mechanism involves addition of the electrons from the bond formed between the alkene donor and palladium to the alkene acceptor, with the end result being a migratory insertion of the donor onto the acceptor. Palladium activation of the alkene acceptor can play a part in this process if there are electron withdrawing groups coordinated to the palladium at this part, but the best reactivity will be observed with an electron deficient terminal alkene on the acceptor. It would therefore be expected that the acrylates **296-299** (**Table 20**, **Entries 1-4**) would be the most reactive due to their good Michael acceptor capability and that the highly electron-rich vinyl acetate **304** (**Table 20**, **Entry 9**) would react poorly.

Scheme 64 A catalytic cycle for the HM coupling, where progression of the cycle involves Michael-type addition onto the acceptor alkene.

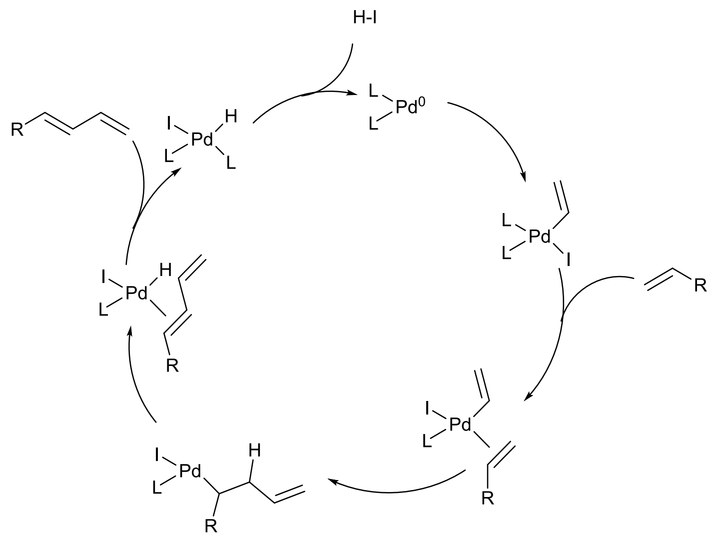

Initially, alkenes **296-299**, and **300-304** were all tested and, surprisingly, all were unreactive towards HM coupling with vinyl iodide. The most reactive was methyl acrylate **296** (**Table 20**, **Entry 1**), the crude ^{1}H NMR of which after 36 hours showed an extremely poor conversion of 3%. This reaction was repeated at reflux and an increased, but still very poor conversion of 7% was achieved. Methyl vinyl ketone **297** (**Table 20**, **Entry 2**) was the only other alkene to give any visible product by ^{1}H NMR, just identifiable at 1% conversion. It appeared that neutral and electron rich alkenes were completely unreactive to HM coupling with vinyl iodide **269**. It was hypothesised that the poor reactivity of these alkenes with respect to the successful vinyl boronate **42** was due to their lack of steric bulk. It seemed possible that the bulk of ester **42** was resulting in a more crowded and therefore less stable palladium species, aiding expulsion of the desired dienyl product and helping catalyst turnover.

Table 20 Yields obtained for HM coupling of a range of different alkenes with vinyl iodide **269**

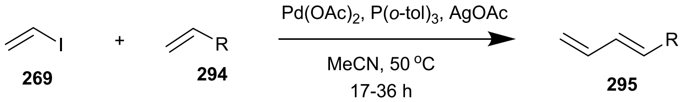

(42)

Entry	Alkene	Yield/ %
1	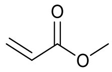 **296**	3, 7[a]
2	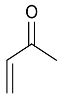 **297**	1
3	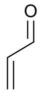 **298**	0
4	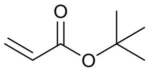 **299**	9
5	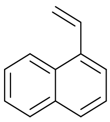 **300**	0
6	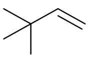 **301**	0
7	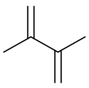 **302**	0
8	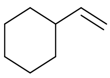 **303**	0

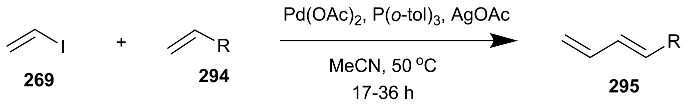

(42)

Entry	Alkene	Yield/ %
9	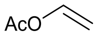 304	0
10	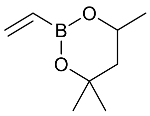 42	73[b]
11	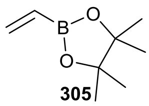 305	72[b]
12	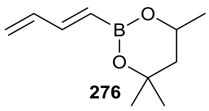 276	0
13	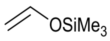 306	0

Product formation monitored by ^{1}H NMR. [a]Reaction done at reflux. [b]Isolated yield.

To this end, *tert*-butyl acrylate **299** was used (**Table 20**, **Entry 4**). The increase in steric bulk did give a small increase in diene formation, at 9%, but not a large enough conversion to establish increased steric bulk as a criterion for successful reaction. Vinylboronic acid pinacol ester **305** (**Table 20**, **Entry 11**) was also reactive, giving the diene in an isolated yield of 72% on the first attempt. Attempts to achieve further homologation with diene **276** were also unsuccessful (**Table 20**, **Entry 12**). Silyl-enol ether **306** (**Table 20**, **Entry 13**) also proved unreactive. The reason for the peculiar reactivity of these substrates is unclear. One theory is that the vinyl boronate interacts with a palladium intermediate in such a way as to make the coupling favourable. Two possible forms **307** and **308** for this interaction have been envisaged, depending on the form of the boronate in solution. As previously discussed, the amount of free acetate present in solution remains unclear, and it is not known whether the boronate will be present as a three-valent species, or as the four-coordinate boronate anion formed by coordination of a free acetate to the boron. In reality, both species will most likely be present. The first possible interaction could be between the empty p-orbital on the three-valent boron and the d-orbitals on the electron rich palladium intermediate, either bringing the alkene closer to the palladium for successful alkene coordination or stabilising the alkene-coordinated intermediate to allow for successful carbometallation (structure **307**). The second possible interaction is a more formal coordination of the acetate on the four-valent boronate anion, forming a stabilising chelate ring (structure **308**). Both of these interactions could also result in a lengthening of the palladium-iodide bond, making it easier for a silver cation to strip it from the palladium and regenerate the active palladium(0) catalyst.

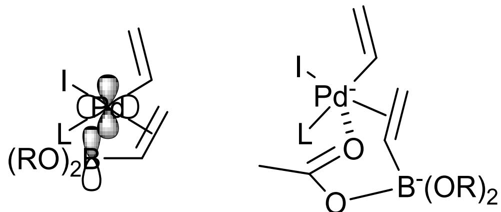

307 **308**

If an interaction such as this is the cause for the increased reactivity of the vinyl boronates to HM coupling with vinyl iodide **269**, it might offer an explanation for the lack of reactivity of diene **276** to further homologation. It is true that the terminal alkene of the diene is likely to be less reactive due to its increased distance from the electronic influence of the boronate ester group. However, the complete lack of reactivity of diene **269** suggests that another contributing factor may also be implicated. The structure **307** requires overlap with the palladium d-orbitals. It may be in the case of diene **276** that the boron is now too far away from the palladium centre and the orbital overlap is not good enough to create an interaction. The interaction depicted in structure **308** involves chelate ring formation, and here the negative effect of diene **276** could be one of coordination ring size. Structure **308** shows a seven-membered chelate, whereas the chelate formed by diene **276** would be a less favourable 9-membered chelate. If structure **307** is possible, then one might expect a vinyl silane to react well in a HM coupling with vinyl iodide. This is because silicon has an empty d-orbital and, in fact, the better matched symmetry between the palladium and silicon orbitals may result in a higher reactivity for vinyl silanes with respect to vinyl boronate species.

In light of this, a range of new vinyl substrates were chosen to investigate their reactivity with vinyl iodide **269** in a HM coupling (**Table 21**, **Equation 43**). A range of vinyl silanes and siloxanes were chosen to see if these could also form a favourable interaction during the carbometallation step (**Table 21**, **Entries 6**, **7** and **11**). Vinyl stannane **248** was also chosen, as it also had the potential to form a favourable interaction (**Table 21**, **Entry 10**). Phosphonate ester **311**, sulfone **312** and vinyl BMIDA **314** were also chosen as substrates that should not be able to form an additional interaction (**Table 21**, **Entries 8**, **9** and **12**). Initially, these couplings were attempted using one equivalent of acceptor with respect to vinyl iodide, as was used for the couplings detailed in **Table 20**. Vinyl silanes **309** and **310** did show an increased level of reactivity when compared to Michael acceptors **296**, **297** and **299**, though these conversions were only modest when compared to the vinyl boronates **42** and **305** (17% and 24% for silanes **309** and **310**, respectively, **Table 21**, **Entries 6** and **7**). This is perhaps not surprising due to the more diffuse nature of the silicon d-orbitals, possibly resulting in a less strong chelation with the palladium complex. Vinyl (triphenyl) silane **313** was investigated as a substrate, as it was thought that the aromatic phenyl groups would be able to stabilise the chelated 'siliconate' anion. However, no reactivity was seen (**Table 21**, **Entry 11**). This was attributed to the large steric bulk of the triphenyl silyl group destabilising the chelate ring.

As expected, vinyl phosphonate **311** and vinyl sulfone **312** displayed very poor reactivity, with less than 5% diene observed for both (**Table 21**, **Entries 8** and **9**). Interestingly, vinyl boronic acid MIDA ester **314** displayed no reactivity (**Table 21**, **Entry 12**). The MIDA ester has all four coordinating sites fully occupied and therefore would not be capable of forming the supposed chelation to facilitate the reaction. This lack of reactivity supports the theory that the effect of the boronate ester and silyl groups is one of chelational assistance.

Table 21 Reactivity of new vinyl acceptors and effect of acceptor loading on reaction conversion.

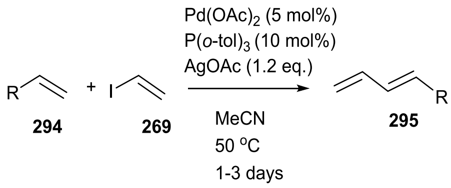

294 + **269** → **295** **(43)**

Entry	Acceptor	(Conversion) [Isolated yield]/ %			
		1 equivalent acceptor	1.2 equivalents acceptor	2 equivalents acceptor	3x scale (2 equivalents acceptor)
1	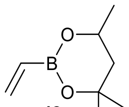 **42**	(100) [72]	-	(94)	-
2	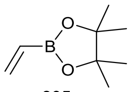 **305**	(91)[72]	-	(55)	-
3	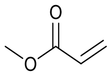 **296**	(3)	-	(24)	(42)
4	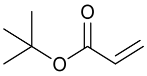 **299**	(9)	-	(42)	(46) [28]
5	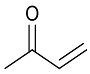 **297**	(1)	-	(48)	(68)
6	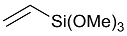 **309**	(17)	(21)	(33)	(42)
7	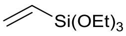 **310**	(24)	(12)	(36)	(50)
8	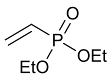 **311**	(<5)	-	(15)	(12)

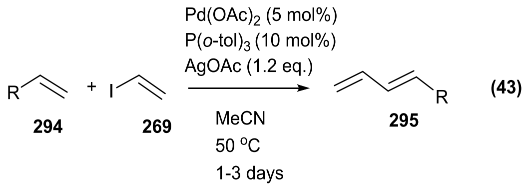

Entry	Acceptor	(Conversion) [Isolated yield]/ %			
		1 equivalent acceptor	1.2 equivalents acceptor	2 equivalents acceptor	3x scale (2 equivalents acceptor)
9	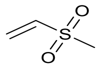 312	(<5)	-	(18)	(14)
10	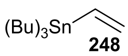 248	-	(0)	-	-
11	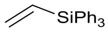 313	(0)	(0)	-	-
12	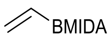 314	(0)	-	-	-

On revisiting a previous substrate screen, it was noted that one attempt to extend methyl acrylate **296** gave a much higher conversion of 19%, compared to the 3% consistently seen beforehand. This experiment had previously been discounted due to an inefficient seal and consequential loss of a significant proportion of the vinyl iodide. This suggested that an excess of acceptor may furnish increased reactivity.

In an attempt to improve the conversions for the vinyl silane acceptors **309** and **310**, 1.2 equivalents of acceptor were used (**Table 21**, **Entries 6** and **7**). For the methyl variant **309**, a 5% increase in conversion was observed (although the ethyl variant **310** gave lower conversions) and hence two equivalents were tried. This gave vastly improved conversions of 33 and 36% for **309** and **310** respectively. On increasing the scale by three times, conversions further increased to 42% and 50%. The reason for this lies in the insolubility of silver(I) acetate. The reaction mixture is a suspension due to this and mass transfer is a key factor in the success of these reactions. It was been found that carrying out these reactions on a larger scale significantly improved the level of stirring that was achieved, and consequently an increase in conversion was generally observed. In fact, the 100% conversion obtained for vinyl boronate **42** (**Table 21**, **Entry 1**) was only ever achieved on larger scales.

These conditions were then applied to other acceptors and these results can be seen in **Table 21**. Acceptors **296**, **297** and **299**, and **309-312** all showed significantly increased conversions, with the starkest improvement being that of methyl vinyl ketone **297** (**Table 21**, **Entry 5**), which went from 1% conversion with one equivalent of acceptor, to 68% with two equivalents on increased scale. Additionally, HM coupling was attempted using 1.2 equivalents of vinyl (tributyl)silane **248**, with exclusive formation of the Stille product observed (**Table 21**, **Entry 10**).

The dramatic increase in yield on increasing the amount of acceptor to two equivalents raises even more mechanistic questions than did the peculiar reactivity of the vinyl boronates **42** and **305**. In particular, the lesser effect observed with the vinyl silanes is intriguing. Methyl acrylate **296** and methyl vinyl ketone **297** showed the greatest improvement, with these substrates also being the least sterically hindered. It is possible that multiple acceptor molecules coordinate to palladium in this mechanism, speeding up the rate of reductive elimination. In the case of *tert*-butyl acrylate **299** and the silanes **309** and **310**, it could be that the steric bulk is slowing this process, leading to a smaller increase in conversion.

Attempts to isolate the dienes formed were met with limited success. The products were highly susceptible to polymerisation; particularly those formed from methyl acrylate **9**, methyl vinyl ketone **297**, and the vinyl silanes **309** and **310**. Dienyl silanes **315** and **316** polymerised within 24 hours at room temperature, even under argon. The crude dienes could be stored, however, at -18 ^{o}C and use of BHT in reaction mixtures, work up solvents and eluents helped to relieve issues with polymerisation in some cases.

The volatility of the acrylates and methyl vinyl ketone **296**, **297** and **297**, allowed the excess acceptor to be easily removed from the crude mixture *in vacuo*. However, only the *tert*-butyl derivative **317** proved stable to silica gel chromatography and could be readily purified. The vinyl silanes **309** and **310**, vinyl phosphonate **311** and vinyl sulfone **312** could not be removed from the crude reaction mixture *in vacuo* and to date a method to separate the vinyl acceptor and diene has not been found due to the similarity of the compounds. Excess acceptor and the resulting dienes have consistently run as one spot on thin layer chromatography (TLC) in all systems attempted. Whilst only dienyl boronates **276** and **318**, and *tert*-butyl derivative **317** were successfully isolated, the other crude dienes were identified using ^{1}H NMR and accurate mass.

Despite the greatly increased conversions seen for substrates **296**, **297** and **299**, and **309-312**, the reaction times were still much longer than those for vinyl boronates **42** and **305** (2-3 days for the prior substrates compared with 3-6 hours for the vinyl boronates). This suggests that the excess acceptor was key for the coupling, but the chelational assistance of the boronate ester group may be more important.

Triene formation was attempted on dienyl boronate **276**, but no triene was observed. If we assume that the facilitation of the HM coupling with vinyl boronates **42** and **305** is due to the formation of 7-membered chelate **308**, then the diene would form a 9-membered chelate, which is less favourable.

Section 2.1.3 Derivatisation of dienes

In light of the instability of the dienes formed in **Section 2.1.2** and the difficulty in separating them from the excess of acceptor used in the reaction mixture, it became desirable to try to functionalise them so that they could be more easily isolated. This was initially done *via* a series of ^{1}H NMR experiments. Attention was focussed on (*1E*)-buta-1,3-dien-1-yltriethoxysilane **316**, due its high susceptibility to polymerisation.

Compound **316** was combined with 2.5 equivalents of three different aryl nitroso compounds with deuterated chloroform ($CDCl_3$) in an attempt to form the cycloadduct (**Table 22**, **Equation 44**). A further NMR experiment where the $CDCl_3$ was first passed through an alumina plug to remove traces of acid was also undertaken, as it had previously been found within the group that acid could have an effect on the reaction. In all cases peaks corresponding to the oxazine were observed. It was found that the more electron withdrawing nitroso dienophiles gave the best conversions (**Table 22**, **Entries 1**, **3** and **4**). It appeared that two regioisomers were formed. Whilst the regioisomers were not isolated and characterised separately, it was presumed that the major regioisomer **321** was the one with least steric hinderance, as this had been observed for other dienyl systems within the group previously[194] (**Equation 44**, **Figure 26**). For the methoxy and methyl carboxylate derivatives of nitrosobenzene **320b** and **320c**, the levels of each regioisomer remained consistent (**Table 22**, **Entries 2** and **3**). However, in the case of nitrosobenzene, a slightly higher proportion of regioisomer **322** was observed after 3 hours (1:0.22 and 0.19, compared with 1:0.14 and 0.13 for **Entries 1** and **4**, respectively). Whilst the difference is small, this could indicate that the oxazine formation is in fact reversible and that a conversion between the kinetic regioisomer **322** and the thermodynamic, less sterically hindered regioisomer **321** may be occurring. (*1E*)-Buta-1,3-dien-1-yltrimethoxysilane **315** was also used to see the difference with the change in alkoxy group size. This methoxy analogue seemed to show a similar level reactivity to ethoxy analogue **316** after 5 hours, although there was not a corresponding ^{1}H NMR to confirm the conversion after 18 hours. Additionally, the level of regioisomer **322** at this time is wass line with that seen for the ethoxy analogue **316**.

Table 22 Attempted functionalization of dienyl silanes **315** and **316**, forming oxazine products.

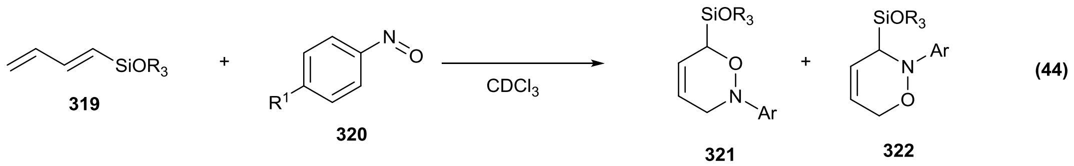

Entry	R group	R^1 group	Conversion (Reaction time)/ %	Regioisomeric ratio **321**:**322**
1	OEt	H (**320a**)	100 (18 h)	1:0.14
2	OEt	OMe (**320b**)	34 (18 h)	1:0.17
3	OEt	COOEt (**320c**)	100 (18 h)	1:0.12
4	OEt	H (**320a**)	94 (18 h) (acid traces removed)	1: 0.13
5	OMe	H (**320a**)	65 (5 h)	1:0.18

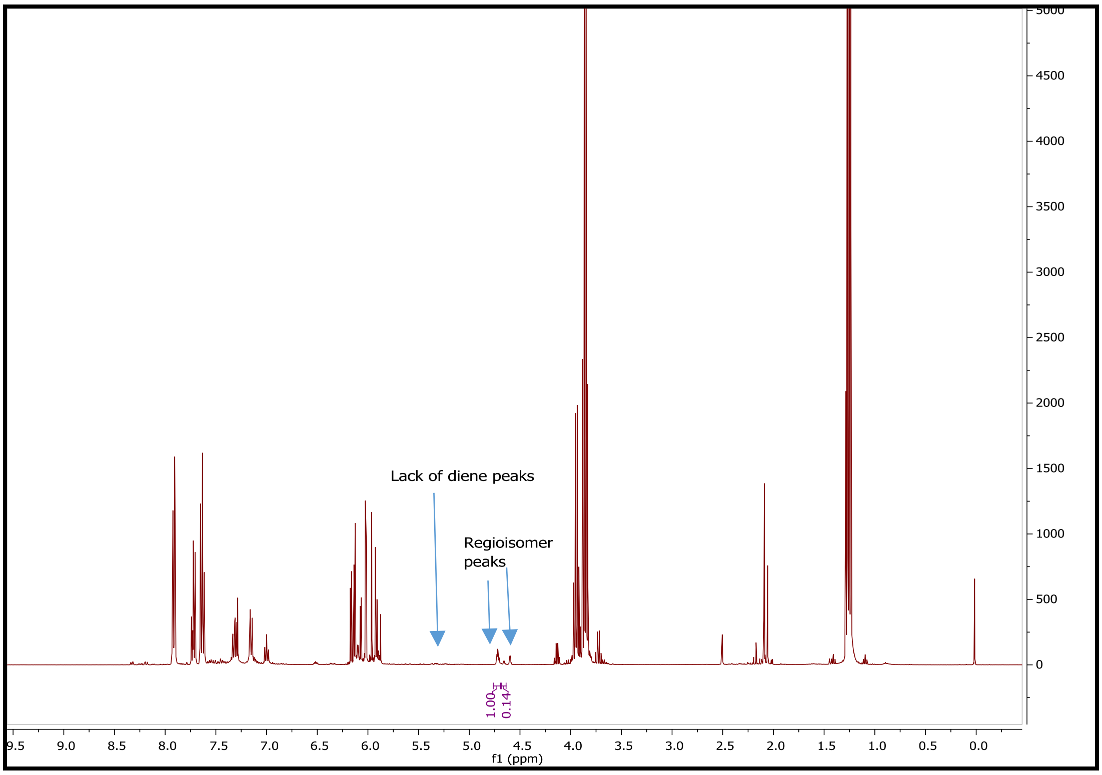

Figure 26 ^{1}H NMR of attempted nitrosocycloaddition onto dienyl silane **316** (**Table 22**, **Entry 1)**, showing the consumption of diene and the two supposed regioisomers **321** and **322**

A Diels-Alder cycloaddition was also attempted on (*1E*)-buta-1,3-dien-1-yltriethoxysilane **316** using 4-phenyl-1,2,4-triazoline-3,5-dione **323**. All of the diene was consumed but no product was visible from the ^{1}H NMR (**Figure 27**, **Equation 45**). However, a precipitate was formed. ^{1}H NMR analysis of this did not indicate presence of the desired cycloadduct **324**.

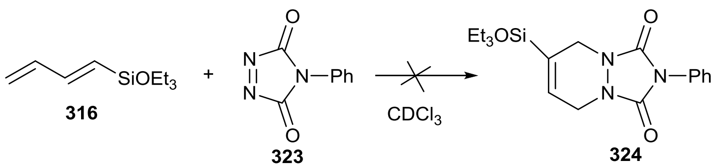

(45)

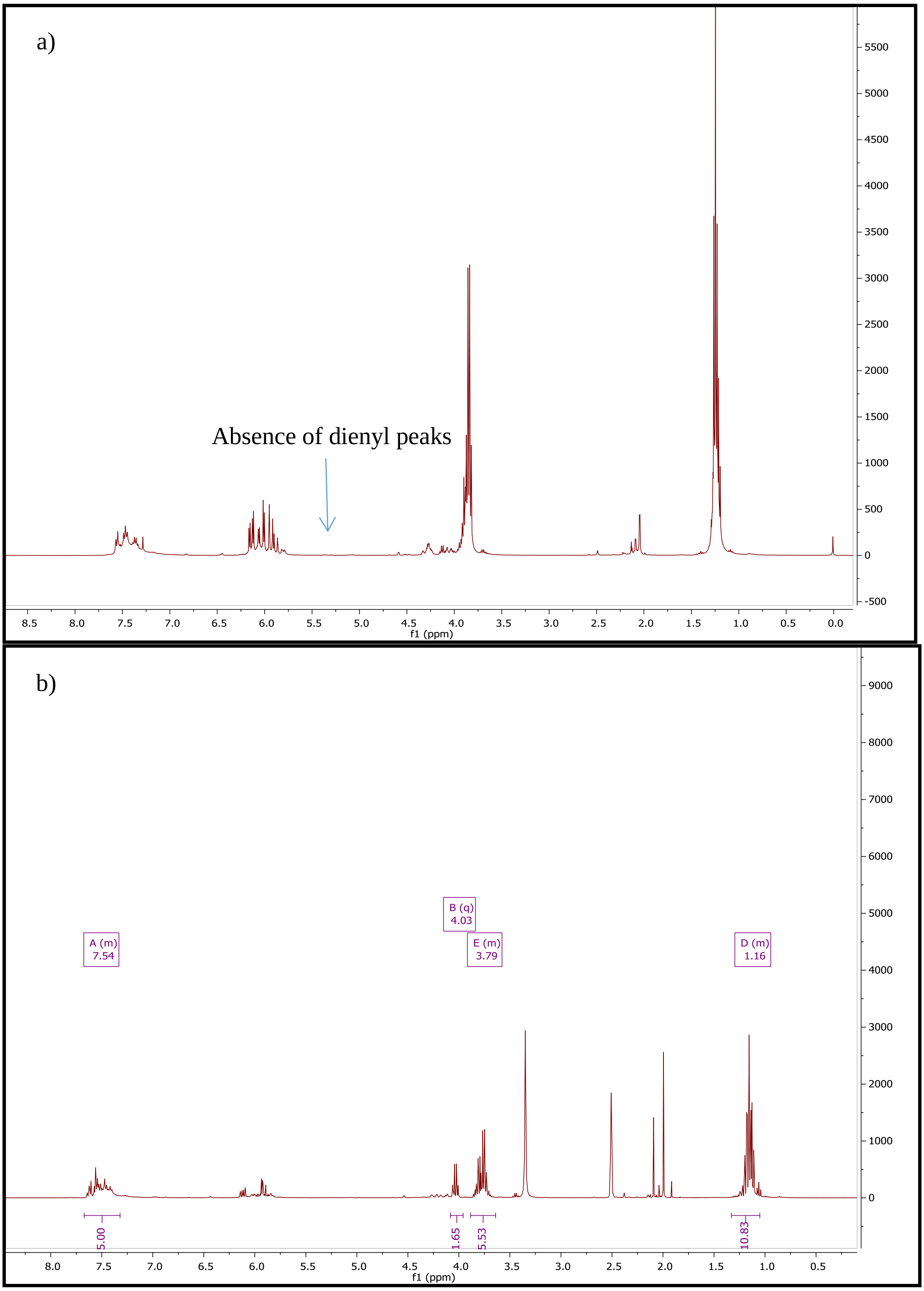

Figure 27 ^{1}H NMR spectrum of **a)** the attempted Diels-Alder cycloaddition, showing complete consumption of diene **316** and **b)** the precipitate formed during the reaction.

A sample of (*1E*)-buta-1,3-dien-1-yltriethoxysilane **316** was dissolved in $CDCl_3$ and acetyl chloride **325** added in an attempt to desilylate the diene (**Equation 46**). **Figure 28** shows the result of treatment with acetyl chloride, the diene peaks shifted downfield and formation of ethyl acetate. However, butadiene **249** was not observed, suggesting that the result of this reaction was actually the reaction between an acyl and an ethoxy on the silicon group, supported by the formation of ethyl acetate. Only one equivalent of acetyl chloride was used, so the exact result of this reaction is unclear.

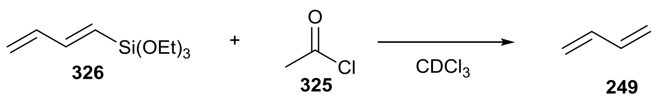

(46)

A sample of methyl (*2E*)-penta-2,4-dienoate **326** was treated with 33% ammonia solution in an attempt to make amide **327** (**Equation 47**). Unfortunately, no change was observed in either the proton or the carbon NMR.

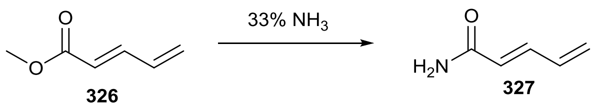

(47)

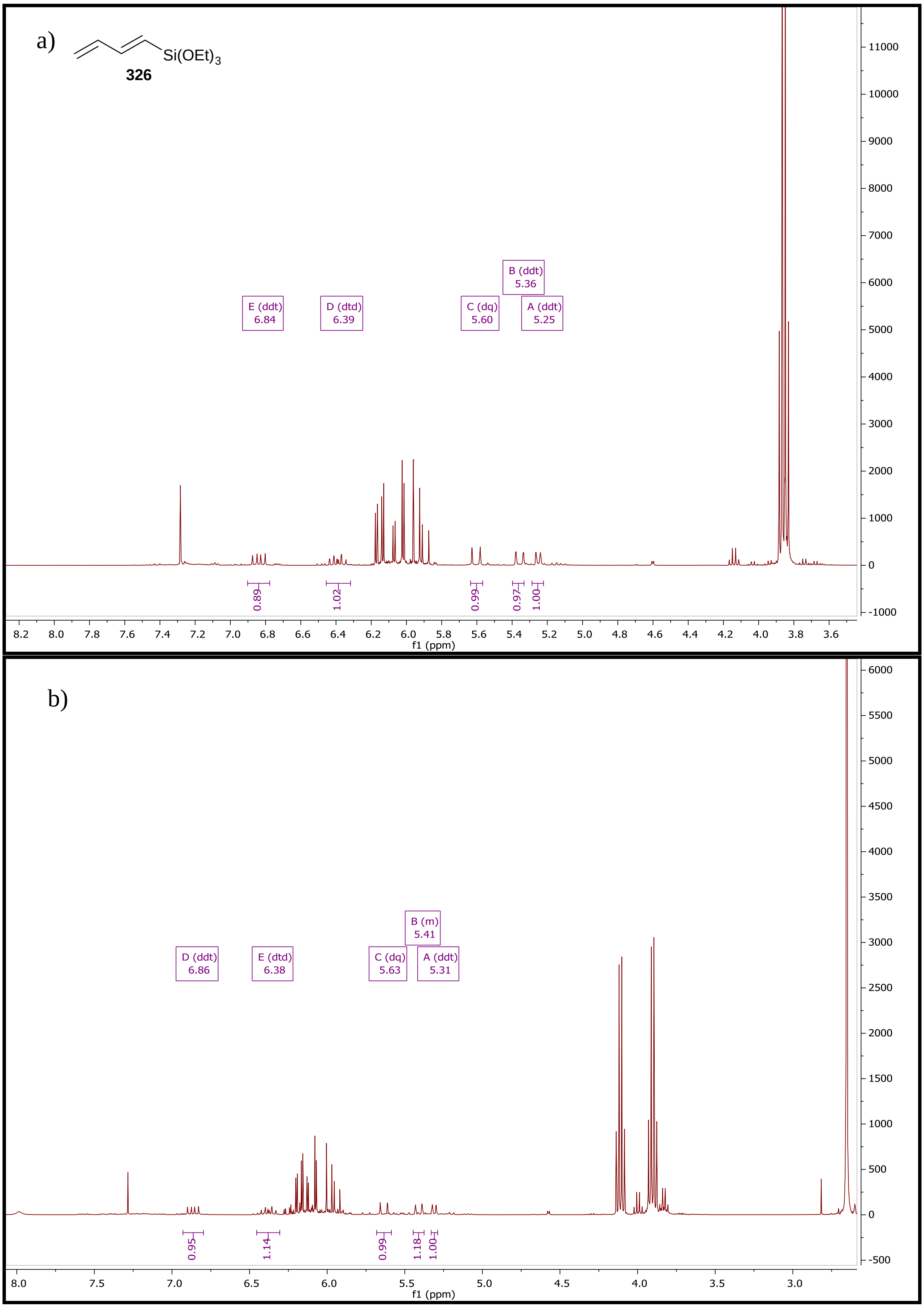

Figure 28 ^{1}H NMR spectrum of **a)** crude (*1E*)-buta-1,3-dien-1-yltriethoxysilane **316** and **b)** (*1E*)-buta-1,3-dien-1-yltriethoxysilane **316** following treatment with acetyl chloride **325**

With the nitroso Diels-Alder cycloaddition appearing a promising route, the focus moved to trapping out the dienes as cycloadducts. A one pot procedure to form dienyl boronate **276** and then effect the cycloaddition using nitrosobenzene was attempted (**Equation 48**). Vinyl boronate **42** was subjected to the optimised HM coupling protocol for boronate esters (one equivalent of acceptor) and after 6 hours, nitrosobenzene **320a** was added and the reaction stirred overnight. ^{1}H NMR analysis after 17.5 hours post addition indicated complete diene consumption and formation of 1-phenyl pyrrole **328**, which was isolated in an 18% yield.

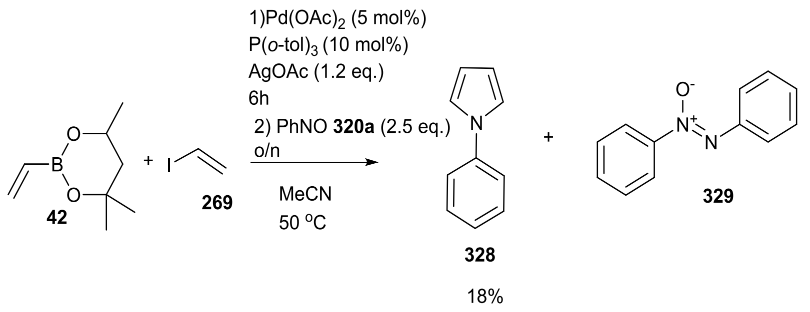

(48)

The isolated yield obtained was disappointing, considering the facile reactivity of the reaction. Unfortunately, large amounts of an azo-oxide **329** (as identified in the group previously)[194,195] was formed during the course of the reaction and this was very difficult to isolate from the desired pyrrole.

The reaction was attempted again, this time initially using 0.9 equivalents of nitrosobenzene and then adding small proportions of nitrosobenzene (0.3 equivalents after 16 hours and then a further 0.2 equivalents 2.5 hours later) as required to effect complete cycloaddition. This was much more successful, resulting in far less formation of azo oxide, and leading to the isolation of **328** in a 48% yield.[173]

A one-pot procedure was also attempted on methyl vinyl ketone **297**, this time attempting to employ ethyl vinyl ether **330** as an electron rich dienophile in an inverse electron demand Diels-Alder reaction (**Equation 49**). Unfortunately, it was found that only a 30% conversion was obtained after six hours, and that the diene that was formed did not undergo a cycloaddition with vinyl ether **330**, even after heating the reaction mixture to reflux for two days.

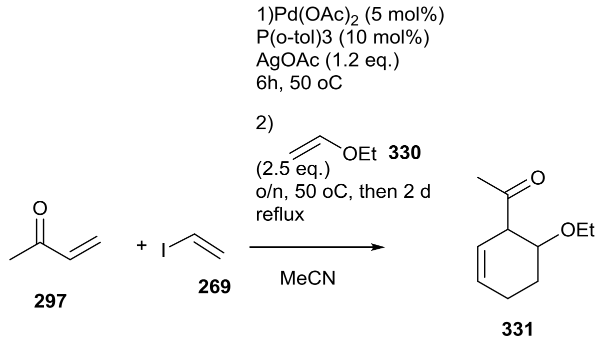

(49)

A sample of crude methyl dienyl ketone **332** was also used in an attempted cycloaddition with nitrosobenzene, following the literature procedure.[195] Diene **332** was dissolved in methanol and nitrosobenzene **320a** added (**Equation 50**). The reaction was then stirred at room temperature. The reaction proved to be extremely facile, with 90% oxazine formation observed after 1 hour and 40 minutes. At this point an approximate regioisomeric ratio of 4:1 was observed for products presumed to be **333** and **334**, respectively.

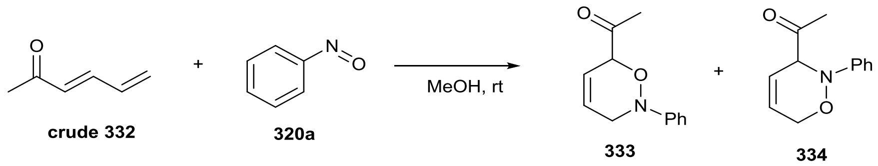

(50)

Section 2.1.4 Capability of (*E*)-2-(buta-1,3-dienyl)-4,4,6-trimethyl-1,3,2-dioxaborinane to act as a four-carbon building block for polyene synthesis

Following the successful isolation of dienylboronate **276**, its utility as a four-carbon, butadienyl dianion equivalent was examined, in a manner analogous to the use of the vinylboronates, such as **42**, as two-carbon, vinyl dianion equivalent building blocks (as in **Scheme 65**, for example).[161,162,164,165,167,192]

Scheme 65 Use of **42** as a two-carbon, vinyl dianion equivalent building block

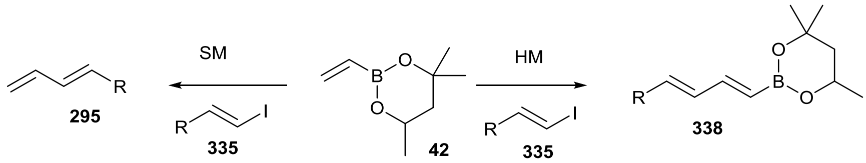

Dienyl boronate **276** was successfully, and consistently, coupled with a number of aryl, heteroaryl and alkenyl halides **51** (**Table 23**, **Equation 51**). A consistent method of purification still remains elusive to date, however, it was found that used of silver(II) nitrate-impregnated silica proved useful in obtaining pure products. In some cases, the instability of the products meant that it was not possible to obtain optimum isolated yields. In many cases, alkenes were isolated with the TMB references. In some cases the products also could not be separated from the starting halide without giving an unacceptable isolated yield. In addition, the dienyl products were susceptible to polymerisation and, as before, BHT had to be used in work up solvents and eluents in order to successfully isolate the products.

Table 23 Results of attempted SM couplings between diene **276** and a range of aryl halides.

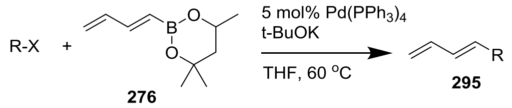

(51)

Entry	R-X	Reaction time/hours	Crude yield (isolated yield)/%
1	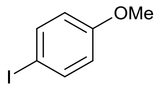 **246**	4.5	76 (69)
2	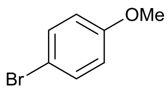 **337**	22	32 (28)
3	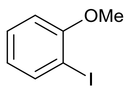 **338**	23	33 (23)
4	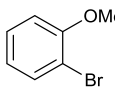 **339**	25	23 (22)
5	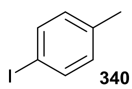 **340**	6	91 (89)
6	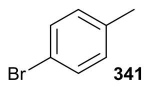 **341**	22	74 (72)
7	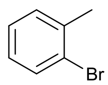 **342**	25	70 (40)

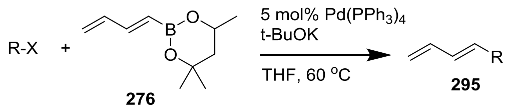

(51)

Entry	R-X	Reaction time/hours	Crude yield (isolated yield)/%
8	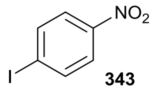 **343**	6	65 (64)
9	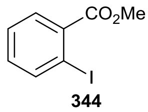 **344**	23	33 (24)
10	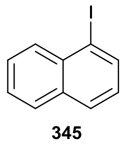 **345**	22	73 (68)
11	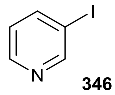 **346**	24	88 (88)
12	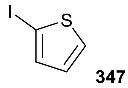 **347**	23	61 (46)
13	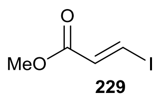 **229**	4	0, 58[b] (53)

[a]Yields determined by ^{1}H NMR and GC on crude product after work up. [b] Ag_2O base used.

Despite this, the ability of dienylboronate **276** to undergo coupling was demonstrated on both electron-donating and electron-withdrawing substrates. It was found that *p*-aryl iodides were coupled in good yields (**Table 23**, **Entries 1**, **5**, **8** and **10**). In the case of *p*-iodoanisole **246** *versus* *p*-bromoanisole **337** (**Table 23**, **Entries 1** and **2**), there was a significant drop in reactivity of the bromide compared to the iodide. There was also a significantly lower reactivity observed for the *o*-iodoanisole **338** compared with *p*-iodoanisole **246** (**Table 23**, **Entries 1** and **3**). With the tolyl derivatives (**Table 23**, **Entries 5**, **6** and **7**), the *o*-aryl halides did display a small drop in reactivity compared to the *p*-derivative, but there was no observed difference between the bromo- and iodo-derivatives and all three were coupled in good yields. Heterocyclic compounds were also coupled (**Table 23**, **Entries 11** and **12**), with 3-iodopyridine giving an isolated yield of 88%. The coupling between iodoacrylate **229** and diene **276** was attempted using both potassium *tert*-butoxide and silver(I) oxide to see if the silver was beneficial to the cross-coupling. The difference between the two bases being apparent by ^{1}H NMR of the two reaction mixtures; *tert*-butoxide resulted in no triene **348**, whereas silver(I) oxide gave a 58% crude yield (**Table 23**, **Entry 13**).

It was considered desirable, due to the tendency for dienyl boronate **276** to polymerise on storage, for the trifluoroborate salt **349** of boronate **276** to be made, as a potentially air-stable and easier to use SM coupling partner. Ideally, in order to overcome the issues with polymerisation of boronate **276** on silica gel chromatography, the trifluoroborate **349** should be isolated directly from the crude boronate **276**. Attempts to functionalise crude diene **276** included the Lloyd-Jones procedure,[196] with KF and (+)-tartaric acid, as well as a procedure using KHF_2. Use of KHF_2 was unsuccessful on diene **276**, and was attempted on the crude pinacol derivative **318** with just as little success. Crude diene **276** was dissolved in a mixture of 1:1 MeOH: MeCN, then a solution of KF in water was added dropwise at room temperature. Addition of (+)-tartaric acid with stirring, followed by dilution with MeCN, filtration to remove the salt and removal of the solvent gave crude trifluoroborate. Unfortunately, any unreacted vinyl boronate **42** left from the previous HM coupling was also converted to trifluoroborate and pure dienyl trifluoroborate **349** could not be isolated, even by recrystallization. The same procedure was attempted on a freshly purified sample of dienyl boronate **276** and trifluoroborate **349** was obtained in a quantitative yield (**Equation 52**).

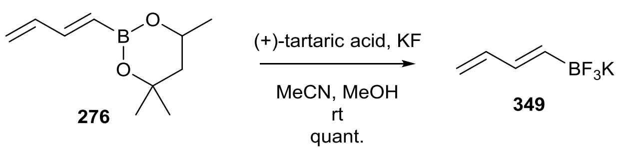

(52)

A SM cross coupling was attempted on trifluoroborate **349** and *para*-iodotoluene, using the conditions detailed in **Table 23**. Unfortunately, the temperature at which the reaction was undertaken appeared to cause decomposition of the trifluoroborate and no SM product was observed (**Equation 53**).

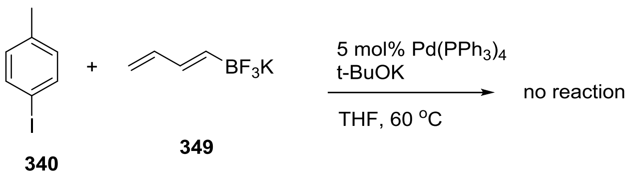

(53)

Given the instability of some of the aryl dienes produced, it seemed appropriate to investigate methods to react them *in situ* to give more readily isolatable products. There was precedent for doing this, with the Thomson group successfully trapping out 2-naphthalenyl diene using a Diels-Alder cycloaddition (**Scheme 66**).[187]

Scheme 66 Successful Diels-Alder cycloaddition of an unsubstituted aryl diene by Thomson *et al*.[187]

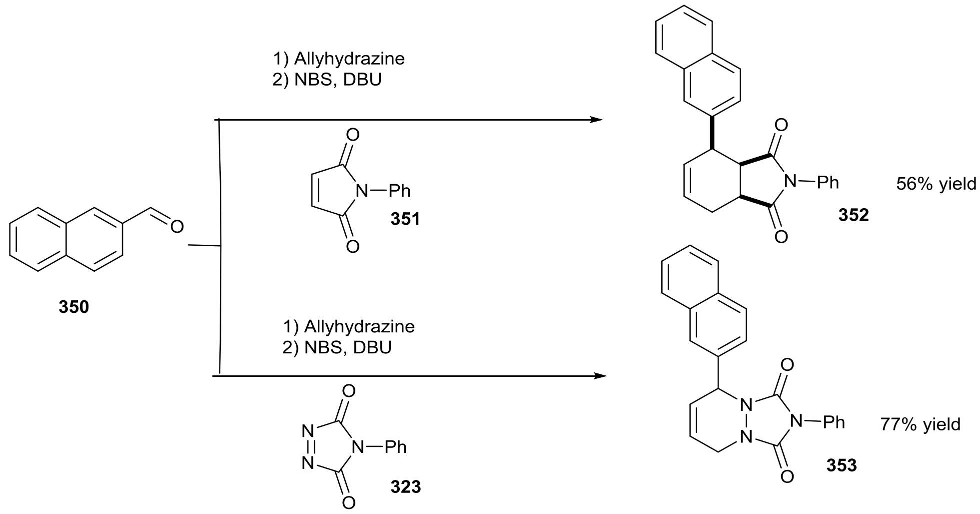

Here, the diene was made *in situ via* bromination of an allyl hydrazone, and then trapped out using either *N*-phenyl maleimide **351** or 4-phenyl-1,2,4-triazoline-3,5-dione **323**, successfully giving cycloadducts **352** and **353** in 56 and 77% isolated yields, respectively.[187]

Using 1-naphthalenyl iodide **345**, the SM coupling to make 1-naphthalenyl diene **354** was undertaken and the cycloaddition with *N*-phenyl maleimide **351** attempted in a one-pot procedure. It was found that the presence of the dienophile from the start of the reaction slowed down the SM coupling. If dienophile **351** was added after reaction completion, no conversion to cycloadduct was observed.

Crude 1-naphthalenyl diene **345** and *p*-tolyl diene **354** were used in attempted cycloadditions with *N*-phenyl maleimide **351**, 4-phenyl-1,2,4-triazoline-3,5-dione **323** and maleic anhydride **356**. In all cases, consumption of the diene was seen, but the corresponding cycloadduct could not be isolated.

A HM coupling was attempted on triene **348**, using iodoacrylate **229**, in an attempt to make the butadienyl diester. Unfortunately, no peaks corresponding to the desired product could be observed in the ^{1}H NMR spectrum after 18 hours

(**Equation 54**).

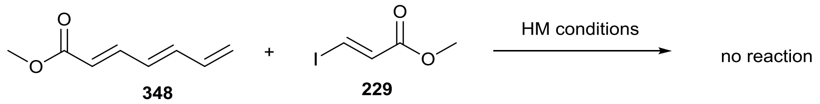

(54)

Section 2.1.5 Summary

The potential for vinyl iodide **269** to act as a HM donor was evaluated, with optimised conditions providing access to key dienyl boronate **276**. The reactivity of vinyl iodide has proven to be unusual, with poor reactivity for all substrates except for the vinyl boronates when using a 1:1 ratio of iodide to alkene acceptor, but in some cases displaying greatly increased reactivity when the ratio of alkene acceptor was increased to 3 equivalents. A chelation effect has been proposed to explain the facile reactivity of the vinyl boronates with vinyl iodide, a theory supported by the moderate reactivity of the vinyl siloxanes and the lack of reactivity of the coordinatively saturated vinyl BMIDA substrate.

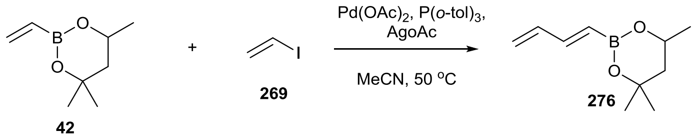

Purification of the terminal dienes formed has proven consistently challenging, with products susceptible to polymerization and difficult to separate from the starting vinyl substrate. Some attempts have been made to trap out these dienes, or else functionalise them directly from a crude reaction mixture, with nitroso-cycloadditions showing the most promise.

Dienyl boronate **269** has been used in a series of SM couplings to furnish a range of dienes and trienes. These products were again highly susceptible to polymerisation, but were more amenable to silica gel chromatography, with silica impregnated with silver(II) nitrate used to effect the best separation.

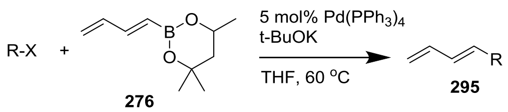

(51)

Section 2.2 Novel, mild Heck-Mizoroki cross-coupling conditions for the stereoselective construction of unstable polyenes

Section 2.2.1 Optimisation for a room temperature HM coupling

Throughout **Section 1**, a recurring theme was one of instability of the polyene intermediates to the temperatures employed in the key cross-coupling reactions. On commencing this project, HM couplings were performed at 50-55 °C and SM couplings were performed at 60 °C. Over time these were shown to cause degradation of the polyenyl intermediate, the aryl building block, or both (see **Sections 1.2**, **1.3** and **1.4**). In **Section 1.3**, issues with stability were circumvented by running HM reactions at 30 °C, as completion was reached, but the SM:HM ratio was too poor at room temperature (**Table 24**, **Equation 55**). In order to access highly the unstable polyenic intermediates, a room temperature protocol for Heck-Mizoroki cross-coupling would be desirable, as degradation of intermediates was observed even at room temperature (**Section 1.3**).

Table 24 Temperature screen for the HM coupling of iodoacrylate **229** and vinyl boronate **42**, showing HM vs competing SM ratios.

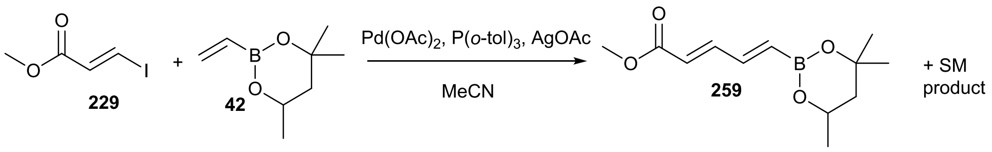

(55)

Entry	Catalyst loading/ mol%	Temperature / ^{o}C	Conversion after 24 h/ %	HM: SM ratio
1	5	50	100	90:10 to 97:3
2	5	40	100	87:13
3	10	40	100	80:20
4	5	30	100	87:13
5	10	30	100	85:15
6	5	rt	100	72:28
7	10	rt	100	68:32

The cause of this increase in SM product at room temperature is unclear and surprising, potentially suggesting that the HM is the thermodynamic preferred pathway, and therefore less favoured at room temperature.

A ligand screen was undertaken in an attempt to optimise the HM:SM product ratio (**Equation 56**), with the results shown in **Table 25.**

Table 25 Ligand screen for the HM coupling of iodoacrylate 229 and vinyl boronate 42, showing HM vs competing SM ratios.[a]

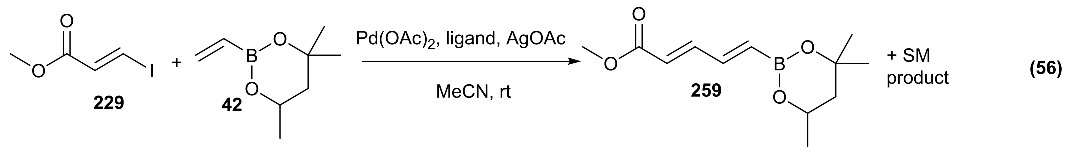

Entry	Ligand	Conversion after 3 h/%	HM: SM ratio
1	No ligand	100	80:20
2	Tri(*o*-tolyl)phosphine	100	68:32
3	Triphenylphosphine	0	-
4	Tris(*o*-methoxyphenyl)phosphine	100	89:11
5	Tris(4-trifluoromethylphenyl)phosphine	0	-
6	Trifurylphosphine	100[b]	89:11

[a]Reaction undertaken using 10 mol% catalyst and 2 equivalents ligand wrt catalyst.
[b]Reaction complete after 1.5 hours

The results were perhaps a little surprising, with the reaction proving to be either highly efficient (going to 100% conversion after 3 hours), or completely unreactive, with no conversion observed at all. It was observed that addition of an electron rich ligand facilitated HM coupling (**Table 25**, **Entries 2**, **4** and **6**), whilst addition of electron deficient ligands resulted in no conversion (**Table 25**, **Entries 3** and **5**). Tris(*o*-methoxyphenyl)phosphine and trifurylphosphine gave the best HM:SM ratio, with the smaller trifurylphosphine also giving a higher level of reactivity, with 100% conversion at the shorter time of 1.5 hours (**Table 25**, **Entries 4** and **6**). It was also noted that addition of no phosphine ligand gave a better ratio than the current phosphine of choice at 50 °C, tri(*o*-tolyl)phosphine. Initially, this observation was put down to steric effects, due to the comparative bulk of tri(*o*-

tolyl)phosphine compared to the most successful trifurylphosphine. The reactivity of tris(*o*-methoxyphenyl)phosphine, however, discounted this.

The optimal catalyst loading was then investigated, using trifurylphosphine as the ligand. The results are shown in **Table 26**, **Equation 57**.

Table 26 Catalyst loading screen for the HM coupling of iodoacrylate **229** and vinyl boronate 4**2**, showing HM vs competing SM ratios.[a]

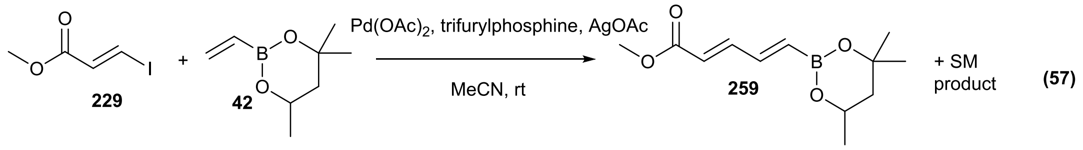

Entry	Catalyst loading/ mol%	Conversion after 3 h/%	HM: SM ratio after 3 h	Conversion after 25 h/%	HM: SM ratio after 25 h
1	10	100	89:11	100	87:13
2	7.5	100	90:10	100	90:10
3	5	100	91:9	100	89:11
4	2.5	100	89:11	100	88:12
5	1	100	88:12	100	89:11
6	0.5	<1	-	31	77:23

[a]Reaction undertaken using 2 equivalents ligand wrt catalyst.

It was found that the reaction could be performed at 1 mol%, achieving 100% conversion after 3 hours, with no reduction in the HM:SM ratio. These conditions showed a great deal of potential for their use in polyene construction *via* iterative cross coupling. Comparison of the *in situ* ^{1}H NMR of the HM coupling between iodoacrylate and vinyl boronate using these conditions, and those originally employed within the group shows a cleaner spectrum for these milder conditions, indicating that the final polyenes may well be easier to purify (**Figure 29**).

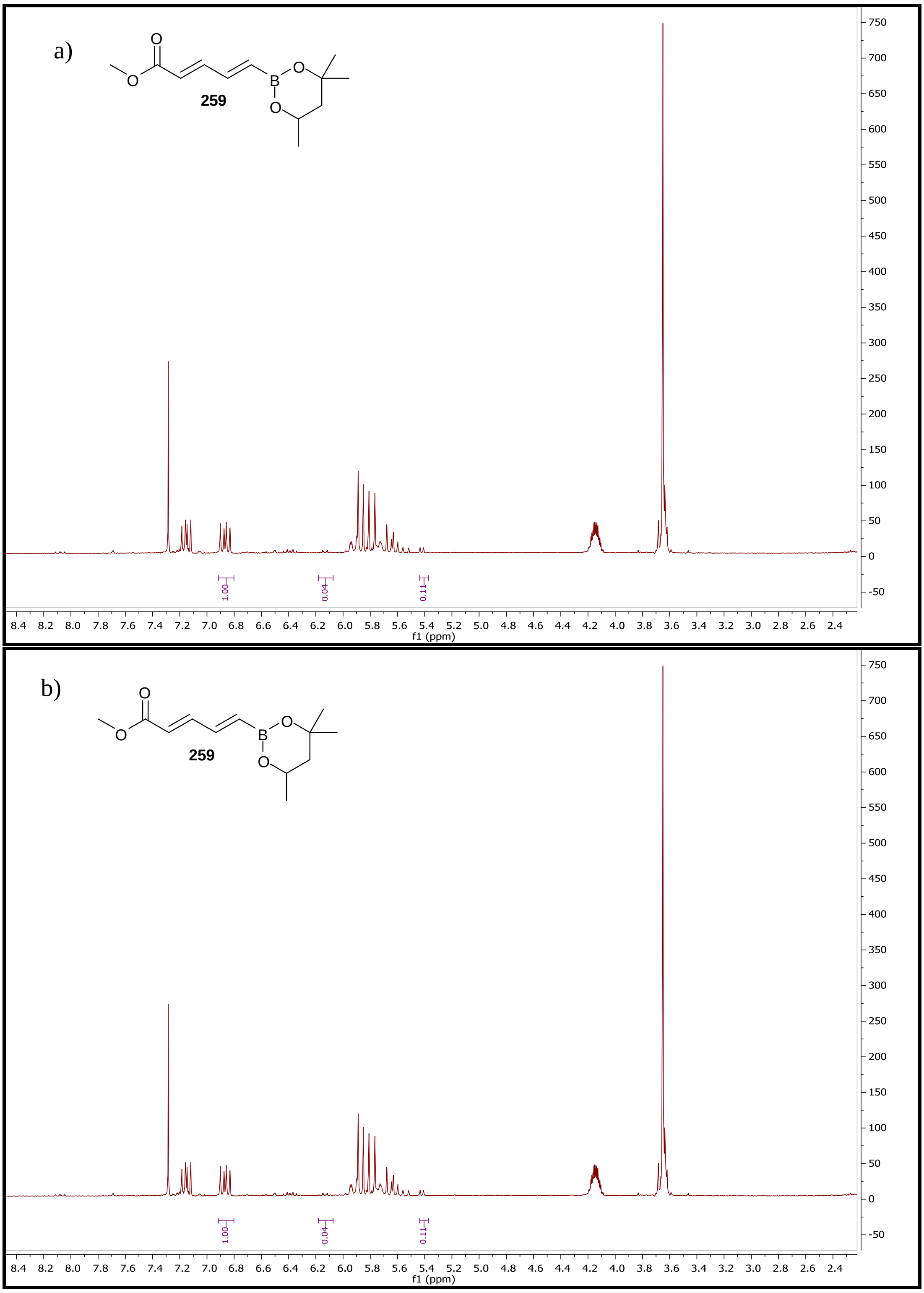

Figure 29 ^{1}H NMR spectra for the HM coupling between iodoacrylate **229** and vinyl boronate **42** under **a)** the group's original conditions and **b)** the newly optimised conditions.

Section 2.2.2 Application of milder methodology

Following on from the identification of optimised conditions for the model reaction between **229** and 4**2**, the scope of this methodology needed to be evaluated. The aim was to apply the optimised conditions to polyenyl systems already reported by ourselves.[1,2] In addition, application to the vinyl iodide methodology needed to be fully investigated, as this proved to be an unreactive system and the products were unstable.[4] Preliminary work was moderately successful, where vinyl iodide **269** was shown to react moderately with vinyl boronate **42** with 10 mol% palladium(II) acetate and 20 mol% tris(*o*-methoxyphenyl)phosphine at room temperature, giving a 48% estimated conversion after 24 hours to dienyl boronate **276** (**Equation 58**).

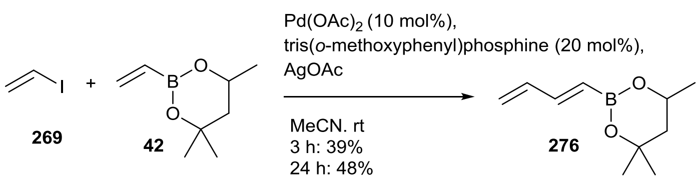

(58)

Initially, there were some concerns that this reactivity would be reduced under the lower catalyst loading employed in the newly optimised conditions. A small substrate screen was undertaken using the new conditions, incorporating the *cis*-iodoacrylate **43** employed in the synthesis of viridenomycin and vinyl iodide **269**, along with 2 different aryl iodides **357** and **246** (**Table 27**, **Equation 59**). *Cis*-iodoacrylate **43** proved highly reactive, comparable with *trans*-iodoacrylate **229** (**Table 27**, **Entry 2**). Vinyl iodide **269** displayed similar reactivity to that observed using the conditions in **Equation 58**, an indication of the highly reactive nature of the palladium(II) acetate/trifurylphosphine system in this case, reaching 52% after 24 hours (**Table 27**, **Entry 5**). Unfortunately, this conversion was considerably worse than that of the iodoacrylates, which reached 100% completion within 3 hours. Aryl iodides **357** and **246** proved unreactive at these temperatures, with no conversion observed for any of these substrates (**Table 27**, **Entries 3-4**).

Table 27 Attempted application of new conditions to the HM coupling of some alkenyl and aryl iodides.

Entry	Substrate	Conversion after 3 h/%	Conversion after 24 h/%
1	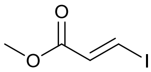 **229**	100	-
2	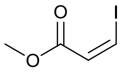 **43**	100	-
3	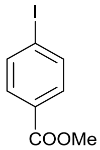 **257**	0	0
4	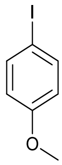 **246**	0	0, 7[a]
5	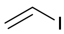 **269**	31	52

[a]Conversion obtained at 40 °C

Section 2.2.3 Summary

In light of the instability of many of the longer chain polyenyl intermediates made during the course of this project, the HM cross-coupling conditions were reoptimised to operate at room temperature. Ligand screening was successful in achieving a comparable HM:SM ratio to the one observed at 50 °C, with the catalyst loading successfully dropped to 1 mol% from 5 mol%. The reaction time has also been greatly reduced from between 1 and 2 days to 3 hours. Aryl iodides are, however, unreactive under these conditions and there is still a need for more general, low temperature HM cross-coupling conditions.

3 Conclusions

The aims of this project were to make progress in the synthesis of xanthomonadin **208**, utilising the group's HM/IDB ICC methodology in the construction of polyene intermediates. After evaluating what was currently known in the literature, the biological action of these compounds was of considerable interest, and the project was widened to include both debrominated xanthomonadin and a number of truncated analogues in the expectation of shedding some light on the behaviour of the *Xanthomonas* pigments.

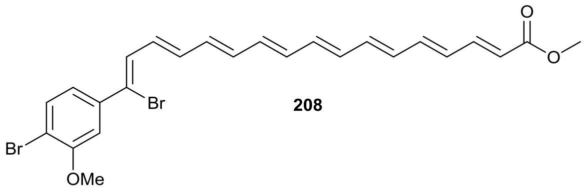
208

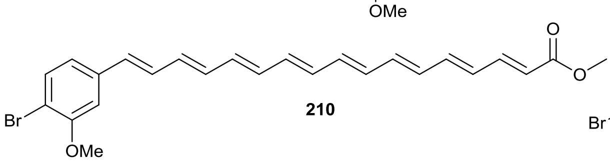
210

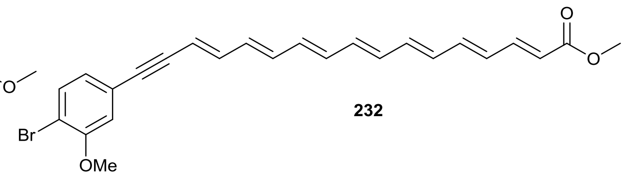
232

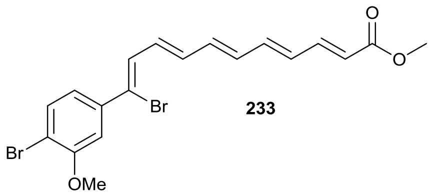
233

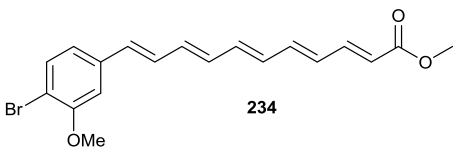
234

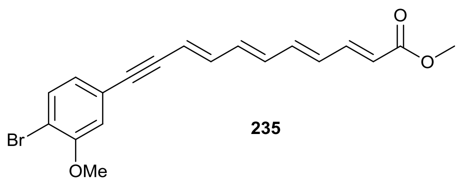
235

The aim was to achieve a convergent and versatile synthetic route, with a number of different aryl building blocks accessed to accomplish this. Considerable challenges were encountered both in the synthesis of brominated styrenyl boronate pinacol ester **228** (where the unwanted production of geminal by-product **236** could be minimised, although not completely eliminated), and in the selection of a suitable cross-coupling reaction to connect a brominated styrenyl building block to the polyenyl section of the pigment. Some inroads were made here, with a SM coupling showing the most promise.

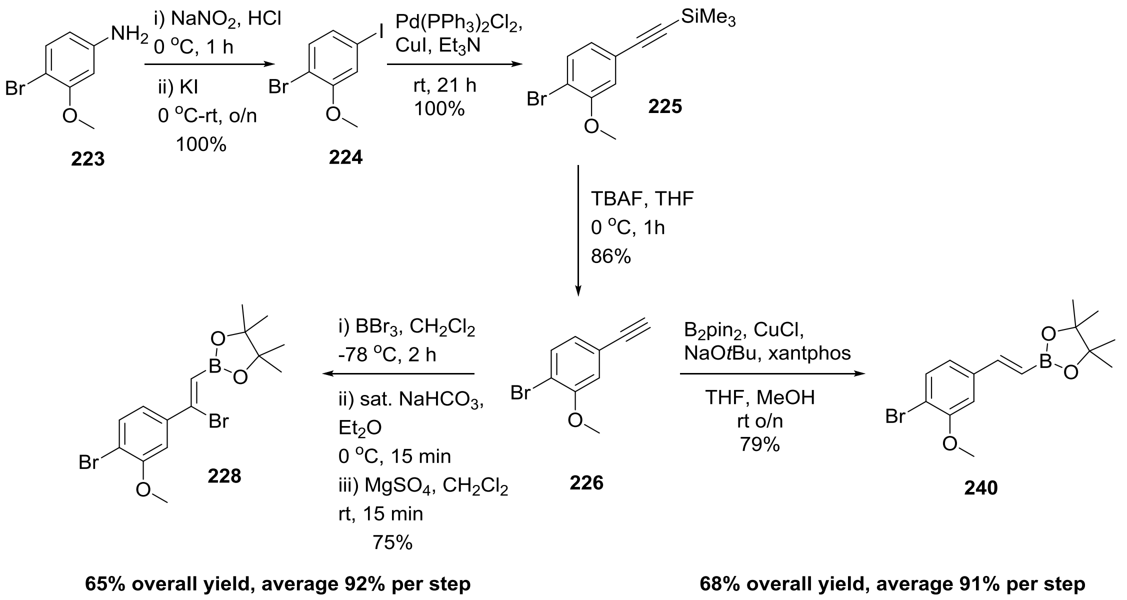

The group's HM/IDB ICC methodology proved to be extremely versatile, providing access to three key polyenyl building blocks. The key issue with this part of the project was the stability of the polyenyl intermediates, especially the polyenyl iodides, which degraded rapidly, in many cases even in the dark and under argon. The HM methodology was reoptimised to operate at lower temperatures in order to minimise degradation of iodide coupling partners, with a room temperature version of the methodology showing promise.

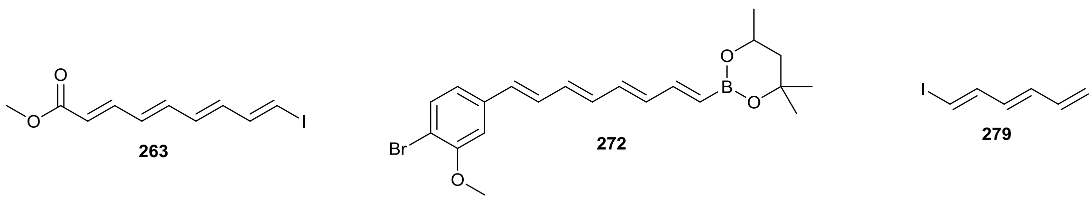

A number of pigments have been successfully made, with dehydro-tetraen-yne xanthomonadin **235** and debrominated pentaenyl xanthomonadin **234** isolated and characterised. Pentaenyl xanthomonadin **233** was also isolated as a mixture with dehydro tetraen-yne xanthomonadin **235**, due to the problematic nature of the final SM coupling with brominated styrenyl boronate pinacol ester **288**. Debrominated xanthomonadin **210** has also been isolated as part of a crude mixture in trace amounts, with purification of the octaenes consistently proving difficult. Some evidence for the successful formation of xanthomonadin **208** in trace amounts has also been found, with the presence of the expected signals in a crude ^{1}H NMR spectrum, and also some promising mass ion peaks in the mass spectrum.

The isolated truncated pigments fit well with the limited characterisation available in the literature for xanthomonadin **208**, with the characteristic signals observed in the ^{1}H NMR spectrum. Studying the behaviour of these pigments by NMR over time provided evidence of a major *cis* isomer of the pigments. This was further corroborated by the presence of a higher energy λ_{max} for both truncated analogues in the UV-Vis spectrum. It also appeared that the pentaenyl xanthomonadin **233** was more stable than the other two analogues, perhaps suggesting a reason for the incorporation of the bromine into the polyene chain itself. Dehydro-tetraen-yne xanthomonadin **235** appeared more stable than debrominated pentaenyl xanthomonadin **234**.

The UV-Vis data was consistent with that obtained by Andrewes *et al*. for pigment mixtures containing xanthomonadin **208**,[151] possessing the same shape of curve and also displaying a λ_{max} consistent with the lower conjugation of these two structures. In addition, it was shown that these two compounds fit with the expected λ_{max} values as predicted by the Fieser-Kuhn rules.[177]

The above data provide strong evidence that we have successfully made compounds analogous to those isolated by Andrewes *et al*., and also support their characterisation.[133,151,154] The data also provide a small insight into the behaviour of such sacrificial pigments and their behaviour towards both oxygen and light. It remains to be seen whether the truncated analogues can provide any photooxidative protection for bacteria that naturally cannot product such pigments for themselves.

There have been opportunities throughout this project to work on optimisation of methodology. The optimisation of the HM methodology used in the HM/IDB ICC construction of key building blocks has already been discussed, but another sub-project was undertaken to establish the potential of vinyl iodide **269** as a HM coupling partner. Through considerable optimisation, this aim was achieved, although isolation of pure reaction products was not possible in many cases. This was due to the instability of the dienes to polymerisation and also to the similarity of the starting alkene to the diene, making them very difficult to separate by silica gel chromatography. This body of work not only showed that vinyl iodide **269** can be used to form a number of dienes, but also highlighted some key mechanistic questions due to the peculiar reactivity of non-coordinatively saturated vinyl boronates. These questions haven't been definitively answered, but it appears that the coupling takes different routes depending on the nature of the substrate.

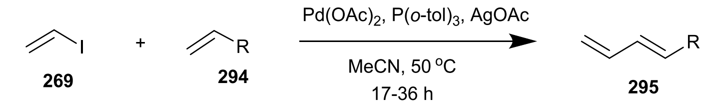

Vinyl iodide **269** was used to readily access key dienyl boronate **276**, which was used in a series of SM couplings to access a range of dienes and trienes, providing a versatile method which could access all of these terminal polyenes where there had previously not been one robust way to do so. Isolation of these compounds was initially hampered by their instability to polymerisation, but use of BHT in all reaction, work up and chromatography solvents solved this problem. Use of silver(I) nitrate impregnated silica allowed for mixtures of these polyenes to be separated, although this did result in a decreased isolated yield.

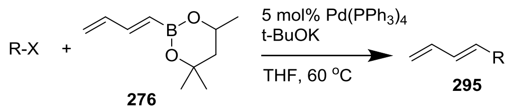

(51)

4 Future work

The potential to access these complex pigment molecules has been established through the work in this thesis. There are still a considerable number of challenges that need to be overcome in order for the natural pigments to be successfully made and isolated on a scale suitable for testing. Suitable purification conditions for the isolation of debrominated xanthomonadin **210** need to be identified. In order to access both xanthomonadin **208** and pentaenyl xanthomonadin **233**, the cross-coupling conditions onto a suitable aryl building block need to be optimised. The current model systems have their limitations in that the desired dienyl analogues have not been successfully isolated. Therefore, the isolation of these dienes needs to be achieved, or suitable alternative models identified. In particular, a lower temperature set of conditions need to be identify as the only conditions that currently give any desired product operate at 60 °C, at which temperature polyenyl iodide intermediates have already been shown to be unstable. In addition, dehydro-heptaen-yne xanthomonadin **232** needs to be synthesised. The relatively simple synthesis of dehydro-tetraen-yne xanthomonadin **235** gives some indication that this analogue should be accessible, though it may suffer from the same instability shown by debrominated xanthomonadin **210** on purification.

The behaviour of all of these target molecules under photooxidative conditions needs to be studied, and the nature of the degradation/polyene isomerisation should be studied in order to understand more about the mechanism of these structures. Work has commenced with Professor Conrad Mullineaux, Queen Mary College London, to investigate the ability for the the two isolated truncated analogues to protect bacteria against photooxidative damage. An ideal solution would be to find a way of quantifying the photoprotective activity of these compounds, in order to begin identifying the most important functional groups for activity.

The next stage in the bacterial pigments project is to access some other pigments found in bacteria (see **Section 1.1**). Through making and testing these pigments, a better understanding of the structure-activity relationship will be obtained for these structures. Some work has already commenced towards this end, with the vision being to access a range of aryl styrenyl boronate esters to be coupled to polyenyl intermediates of varying length.

The optimised HM/IDB ICC methodology needs to be applied to the synthesis of our key polyenyl building blocks, to assess the possibility of operating these at room temperature. Following this, the methodology could be applied to the synthesis of the northern hemisphere of viridenomycin **18**, the total synthesis of which is part way through completion (see **Introduction**). **Scheme 67** shows the yields previously obtained for the synthesis of this key building block. The final HM has considerable room for improvement, and it could well be that the poor yield is due to the instability of the trienyl iodide to the reaction temperature. Further work needs be undertaken into the cause of HM *vs* SM selectivity, with the hope of better understanding the intriguing switch in reactivity on operating at a lower temperature. With the development of milder HM methodology, the HM coupling onto brominated styrenyl iodide **238** needs to be reinvestigated, as this could open up the potential of building xanthomonadin **208** utilising two tetraenyl intermediates, in an approach analogous to that of the synthesis of debrominated xanthomonadin **210**.

Scheme 67 Previously developed route to the northern hemisphere of viridenomycin **18**

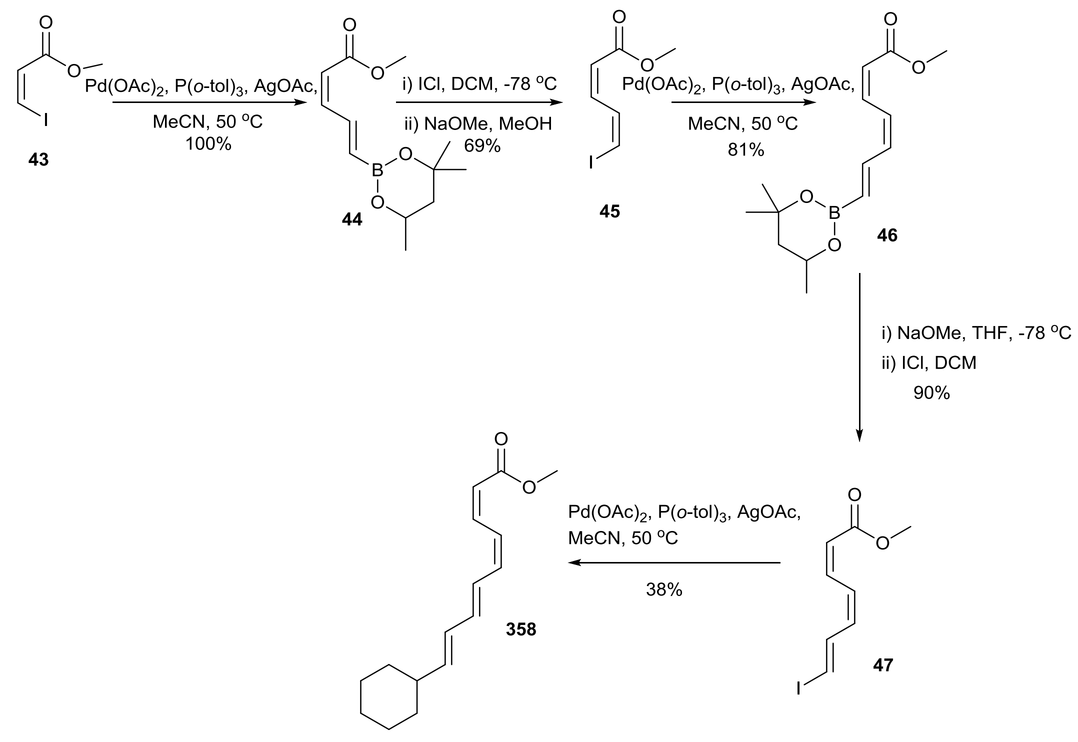

The mechanisms involved in the cross-coupling of vinyl iodide with different alkenyl substrates needs to be further investigated, with DFT calculations currently being performed on the vinyl iodide-vinyl boronate system to evaluate the validity of the chelation theory. The cause of the greatly increased reactivity of some of the Michael acceptor substrates when 3 equivalents is used also needs to be investigated. There are still considerable issues with the isolation of the products from these couplings, and this needs to be addressed. Methods of functionalising these dienes have been briefly explored, but little progress has been made so far.

5 Experimental

5.1 General experimental details

All reactions were carried out in oven-dried glassware with magnetic stirring unless otherwise stated. All chemicals were purchased from commercial suppliers and used without further purification. Where petroleum ether is stated, this refers to petroleum ether bp 40-60 °C. Anhydrous acetonitrile was obtained by distillation of HPLC grade acetonitrile over calcium hydride. Anhydrous THF was obtained by distillation of HPLC grade THF over sodium metal, with a benzophenone indicator. Solvents were degassed, unless stated otherwise, by sparging with argon for 20 minutes. For all palladium cross-coupling reactions, cross-shaped stirrer bars were used for the most efficient stirring. Where reagents were added dropwise, these were added at a rate of 1 drop per second unless otherwise stated. Monitoring of reactions was achieved using any of TLC, ^{1}H NMR and GC. TLC was performed using silica plates. The silica plates were polyester-backed silica TLC plates with 0.2 mm silica gel and fluorescent indicator. Spots were visualised using an ultraviolet (UV) lamp and $KMnO_4$ dip, visualising in both long wave and short wave UV. Where a reference was used, naphthalene or 1,3,5-trimethoxybenzene were used as a reference for conversion calculations. HMR experiments were carried out on either a Bruker Avance-400 or a Varian VNMRS-700 spectrometer in deuterated chloroform ($CDCl_3$-d), deuterated methanol (MeOD-d_4), or deuterated dimethyl sulfoxide (DMSO-d_6). Chemical shifts are reported in ppm relative to tetramethylsilane (TMS) reference. Experiments undertaken included ^{1}H, ^{11}B, ^{19}F, ^{13}C, COSY, PSYCHE, HSQC and HMBC NMR. NMR experiments were not boron-decoupled, but in all cases the coupling constant proved too small to be visible on the resulting spectra. GC data was obtained by removing 0.01 mL samples from the reaction mixture and diluting into 1 mL acetonitrile. GC experiments were run on a Hewlett Packard 5890 Series II Gas Chromatograph fitted with a Hewlett Packard 6890 series injector, using a FactorFour™ capillary column VF-5 ms, 30 m, 0.25 mm, 0.25 µm. The experiment conditions were an initial temperature of 30 °C, held for 5 minutes, followed by a gradient of 20 °C/ minute to 150 °C, with a hold time of 11 minutes. Celite/silica filtration used Celite® S and technical grade silica gel: pore size 60 Å, 230-400 mesh particle size, 40-63 µm particle size. The term ‘evaporated’ refers to the removal of solvent *in vacuo*. Silica gel chromatography used technical grade silica gel: pore size 60 Å, 230-400 mesh particle size, 40-63 μm particle size. Where silver nitrate-impregnated silica gel was used, this was prepared according to Li and coworkers.[197] Alumina chromatography used activated, neutral, brockmann I standard grade aluminium oxide with ~150 mesh and 58 Å pore size. Electrospray ionisation (ESI) mass spectrometry was undertaken using a LTQ FT (ThermoFinnigan) high resolution, accurate mass LC ES MS/MS or a Thermo Scientific LTQ Orbitrap XL. Samples were made up as 1 mg per mL solutions in acetonitrile. GC/MS EI was undertaken using a Waters GCT Premier. Atmospheric solids analysis probe (ASAP) mass spectrometry was undertaken using LCT Premier XE (Waters) high resolution, accurate mass ultra performance liquid chromatography (UPLC) ASAP or a Thermo Scientific LTQ Orbitrap XL. Samples were either made up as 1 mg per mL solutions in acetonitrile or run as solids. Infra-red (IR) spectroscopy was undertaken using a Perkin Elmer-1600 FTIR, using both liquid and solid samples. Melting point measurements were undertaken using a Gallenkamp melting point apparatus. Where products were susceptible to polymerisation, these were stored with approximately 20 ppm BHT under argon at either 4 ^{o}C or -18 ^{o}C.UV-Vis measurements were carried out on a Varian Cary 100 Bio UV-Visible Spectrophotometer. Fluorescence measurements were carried out on a PerkinElmer LS 55 Fluorescence Spectrometer. Both UV-Vis and fluorescence measurements were carried out using quartz cuvettes, with samples dissolved in either spectrophotometric grade diethyl ether, or spectrophotometric grade chloroform.

5.2 Specific experimental procedures

Methyl (2E)-3-iodoprop-2-enoate **229**

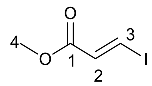

A solution of propiolic acid (5.00 g, 71.0 mmol) in aq. HI (57%, 25 mL) was heated under reflux for 0.5 hours, after which time the reaction was cooled to 0 ^{o}C. The resulting crystals were then filtered, washed with water (3 x 20 mL) and air-dried to afford 14.2 g of (*E*)-3-iodoprenoic acid as an off-white solid. The stereochemistry as the (*E*)-isomer was confirmed by X-ray crystallography following slow evaporation from EtOAc. (*E*)-3-Iodopropenoic acid (14.0 g, 70.7 mmol) was dissolved in MeOH (20 mL) and conc. H_2SO_4 (1 mL) was added. The reaction mixture heated under reflux for 24 hours, after which the solvent was removed *in vacuo***.** The resulting crude product was dissolved in Et_2O (100 mL), washed with H_2O (50 mL), sat. $NaHCO_3$ (2 x 50 mL), sat. Na2S2O5 (2 x 50 mL) and brine (50 mL). The organic extracts were then dried over $MgSO_4$ and evaporated to yield methyl (2*E*)-3-iodoprop-2-enoate as an off-white solid (12.9 g, 86% over two steps), mp 48.5-51.3 ^{o}C. ^{1}H NMR (400 MHz, $CDCl_3$): δ 3.75 (3H, s, CH_3), 6.88 (1H, d, J=14.8 Hz, H_3), 7.89 (1H, d, J=14.8 Hz, H_2). All spectroscopic data were consistent with those reported previously.[198]

1-Bromo-4-iodo-2-methoxybenzene **224**

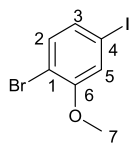

4-Bromo-3-methoxyaniline (5.00 g, 24.8 mmol) was stirred in aqueous HCl (37%, 250 mL) at 80 $^{\circ}$C to ensure complete dissolution. This was then cooled to 0 $^{\circ}$C and a cold solution of $NaNO_2$ (2.22 g, 32.2 mmol) in H_2O (125 mL) was added dropwise, keeping the temperature constant. The reaction mixture was stirred at 0 $^{\circ}$C for 1 hour and a cold solution of KI (12.5 g, 74.3 mmol) was carefully added dropwise at 0 $^{\circ}$C over a period of 1 hour. The resulting dark brown solution was stirred and allowed to reach room temperature overnight. The reaction mixture was diluted with EtOAc (250 mL) and the layers separated. The aqueous layer was extracted using EtOAc (2 x 250 mL). The organic layers were combined and washed sequentially with sat. $NaHCO_3$ (125 mL) and H_2O (125 mL) until neutral pH. The organic layers were then washed with 5% $Na_2S_2O_5$ (125 mL) and saturated brine (125 mL), dried over $MgSO_4$ and the solvent evaporated to afford a dark brown oil, from with the desired product spontaneously crystallised to give 1-bromo-4-iodo-2-methoxybenzene as a dark brown solid (7.8 g, 100 %), mp 53.1-55.6 ^oC. ^1H NMR (400 MHz, $CDCl_3$): δ 3.88 (3H, s, OCH_3), 7.14-7.18 (2H, m, $H_{5,3}$), 7.22-7.25 (1H, m, H_2). All spectroscopic data were consistent with those reported previously.[168]

((4-Bromo-3-methoxyphenyl)ethynyl)trimethylsilane **225**

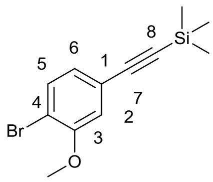

1-Bromo-4-iodo-2-methoxybenzene (7.71 g, 24.8 mmol), $Pd(PPh_3)_2Cl_2$ (0.173 g, 0.242 mmol) and CuI (47 mg, 0.242 mmol) were added to a dry flask. After purging the flask with argon for 5 minutes, dry, degassed Et_3N (139 mL) was added to the tube under argon, followed by TMS acetylene (4.0 mL, 29.8 mmol). The reaction was stirred at room temperature in the dark for 16 hours. The solvent was then evaporated and the residue was passed through a silica gel column, eluent 5% EtOAc in petroleum ether. Fractions containing the compound were evaporated to give desired product as an orange oil (7.11 g, 100%). ^1H NMR (600 MHz, $CDCl_3$): δ 0.25 (9H, s, $SiMe_3$), 3.89 (3H, s, OCH_3), 6.92-6.98 (2H, m, H_2, H_6), 7.45 (1H, d, J=8.1 Hz, H_5). ^{29}Si NMR (139 MHz, $CDCl_3$): δ -17.47 (s); ^{13}C NMR (151 MHz, $CDCl_3$): δ -0.2 ($SiMe_3$), 56.2 (OMe), 95.0 (C_8), 104.0 (C_7), 112.5 (C_4), 115.0 (C_6), 123.3 (C_1), 125.4 (C_2), 133.1 (C_5), 155.4 (C_3); IR (ν_{max}, cm^{-1}) 2157.0 (w, alkyne C-C), 2959.0 (m, arom. C-H), *inter alia*; LRMS (ASAP) 282.0 (M^+-^{79}Br, 50%), 284.0 (M^+-^{81}Br, 58); HRMS (ASAP) [$C_{12}H_{15}OSi^{79}Br$] calculated 282.0076, found

282.0083.

1-Bromo-4-ethynyl-2-methoxybenzene **226**

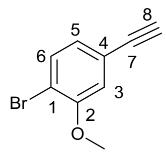

((4-Bromo-3-methoxyphenyl)ethynyl)trimethylsilane (4.09 g, 14.5 mmol) was dissolved in THF (285 mL) and cooled to 0 °C under argon. TBAF (20.2 mL, 20.2 mmol) was then added dropwise at 0 °C. The reaction was allowed to warm to room temperature, then stirred at this temperature for 1 hour. This mixture was then evaporated to give a black oil. The residue was redissolved in EtOAc (500 mL) and then passed through a Celite plug, washed with water (2 x 250 mL), then brine (250 mL), dried over $MgSO_4$, filtered and evaporated to give a brown oil. The crude product was purified by silica gel chromatography, eluent 5% EtOAc in hexane. Pure fractions were evaporated to give desired product as an orange solid (2.1 g, 69%), mp 37.4-38.8 °C. ^{1}H NMR (400 MHz, $CDCl_3$): δ 3.12 (1H, s, H_8), 3.89 (3H, s, OMe), 6.92-7.01 (2H, m, $H_{3,6}$), 7.48 (1H, d, J=8.1 Hz, C_5); ^{13}C NMR (176 MHz, $CDCl_3$): δ 56.2 (OMe), 77.9 (C_8), 82.8 (C_7), 112.9 (C_1), 115.2 (C_6), 122.3 (C_2), 125.5 (C_3), 133.2 (C_5), 155.6 (C_4); IR (ν_{max}, cm^{-1}) 2051.4 (w, alkyne C-C), 2938.5 (w, alkene C-H), 3257.6 (s, alkyne C-H), *inter alia*; LRMS (ASAP) 210.0 (M^+-^{79}Br, 54%), 212.0 (M^+-^{81}Br, 57); HRMS (ASAP) [$C_9H_7O^{79}Br$] calculated 209.9680, found 209.9689.

[(Z)-7-Bromo-7-(4-bromo-3-methoxyphenyl)ethenyl] boronic acid **227**

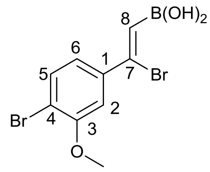

To a well-stirring solution of BBr_3 (0.19 mL, 1.92 mmol) in DCM (18 mL) was added 1-bromo-4-ethynyl-2-methoxybenzene (0.402 g, 1.92 mmol) at -78 °C under a positive pressure of argon. The resulting purple solution was stirred at – 78 °C for

2 hours and warmed to 0 °C before adding $NaHCO_3$ (0.323 g, 3.84 mmol) dissolved in H_2O (13 mL). The resulting pale yellow solution was stirred for 25 minutes, then transferred to a separating funnel. The mixture was extracted with DCM (2 x 20 mL) and the organics washed with H_2O (20 mL) and brine (20 mL), dried over $MgSO_4$, filtered and evaporated to yield [(*Z*)-7-bromo-7-(4-bromo-3-methoxyphenyl)ethenyl] boronic acid as an unstable pale yellow solid (0.522 g, 81%), mp 115.3-118.1 °C. ^{1}H NMR (400 MHz, $CDCl_3$): δ 3.94 (3H, s, CH_3), 6.47 (1H, s, H_8), 7.03-7.19 (2H, m, $H_{2,6}$), 7.45-7.60 (1H, m, H_5); ^{11}B NMR (128 MHz, $CDCl_3$): δ 27.61. The compound was taken on to the next stage without any further purification or characterisation. All spectroscopic data were consistent with those reported previously.[168]

(Z)-2-(2-Bromo-2-(4-bromo-3-methoxyphenyl)vinyl)-4,4,5,5-tetramethyl-1,3,2-dioxaborolane **228**

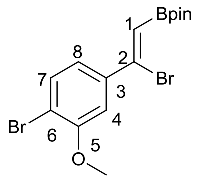

To a well-stirring solution of BBr_3 (6.0 mL, 6.0 mmol, 1.0 M in DCM) in DCM (57 mL) was added 1-bromo-4-ethynyl-2-methoxybenzene (1.25 g, 6.0 mmol) in DCM (10 mL) at -78 °C under a positive pressure of argon. The resulting purple solution was stirred at – 78 °C for 2 hours and warmed to 0 °C before adding sat. $NaHCO_3$ (19 mL). The resulting orange solution was stirred for 10 minutes, then transferred to a separating funnel. The mixture was extracted with DCM (2 x 114 mL) and the organics washed with H_2O (114 mL) and brine (114 mL), dried over $MgSO_4$, filtered and evaporated to yield a brown oil. This crude residue was then redissolved in DCM (63 mL) and $MgSO_4$ (1.46 g, 12.1 mmol) and pinacol (0.716 g, 6 mmol) were added. The reaction mixture was stirred for 1 hour at room temperature, then the solution was filtered and evaporated to give desired product as a brown solid (1.88 g, 75%), mp 74.8-77.0 °C.[168] ^{1}H NMR (700 MHz, $CDCl_3$): δ 1.35 (12H, s, Bpin), 3.91 (3H, s, OMe), 6.43 (1H, s, H_1), 7.07-7.13 (2H, m, $H_{4,8}$), 7.49 (1H, d, J=8.3 Hz, H_7); ^{11}B NMR (128 MHz, $CDCl_3$): δ 29.18; ^{13}C NMR (176 MHz, $CDCl_3$): δ 25.0 (Bpin), 56.4 (OMe), 84.2 (C_2), 111.3 (C_4), 113.2 (C_6), 120.9 (C_8), 133.1 (C_7), 138.9 (C_3), 141.8 (C_1), 155.6 (C_5); IR (ν_{max}, cm^{-1}) KBr disk 2978 (m), 2942 (m), *inter alia*;[168] LRMS (ASAP) 415.0 (M^+-$^{10}B^{79}Br$, 11%), 416.0 (M^+-$^{11}B^{79}Br$, 57), 417.0 (M^+-$^{10}B^{81/79}Br$, 88), 418.0 (M^+-$^{11}B^{81/79}Br$, 99), 419.0 (M^+-$^{10}B^{81}Br$, 100), 420.0 (M^+-$^{11}B^{81}Br$, 65); HRMS (ASAP) [$C_{15}H_{19}{}^{10}BO_3Br_2$] calculated 414.9830, found 414.9826. Structure confirmed by X-ray crystallography.[168]

1-[(Z)-7-Bromo-8-iodoethenyl]-3-methoxy-4-bromobenzene **238**

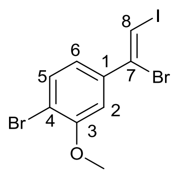

To a solution of [(*Z*)-7-bromo-7-(4-bromo-3-methoxyphenyl)ethenyl] boronic acid (0.972 g, 2.90 mmol) in MeCN (17 mL), protected from light, was added *N*-iodosuccinimide (0.780 g, 3.48 mmol) and the reaction mixture was stirred for 3 hours at room temperature. The reaction mixture was diluted with EtOAc (60 mL) and washed with 5% $Na_2S_2O_5$ (2 x 60 mL), H_2O (2 x 60 mL) and brine (60 mL). The organic layer was dried over $MgSO_4$, filtered and evaporated to yield 1.05 g of a crude orange oil. The crude product was purified by silica gel chromatography at 0 °C, eluent 5% EtOAc in petroleum ether. Pure fractions were evaporated to yield 1-[(*Z*)-7-bromo-8-iodoethenyl]-3-methoxy-4-bromobenzene as a pale yellow amorphous powder (0.947 g, 78%). ^1H NMR (400 MHz, $CDCl_3$) δ: 3.92 (3H, s, Me), 6.98 (1H, dd, *J* = 8.3, 2.1 Hz, H_2), 7.03 (d, *J* = 2.1 Hz, 1H, H_6), 7.44 (1H, s, H_8), 7.50 (d, J=8.2 Hz, 1H, H_5); ^{13}C NMR (176 MH z, $CDCl_3$) δ: 56.3 (Me), 83.7 (C_8), 111.4 (C_6), 113.1 (C_1), 120.9 (C_2), 133.1 (C_5), 136.5 (C_4), 140.0 (C_7), 155.7 (C_3); IR (ν_{max}, cm^{-1}) 3044.4 (w, arom. C-H), 2939.5 (w, alkene C-H), 1585.7 (m, arom. C=C), 1581.5 (m, arom. C=C), 1546.2 (m, arom. C=C); LCMS (ASAP) 416.8 (M^+-^{79}Br, 55%), 418.8 (M^+-$^{81/79}Br$, 100), 420.8 (M^+-^{81}Br, 53); HRMS (ASAP) calculated [$C_9H_7Br_2IO$] 417.8065, found 417.7909.

1-Bromo-4-(1-bromoethenyl)-2-methoxybenzene **236**

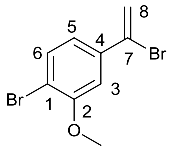

To a well-stirring solution of BBr_3 (4.8 mL, 4.78 mmol, 1.0 M solution in DCM) in DCM (45 mL) at -78 ^{o}C was added a solution of 1-bromo-4-ethynyl-2-methoxybenzene (1.0 g, 4.78 mmol) dropwise. The resulting deep pink solution was then stirred at -78 $^{\circ}$C for 3 hours. The reaction mixture was then allowed to warm to 0 $^{\circ}$C and sat. $NaHCO_3$ (15 mL), followed by Et_2O (30 mL), were added dropwise at 0 $^{\circ}$C. The now pale yellow reaction mixture was then stirred at this temperature for 2 hours. The reaction mixture was then transferred to a separating funnel and the layers separated. The aqueous layer was then washed with DCM (2 x 100 mL), then the organics was with H_2O (100 mL) and then brine (100 mL). The organics were then dried over $MgSO_4$, filtered and evaporated to yield 1.4 g of a pale yellow solid. The crude solid was then purified by silica gel chromatography, elution gradient 0% to 10% to 50% EtOAc in hexane. Pure fractions were evaporated to give 0.411 g of a pale yellow solid containing 41% desired product (0.173 g, 13%). ^{1}H NMR (600 MHz, $CDCl_3$): δ; 3.93 (3H, s, OMe), 5.80 (1H, d, J=2.1 Hz, H_8), 6.12 (1H, d, J=2.1 Hz, H_8), 7.02-7.12 (2H, m, $H_{3,5}$), 7.50 (1H, d, J= 8.2 Hz, H_6); ^{13}C NMR (151 MHz, $CDCl_3$): δ 56.4 (OMe), 111.2 (C_3), 112.7 (C_1), 118.4 (C_8), 120.5 (C_5), 129.7 (C_7) 132.92 (C_6), 139.2 (C_4) 156.5 (C_2); IR (ν_{max}, cm^{-1}) : 2836 (m, C=C-H), 2943 (m, C=C-H), 2970 (m, C=C-H) *inter alia*; LCMS (ASAP); 289.9 (M^+-^{79}Br, 2%), 291.1 (M^+-$^{81/79}$Br, 5), 293.9 (M^+-^{81}Br, 3); HRMS (ASAP) calculated [$C_9H_8O^{79}Br_2$] 289.8959, found 289.8942.

2-[(E)-2-(4-Bromo-3-methoxyphenyl)ethenyl]-4,4,5,5-tetramethyl-1,3,2-dioxaborolane **240**

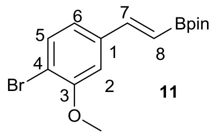

Copper(I) chloride (16 mg, 0.158 mmol), xantphos (92 mg, 0.158 mmol), sodium *tert*-butoxide (31 mg, 0.32 mmol) and 4,4,5,5-tetramethyl-2-(tetramethyl-1,3,2-dioxaborolan-2-yl)-1,3,2-dioxaborolane (1.33 g, 5.28 mmol) were added to a dry flask fitted with a Schlenk tap under argon. Dry THF (11 mL) was then added and the reaction stirred for 5 minutes. 1-bromo-4-ethynyl-2-methoxybenzene (1.11 g, 5.28 mmol) was then added and the reaction stirred for 5 minutes, then dry MeOH (0.42 mL) was added. The reaction was stirred at room temperature overnight. The reaction mixture was diluted with EtOAc (110 mL) and washed with H_2O (105 mL) and then brine (105 mL). The organics were dried over $MgSO_4$, filtered and evaporated to yield 2.40 g of a dark yellow oil. The crude product was purified by silica gel chromatography, eluent 0-5% EtOAc in hexane. Pure fractions were evaporated to yield desired product as a yellow oil, which became a yellow solid on standing (1.40 g, 79%), mp 66.9-69.3 ^oC. ^1H NMR (400 MHz, $CDCl_3$) δ 1.31 (12H, s, Bpin), 3.90 (3H, s, Me), 6.16 (1H, d, J=18.4 Hz, H_8), 6.91-7.06 (2H, m, $H_{2,6}$), 7.33 (1H, d, J=18.4 Hz, H_7), 7.49 (1H, d, J=8.1 Hz, H_5); ^{11}B NMR (128 MHz, $CDCl_3$) δ 29.69; ^{13}C NMR (101 MHz, $CDCl_3$) δ 25.0 (Bpin), 56.2 (Me), 83.7 (C_8), 110.1 (C_7), 112.5 (C_4), 120.8 (C_6), 133.5 (C_1), 138.4 (C_2), 148.6 (C_5), 156.1 (C_3); IR (ν_{max}, cm^{-1}) 1548.4 (m, arom. C=C), 1619.8 (m, arom. C=C) *inter alia*; LRMS (ESI) 339.1 ([M+H]-^{79}Br, 47%), 341.1 ([M+H]-^{81}Br, 50); HRMS (ESI) [$C_{15}H_{21}{}^{10}BO_3{}^{79}Br$] calculated 338.0803, found 338.0814.

1-Bromo-4-[(1Z)-1-bromobuta-1,3-dien-1-yl]-2-methoxybenzene **244**

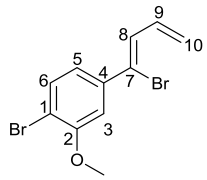

$Pd(PPh_3)_2Cl_2$ (2 mg, 0.024 mmol) and 1-[(*Z*)-7-bromo-8-iodoethenyl]-3-methoxy-4-bromobenzene (0.20 g, 0.481 mmol) were added to a dry flask, and the flask purged with argon for 5 minutes. Dry, degassed MeCN (5.0 mL) was added, followed tributyl(vinyl)tin (0.14 mL, 0.481 mmol). The reaction was then stirred at room temperature for 16 hours, then at 50 °C for 2 days. The reaction mixture was diluted with EtOAc containing ~ 3 ppm BHT (20 mL) and passed through a Celite/silica plug, then the solvent evaporated to give 0.408 g of a dark yellow oil. The crude product mixture was purified by silica gel chromatography, elution gradient 0-5% EtOAc in petroleum ether. Fractions containing product were evaporated to give 0.185 g of a dark yellow oil as a mixture containing desired product (26 mg, 17%). ^{1}H NMR (600 MHz, $CDCl_3$) δ 3.92 (3H, s, OMe), 5.43 (1H, dd, J=9.6, 1.5 Hz, $H_{10\textit{cis}}$), 5.49-5.61 (1H, m, $H_{10\textit{trans}}$), 6.75-6.84 (2H, m, $H_{8,9}$), 7.04-7.12 (3H, m, $H_{3,5,6}$); LRMS (ASAP) 315.9 (M^+-^{79}Br, 2%), 317.9 (M^+-$^{79/81}$Br, 4), 319.9 (M^+-^{81}Br, 3); HRMS (ASAP) [$C_{11}H_{11}Br_2O$] calculated 316.9177, found 316.9188. No further characterisation was performed.

[(3Z)-4-Bromo-4-(4-bromo-3-methoxyphenyl)but-3-en-1-yn-1-yl]trimethylsilane **251**

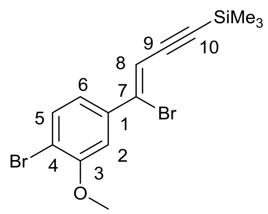

$Pd(PPh_3)_2Cl_2$ (2 mg, 0.024 mmol), copper (I) iodide (1 mg, 0.048 mmol) and 1-[(*Z*)-7-bromo-8-iodoethenyl]-3-methoxy-4-bromobenzene (0.2 g, 0.481 mmol) were added to a dry flask, and the flask sealed and purged with argon for 5 minutes. Dry, degassed Et_3N (3.0 mL) was added, followed by ethynyl trimethylsilane (0.08 mL, 0.577 mmol). The reaction was then stirred at room temperature for 3 days. The solvent was evaporated to give 0.353 g of a dark brown residue, which was subjected to silica gel chromatography, eluent 5% EtOAc in hexane. Fractions containing product were evaporated to give 0.202 g of a light brown solid which was a mixture containing desired product. ^{1}H NMR (400 MHz, $CDCl_3$) δ 0.19 (9H, s, $SiMe_3$ (under TMS signal)), 3.91 (3H, s, OMe) 6.32 (1H, s, H_8), 7.07 (1H, dd, J=8.3, 2.0 Hz, H_6), 7.16 (1H, d, J=2.0 Hz, H_2), 7.49 (1H, d, J=8.2 Hz, H_5); LRMS (ASAP) 385.9 (M^+-^{79}Br, 6%) 387.9 (M^+-$^{79/81}$Br, 14), 389.9 (M^+-^{81}Br, 10); HRMS (ASAP) calculated [$C_{14}H_{16}{}^{79}Br_2OSi$] 385.9337, found 385.9349. No further characterisation was performed (see main discussion).

Methyl (2E)-5-(4-bromo-3-methoxyphenyl)pent-2-en-4-ynoate **252**

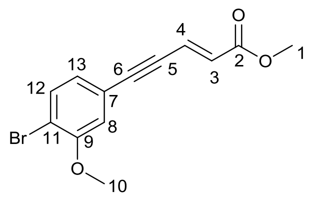

1-bromo-4-ethynyl-2-methoxybenzene (0.175 g, 0.833 mmol), methyl(2*E*)-3-iodoprop-2-enoate (0.147 g, 0.694 mmol), bis(triphenylphosphine)palladium(II) dichloride (49 mg, 0.007 mmol) and copper (I) iodide (1 mg, 0.007 mmol) were added to a flask, which was then purged with argon for 5 minutes. Dry, degassed Et_3N (3.9 mL) was then added and the reaction stirred in the dark at room temperature for 3 days. The solvent was then evaporated to give 0.347 g of a dark yellow solid. This residue was then purified using silica gel chromatography, eluent 25% EtOAc in hexane. Pure fractions were evaporated to give desired product as a yellow solid (0.204 g, 89%), mp 85.8-86.8 ^oC. ^1H NMR (700 MHz, $CDCl_3$): δ 3.78 (3H, s, H_1), 3.90 (3H, s, H_{10}), 6.32 (1H, d, J= 15.8 Hz, H_3), 6.89-6.99 (3H, m, H_4, H_8, H_{13}), 7.50 (1H, d, J= 8.0 Hz, H_{12}); ^{13}C NMR (176 MHz, $CDCl_3$): δ 51.9 (C_1), 56.3 (C_{10}), 86.8 (C_5), 97.4 (C_6), 113.6 (C_{11}), 114.8 (C_{13}), 122.3 (C_9), 124.9 (C_4), 125.4 (C_{12}), 130.0 (C_3), 133.4 (C_8), 155.7 (C_7), 166.2 (C_2); IR (ν_{max}, cm^{-1}) 1713.9 (s, C=O), 2198.7 (s, alkyne), 2947.3 (w, alkene C-H) *inter alia*; LRMS (ASAP) 295.0 ([M+H]-^{79}Br, 100%), 297.0 ([M+H]-^{81}Br, 100); HRMS (ASAP) calculated [$C_{13}H_{12}O_3{}^{79}Br$] 294.9969, found 294.9970. Structure determined by X-ray crystallography.

Silver(I) oxide

A 1 M solution of NaOH in H_2O (100 mL) was added slowly to a well-stirring 1 M solution of $AgNO_3$ in H_2O (100 mL) and the resulting flocculating solid suspension stirred for 5 minutes. The solid was filtered and dried to give desired product as a brown solid (15.4 g, 67%).

Methyl (2E,4E)-5-(4-bromo-3-methoxyohenyl)penta-2,4-dienoate **253**

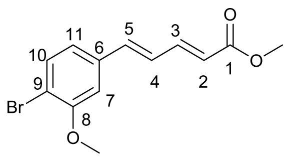

2-[(*E*)-2-(4-Bromo-3-methoxyphenyl)ethenyl]-4,4,5,5-tetramethyl-1,3,2-dioxaborolane (0.256 g, 0.76 mmol), methyl (2*E*)-3-iodoprop-2-enoate (0.129 g, 0.61 mmol), $Pd(PPh_3)_2Cl_2$ (22 mg, 0.031 mmol) and silver oxide (0.174 g, 0.76 mmol) were added to a dry flask and the flask sealed and purged with argon. Dry, degassed DME (4.6 mL) was then added and the reaction stirred at 60 °C for 2 days

17 hours. The reaction mixture was then diluted with EtOAc (50 mL) and passed through a short Celite/silica plug. The solvent was evaporated to give 0.340 g of a crude green/yellow solid. The crude residue was purified by silica gel chromatography, eluent 0-5% EtOAc in hexane to give 0.110 g of a bright yellow solid which rapidly polymerised, but from which the desired product could be identified (est. 41% I.Y. by ^{1}H NMR). ^{1}H NMR (400 MHz, $CDCl_3$) δ: 3.69 (3H, s), 3.86 (3H, s), 5.96 (1H, d, J=15.3 Hz), 6.85-6.93 (2H, m), 7.33 (1H, d, J=10.0 Hz), 7.45-7.52 (1H, m), 7.55-7.50 (2H, m); LRMS (ASAP) 297.0 ([M+H] -^{79}Br, 100%), 299.0 ([M+H] -^{79}Br, 99%) ; HRMS (ASAP) [$C_{13}H_{14}O_3Br$] calculated 297.0126, found, 297.0128. No further characterisation was performed due to instability.

Methyl (2E,4Z)-5-bromo-5-(4-bromo-3-methoxyohenyl)penta-2,4-dienoate **241**

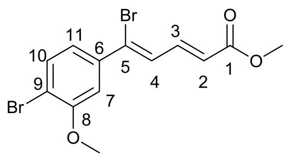

2-[(*Z*)-2-Bromo-2-(4-bromo-3-methoxyphenyl)ethenyl]-4,4,5,5-tetramethyl-1,3,2-dioxaborolane (60 mg, 0.144 mmol), methyl (2*E*)-3-iodoprop-2-enoate (25 mg, 0.12 mmol), $Pd(PPh_3)_2Cl_2$ (4.2 mg, 0.006 mmol) and silver oxide (33 mg, 0.144 mmol) were added to a dry flask and the flask sealed and purged with argon. Dry, degassed DME (1.1 mL) was then added and the reaction stirred at 60 °C for 2 days 15 hours. The reaction mixture was then diluted with EtOAc (10 mL), passed through a short plug of Celite and the solvent evaporated to give 57 mg of a crude brown oil from which the desired product could be identified. ^{1}H NMR (400 MHz, $CDCl_3$) δ: 3.74 (3H, s), 3.90 (3H, s), 6.12 (1H, dd, J=15.4, 0.9 Hz), 7.03-7.12 (2H, m), 7.35 (1H, dd, J=8.1, 2.0 Hz), 7.46 (2H, d, J=8.0 Hz); LRMS (ASAP) 374.9 ([M+H]-^{79}Br, 36%), 376.9 ([M+H]-$^{79/81}$Br, 68%), 378.9 ([M+H]-^{81}Br, 36%). HRMS (ASAP) [$C_{13}H_{13}O_3Br_2$] calculated 374.9231, found 374.9247. No further characterisation was performed (see main discussion).

(2E,4E)-5-(4,4,6-Trimethyl-[1,3,2-dioxaborinan-2-yl]-penta-2,4-dienoic acid methyl ester **259**

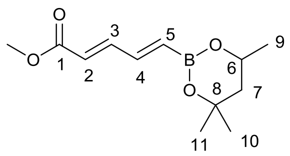

Method 1: To a dry Schlenk flask was added $Pd(OAc)_2$ (36 mg, 0.160 mmol), $P(o\text{-tol})_3$ (0.10 g, 0.330 mmol) and AgOAc (0.601 g, 3.60 mmol). The flask was purged with argon, and dry, degassed MeCN (10 mL) was added. 4,4,6-Trimethyl-2-vinyl-1,3,2-dioxaborinane (0.655 mL, 3.80 mmol) was then added, followed by methyl (2*E*)-3-iodoprop-2-enoate (0.704 g, 3.32 mmol). The vessel was purged further with argon, and the reaction mixture was then heated to 50 °C with vigorous stirring for 2 days. The mixture was allowed to cool, then diluted with Et_2O (280 mL) and passed through a short Celite/silica plug. The organic extracts were washed with 5% HCl (40 mL), H_2O (80 mL) and brine (80 mL), dried over $MgSO_4$ and evaporated to yield 0.980 g of crude product as an orange oil. The crude product was purified by silica gel chromatography, eluent 10% EtOAc in hexane elution. Pure fractions were evaporated to yield (2*E*,4*E*)-5-(4,4,6-trimethyl-[1,3,2-dioxaborinan-2-yl]-penta-2,4-dienoic acid methyl ester as a yellow oil (0.404 g, 51%). ^{1}H NMR (400 MHz, $CDCl_3$): δ 1.35-1.24 (9H, m, $H_{9,10,11}$), 1.5-1.47 (1H, m, H_7), 1.81 (1H, dd, J=14.0, 2.9 Hz, H_7), 3.75 (3H, s, Me), 4.24 (1H, dqd, J=12.3, 6.2, 2.9 Hz, H_6), 5.99-5.86 (2H, m, $H_{2,5}$), 6.97 (1H, ddd, J=17.3, 11.0, 0.7 Hz, H_4), 7.33-7.21 (1H, m, H_3); ^{11}B NMR (128 MHz, $CDCl_3$): δ 25.52; ^{13}C NMR (101 MHz, $CDCl_3$): δ 23.58 ($C_{9,10,11}$), 28.62 ($C_{9,10,11}$), 31.65 ($C_{9,10,11}$), 46.41 (C_7), 52.12 (Me), 65.52 (C_6), 71.67 (C_8), 123.17 ($C_{2,5}$), 143.89 (C_4), 146.54 (C_3), 167.93 (C_1); IR (ν_{max}, cm^{-1}) 2974.3 (w, C=C-H) 1719.5 (s, C=O) *inter alia*; LCMS (ESI) 237.1 (M^+-^{10}B, 5%), 238.1 (M^+-^{11}B, 59); HRMS (ESI+) calculated $[C_{12}H_{19}BO_4+H]^+$ 238.1470, found 238.1491.

Method 2: To a dry flask was added methyl (2*E*)-3-iodoprop-2-enoate (2.82 g, 13.3 mmol), $Pd(OAc)_2$ (0.150 g, 0.67 mmol), $P(o\text{-tol})_3$ (0.408 g, 1.34 mmol) and AgOAc (2.41 g, 14.4 mmol). The flask was purged with argon, and dry, degassed

MeCN (80 mL) was added. 4,4,6-Trimethyl-2-vinyl-1,3,2-dioxaborinane (2.6 mL, 15.2 mmol) was then added, the vessel was purged further with argon, and the reaction mixture was then heated to 50 °C with vigorous stirring for 23 hours. The mixture was allowed to cool, then diluted with Et_2O (200 mL) and passed through a short Celite/silica plug. The organic extracts were washed with NH_4Cl (200 mL), H_2O (200 mL) and brine (200 mL), dried over $MgSO_4$, filtered and evaporated to give crude product as a yellow oil (2.65g, 83%). The compound was taken on to the next stage without any further purification or characterisation.

Method 3: To a dry flask was added methyl (2*E*)- 3-iodoprop-2-enoate (2.82 g, 13.3 mmol), $Pd(OAc)_2$ (0.150 g, 0.67 mmol), P(*o*-tol)$_3$ (0.408 g, 1.34 mmol) and AgOAc (2.41 g, 14.4 mmol). The flask was purged with argon, and dry, degassed MeCN (72 mL) was added. 4,4,6-Trimethyl-2-vinyl-1,3,2-dioxaborinane (2.6 mL, 15.2 mmol) was then added, the vessel was purged further with argon, and the reaction mixture was then heated to 30 °C with vigorous stirring for 19 hours. The mixture was allowed to cool, then diluted with Et_2O (200 mL) and passed through a short Celite/silica plug. The solvent was evaporated to give crude product as a yellow oil (2.84g, 89%). The compound was taken on to the next stage without any further purification or characterisation.

Method 4: To a dry flask was added methyl (2*E*)-3-iodoprop-2-enoate (1.0 g, 4.72 mmol), $Pd(OAc)_2$ (0.011 g, 0.0472 mmol), tri(2-furyl)phosphine (0.022 g, 0.094 mmol) and AgOAc (0.851 g, 5.11 mmol). The flask was purged with argon, and dry, degassed MeCN (28 mL) was added. 4,4,6-Trimethyl-2-vinyl-1,3,2-dioxaborinane (0.93 mL, 5.4 mmol) was then added, the vessel was purged further with argon, and the reaction mixture was stirred vigorously at room temperature for 3 hours. The mixture was diluted with Et_2O (71 mL) and passed through a short Celite/silica plug. The solvent was evaporated to give crude product as a pale yellow oil (1.0 g, 89%). The compound was taken on to the next stage without any further purification or characterisation.

Methyl (2E,4E)-5-iodopenta-2,4-dienoate **260**

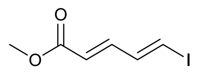

Method 1: NaOMe (4.2 mL, 2.10 mmol, 0.5 M solution in MeOH) was added dropwise to a solution of (2*E*,4*E*)-5-(4,4,6-trimethyl-[1,3,2-dioxaborinan-2-yl]-penta-2,4-dienoic acid methyl ester (0.404 g, 1.70 mmol) in THF (6.0 mL) cooled to -78 °C for 1 hour 50 minutes. The reaction mixture was allowed to warm to room temperature whilst stirring. The mixture was diluted with Et_2O (60 mL) and washed with 5% $Na_2S_2O_5$ (2 x 20 mL), H_2O (20 mL) and brine (20 mL). The organic extracts were dried over $MgSO_4$, filtered and evaporated to yield a pale orange solid. The crude material was purified by silica gel chromatography, eluent 5% EtOAc in petroleum ether at 0 °C. Pure fractions were evaporated to yield methyl (*2E,4E*)-5-iodopenta-2,4-dienoate as a white solid (0.337 g, 83%). ^{1}H NMR (400 MHz, $CDCl_3$): δ 3.75 (3H, s), 5.84-5.98 (1H, m), 6.89-6.98 (1H, m), 7.12-7.22 (2H, m); ^{13}C NMR (101 MHz, $CDCl_3$): δ 51.6, 89.6, 92.0, 121.0, 125.1, 136.4, 142.9. The compound was taken on to the next stage without any further characterisation.

Method 2: NaOMe (28 mL, 14.2 mmol, 0.5 M solution in MeOH) was added dropwise to a solution of (2*E*,4*E*)-5-(4,4,6-trimethyl-[1,3,2-dioxaborinan-2-yl]-penta-2,4-dienoic acid methyl ester (2.84 g, 11.9 mmol) in THF (44 mL) cooled to -78 °C under argon in the absence of light. The mixture was stirred at this temperature for 1 hour 5 minutes and iodine monochloride (12 mL, 12.1 mmol, of a 1.0 M solution in DCM) was added dropwise. The mixture was stirred at -78 °C for 2 hours, then allowed to warm to room temperature whilst stirring. The mixture was diluted with Et_2O (356 mL) and washed with 5% $Na_2S_2O_5$ (2 x 142 mL), water (142 mL) and brine (142 mL). The organic extracts were dried over $MgSO_4$, filtered and evaporated to 3.2 g of a brown oil containing desired product (2.14 g, 76%). The compound was taken on to the next stage without any further purification or characterisation.

Methyl (2E,4E,6E)-7-(4,4,6-trimethyl-1,3,2-dioxaborinane-2-yl)hepta-2,4,6-trienoate **261**

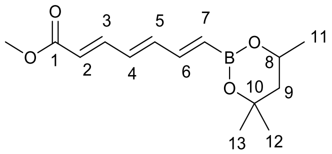

Method 1: To a dry Schlenk flask was added $Pd(OAc)_2$ (16 mg, 0.0710 mmol), P(*o*-tol)$_3$ (43 mg, 0.142 mmol) and AgOAc (0.284 g, 1.70 mmol), followed by a solution of (*2E,4E*)-5-iodopenta-2,4-dienoate (0.337 g, 1.42 mmol) in dry, degassed MeCN (4.5 mL). 4,4,6-Trimethyl-2-vinyl-1,3,2-dioxaborinane (0.24 mL, 1.42 mmol) was then added and the reaction mixture was then heated to 50 °C with vigorous stirring for 2 days. The mixture was allowed to cool, then diluted with Et_2O (80 mL) and passed through a short Celite/silica plug. The organic extracts were washed with H_2O (40 mL) and brine (40 mL), dried over $MgSO_4$, filtered and evaporated to yield 0.333 g of crude product as an orange oil. The crude product was purified by silica gel chromatography, eluent 10% EtOAc in hexane, to yield methyl (*2E*,*4E*,*6E*)-7-(4,4,6-trimethyl-1,3,2-dioxaborinane-2-yl)hepta-2,4,6-trienoate as a pale yellow solid (78 mg, 21%), mp 80.1-82.1°C. ^{1}H NMR (400 MHz, $CDCl_3$): δ 1.36-1.23 (9H, m, $H_{11,12,13}$), 1.56-1.47 (1H, m, H_9), 1.80 (1H, dd, J=13.9, 3.0 Hz, H_9), 3.75 (3H, s, Me), 4.24 (1H, dqd, J=12.3, 6.2, 3.2 Hz, H_8), 5.71 (1H, d, J=17.4 Hz, H_7), 5.92 (1H, d, J=15.3 Hz, H_2), 6.46-6.33 (1H, m, H_4), 6.58 (1H, ddd, J=15.0, 10.7, 0.9 Hz, H_5), 6.97 (1H, dd, J=17.4, 10.7 Hz, H_6), 7.35-7.27 (1H, m, H_3); ^{11}B NMR (128 MHz, $CDCl_3$): δ 25.90; ^{13}C NMR (101 MHz, $CDCl_3$): δ 23.1 ($C_{11,12,13}$), 28.1 ($C_{11,12,13}$), 31.2 ($C_{11,12,13}$), 46.0 (C_9), 51.6 (Me), 64.9 (C_8), 71.0 (C_{10}), 121.5 ($C_{2,7}$), 131.7 (C_4), 142.4 (C_5), 144.5 (C_3), 145.2 (C_6), 167.4 (C_1); IR (ν_{max}, cm^{-1}) 2972.0 (w, C=C-H), 2949.7 (w, C=C-H), 2924.1 (w, C=C-H) 1705.9 (C=O) *inter alia*; LCMS (ESI) 263.2 (M^+-^{10}B, 5%), 264.2 (M^+-^{11}B, 45); HRMS (ESI+) calculated $[C_{14}H_{21}BO_4+H]^+$ 264.1620, found 264.1647.

Method 2: To a dry flask was added $Pd(OAc)_2$ (0.120 g, 0.525 mmol), P(*o*-tol)$_3$ (0.315 g, 1.50 mmol) and AgOAc (1.89 g, 11.3 mmol). The flask was purged with argon, and a solution of (*2E,4E*)-5-iodopenta-2,4-dienoate (2.50 g, 10.5 mmol) in dry, degassed MeCN (63 mL) was added. 4,4,6-Trimethyl-2-vinyl-1,3,2-dioxaborinane (2.2 mL, 12.6 mmol) was then added, the vessel was purged further with argon, and the reaction mixture was then heated to 50 °C with vigorous stirring for 19.5 hours. The mixture was allowed to cool, then diluted with Et_2O (180 mL) and passed through a short Celite/silica plug. The organic extracts were washed with NH_4Cl (180 mL), H_2O (180 mL) and brine (100 mL), dried over $MgSO_4$, filtered, evaporated and dried on the high vacuum line for 2 days to give crude product as a brown oil (1.7 g, 48% from starting acrylate). The compound was taken on to the next stage without any further purification or characterisation.

Method 3: To a dry flask was added $Pd(OAc)_2$ (0.102 g, 0.460 mmol), P(*o*-tol)$_3$ (0.276 g, 0.911 mmol) and AgOAc (1.64 g, 9.81 mmol), followed by a solution of (*2E,4E*)-5-iodopenta-2,4-dienoate (2.14 g, 8.99 mmol) in dry, degassed MeCN (54 mL). 4,4,6-Trimethyl-2-vinyl-1,3,2-dioxaborinane (1.8 mL, 10.3 mmol) was then added and the reaction mixture was then heated to 30 °C with vigorous stirring for 18.5 hours. The mixture was allowed to cool, then diluted with Et_2O (136 mL) and passed through a short Celite/silica plug. The solvent was evaporated to yield 3.8 g of a crude yellow solid containing desired product (2.28 g, 96%). The compound was taken on to the next stage without any further purification or characterisation.

Methyl (2E,4E,6E)-7-iodohepta-2,4,6-trienoate **230**

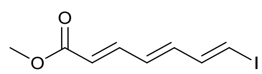

NaOMe (21 mL, 10.3 mmol, 0.5 M solution in MeOH) was added dropwise to a solution of methyl (2*E*,4*E*,6*E*)-7-(4,4,6-trimethyl-1,3,2-dioxaborinane-2-yl)hepta-2,4,6-trienoate (2.28 g, 8.6 mmol) in THF (32 mL) cooled to -78 °C under argon in the absence of light. The mixture was stirred at this temperature for 40 minutes and iodine monochloride (8.8 mL, 8.77 mmol, 1.0 M solution in DCM) was added dropwise. The mixture was stirred at -78 °C for 2 hours, then allowed to warm to room temperature whilst stirring. The mixture was diluted with Et_2O (258 mL) and washed with $Na_2S_2O_5$ (2 x 103 mL), water (103 mL) and brine (103 mL). The organic extracts were dried over $MgSO_4$, filtered and evaporated to yield 4.9 g of a red solid, from which completion was assumed. ^1H NMR (400 MHz, $CDCl_3$): δ 3.74 (3H,s), 5.98 (1H, d, J=15.3 Hz), 6.24-6.47 (2H, m), 6.61-6.71 (1H, m), 7.08-7.18 (1H, m), 7.20-7.31 (1H, m). The compound was taken on to the next stage without any further purification or characterisation.

Methyl (2E,4E,6E,8E)-9-(4,4,6-trimethyl-1,3,2-dioxaborinan-2-yl)nona-2,4,6,8-tetraenoate **262**

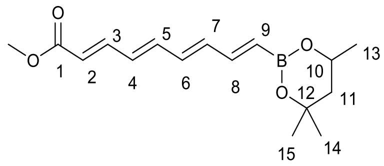

Method 1: To a dry flask was added $Pd(OAc)_2$ (82 mg, 0.357 mmol), P(*o*-tol)$_3$ (0.214 g, 0.714 mmol) and AgOAc (1.29 g, 7.71 mmol), followed by a solution of *methyl* (2*E*, 4*E*, 6*E*)-7-iodohepta-2,4,6-trienoate (1.70 g, 6.44 mmol) in dry, degassed MeCN (43 mL), which had been previously degassed by a bubbling argon needle. 4,4,6-trimethyl-2-vinyl-1,3,2-dioxaborinane (1.5 mL, 8.57 mmol) was then added and the reaction mixture was then heated to 50 °C with vigorous stirring for 21 hours. The mixture was allowed to cool, then diluted with Et_2O (150 mL) and passed through a short Celite/silica plug. The organic extracts were washed with H_2O (150 mL) and brine (150 mL), dried over $MgSO_4$, filtered and evaporated to yield 2.2 g of crude product as a brown oil. After drying the crude product on the high vacuum line for 2 days, 1.2 g of an orange solid was obtained. The compound was taken on to the next stage without any further purification or characterisation.

Method 2: To a dry flask was added $Pd(OAc)_2$ (98 mg, 0.44 mmol), P(*o*-tol)$_3$ (0.265 g, 0.875 mmol) and AgOAc (1.57 g, 9.42 mmol), followed by a solution of methyl (2*E*, 4*E*, 6*E*)-7-iodohepta-2,4,6-trienoate (2.28 g, 8.60 mmol) in dry, degassed MeCN (52 mL). 4,4,6-Trimethyl-2-vinyl-1,3,2-dioxaborinane (1.4 mL, 8.60 mmol) was then added and the reaction mixture was then heated to 30 °C with vigorous stirring for 15.5 hours. The mixture was allowed to cool, then diluted with Et_2O (131 mL) and passed through a short Celite/silica plug. The solvent was evaporated to yield 3.95 g of a crude viscous orange oil containing desired product (1.90 g, 76%). After drying the crude product on the high vacuum line for 2 days, 1.2 g of an orange solid was obtained. The compound was taken on to the next stage without any further purification or characterisation.

Method 3: To a dry flask was added $Pd(OAc)_2$ (0.134 g, 0.440 mmol), P(*o*-tol)$_3$ (0.364 g, 1.20 mmol) and AgOAc (2.16 g, 13.0 mmol), followed by a solution of methyl (2*E*, 4*E*, 6*E*)-7-iodohepta-2,4,6-trienoate (3.14 g, 11.9 mmol) in dry, degassed MeCN (72 mL). 4,4,6-Trimethyl-2-vinyl-1,3,2-dioxaborinane (2.0 mL, 11.9 mmol) was then added and the reaction mixture was then heated to 30 °C with vigorous stirring for 18 hours. The mixture was allowed to cool, then diluted with Et_2O (180 mL) and passed through a short Celite/silica plug. The solvent was evaporated to yield 4.5 g of a crude viscous orange oil. The crude product was purified by silica gel chromatography, eluent 5% EtOAc in petroleum ether, to give desired product as a bright yellow solid (0.9 g, 23% from iodoacrylate). ^{1}H NMR (700 MHz, $CDCl_3$): δ 1.23-1.33 (9H, m, $H_{13,14,15}$), 1.45-1.56 (1H, m, H_{11}), 1.79 (1H, dd, J=13.9, 2.9 Hz, H_{11}), 3.74 (3H, s, Me), 4.22 (1H, dqd, J=11.5, 6.1, 2.9 Hz, H_{10}), 5.59-5.65 (1H, m, H_9), 5.84-5.93 (1H, m, H_2), 6.27-6.46 (3H, m, $H_{4,6,7}$), 6.54-6.63 (1H, m, H_5), 6.91-7.00 (1H, m, H_8), 7.28-7.37 (1H, m, H_3); ^{11}B NMR (128 MHz, $CDCl_3$): δ 25.92; ^{13}C NMR (176 MHz, $CDCl_3$): δ 23.1 ($C_{13,14,15}$), 28.1 ($C_{13,14,15}$), 31.2 ($C_{13,14,15}$), 45.9 (C_{11}), 51.5 (Me), 64.8 (C_{10}), 70.9 (C_{12}), 110.1 (C_9), 120.6 (C_2), 130.9 ($C_{4,6,7}$), 133.6 ($C_{4,6,7}$), 138.9 ($C_{4,6,7}$), 140.6 (C_5), 144.4 (C_3), 145.8 (C_8), 167.4 (C_1); LCMS (ASAP) 289.2 (M^+-^{10}B, 3%), 290.2 (M^+-^{11}B, 15); HRMS (ASAP) calculated [$C_{16}H_{24}{}^{10}BO_4$] 290.1804, found 290.1777. The compound was taken on to the next stage without any further purification or characterisation.

Methyl (2E,4E,6E,8E)-9-iodonona-2,4,6,8-tetraenoate **263**

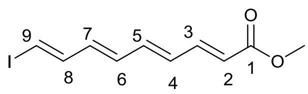

NaOMe (26 mL, 13.1 mmol, 0.5 M solution in MeOH) was added dropwise over 5 minutes to a solution of a crude mixture containing methyl (2*E*,4*E*,6*E*,8*E*)-9-(4,4,6-

trimethyl-1,3,2-dioxaborinan-2-yl)nona-2,4,6,8-tetraenoate (3.20 g, 10.9 mmol) in dry THF (41 mL) cooled to -78 °C under argon in the absence of light. The mixture was stirred at this temperature for 50 minutes and iodine monochloride (2.10 g, 11.3 mmol) in dry DCM (11 mL) was added dropwise over 5 minutes. The mixture was stirred at -78 °C for 3 hours 40 minutes, then allowed to warm to room temperature. The mixture was diluted with Et_2O (329 mL) and washed with $Na_2S_2O_5$ (2 x 132 mL), H_2O (132 mL) and brine (132 mL). The organic extracts were dried over $MgSO_4$, filtered and evaporated to yield 3.3 g of a dark brown solid. The crude product was purified by silica gel chromatography at 0 ^oC, eluent 0-5 % EtOAc in petroleum ether. Pure fractions were evaporated to yield desired product as an unstable yellow solid (0.754 g, 20% from starting iodoacrylate) ^1H NMR (700 MHz, $CDCl_3$): δ 3.75 (3H,s, OMe), 5.92 (1H, d, J=15.0 Hz, H_2), 6.29 (1H, dd, J=8.7, 6.1 Hz, H_7), 6.38-6.45 (1H, m, H_4), 6.47-6.55 (2H, m, $H_{5,8}$), 7.07-7.14 (1H, m, H_6), 7.27-7.34 (2H, m, $H_{3,9}$); ^{13}C NMR (176 MHz, $CDCl_3$) δ 51.7 (Me), 121.3 (C_2), 131.9 (C_4), 132.1 (C_7), 135.7 (C_8), 139.8 (C_5), 141.1 (C_9), 144.2 (C_3), 145.0 (C_6), 167.5 (C_1); LRMS (ASAP) [M+H]= 291.0. HRMS (ASAP) [$C_{10}H_{12}O_2{}^{127}I$], calculated 290.9882, found 290.9896.

Methyl (2E,4E,6E,8E,10E)-11-(4,4,6-trimethyl-1,3,2-dioxaborinan-2-yl)undeca-2,4,6,8,10-pentaenoate **231**

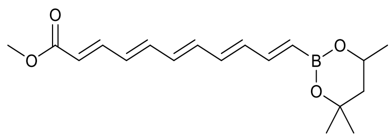

To a dry flask was added $Pd(OAc)_2$ (45 mg, 0.197 mmol), P(*o*-tol)$_3$ (0.117 g, 0.394 mmol) and AgOAc (0.713 g, 4.26 mmol), followed by a solution of methyl (2*E*,4*E*,6*E*,8*E*)-9-iodonona-2,4,6,8-tetraenoate (1.10 g, 3.79 mmol) in dry, degassed MeCN (24 mL). 4,4,6-Trimethyl-2-vinyl-1,3,2-dioxaborinane (0.75 mL, 4.34 mmol) was then added and the reaction mixture was then heated to 50 °C with vigorous stirring for 21 hours. The mixture was allowed to cool, then diluted with Et_2O (100 mL) and passed through a short Celite/silica plug. The organic extracts were washed with H_2O (100 mL) and brine (100 mL), dried over $MgSO_4$, filtered and evaporated to yield 1.2 g of crude product a deep red solid. A small portion (0.153 g) was taken and purified by silica gel chromatography, eluent 10% EtOAc in petroleum ether 40-60 °C to verify presence of product. ^{1}H NMR (400 MHz, $CDCl_3$): δ 1.21-1.35 (9H, m), 1.41-1.51 (1H, m), 1.72-1.88 (1H, m), 3.74 (3H, s), 4.23 (1H, dqd, J=12.2, 6.2, 2.9 Hz), 5.56-5.68 (1H, m), 5.88 (1H, d, J=15.3 Hz), 6.25-6.50 (5H, m), 6.92-7.02 (1H, m), 7.32 (1H, ddd, J=13.0, 11.0, 3.7 Hz); ^{11}B NMR (128 MHz, $CDCl_3$) δ 23.80. The compound was taken on to the next stage without any further purification or characterisation.

Methyl (2E,4E,6E,8E,10E)-11-iodoundeca-2,4,6,8,10-pentaenoate **264**

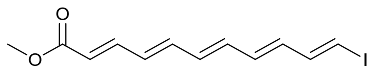

NaOMe (7.0 mL, 3.49 mmol, 0.5 M solution in MeOH) was added dropwise to a solution of (2*E*,4*E*,6*E*,8*E*,10*E*)-11-(4,4,6-trimethyl-1,3,2-dioxaborinan-2-yl)undeca-2,4,6,8,10-pentaenoate (1.05 g, 3.33 mmol) in THF (12 mL) cooled to -78 °C under argon in the absence of light. The mixture was stirred at this temperature for 1 hour 25 minutes and iodine monochloride (3.0 mL, 3.0 mmol, a 1.0 M solution in DCM) was added dropwise. The mixture was stirred at -78 °C for 1.5 hours, then allowed to warm to room temperature while stirring. The mixture was diluted with Et_2O (150 mL) and washed with 5% $Na_2S_2O_5$ (2 x 60 mL), H_2O (60 mL) and brine (60 mL). The organic extracts were dried over $MgSO_4$, filtered and evaporated to yield 0.70 g of a dark brown solid. ^{1}H NMR (400 MHz, $CDCl_3$): δ 3.75 (3H, s), 5.72-5.84 (1H, m), 5.85-5.96 (1H, m), 6.16-6.47 (5H, m), 6.47-6.69 (1H, m), 7.02-7.13 (1H, m), 7.28-7.37 (1H, m). The compound was taken on to the next stage without any further purification or characterisation.

Methyl (2E,4E,6E,8E,10E,12E)-13-(4,4,6-trimethyl-1,3,2-dioxaborinan-2-yl)trideca-2,4,6,8,10,12-hexaenoate **265**

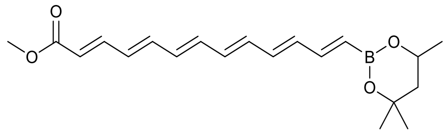

To a dry flask was added $Pd(OAc)_2$ (26 mg, 0.110 mmol), P(*o*-tol)$_3$ (68 mg, 0.210 mmol) and AgOAc (0.414 g, 2.26 mmol), followed by a solution of methyl (2*E*,4*E*,6*E*,8*E*,10*E*)-11-iodoundeca-2,4,6,8,10-pentaenoate (0.70 g, 2.20 mmol) in dry, degassed THF(4 mL) and dry, degassed MeCN (13 mL), which had been previously degassed by a bubbling argon needle. 4,4,6-Trimethyl-2-vinyl-1,3,2-dioxaborinane (0.44 mL, 2.52 mmol) was then added and the reaction mixture was then heated to 50 °C with vigorous stirring for 20 hours. The mixture was allowed to cool, then diluted with Et_2O (100 mL) and passed through a short Celite/silica plug. The organic extracts were washed with H_2O (100 mL) and brine (100 mL), dried over $MgSO_4$, filtered and evaporated to yield 0.661 g of crude product a neon orange solid. ^{1}H NMR (400 MHz, $CDCl_3$) δ 1.15-1.35 (9H, m), 1.50 (1H, dd, J=13.9, 11.6 Hz), 1.79 (1H, dd, J=13.9, 2.9 Hz), 3.75 (3H, s), 4.22 (1H, dqd, J=11.7, 6.2, 3.0 Hz), 6.22-6.48 (7H, m), 6.49-6.70 (1H, m), 7.01-7.18 (2H, m), 7.28-7.36 (2H, m). LRMS (ESI) M=342.1. The compound was taken on to the next stage without any further purification or characterisation.

Methyl (2E,4E,6E,8E,10E,12E)-13-iodotrideca-2,4,6,8,10,12-hexaenoate **266**

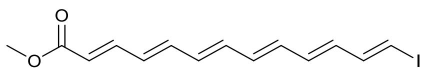

NaOMe (4.6 mL, 2.31 mmol, 0.5 M solution in MeOH) was added dropwise to a solution of methyl (2*E*,4*E*,6*E*,8*E*,10*E*,12*E*)-13-(4,4,6-trimethyl-1,3,2-dioxaborinan-2-yl)trideca-2,4,6,8,10,12-hexaenoate (0.661 g, 1.93 mmol) in THF (7.2 mL) cooled to -78 °C under argon in the absence of light. The mixture was stirred at this temperature for 50 minutes and iodine monochloride (2.0 mL, 1.99 mmol, 1.0 M solution in DCM) was added dropwise. The mixture was stirred at -78 °C for 1 hour

20 minutes, then allowed to warm to room temperature while stirring. The mixture was diluted with Et_2O (100 mL) and washed with 5% $Na_2S_2O_5$ (2 x 50 mL), H_2O (50 mL) and brine (50 mL). The organic extracts were dried over $MgSO_4$, filtered and evaporated to yield 0.523 g of a dark brown solid. The compound was taken on to the next stage without any further purification or characterisation (see main discussion).

Methyl (2E,4E,6E,8E,10E,12E,14E)-15-(4,4,6-trimethyl-1,3,2-dioxaborinan-2-yl)pentadeca-2,4,6,8,10,12,14-heptaenoate **267**

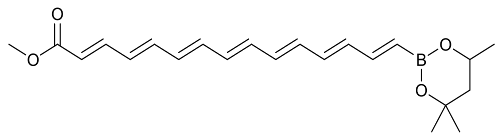

To a dry flask was added $Pd(OAc)_2$ (14 mg, 0.0610 mmol), P(*o*-tol)$_3$ (37 mg, 0.120 mmol) and AgOAc (0.223 g, 1.24 mmol), followed by a solution of methyl (2*E*,4*E*,6*E*,8*E*,10*E*,12*E*)-13-iodotrideca-2,4,6,8,10,12-hexaenoate (0.418 g, 1.22 mmol) in dry, degassed THF (3.1 mL) and dry, degassed MeCN (7.7 mL). 4,4,6-Trimethyl-2-vinyl-1,3,2-dioxaborinane (0.24 mL, 1.37 mmol) was then added and the reaction mixture was then heated to 50 °C with vigorous stirring for 17 hours. The mixture was allowed to cool, then diluted with Et_2O (80 mL) and passed through a short Celite/silica plug. The organic extracts were washed with H_2O (80 mL) and brine (80 mL), dried over $MgSO_4$, filtered and evaporated to yield 0.440 g of crude product a neon orange solid. The compound was taken on to the next stage without any further purification or characterisation (see main discussion).

Methyl (2E,4E,6E,8E,10E,12E,14E)-15-iodopentadeca-2,4,6,8,10,12,14-heptaenoate **268**

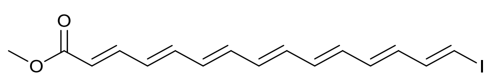

NaOMe (2.5 mL, 1.25 mmol, 0.5 M solution in MeOH) was added dropwise to a solution of methyl (2*E*,4*E*,6*E*,8*E*,10*E*,12*E*,14*E*)-15-(4,4,6-trimethyl-1,3,2-dioxaborinan-2-yl)pentadeca-2,4,6,8,10,12,14-heptaenoate (0.440 g, 1.20 mmol) in

THF (4.4 mL) cooled to -78 °C under argon in the absence of light. The mixture was stirred at this temperature for 50 minutes and iodine monochloride (1.1 mL, 1.08 mmol, 1.0 M solution in DCM) was added dropwise. The mixture was stirred at -78 °C for 1 hour 5 minutes, then allowed to warm to room temperature while stirring. The mixture was diluted with Et_2O (80 mL) and washed with 5% $Na_2S_2O_5$ (2 x 40 mL), water (40 mL) and brine (40 mL). The organic extracts were dried over $MgSO_4$, filtered and evaporated to yield 0.287 g of an orange solid. The compound was taken on to the next stage without any further purification or characterisation (see main discussion).

Methyl (2E)-5-(trimethylsilyl)pent-2-en-4-ynoate **283**

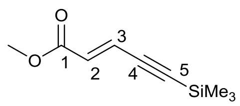

(2*E*)-3-iodoprop-2-enoate (5.0 g, 23.5 mmol), $Pd(PPh_3)_2Cl_2$ (0.160 g, 0.240 mmol) and copper (I) iodide (45 mg, 0.240 mmol) were added to a dry 3-neck flask and the vessel purged with argon for 5 minutes. Dry, degassed THF (60 mL) was added and then the solution was cooled to 0 °C. Et_3N (6.5 mL, 47.0 mmol) was added, followed by ethynyltrimethylsilane (3.3 mL, 23.5 mmol) and the flask was purged with argon for 2 minutes. The reaction mixture was stirred at room temperature for 19 hours. The reaction mixture was diluted with Et_2O (200 mL) and passed through a silica plug, then the solvent evaporated to give 5.44 g of a brown oil. The crude product was purified by silica gel chromatography, eluent 0-5% EtOAc in hexane. Pure fractions were evaporated to give desired product as a dark orange oil (4.21 g, 98%). ^1H NMR (400 MHz, $CDCl_3$): δ 0.19 (9H, s, $SiMe_3$), 3.73 (3H, s, OMe), 6.23 (1H, d, J=15.9 Hz, H_3), 6.72 (1H, d, J=15.9 Hz, H_2); ^{29}Si (139 MHz, $CDCl_3$) δ -16.84; ^{13}C NMR (101 MHz, $CDCl_3$): δ -0.3 ($SiMe_3$), 52.0 (OMe), 101.4 (C_4), 105.1 (C_5), 125.6 (C_2), 130.8 (C_3), 166.3 (C_1). Other spectroscopic data were consistent with those reported previously.[176]

(2E)-5-(Trimethylsilyl)pent-2-en-4-yn-1-ol **284**

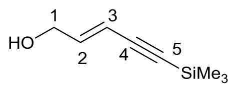

A solution of methyl (*2E*)-5-(trimethylsilyl)pent-2-en-4-ynoate (1.0 g, 5.50 mmol) in dry DCM (28 mL) was cooled to -78 ^{o}C and DIBAL (11 mL, 11.0 mmol, 1.0 M solution in hexanes) was added dropwise under argon. The reaction mixture was stirred at this temperature for 4 hours. A solution of 1M HCl (15 mL) was added and the reaction allowed to reach room temperature. The organic layer was washed with sat. $NaHCO_3$ (25 mL) to reach pH 7 and the aqueous washed with DCM (3 x 25 mL), then the organic extracts combined and washed with H_2O (25 mL) and brine (25 mL), dried over $MgSO_4$, filtered and evaporated to give desired product as a yellow oil (0.842 g, 95%). ^{1}H NMR (400 MHz, $CDCl_3$): δ 0.19 (9H, s, $SiMe_3$), 1.45 (1H, s, br, OH), 4.21 (2H, dd, J=5.1, 2.0 Hz, H_1), 5.77 (1H, dt, J=16.0, 1.95 Hz, H_3), 6.31 (1H, dt, J=16.0, 5.1 Hz, H_2); ^{29}Si NMR (139 MHz, $CDCl_3$) δ -18.01; ^{13}C NMR (101 MHz, $CDCl_3$): δ 0.04 ($SiMe_3$), 63.0 (C_1), 95.5 (C_5), 103.1 (C_4), 110.5 (C_3), 143.1 (C_2). Other spectroscopic data were consistent with those reported previously.[176]

(2E)-Pent-2-en-4-yn-1-ol **285**

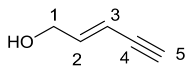

(*2E*)-5-(Trimethylsilyl)pent-2-en-4-yn-1-ol (1.48 g, 9.50 mmol) was dissolved in MeOH (38 mL) and cooled to -10 ^{o}C under argon. Aqueous NaOH (9.5 mL of a 2.5 M solution) was added slowly and the reaction stirred at this temperature for a further 2 hours. The reaction mixture was allowed to warm to room temperature and diluted with Et_2O (40 mL). The aqueous layer was further washed with Et_2O (40 mL), then the organics were washed with H_2O (40 mL) and brine (40 mL), dried over $MgSO_4$, filtered and evaporated to give desired product as a yellow oil (0.620 g, 79%). ^1H NMR (400 MHz, $CDCl_3$): δ 1.65 (1H, s, br, OH), 2.89 (1H, dq, J=2.2, 0.7 Hz, H_5), 4.14-4.28 (2H, m, H_1), 5.74 (1H, dq, J=16.0, 2.1 Hz, H_3), 6.35 (1H, dtd, J=16.0, 5.0, 0.7 Hz, H_2). Other spectroscopic data were consistent with those reported previously.[176]

(2E,4E)-5-(Tributylstannyl)penta-2,4-dien-1-ol **286**

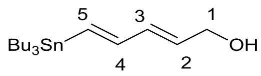

Pd_2dba_3 (35 mg, 0.038 mmol), $P(Cy)_3BF_4$ (56 mg, 0.152 mmol) and *N*,*N*-diisopropylethylamine (0.05 mL, 0.304 mmol) were added to dry, degassed DCM (76 mL) under a positive pressure of argon, then stirred for 10 minutes. A solution of (*2E*)-pent-2-en-4-yn-1-ol (0.620 g, 7.60 mmol) in DCM (20 mL) was added and the reaction cooled to 0 °C. Tributyltin hydride (2.43 mL, 9.12 mmol) in DCM (4 mL) was then added dropwise and the reaction stirred at 0 °C for 2 hours. The reaction was then allowed to warm to room temperature whilst stirring. The solvent was evaporated to give 3.50 g of a brown oil. The mixture was diluted with DCM (100 mL) and passed through Celite, then the solvent removed to give 3.34 g of a brown oil which was taken straight into the next stage. ^1H NMR (400 MHz, $CDCl_3$): δ 0.79-1.05 (15H, m, $SnBu_3$), 1.14-1.36 (6H, m, $SnBu_3$), 1.42-1.61 (6H, m, $SnBu_3$), 4.21 (2H, tdd, J=7.8, 4.4, 1.8 Hz, H_1), 5.58-5.93 (1H, m, H_2), 6.09-6.33 (2H, m, $H_{3,4,5}$), 6.47-6.63 (1H, m, $H_{3,4,5}$). Other spectroscopic data were consistent with those reported previously.[174]

(2E,4E)-5-(Tributylstannyl)penta-2,4-dienal **287**

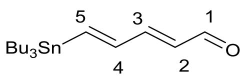

Activated MnO_2 was placed in a dry flask and the flask purged with argon, then suspended in DCM (19 mL) and stirred while continuing to purge with argon. A solution of (*2E*,*4E*)-5-(tributylstannyl)penta-2,4-dien-1-ol in DCM (11 mL) was added slowly to the suspension and the reaction stirred at room temperature for

2 hours 15 minutes. The reaction mixture was passed through a plug of Celite, then the filter cake washed with DCM (56 mL), then EtOAc (94 mL). The solvent was evaporated to give 0.823 g of a crude brown oil, containing desired product (0.412 g, 69% over the two steps). ^{1}H NMR (400 MHz, $CDCl_3$): δ 0.64-1.06 (15H, m, $SnBu_3$), 1.16-1.38 (6H, m, $SnBu_3$), 1.44-1.64 (6H, m, $SnBu_3$), 5.89-6.18 (1H, m, H_2), 6.70-6.87 (1H, m, H_5), 6.93-7.07 (2H, m, $H_{3,4}$), 9.57 (1H, d, J=8.0 Hz, H_1). Other spectroscopic data were consistent with those reported previously.[174]

(Dichloromethyl)boronic acid **289**

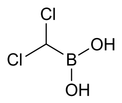

Dry DCM (0.75 mL, 11.8 mmol) was added to dry THF (21 mL) in a dry flask under argon and the solution cooled to -100 °C. *n*-BuLi (4.3 mL, 10.7 mmol, 2.5 M solution in hexanes) was added dropwise and the reaction stirred at -100 °C for 30 minutes. Trimethyl borate (1.3 mL, 11.8 mmol) was added all in one portion and the reaction stirred for 35 minutes. 5M HCl (2.1 mL) was then added and the reaction mixture was allowed to warm to room temperature. Et_2O (10 mL) was added and the layers separated. The aqueous was extracted with Et_2O (2 x 10 mL). The organics were combined, dried over $MgSO_4$, filtered and evaporated to a crude viscous pale yellow residue which became a solid on standing (1.54 g, 100 %). ^{1}H NMR (400 MHz, MeOD): δ 5.47; ^{11}B NMR (128 MHz, MeOD): δ 22.6; ^{13}C NMR (101 MHz, MeOD): δ 68.9. The compound was taken on to the next stage without any further purification or characterisation.

(Dichloromethyl)-4,4,5,5-tetramethyl-1,3,2-dioxaborolane **290**

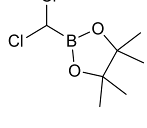

(Dichloromethyl) boronic acid (1.51 g, 11.8 mmol), $MgSO_4$ (2.84 g, 23.6 mmol) and pinacol (1.39 g, 11.8 mmol) were placed in a flask and the flask purged with argon.

Dry THF (16 mL) was then added and the reaction stirred at room temperature for 3 days. The reaction mixture was then filtered and the $MgSO_4$ washed with DCM, then the solvent evaporated to give desired product as a pale yellow oil (2.15 g, 86%). ^{1}H NMR (400 MHz, $CDCl_3$): δ 1.31 (12H, s, pinacol ester), 5.33 (1H, S, tertiary carbon). ^{11}B NMR (128 MHz, $CDCl_3$): δ 29.0; LRMS (ASAP) 210.1 (M^+-$^{10}B^{35}Cl$, 3%), 211.0 (M^+-$^{11}B^{35}Cl$, 8), 212.0 (M^+-$^{10}B^{35/37}Cl$, 2), 213.0 (M^+-$^{11}B^{35/37}Cl$, 6), 214.1 (M^+-$^{10}B^{37}Cl$, 5), 215.1 (M^+-$^{11}B^{37}Cl$, 5); HRMS (ASAP) calculated [$C_7H_{14}{}^{10}BO_2Cl_2$] 210.0500, found 210.0491. The compound was taken on to the next stage without any further purification or characterisation.

1-Bromo-4-[(E)-2-iodoethenyl]-2-methoxybenzene **273**

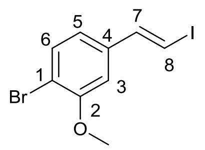

2-[(*E*)-2-(4-Bromo-3-methoxyphenyl)ethenyl]-4,4,5,5-tetramethyl-1,3,2-dioxaborolane (1.30 g, 3.85 mmol) was dissolved in dry THF (14 mL) and cooled to -78 °C under argon. NaOMe (9.2 mL, 4.62 mmol, 0.5 M in MeOH) was added dropwise and then reaction mixture stirred at -78 °C for 1 hour 15 minutes. Iodine monochloride (0.736 g, 3.95 mmol) in dry DCM (3.9 mL) was then added dropwise at this temperature and the reaction mixture stirred at -78 °C for a further 2 hours 10 minutes. The reaction mixture was allowed to warm to room temperature and diluted with Et_2O (116 mL), then washed with 5% $Na_2S_2O_5$ (2 x 46 mL), H_2O (46 mL) and brine (46 mL). The organics were dried over $MgSO_4$ under argon, filtered and evaporated to give 1.30 g of a crude yellow solid containing desired product (0.863 g, 66%). ^{1}H NMR (400 MHz, $CDCl_3$): δ 3.90 (3H, s), 6.75-6.82 (2H, m), 6.88 (1H, d, J=14.9 Hz), 7.37 (1H, d, J=14.9 Hz), 7.48 (1H, d, J=7.9 Hz). The compound was taken on to the next stage without any further purification or characterisation.

2-[(1E,3E)-4-(4-Bromo-3-methoxyphenyl)buta-1,3-dien-1-yl]-4,4,6-trimethyl-1,3,2-dioxaborinane **270**

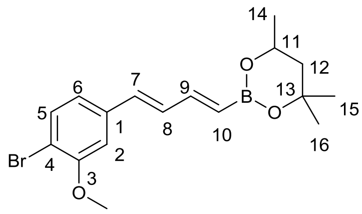

Method 1: 1-Bromo-4-[(*E*)-2-iodoethenyl]-2-methoxybenzene (0.863 g, 2.55 mmol) was dissolved in dry, degassed MeCN (15 mL) and added to a dry, argon-purged flask containing $Pd(OAc)_2$ (29 mg, 0.130 mmol), P(*o*-tol)$_3$ (77 mg, 0.255 mmol) and AgOAc (0.458 g, 2.74 mmol). 4,4,6-Trimethyl-2-vinyl-1,3,2-dioxaborinane (0.50 mL, 2.92 mmol) was then added and the reaction mixture heated to 50 $^{\circ}$C for 18 hours. The reaction mixture was allowed to cool to room temperature, then diluted with Et_2O containing ~3 ppm BHT (38 mL) and passed through a short Celite/silica plug. The solvent was evaporated to give 1.37 g of crude product as a viscous orange oil. The crude product was purified by silica gel chromatography, elution gradient 0-10 % EtOAc in petroleum ether. Pure fractions were evaporated to give desired product as a viscous yellow oil (0.725 g, 78%). ^{1}H NMR (600 MHz, $CDCl_3$): δ 1.23-1.33 (9H, m, $H_{14,15,16}$), 1.46-1.53 (1H, m, H_{12}), 1.80 (1H, ddd, J=14.0, 11.2, 2.9 Hz, H_{12}), 3.92 (3H, s, OMe), 4.24 (1H, dqd, J=14.8, 6.1, 3.1 Hz, H_{11}), 5.64 (1H, d, J=17.4 Hz, H_{10}), 6.59 (1H, d, 15.6 Hz, H_7), 6.77-6.84 (1H, m, H_8), 6.87-6.94 (2H, m, $H_{2,6}$), 7.06 (1H, dd, J=17.3, 10.5 Hz, H_9), 7.42-7.47 (1H, m, H_5); ^{11}B NMR (128 MHz, $CDCl_3$): δ 25.56; ^{13}C NMR (151 MHz, $CDCl_3$): δ 23.1, 28.1, 31.2 ($C_{14,15,16}$), 46.0 (C_{12}), 64.8 (C_{11}), 70.8 (C_{13}), 109.7 (C_6), 111.3 (C_4), 120.3 (C_2), 131.7 (C_8), 133.3 (C_5), 133.6 (C_{10}), 134.9 (C_7), 137.9 (C_1), 146.3 (C_9), 155.9 (C_3); LRMS (ASAP) 363.1 (M^+-$^{10}B^{79}Br$, 7%), 364.1 (M^+-$^{11}B^{79}Br$, 36), 365.1 (M^+-$^{10}B^{81}Br$, 100, includes [M+H]), 366.1 (M^+-$^{11}B^{81}Br$, 51); HRMS (ASAP) [$C_{17}H_{23}{}^{10}BO_3Br$] calculated 364.0960, found 364.0958.

Method 2: 1-Bromo-4-[(*E*)-2-iodoethenyl]-2-methoxybenzene (1.40 g, 4.15 mmol) was dissolved in dry, degassed MeCN (24 mL) and added to a dry, argon-purged flask containing $Pd(OAc)_2$ (46 mg, 0.208 mmol), P(*o*-tol)$_3$ (0.123 g, 0.408 mmol) and AgOAc (0.733 g, 4.38 mmol). 4,4,6-Trimethyl-2-vinyl-1,3,2-dioxaborinane (0.80 mL, 4.75 mmol) was then added and the reaction mixture heated to 30 °C for 21.5 hours. The reaction mixture was allowed to cool to room temperature, then diluted with Et_2O containing ~3 ppm BHT (61 mL) and passed through a short Celite/silica plug. The solvent was evaporated to give 1.67 g of crude product as a viscous orange oil. The crude product was purified by silica gel chromatography, elution gradient 0-10 % EtOAc in petroleum ether. Pure fractions were evaporated to give desired product as a viscous yellow oil (1.10 g, 73% over the two steps).

1-Bromo-4-[(1E,3E)-4-iodobuta-1,3-dien-1-yl]-2-methoxybenzene **274**

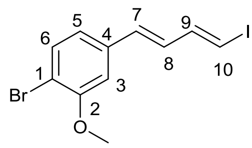

The crude mixture containing 2-[(*1E*,*3E*)-4-(4-bromo-3-methoxyphenyl)buta-1,3-dien-1-yl]-4,4,6-trimethyl-1,3,2-dioxaborinane (0.725 g, 1.99 mmol) was dissolved in dry THF (7.3 mL) and cooled to -78 °C under argon. NaOMe (4.8 mL, 2.4 mmol, 0.5 M in MeOH) was added dropwise and then reaction mixture stirred at -78 °C for 55 minutes. Iodine monochloride (0.383 g, 2.054 mmol) in dry DCM (2.0 mL) was then added dropwise at this temperature and the reaction mixture stirred at -78 °C for a further 2 hours. The reaction mixture was allowed to warm to room temperature and diluted with Et_2O (60 mL), then washed with 5% $Na_2S_2O_5$ (2 x 24 mL), H_2O (24 mL) and brine (24 mL). The organics were dried over $MgSO_4$ under argon, filtered and evaporated to give a crude yellow solid containing desired product (0.708g, 98%). ^{1}H NMR (400 MHz, $CDCl_3$): δ 3.92 (3H, s), 6.47-6.49 (1H, m), 6.51-6.53 (1H, m), 6.67 (1H, ddd, J=15.6, 10.6, 0.7 Hz), 6.85-6.91 (2H, m), 7.17 (1H, ddd, J=14.4, 10.6, 0.7 Hz), 7.44-7.48 (1H, m). The compound was taken on to the next stage without any further purification or characterisation.

2-[(1E,3E,5E)-6-(4-Bromo-3-methoxyphenyl)hexa-1,3,5-trien-1-yl]-4,4,6-trimethyl-1,3,2-dioxaborinane **270**

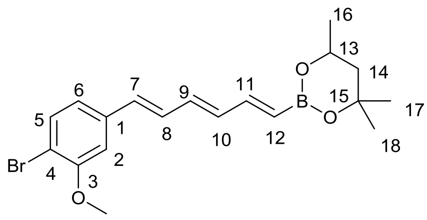

Method 1: 1-Bromo-4-[(*1E,3E*)-4-iodobuta-1,3-dien-1-yl]-2-methoxybenzene (0.708 g, 1.95 mmol) was dissolved in dry, degassed MeCN (11.6 mL) and added to a dry, argon-purged flask containing $Pd(OAc)_2$ (22 mg, 0.10 mmol), P(*o*-tol)$_3$ (59 mg, 0.190 mmol) and AgOAc acetate (0.348 g, 2.08 mmol). 4,4,6-Trimethyl-2-vinyl-1,3,2-dioxaborinane (0.38 mL, 2.23 mmol) was then added and the reaction mixture heated to 50 °C for 2 days 17 hours. The reaction mixture was allowed to cool to room temperature then diluted with Et_2O containing ~ 3 ppm BHT (29 mL) and passed through a short Celite/silica plug. The solvent was evaporated to give 1.031 g of crude product as a brown oil. The crude product was purified by silica gel chromatography, elution gradient 0-10% EtOAc in petroleum ether. Pure fractions were evaporated to yield desired product as a bright yellow oil (0.470 g, 62%). ^{1}H NMR (600 MHz, $CDCl_3$): δ 1.14-1.9 (1H, m, $H_{16,17,18}$), 1.46-1.55 (1H, m, H_{14}), 1.80 (1H, dd, J=13.9, 2.9 Hz, H_{14}), 3.92 (3H, s, OMe), 4.24 (1H, dqd, J=12.3, 6.2, 3.0 Hz, H_{13}), 5.58 (1H, d, J=17.4 Hz, H_{12}), 6.39-6.55 (3H, m, $H_{8,9,10}$), 6.82 (1H, dd, J=15.5, 10.0 Hz, H_7), 6.82-6.92 (2H, m, $H_{2,6}$), 7.00 (1H, dd, J=17.3, 9.9 Hz, H_{11}), 7.45 (1H, d, J=8.1 Hz, H_5); ^{11}B NMR (128 MHz, $CDCl_3$): δ 25.49; ^{13}C NMR (151 MHz, $CDCl_3$): δ 23.3, 28.3, 31.4 ($C_{16,17,18}$), 46.2 (C_{14}), 56.3 (OMe), 65.0 (C_{13}), 71.0 (C_{15}), 109.5 (C_6), 111.0 (C_4), 120.3 (C_2), 130.0 (C_7), 132.7 ($C_{8,9,10}$), 133.5 (C_5), 134.8 ($C_{8,9,10}$), 136.2 ($C_{8,9,10,12}$), 138.2 (C_1), 146.5 (C_{11}), 156.1 (C_3); LRMS (ASAP) 389.1 (M^+-$^{10}B^{79}Br$, 12%), 390.1 (M^+-$^{11}B^{79}Br$, 47), 391.1 (M^+-$^{10}B^{81}Br$, 100, includes [M+H]), 392.1 (M^+-$^{11}B^{81}Br$, 60);. HRMS (ASAP) [$C_{19}H_{24}{}^{10}BO_3Br$] calculated 389.1038, found 389.1023.

Method 2: 1-Bromo-4-[(*1E,3E*)-4-iodobuta-1,3-dien-1-yl]-2-methoxybenzene (1.0 g, 2.75 mmol) was dissolved in dry, degassed MeCN (16 mL) and added to a dry, argon-purged flask containing $Pd(OAc)_2$ (31 mg, 0.141 mmol), P(*o*-tol)$_3$ (83 mg, 0.268 mmol) and AgOAc (0.491 g, 2.93 mmol). 4,4,6-Trimethyl-2-vinyl-1,3,2-dioxaborinane (0.53 mL, 3.14 mmol) was then added and the reaction mixture heated to 30 °C for 18 hours. The reaction mixture was allowed to cool to room temperature then diluted with Et_2O containing ~ 3 ppm BHT (41 mL) and passed through a short Celite/silica plug. The solvent was evaporated to give 1.10 g of crude product as a viscous orange oil. The crude product was purified by silica gel chromatography, elution gradient 0-10% EtOAc in petroleum ether. Pure fractions were evaporated to yield desired product as a viscous yellow oil (0.600 g, 56%).

1-Bromo-4-[(1E,3E,5E)-6-iodohexa-1,3,5-trien-1-yl]-2-methoxybenzene **275**

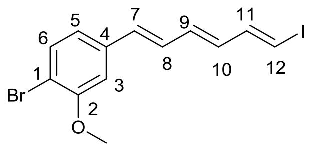

The crude mixture containing 2-[(*1E*,*3E*,*5E*)-6-(4-bromo-3-methoxyphenyl)hexa-1,3,5-trien-1-yl]-4,4,6-trimethyl-1,3,2-dioxaborinane (0.60 g, 1.54 mmol) was dissolved in dry THF (5.7 mL) and cooled to -78 °C under argon. NaOMe (3.7 mL, 1.86 mmol, 0.5 M in MeOH) was added dropwise and then reaction mixture stirred at -78 °C for 40 minutes. Iodine monochloride (0.296 g, 1.59 mmol) in dry DCM (1.2 mL) was then added dropwise at this temperature and the reaction mixture stirred at -78 °C for a further 2 hours. The reaction mixture was allowed to warm to room temperature and diluted with Et_2O (47 mL), then washed with 5% $Na_2S_2O_5$ (2 x 19 mL), H_2O (19 mL) and brine (19 mL). The organics were dried over $MgSO_4$ under argon, filtered and evaporated to give a bright yellow solid containing desired product (est 0.506 g, 84%), which was found to rapidly decompose. ^1H NMR (400 MHz, $CDCl_3$): δ 3.93 (3H, s), 6.34 (1H, dd, J=7.4, 1.2 MHz), 6.56-6.63 (2H, m), 6.81 (1H, dd, J=9.9, 7.6 Hz), 6.86-6.94 (3H, m), 7.11 (1H, dd, J=14.3, 10.6 Hz), 7.45-7.49 (1H, m). The compound was taken on to the next stage without any further purification or characterisation.

2-[(1E,3E,5E,7E)-8-(4-Bromo-3-methoxyphenyl)octa-1,3,5,7-tetraen-1-yl]-4,4,6-trimethyl-1,3,2-dioxaborinane **272**

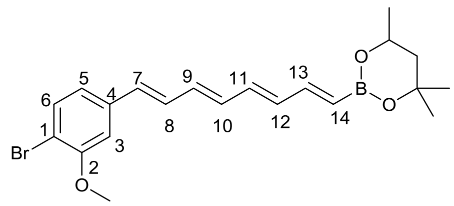

Method 1: 1-Bromo-4-[(*1E,3E,5E*)-6-iodohexa-1,3,5-trien-1-yl]-2-methoxybenzene (0.233 g, 0.60 mmol) was dissolved in dry, degassed MeCN (3.7 mL) and added to a dry, argon-purged flask containing $Pd(OAc)_2$ (7 mg, 0.031 mmol), P(*o*-tol)$_3$ (18 mg, 0.060 mmol) and AgOAc (0.109g, 0.645 mmol). 4,4,6-Trimethyl-2-vinyl-1,3,2-dioxaborinane (0.12 mL, 0.690 mmol) was then added and the reaction mixture heated to 50 °C for 20 hours. The reaction mixture was allowed to cool to room temperature, then diluted with Et_2O containing ~3 ppm BHT (25 mL) and passed through a short Celite/silica plug. The solvent was evaporated to give 0.296 g of crude product as a dark red viscous oil. The crude product was purified by silica gel chromatography, elution gradient 0-10% EtOAc in petroleum ether. Pure fractions were evaporated to give desired product as a bright orange gum (0.146 g, 58%).

Method 2: 1-Bromo-4-[(*1E,3E,5E*)-6-iodohexa-1,3,5-trien-1-yl]-2-methoxybenzene (0.506 g, 1.30 mmol) was dissolved in dry, degassed MeCN (7.8 mL) and added to a dry, argon-purged flask containing $Pd(OAc)_2$ (15 mg, 0.067 mmol), P(*o*-tol)$_3$ (39 mg, 0.127 mmol) and AgOAc (0.232 g, 1.39 mmol). 4,4,6-Trimethyl-2-vinyl-1,3,2-dioxaborinane (0.25 mL, 1.49 mmol) was then added and the reaction mixture heated to 30 °C for 18.5 hours. The reaction mixture was allowed to cool to room temperature, then diluted with Et_2O containing ~3 ppm BHT (19 mL) and passed through a short Celite/silica plug. The solvent was evaporated to give 0.704 g of crude product as a dark red viscous oil. The crude product was purified by silica gel chromatography, elution gradient 0-10% EtOAc in petroleum ether. Pure fractions were evaporated to give desired product as a bright orange gum (0.289 g, 53%). ^{1}H NMR (600 MHz, $CDCl_3$): δ 1.24-1.6 (9H, m, $H_{18,19,20}$), 1.46-1.54 (1H, m, H_{16}), 1.79 (1H, dd, J=13.8, 3.0 Hz, H_{16}), 3.92 (3H, s, OMe), 4.24 (1H, dqd, J=12.3, 6.0, 2.9 Hz, H_{15}), 5.55 (1H, d, J=17.3 Hz, H_{14}), 6.03-6.18 (1H, m, H_{11}), 6.39-6.44 (3H, m, $H_{9,10,12}$), 6.48-6.52 (1H, m, H_8), 6.84-6.94 (3H, m, $H_{3,5,7}$), 6.95-7.04 (1H, m, H_{13}), 7.45 (1H, d, J=8.1 Hz, H_6); ^{11}B NMR (128 MHz, $CDCl_3$): δ 25.37; ^{13}C NMR (151 MHz, $CDCl_3$): δ 23.3, 28.3, 31.4 ($C_{18,19,20}$), 46.2 (C_{16}), 56.3 (OMe), 64.9 (C_{15}), 71.0 (C_{17}), 109.6 (C_5), 110.9 (C_4), 120.2 (C_1), 129.7 (C_7), 130.0 (C_{14}), 132.0 (C_{11}), 133.5 (C_6), 134.1 (C_9), 134.2 (C_8), 135.1 (C_{10}), 135.8 (C_{12}), 138.3 (C_3), 146.7 (C_{13}), 156.1 (C_2); IR (ν_{max}, cm^{-1}) 1568.7 (m, alkene C=C), 1587.0 (m, alkene C=C), 1607.7 (m, alkene C=C), 2911.1 (m, C=CH), 2938.7 (m, C=CH), 2971.6 (m, C=CH) *inter alia*; LRMS (ASAP) 415.1 (M^+-$^{10}B^{79}Br$, 16%), 416.1 (M^+-$^{11}B^{79}Br$, 66), 417.1 (M^+-$^{10}B^{81}Br$, 100, includes [M+H]), 418.1 (M^+-$^{11}B^{81}Br$, 71);. HRMS (ESI) [$C_{21}H_{26}{}^{10}BO_3Br$] calculated 415.1195, found 415.1213.

(3E)-4-Iodobuta-1,3-diene **277**

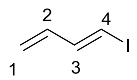

(*E*)-2-(Buta-1,3-dienyl)-4,4,6-trimethyl-1,3,2-dioxaborinane (2.77 g, 12.9 mmol) was dissolved in dry THF (48 mL) and cooled to -78 °C under argon. NaOMe (31 mL, 15.5 mmol, 0.5 M in MeOH) was added dropwise and then the reaction mixture stirred at -78 °C for 30 min. Iodine monochloride (2.47 g, 13.3 mmol) in dry DCM (13 mL) was then added dropwise at this temperature and the reaction mixture stirred at -78 °C for a further 2 hours. The reaction mixture was allowed to warm to room temperature and diluted with Et_2O (400 mL), then washed with 5% $Na_2S_2O_5$ (2 x 160 mL), H_2O (160 mL) and brine (160 mL). The organics were dried over $MgSO_4$ under argon, filtered and evaporated to give 3.40 g of crude product as a dark brown oil. ^1H NMR (400 MHz, $CDCl_3$): δ 5.07 (1H, ddt, J=10.2, 1.4, 0.7 Hz, H_{1cis}), 5.21 (1H, ddt, J=17.0, 1.5, 0.8 Hz, H_{1trans}), 6.23 (1H, dddd, J=17.0, 10.7, 10.1, 0.6 Hz, H_2), 6.35 (1H, dq, J=14.4, 0.7 Hz, H_4), 7.01 (1H, dd, J=14.4, 10.6 Hz, H_3). The compound was taken on to the next stage without any further purification or characterisation.

2-[(1E,3E)-Hexa-1,3,5-trien-1-yl]-4,4,6-trimethyl-1,3,2-dioxaborinane **278**

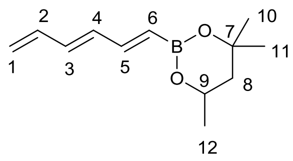

(3*E*)-4-Iodobuta-1,3-diene (2.77 g, 12.9 mmol) was dissolved in dry, degassed MeCN (78 mL) and added to a dry, argon purged flask containing $Pd(OAc)_2$ (0.146 g, 0.650 mmol), P(*o*-tol)$_3$ (0.395 g, 1.30 mmol) and AgOAc (2.60 g 15.6 mmol). 4,4,6-Trimethyl-2-vinyl-1,3,2-dioxaborinane (2.5 mL, 14.7 mmol) was then added and the reaction mixture stirred at 50 °C for 20.5 hours. The reaction mixture was allowed to cool, diluted with 250 mL EtOAc containing ~3 ppm BHT and passed through a Celite/silica plug. The solvent was evaporated to give 5.90 g of a brown oil. The crude product was purified by silica gel chromatography, eluent 0-5% EtOAc in petroleum ether (eluents containing ~3 ppm BHT), to yield 1.50 g of a yellow oil containing desired product (est 0.462 g, 17% from vinyl boronate). ^{1}H NMR (400 MHz, $CDCl_3$): δ 1.24-1.32 (12H, m, $H_{10,11,12}$), 1.42-1.56 (1H, m, H_8), 1.79 (1H, ddd, J=13.9, 3.0, 0.7Hz, H_8), 4.17-4.28 (1H, m, H_9), 5.14 (1H, dd, J=9.4, 1.8 Hz, $H_{1\mathit{cis}}$), 5.26 (1H, dd, J=16.1, 1.6 Hz, $H_{1\mathit{trans}}$), 5.52 (1H, d, J=17.4 Hz, H_6), 6.22-6.43 (3H, m, $H_{2,3,4}$), 6.88-6.99 (1H, m, H_5); ^{11}B NMR (128 MHz, $CDCl_3$): δ 25.81; ^{13}C NMR (101 MHz, $CDCl_3$): δ 23.3, 28.2, 31.4, 46.1, 64.9, 70.9, 118.7, 133.9, 135.4, 135.6, 137.1, 146.6.; LRMS (ASAP) 206.1 ([M+H]- ^{10}B, 5%) 207.1 ([M+H]- ^{11}B, 18); HRMS (ASAP) [$C_{12}H_{20}O_2{}^{10}B$] calculated 206.1593, found 206.1569.

(3E,5E)-6-Iodohexa-1,3,5-triene **279**

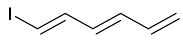

Crude mixture containing 2-[(1*E*,3*E*)-hexa-1,3,5-trien-1-yl]-4,4,6-trimethyl-1,3,2-dioxaborinane (1.50 g, 8.86 mmol) was dissolved in dry THF (33 mL) and cooled to -78 °C under argon. NaOMe (21 mL, 10.7 mmol, 0.5 M in MeOH) was added dropwise and then the reaction mixture stirred at -78 °C for 40 minutes. Iodine monochloride (1.65 g, 7.97 mmol) in dry DCM (7.9 mL) was then added dropwise at this temperature and the reaction mixture stirred at -78 °C for a further 2.5 hours. The reaction mixture was allowed to warm to room temperature and diluted with Et_2O (280 mL), then washed with 5% $Na_2S_2O_5$ (2 x 96 mL), H_2O (96 mL) and brine (96 mL). The organics were dried over $MgSO_4$ under argon, filtered and evaporated to give 0.941 g of crude product as a yellow oil containing desired product (0.282 g, 11% from vinyl boronate). ^{1}H NMR (400 MHz, $CDCl_3$): δ 5.19-5.24 (1H, m), 5.29-5.36 (1H, m), 6.08-6.38 (4H, m), 7.04 (1H, dd, J=14.4, 10.5 Hz). The compound was taken on to the next stage without any further purification or characterisation.

Methyl (2E,4E,6E,8E)-11-(4-bromo-3-methoxyphenyl)undeca-2,4,6,8-tetraen-10-ynoate **235**

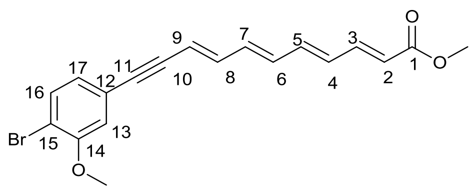

$Pd(PPh_3)_2Cl_2$ (1 mg, 0.002 mmol), copper (I) iodide (0.3 mg, 0.002 mmol), 1-bromo-4-ethynyl-2-methoxybenzene (43 mg, 0.20 mmol) and methyl (*2E*,*4E*,*6E*,*8E*)-9-iodonona-2,4,6,8-tetraenoate (50 mg, 0.170 mmol) were added to a dry flask and the vessel purged with argon. Dry, degassed Et_3N (0.90 mL) was then added and the mixture was briefly degassed. The reaction mixture was then stirred at room temperature overnight. The solvent was removed to give a dark red residue, which was purified by silica gel chromatography at 0 °C, elution gradient 0-10% EtOAc in hexane. Pure fractions were evaporated to give desired product as a bright yellow amorphous solid (36 mg, 56%). ^{1}H NMR (400 MHz, $CDCl_3$): δ 3.76 (s, 3H, COO*Me*), 3.90 (s, 3H, aryl O*Me*), 5.91 (dd, *J* = 15.3, 6.1 Hz, 2H, $H_{2,9}$), 6.29-6.54 (m, 3H, $H_{4,6,7}$), 6.60 (dd, *J* = 14.8, 10.5 Hz, 1H, H_5), 6.75 (dd, *J* = 15.4, 10.4 Hz, 1H, H_8), 6.89-6.99 (m, 2H, $H_{13,17}$), 7.28-7.39 (m, 1H, H_{16}), 7.49 (dd, *J* = 11.4, 8.3 Hz, 1H, H_{13}). ^{13}C NMR (101 MHz, $CDCl_3$): δ 51.6 (COO*Me*), 56.2 (aryl O*Me*), 90.0 (C_{11}), 93.7 (C_{10}), 112.4 (C_{13}), 113.1 (C_9), 114.5 (C_{16}), 121.2 (C_2), 123.4 (C_{12}), 124.9 (C_{15}), 131.7 (C_7), 133.3 (C_{17}), 134.1 (C_6), 135.7 (C_4), 139.9 (C_5), 141.4 (C_8), 144.1 (C_3), 155.6 (C_{14}), 167.4 (C_1). IR (ν_{max}, cm^{-1}) 1706.4 (C=O), 2184.6 (alkyne), 2956.1 (C-H), *inter alia*. LRMS (ASAP) 373.0 ([M+H]- ^{79}Br, 100%) 375.0 ([M+H]- ^{81}Br, 98); HRMS (ASAP) [$C_{19}H_{17}O_3Br$] calculated 372.0361, found 372.0357; UV (Et_2O 5μM, nm) 370 (ε 148 400), 391 (ε 117 200); Fluorescence (Et_2O 100 nM, nm) 439.5, 467.5, 493.5.

1-Bromo-4-[(1Z,3E,5E)-1-bromoocta-1,3,5,7-tetraen-1-yl]-2-methoxybenzene **280**

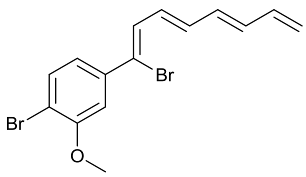

(3*E*,5*E*)-6-Iodohexa-1,3,5-triene (0.120 g, 0.583 mmol), (*Z*)-2-(2-bromo-2-(4-bromo-3-methoxyphenyl)vinyl)-4,4,5,5-tetramethyl-1,3,2-dioxaborolane (0.243 g, 0.583 mmol), $Pd(PPh_3)_4$ (35 mg, 0.030 mmol) and Ag_2O (0.161 g, 0.70 mmol) were added to a dry flask, then the flask purged with argon. Dry, degassed DME (5.3 mL) was then added and the reaction mixture heated to 60 $^{\circ}$C for 20 hours. The reaction mixture was allowed to cool, diluted with Et_2O containing ~3 ppm BHT (40 mL) and passed through a Celite/silica plug. The solvent was evaporated to give 0.634 g of a red oil. The crude product was purified using silica gel chromatography, eluent 0-5% EtOAc in hexane (eluents containing ~ 3 ppm BHT) to give 0.125 g of a wet orange solid containing desired product (59 mg, 28%). Partial ^{1}H NMR (400 MHz, $CDCl_3$) δ: 5.22 (1H, dd, J=7.3, 2.5 Hz), 5.33 (1H, d, J=15.1 Hz), *inter alia*; LRMS (ASAP) 368.9 ([M+H]- ^{79}Br, 36%), 370.9 ([M+H]- $^{79/81}$Br, 68), 372.9 ([M+H]- ^{81}Br, 37); HRMS (ASAP) [$C_{15}H_{15}OBr_2$], calculated 368.9490, found 368.9500. The compound was taken on to the next stage without any further purification or characterisation.

1-Bromo-2-methoxy-4-[(1E,3E,5E)-octa-1,3,5,7-tetraen-1-yl]benzene **292**

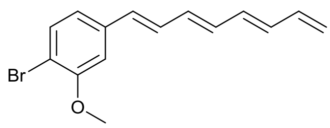

2-[(*E*)-2-(4-Bromo-3-methoxyphenyl)ethenyl]-4,4,5,5-tetramethyl-1,3,2-dioxaborolane (0.165 g, 0.490 mmol), (3*E*,5*E*)-6-iodohexa-1,3,5-triene (0.10 g, 0.490 mmol), $Pd(PPh_3)_4$ (29 mg, 0.0250 mmol) and Ag_2O (0.135 g, 0.588 mmol) were added to a dry flask, then the flask purged with argon. Dry, degassed DME (4.4 mL) was then added and the reaction mixture heated to 60 °C for 22.5 hours. The reaction mixture was allowed to cool, diluted with Et_2O containing ~3 ppm BHT (30 mL) and passed through a Celite/silica plug. The solvent was evaporated to give 0.440 g of a red oil. The crude product was purified using silica gel chromatography, eluent 0-5% EtOAc in hexane (eluents containing ~3 ppm BHT) to give 0.172 g of a wet orange solid that was rapidly polymerised, but from which the desired product could be identified. Partial ^{1}H NMR (400 MHz, $CDCl_3$) δ: 5.13 (1H, d, J=8.4 Hz), 5.26 (1H, dd, J=16.7, 1.6 Hz), *inter alia*; LRMS (ASAP) 289.0 ([M-H]- ^{79}Br, 33%), 291.0 ([M-H]- ^{81}Br, 31).; HRMS (ASAP) [$C_{15}H_{14}OBr$], calculated 289.0228, found 289.0319. No further characterisation was performed due to instability.

Methyl (2E,4E,6E,8E,10Z)-11-bromo-11-(4-bromo-3-methoxyphenyl)undeca-2,4,6,8,10-pentaenoate **233**

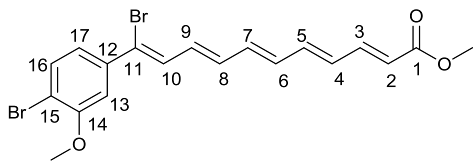

2-[(*Z*)-2-Bromo-2-(4-bromo-3-methoxyphenyl)ethenyl]-4,4,5,5-tetramethyl-1,3,2-dioxaborolane (0.10 g, 0.240 mmol), methyl (*2E,4E,6E,8E*)-9-iodonona-2,4,6,8-tetraenoate (58 mg, 0.20 mmol), $Pd(PPh_3)_4$ (12 mg, 0.010 mmol) and Ag_2O (55 mg, 0.240 mmol) were added to a dry flask and the flask purged with argon. Dry, degassed DME (1.8 mL) was then added and the reaction stirred at 60 °C for 16 hours. The reaction mixture was then diluted with EtOAc (10 mL) and passed through a short plug of Celite/silica. The solvent was evaporated to give 0.106 g of a crude brown oil. The crude product was purified by silica gel chromatography at 0 °C, elution gradient 0-10% EtOAc in hexane, to give 31 mg of an orange solid from which the desired product could be identified. ^{1}H NMR (700 MHz, $CDCl_3$): δ 3.75 (3H, s), 3.89 (3H, s), 5.91 (2H, dd, J=15.4, 10.4 Hz), 6.35-6.50 (3H, m), 6.56-6.67 (2H, m), 6.70-6.77 (1H, m), 6.84-7.01 (2H, m), 7.29-7.34 (1H, m), 7.44-7.51 (1H, m); LRMS (ASAP) 452.0 (M^+- ^{79}Br, 7%), 454.0 (M^+- $^{79/81}$Br, 15), 456.0

(M^+- ^{81}Br, 11); HRMS (ASAP) [$C_{19}H_{18}O_3Br_2$] calculated 451.9623, found 451.9631.

Methyl (2E,4E,6E,8E,10E,12E,14E,16Z)-17-bromo-17-(4-bromo-3-methoxyphenyl)heptadeca-2,4,6,8,10,12,14,16-octaenoate **208**

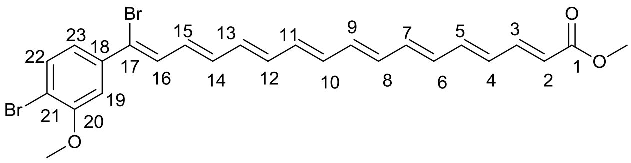

1-Bromo-4-[(1*Z*,3*E*,5*E*)-1-bromoocta-1,3,5,7-tetraen-1-yl]-2-methoxybenzene (59 mg, 0.160 mmol) was dissolved in dry, degassed THF (0.50 mL) and dry, degassed MeCN (1.3 mL), then added to a dry, argon purged flask containing methyl (2*E*,4*E*,6*E*,8*E*)-9-iodonona-2,4,6,8-tetraenoate (63 mg, 0.220 mmol), $Pd(OAc)_2$ (2 mg, 0.0101 mmol), P(*o*-tol)$_3$ (6 mg, 0.0220 mmol) and AgOAc (38 mg, 0.230 mmol). The reaction mixture was degassed for 5 minutes and then heated to 50 °C for 24 hours. The reaction mixture was allowed to cool, then diluted with Et_2O containing ~3 ppm BHT (25mL) and passed through a Celite/silica plug. The solvent was evaporated to yield 96 mg of a bright red gum. The crude product was purified by silica gel chromatography at 0 °C, eluent 0-10% EtOAc in hexane (eluents containing ~ 3ppm BHT) to give 25 mg of a yellow solid, which contained small amounts of desired product (see main discussion).

Methyl (2E,4E,6E,8E,10E)-11-(4-bromo-3-methoxyphenyl)undeca-2,4,6,8,10-pentaenoate **234**

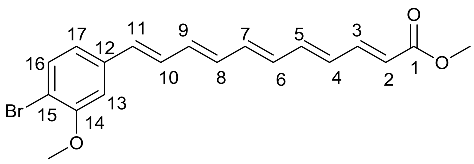

Method 1: 2-[(*E*)-2-(4-Bromo-3-methoxyphenyl)ethenyl]-4,4,5,5-tetramethyl-1,3,2-dioxaborolane (26 mg, 0.0760 mmol), methyl (*2E, 4E, 6E,8E*)-9-iodonona-2,4,6,8-tetraenoate (18 mg, 0.0610 mmol), $Pd(PPh_3)_4$ (7 mg, 0.0061 mmol) and Ag_2O (17 mg, 0.0760 mmol) were added to a dry flask and the flask purged with argon.

Dry, degassed DME (0.46 mL) was then added and the reaction stirred at 40 °C for 17 hours. The reaction mixture was then diluted with EtOAc containing ~ 3ppm BHT (6.0 mL) and passed through a short plug of Celite/silica. The solvent was evaporated to give 55 mg of a green residue. The crude product was purified by silica gel chromatography at 0 °C, eluent benzene, to give desired product as a bright yellow solid (10 mg, 42%), mp 207.3-208.9 °C. ^{1}H NMR (700 MHz, $CDCl_3$): δ 3.75 (3H, s, ester OMe), 3.92 (3H, s, aryl OMe), 5.89 (1H, d, J=15.2 Hz, H_2), 6.37 (2H, ddd, J=15.1, 11.2, 4.3 Hz, $H_{4,6}$), 6.41-6.52 (3H, m, $H_{7,8,9}$), 6.55 (1H, d, J=15.5 Hz, H_{11}), 6.62 (1H, dd, J=14.7, 11.2 Hz, H_5), 6.80-6.85 (1H, m, H_{10}), 6.87-6.93 (2H, m, $H_{13,17}$), 7.29-7.35 (1H, m, H_3), 7.47 (1H, d, J=8.1 Hz, H_{16}); ^{13}C NMR (176 MHz, $CDCl_3$): δ 51.7 (ester OMe), 56.3 (aryl OMe), 109.6 (C_{17}), 111.3 (C_{15}), 120.3 (C_{13}), 120.5 (C_2), 129.7 (C_{10}), 130.5 ($C_{4,6}$), 132.6 ($C_{4,6}$), 133.1 (C_{11}), 133.5 (C_{16}), 133.7 ($C_{7,8,9}$), 135.4 ($C_{7,8,9}$), 137.2 ($C_{7,8,9}$), 138.0 (C_{12}), 140.8 (C_5), 144.7 (C_3), 156.2 (C_{14}), 167.7 (C_1); IR (ν_{max}, cm^{-1}) *inter alia* 1703.9 (m, C=O), 2912.8 (w, C-H alkene), 2924.4 (w, C-H alkene), 2938.4 (w, C-H alkene), 2952.3 (w, C-H alkene); LRMS (ASAP) 375.1 ([M+H]- ^{79}Br, 92%), 377.1 ([M+H]- ^{81}Br, 95); HRMS (ASAP) [$C_{19}H_{19}O_3Br$] calculated 374.0499, found 374.050. UV ($CHCl_3$ 5μM, nm) 397 (ε 67 000), 417 (ε 56 000). Fluorescence ($CHCl_3$ 100 nM, nm) 498, 527, 566, 594.

Method 2: 2-[(*E*)-2-(4-Bromo-3-methoxyphenyl)ethenyl]-4,4,5,5-tetramethyl-1,3,2-dioxaborolane (26 mg, 0.0760 mmol), methyl (*2E, 4E, 6E,8E*)-9-iodonona-2,4,6,8-tetraenoate (18 mg, 0.0610 mmol), $Pd(OAc)_2$ (1 mg, 0.0061 mmol), PPh_3 (5 mg, 0.0183 mmol) and Ag_2CO_3 (34 mg, 0.122 mmol) were added to a dry flask and the flask purged with argon. Dry, degassed MeCN (0.46 mL) was then added and the reaction stirred at room temperature for 17 hours. The reaction mixture was then diluted with EtOAc containing ~ 3ppm BHT (6.0 mL) and passed through a short plug of Celite/silica. The solvent was evaporated to give 82 mg of a green residue. The crude product was purified by silica gel chromatography at 0 ^{o}C, eluent benzene, to give desired product as a bright yellow solid (est. 19 mg, 81%).

Methyl (2E,4E,6E,8E,10E,12E,14E,16E)-17-(4-bromo-3-methoxyphenyl)heptadeca-2,4,6,8,10,12,14,16-octaenoate **210**

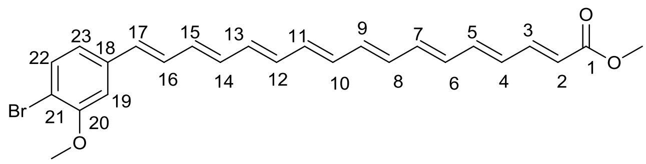

2-[(*1E*,*3E*,*5E*,*7E*)-8-(4-Bromo-3-methoxyphenyl)octa-1,3,5,7-tetraen-1-yl]-4,4,6-trimethyl-1,3,2-dioxaborinane (27 mg, 0.0650 mmol), methyl (*2E*,*4E*,*6E*,*8E*)-9-iodonona-2,4,6,8-tetraenoate (16 mg, 0.0550 mmol), $Pd(PPh_3)_4$ (7 mg, 0.0250 mmol) and Ag_2O (15 mg, 0.065 mmol) were added to a dry flask and purged with argon. Dry, degassed DME (0.50 mL) was added and the reaction heated to 40 °C for 26 hours. The reaction mixture was allowed to cool to room temperature and then diluted with Et_2O containing ~ 3 ppm BHT (10 mL) and passed through a Celite plug. The organics were evaporated to give 25 mg of an orange residue. The crude product was dissolved in $CDCl_3$, and then cooled to 0 °C. Petroleum ether was added until precipitation of a red solid was achieved. The solid was collected on a sinter funnel and washed with cold petroleum ether, then the solid collected by dissolving in $CHCl_3$ and then removing the solvent *in vacuo* to give 7 mg of a red solid containing desired product (0.5 mg, 2 %). ^{1}H NMR (700 MHz, $CDCl_3$): δ 3.74 (3H, s), 3.95 (3H, s), 5.91-5.99 (3H, m), 6.24-6.47 (12H, m), 6.85-6.92 (2H, m), 7.43-7.50 (2H, m); LRMS (ASAP) 453.1 ([M+H]- ^{79}Br, 23%), 455.1 ([M+H]- ^{81}Br, 22); HRMS (ASAP) [$C_{25}H_{26}O_3Br$] calculated 453.1065, found 453.1058.

Methyl (2Z)-3-iodoprop-2-enoate **43**

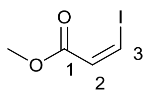

Sodium iodide (14.4 g, 96 mmol) and methyl propiolate (5.3 mL, 59.6 mmol) were added to a flask and acetic acid (22 mL) added. The reaction mixture was then heated to 115 °C for 1 hour. The mixture was poured onto H_2O (100 mL) whilst stil hot, then extracted with Et_2O (3 x 100 mL) and washed with sat. $NaHCO_3$ (4 x 50 mL), 5% $Na_2S_2O_5$ (50 mL) and brine (50 mL). The organic extracts were then dried over $MgSO_4$, filtered and evaporated to give desired product as a yellow oil (12.1 g, 96%). ^1H NMR (400 MHz, $CDCl_3$) δ 3.77 (3H, s, OMe), 6.90 (1H, d, J=8.9 Hz, H_3), 7.46 (1H, d, J=8.9 Hz, H_2); ^{13}C NMR (101 MHz, $CDCl_3$) δ 51.8 (OMe), 95.2 (C_3), 129.7 (C_2), 165.1 (C_1). All spectroscopic data were consistent with those reported previously.[199]

(E)-2-(Buta-1,3-dienyl)-4,4,6-trimethyl-1,3,2-dioxaborinane **276**

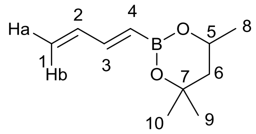

Method 1: To a dry Schlenk flask under argon was added a solution of vinyl iodide (0.19 mL, 2.50 mmol) in dry MeCN (4.5 mL). To the solution was added $Pd(OAc)_2$ (0.280 g, 1.25 mmol). The reaction was degassed using the freeze-pump-thaw method (2 x cycles). 4,4,6-Trimethyl-2-vinyl-1,3,2-dioxaborinane (1.8 mL, 10.3 mmol) was then added and the mixture further degassed (2 x cycles). The reaction was then heated to 55 °C with vigorous stirring. After 2 days, the reaction was cooled to room temperature, diluted with Et_2O (80 mL), filtered through Celite and then washed with 5% HCl (2 x 20 mL), H_2O (40 mL) and brine (40 mL). The organics were dried over $MgSO_4$, filtered and evaporated to yield crude product (1.21 g) as a brown oil which partially crystallised on standing. The crude product was purified by silica chromatography, eluent 15% EtOAc in hexane, to yield an impure yellow oil. The crude product was further purified by silica chromatography, eluent 5% EtOAc in petroleum ether, to yield desired product as a yellow oil (0.325 g, 78%).

Method 2: To a dry flask were added $Pd(OAc)_2$ (0.146 g, 0.650 mmol), P(*o*-tol)$_3$ (0.395 g, 1.30 mmol) and AgOAc (2.60 g 15.6 mmol). Dry, degassed MeCN (24 mL) was added together with vinyl iodide (0.96 mL, 13.0 mmol) and 4,4,6-trimethyl-2-vinyl-1,3,2-dioxaborinane (2.2 mL, 13.0 mmol). The reaction mixture was heated at 50 °C for 48 hours with vigorous stirring. The reaction mixture was allowed to cool, then diluted with Et_2O (250 mL) and passed through a short Celite/silica plug. The organic extracts were evaporated to yield 2.60 g of crude product as an orange oil. The crude product was purified by silica chromatography, elution gradient 0-4% EtOAc in petroleum ether. Pure fractions were evaporated to yield (*E*)-2-(buta-1,3-dienyl)-4,4,6-trimethyl-1,3,2-dioxaborinane as a pale yellow oil (1.71 g, 73%). ^{1}H NMR (400 MHz, $CDCl_3$): δ 1.33-1.26 (9H, m, $H_{8,9,10}$), 1.50 (1H, dd, J=13.9, 11.7 Hz, H_6), 1.81-1.76 (1H, m, H_6), 4.22 (1H, dqd, J=12.2, 6.3, 2.7 Hz, H_5), 5.18 (1H, dd, J=9.8, 1.7 Hz, H_{1a}), 5.32 (1H, dd, J=17.1, 1.7 Hz, H_{1b}), 5.51 (1H, d, J=17.5, H_4), 6.39 (1H, dt, J=17.1, 10.2 Hz, H_2), 6.91 (1H, dd, J=17.6, 10.5 Hz, H_3); ^{11}B NMR (128 MHz, $CDCl_3$): δ 26.19; ^{13}C NMR (101 MHz, $CDCl_3$): δ 23.1 ($C_{8,9,10}$), 28.0 ($C_{8,9,10}$), 31.2 ($C_{8,9,10}$), 46.0 (C_6), 64.71 (C_5), 70.7 (C_7), 119.5 (C_1), 139.1 (C_2), 147.2 (C_3, C_4); IR (ν_{max}, cm^{-1}) 2973.5 (m, C=C-H), 1591 (m, C=C), *inter alia*; LCMS (ASAP) 180.1 (M^+- ^{10}B, 9%) 181.1 (M^+- ^{11}B, 33); HRMS (ASAP) calculated [$C_{10}H_{17}{}^{10}BO_2$+H] 180.1428, found 180.1431.

Method 3: To an oven dried round bottomed flask were added $Pd(OAc)_2$ (0.146 g, 0.650 mmol), P(*o*-tol)$_3$ (0.395 g, 1.30 mmol) and AgOAc (2.60 g 15.6 mmol). MeCN (24 mL), previously degassed by a bubbling argon needle, was added together with vinyl iodide (1.154 mL, 15.6 mmol) and 4,4,6-trimethyl-2-vinyl-1,3,2-dioxaborinane (2.2 mL, 13.0 mmol). The reaction mixture was heated at 50 °C for 2 days 17 hours with vigorous stirring. The reaction mixture was allowed to cool, then diluted with Et_2O containing ~ 3 ppm BHT (250 mL) and passed through a short Celite/silica plug. The organic extracts were evaporated to yield 3.1 g of crude product as an orange oil (2.77 g, 99%).

2-[(1E)-Buta-1,3,-dienyl-4,4,5,5-tetramethyl-1,3,2-dioxaborolane **318**

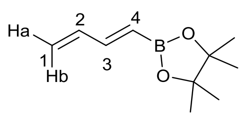

To a dry Schlenk flask was added $Pd(OAc)_2$ (29 mg, 0.125 mmol), P(*o*-tol)$_3$ (76 mg, 0.250 mmol) and AgOAc (0.50 g, 3.0 mmol), followed by dry, degassed MeCN (4.5 mL). Vinylboronic acid pinacol ester (0.42 mL, 2.50 mmol) was then added, followed by vinyl iodide (0.19 mL, 2.50 mmol). The reaction mixture was then heated to 55 °C with vigorous stirring for 2 days. The mixture was allowed to cool, then diluted with Et_2O (280 mL) and passed through a short Celite/silica plug. The organic extracts were washed with 5% HCl (40 mL), H_2O (80 mL) and brine (80 mL), dried over $MgSO_4$ and evaporated to yield 0.980 g of crude product as an orange oil. The crude product was purified by silica gel chromatography, eluent 10% EtOAc in hexane. Pure fractions were evaporated to yield 2-[(*1E*)-buta-1,3,-dienyl-4,4,5,5-tetramethyl-1,3,2-dioxaborolane as a an orange oil (0.318 g, 72%). ^1H NMR (400 MHz, $CDCl_3$): δ 1.30 (12H, s, Bpin), 5.28 (1H, ddt, J=10.0, 1.5, 0.7, H_{1a}), 5.40 (1H, ddt, J=17.1, 1.6, 0.8 Hz, H_{1b}), 5.60 (1H, dq, J=17.7, 0.7 Hz, H_4), 6.44 (1H, dddd, J=16.9, 10.5, 9.9, 0.8 Hz, H_2), 7.03 (1H, dd, J=17.8, 10.4 Hz, H_3); ^{11}B NMR (128 MHz, $CDCl_3$): δ 29.84. All spectroscopic data were consistent with those reported previously.[200]

General conditions used for chain extension using vinyl iodide

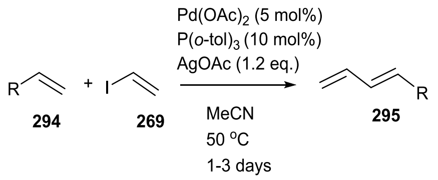

(43)

Method 1: $Pd(OAc)_2$ (0.0975 mmol), P(*o*-tol)$_3$ (0.195 mmol) and AgOAc (2.34 mmol) were added to a dry flask under argon in the absence of light. Degassed MeCN (6.0 mL) was added, followed by alkene (3.90 mmol) and then vinyl iodide (1.95 mmol) under a positive pressure of argon. The flask was then purged with argon for 2 minutes, and then stirred at 50 °C for between 17 hours and 3 days. Conversion was determined by ^1H NMR. The reaction mixture was diluted with EtOAc containing ~ 3 ppm BHT (60 mL) and passed through a short Celite/silica plug. This was then evaporated to give crude product which was then analysed by ^1H NMR. Where purification was undertaken, this was achieved through silica gel chromatography.

Method 2: $Pd(OAc)_2$ (0.0325 mmol), P(*o*-tol)$_3$ (0.0650 mmol) and AgOAc (0.780 mmol) were added to a dry flask under argon in the absence of light. Degassed MeCN (2.0 mL) was added, followed by TMB (0.65 mL, 0.65 mmol, 1 M solution in MeCN), BHT (0.01 mL, 10-20 ppm,1x10^{-3} M solution in MeCN), alkene

(1.30 mmol) and then vinyl iodide (0.650 mmol) under a positive pressure of argon. The flask was then purged with argon for 2 minutes, and then stirred at 50 °C for between 17 hours and 3 days. Conversion was determined by ^{1}H NMR. The reaction mixture was diluted with EtOAc containing ~ 3 ppm BHT (20 mL) and passed through a short Celite/silica plug. This was then evaporated to give crude product which was then analysed by ^{1}H NMR. Where purification was undertaken, this was achieved through silica gel chromatography.

Method 3: $Pd(OAc)_2$ (0.0325 mmol), P(*o*-tol)$_3$ (0.0650 mmol) and AgOAc (0.780 mmol) were added to a dry flask under argon in the absence of light. Degassed MeCN (2.0 mL) was added, followed by TMB (0.65 mL, 0.65 mmol, 1 M solution in MeCN), BHT (0.01 mL, 10-20 ppm,$1x10^{-3}$ M solution in MeCN), alkene (0.780 mmol) and then vinyl iodide (0.650 mmol) under a positive pressure of argon. The flask was then purged with argon for 2 minutes, and then stirred at 50 °C for between 17 hours and 3 days. Conversion was determined by ^{1}H NMR. The reaction mixture was diluted with EtOAc containing ~ 3 ppm BHT (20 mL) and passed through a short Celite/silica plug. This was then evaporated to give crude product which was then analysed by ^{1}H NMR. Where purification was undertaken, this was achieved through silica gel chromatography.

Method 4: $Pd(OAc)_2$ (0.0325 mmol), P(*o*-tol)$_3$ (0.0650 mmol) and AgOAc (0.780 mmol) were added to a dry flask under argon in the absence of light. Degassed MeCN (2.0 mL) was added, followed by alkene (0.650 mmol) and then vinyl iodide (0.650 mmol) under a positive pressure of argon. The flask was then purged with argon for 2 minutes, and then stirred at 50 °C for between 17 hours and 3 days. Conversion was determined by ^{1}H NMR.

Method 5: $Pd(OAc)_2$ (0.0325 mmol), P(o-tol)$_3$ (0.0650 mmol) and AgOAc (0.780 mmol) were added to dry Radleys Carousel reaction tubes under argon. MeCN (2.0 mL), previously degassed by the freeze-pump-thaw method (4 cycles), was added, the tubes were purged with argon, and vinyl iodide (0.650 mmol), followed by the alkene (0.650 mmol) were added. The tubes were heated to 50 °C with vigorous stirring for 2 days. Conversion was determined by ^{1}H NMR.

Methyl (2E)-penta-2,4-dienoate **326**

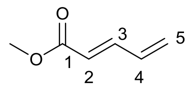

After a 3 day reaction time, desired product was obtained as a crude orange oil, 42% conversion. ^{1}H NMR (400 MHz, $CDCl_3$): δ 3.76 (3H, s), 5.50 (1H, ddt, J=10.0, 1.4, 0.7 Hz), 5.61 (1H, ddt, J=16.9, 1.5, 0.8 Hz), 5.92 (1H, dq, J=15.4, 0.7 Hz), 6.46 (1H, dddd, J=16.9, 10.9, 10.0, 0.7 Hz), 7.22-7.32 (1H, m, plus $CDCl_3$); LCMS (EI) 112.1; HRMS (EI) calculated [$C_6H_7O_2$+H] 112.0516, found 112.0519. All spectroscopic data were consistent with those reported previously.[201]

Tert-butyl (2E)-penta-2,4-dienoate **317**

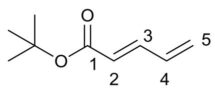

After a 2 day reaction time, desired product obtained as a pale yellow oil (84 mg, 28%). ^{1}H NMR (700 MHz, $CDCl_3$): δ 1.49 (9H, s, *t*-Bu), 5.44 (1H, ddd, J=10.0, 1.5, 0.8 Hz, H_{5cis}), 5.57 (1H, ddt, J=17.0, 1.6, 0.8 Hz, H_{5trans}), 5.84 (1H, dd, J=15.4, 0.8 Hz, H_2), 6.43 (1H, dddd, J=16.9, 10.9, 10.0, 0.8 Hz, H_3), 7.16 (1H, ddt, J=15.4, 11.0, 0.8 Hz, H_4); ^{13}C NMR (176 MHz, $CDCl_3$): δ 28.1 (*t*-Bu), 124.2 (C_2), 124.7 (C_5), 134.8 (C_3), 143.5 (C_4), 166.1 (C_1); IR (ν_{max}, cm^{-1}) : 3008.3 (m, C=C-H), 2980.6 (m, C=C-H), 2935.5 (m, C=C-H), 1707.6 (m, C=C) *inter alia*; LCMS (ESI) 326.2; HRMS (ASAP) calculated [$C_{18}H_{32}O_4$ (2M)+NH_4] 326.2326, found 326.2326.

(3E)-Hexa-3,5-dien-2-one **332**

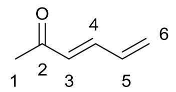

After a 3 day reaction time, desired product was obtained as a crude dark orange oil, 68% conversion. ^{1}H NMR (400 MHz, $CDCl_3$): δ 2.29 (3H,s), 5.48-5.57 (1H, m), 5.61-5.71 (1H, m), 6.16 (1H, d, J=15.7 Hz), 6.47 (1H, dddd, J=16.9, 10.8, 9.9, 0.7 Hz), 7.10 (1H, ddt, J=15.8, 10.8, 0.8 Hz); LCMS (EI) 96.1; HRMS (EI) calculated [C_6H_8O] 96.0577, found 96.0575. All spectroscopic data were consistent with those reported previously.[202]

(1E)-Buta-1,3-dien-1-yltrimethoxysilane **315**

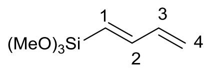

After a 3 day reaction time, desired product was obtained as a crude yellow oil, 42 % conversion. ^{1}H NMR (700 MHz, $CDCl_3$): δ 3.58 (9H, s, plus starting acceptor), 5.25 (1H, ddt, J=10.0, 1.5, 0.7 Hz), 5.36 (1H, ddt, J=17.0, 1.5, 0.7 Hz), 5.55 (1H, dq, J=18.6, 0.7 Hz), 6.38 (1H, dtd, J=17.0, 10.0, 0.8 Hz), 6.82 (1H, ddt, J=18.6, 10.2, 0.8 Hz); LCMS (EI) 174.1; HRMS (EI) calculated [$C_7H_{14}O_3Si$] 174.0703, found 174.0707.

(1E)-Buta-1,3-dien-1-yltriethoxysilane **316**

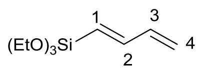

After a 3 day reaction time, desired product was obtained as a crude orange oil, 50% conversion. ^{1}H NMR (700 MHz, $CDCl_3$): δ 1.23 (9H, t, J=7.0 Hz, plus starting acceptor), 3.83 (6H, q, J=7.0Hz, plus starting acceptor), 5.23 (1H, ddt, J=10.0, 1.5, 0.7 Hz), 5.33 (1H, ddt, J=17.0, 1.5, 0.7 Hz), 5.58 (1H, dq, J=18.5, 0.7 Hz), 6.37 (1H, dtd, J=17.0, 10.1, 0.9 Hz), 6.81 (1H, ddt, J=18.6, 10.2, 0.8 Hz); LCMS (EI) 216.1; HRMS (EI) calculated [$C_{10}H_{20}O_3Si$] 216.1175, found 216.1177.

Dimethyl [(1E)-buta-1,3-dien-1-yl)]phosphonate **359**

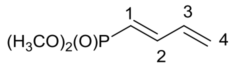

After a 3 day reaction time, desired product was obtained as a crude dark orange oil, 12% conversion. ^{1}H NMR (600 MHz, $CDCl_3$): δ 2.04 (6H, s), 5.44-5.49 (1H, m), 5.52-5.60 (1H, m), 5.64-5.68 (1H, m), 6.41 (1H, dtd, J=17.0, 10.3, 1.9 Hz), 7.04-7.13 (1H, m); LRMS (ASAP) 163.1; HRMS (ASAP) calculated [$C_6H_{11}O_3P$+H] 163.0515, found 163.0519.

(3E)-4-Methanesulfonylbuta-1,3-diene **360**

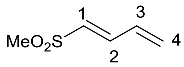

After a 3 day reaction time, desired product was obtained as a crude dark orange oil, 14% conversion. ^{1}H NMR (600 MHz, $CDCl_3$): δ 2.94 (3H, s), 5.61-5.65 (m, 1H), 5.72 (1H, dt, J=16.8, 0.9 Hz), 6.11 (1H, underneath signal for starting acceptor), 6.43 (1H, underneath signal for starting acceptor), 7.13-7.20 (m, 1H); LCMS (EI) 132.0; HRMS (EI) calculated [$C_5H_8O_2S$] 132.0247, found 132.0245. All spectroscopic data were consistent with those reported previously.[203]

N-Phenyl pyrrole **328**

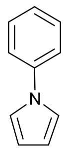

$Pd(OAc)_2$ (48 mg, 0.195 mmol), $P(o\text{-}tol)_3$ (0.119 g, 0.390 mmol) and AgOAc (0.780 g, 4.68 mmol) were added to a dry flask under argon in the absence of light. Dry, degassed MeCN (6.0 mL) was added, followed by vinyl iodide (0.29 mL, 3.90 mmol) and then 4,4,6-trimethyl-2-vinyl-1,3,2-dioxaborinane (0.67 mL, 1.95 mmol) under a positive pressure of argon. The flask was purged with argon for 5 minutes and stirred at 50 °C for 6 hours. Nitrosobenzene (0.379 g, 3.51 mmol) was then added and the reaction stirred at the same temperature overnight. A further

0.3 equivalents of nitrosobenzene was added (0.126 g, 1.17 mmol) and the reaction stirred for a further 2.5 hours. 0.2 equivalents of nitrosobenzene was then added (84 mg, 0.78 mmol) and the reaction stirred overnight. The reaction was allowed to cool, then diluted with DCM (120 mL) and passed through a short Celite/silica plug. Concentration *in vacuo* gave 1.1 g of a dark brown oil. The crude product was purified by silica gel chromatography, elution gradient 2-10% toluene in hexane to give desired product as a white solid (0.267 g, 48%), mp 60.8-62.2 ^{o}C; ^{1}H NMR (400 MHz, $CDCl_3$) δ 6.35 (2H, t, J=2.2 Hz), 7.10 (2H, t, 2.2 Hz), 7.21-7.29 (1H, m), 7.36-7.46 (4H, m). Other spectroscopic data are consistent with those reported previously.[195]

^{1}H NMR reaction scale cycloadditions of dienyl silanes

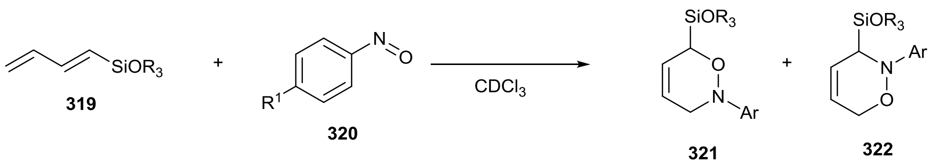

(44)

The dienyl silane (0.139 mmol) and the nitrosobenzene (2.5 equivalents) were added to a vial and dissolved in 1.0 mL $CDCl_3$. Where necessary the $CDCl_3$ was passed through a short plug of alumina before dissolution. The solution was transferred to a pre-cooled NMR tube and ^{1}H NMR experiments performed at 30 minutes, and then at the time specified in the table.

General conditions used for SM couplings on dienyl boronate

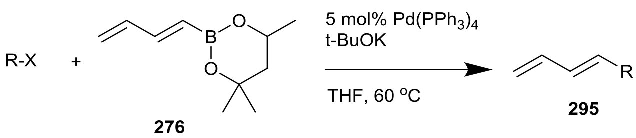

(51)

To a completely cooled, oven dried round bottomed flask was added (*E*)-2-(buta-1,3-dienyl)-4,4,6-trimethyl-1,3,2-dioxaborinane (0.183 g, 1.01 mmol), followed by BHT (0.01 mL, 10-20 ppm, 1x10^{-3} M solution in THF), TMB (0.68 mL, 0.675 mmol, 1 M solution in THF), aryl or vinyl halide (0.675 mmol), *t*-BuOK (91 mg, 0.810 mmol) and $Pd(PPh_3)_4$ (39 mg, 0.0338 mmol). After purging with argon for 2 minutes, degassed THF (6.0 mL) was added, and the reaction mixture further degassed for

2 minutes. The reaction mixture was heated to 60 °C. After the reaction was complete, the mixture was allowed to cool, diluted with EtOAc containing ~ 3 ppm BHT
(80 mL) and passed through a short Celite/silica gel plug and the organic extracts were evaporated to yield crude product. A small portion of the crude product was used for GC and ^{1}H NMR analysis to determine crude yield. The crude product was purified by silica gel chromatography to yield the desired polyene.

1-[(1E)-Buta-1,3-dien-1-yl]-4-methoxybenzene **361**

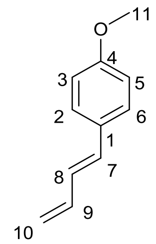

After a 4.5 hour reaction time, product obtained as a colourless oil (84 mg, 78%) following silica gel chromatography on silver nitrate impregnated silica, eluent 5% EtOAc in hexane. ^{1}H NMR (400 MHz, $CDCl_3$): δ 3.81 (3H, s, Me), 5.11 (1H, ddt, J= 10.7, 1.5, 0.7 Hz, $H_{10\textit{cis}}$), 5.28 (1H, ddt, J=16.9, 1.6, 0.8 Hz, $H_{10\textit{trans}}$), 6.44-6.54 (2H, m, $H_{7,8}$), 6.67 (1H, ddt, J=15.5, 10.5, 0.8 Hz, H_9), 6.83-6.87 (2H, m, $H_{2,6}$), 7.32-7.38 (2H, m, $H_{3,5}$). 13C NMR: (176 MHz, CDCl3) δ 55.7 (C_{11}), 114.4 ($C_{2,6}$), 116.8 (C_{10}), 127.67 ($C_{3,5,8}$), 130.3 (C_1), 132.7 (C_8), 137.7 (C_7), 159.6 (C_4). All spectroscopic data were consistent with those reported previously.[187]

1-[(1E)-Buta-1,3-dien-1-yl]-2-methoxybenzene **362**

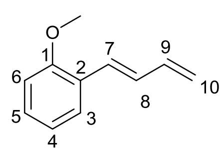

After a 25 hour reaction time, product obtained as a colourless oil containing 0.87:1 reference:product (25 mg, 23%), following silica gel chromatography on silver nitrate impregnated silica, eluent 5% EtOAc in hexane. ^{1}H NMR (700 MHz, $CDCl_3$):

δ 3.86 (3H, s, OMe), 5.15 (1H, ddt, J=10.0, 1.5, 0.7 Hz, H_{10cis}), 5.31 (1H, ddt, J=16.9, 1.6, 0.8 Hz, $H_{10trans}$), 6.55 (1H, dtd, J=17.0, 10.2, 0.7 Hz, H_9), 6.79-6.85 (1H, m, H_8), 6.87 (1H, dd, J=8.3, 1.1 Hz, H_7), 6.90-6.95 (2H, m, $H_{3,4}$), 7.22 (1H, ddd, J=8.2, 7.3, 1.7 Hz, H_6), 7.48 (1H, dd, J=7.6, 1.7 Hz, H_5). ^{13}C NMR (176 MHz, $CDCl_3$): δ 55.4 (OMe), 85.9 (C_2), 110.9 (C_7), 116.9 (C_{10}), 120.6 (C_3), 126.5 (C_5), 127.6 (C_4), 128.6 (C_6), 130.2 (C_8), 137.9 (C_9), 156.8 (C_1). All spectroscopic data were consistent with those reported previously.[187]

1-[(1E)-Buta-1,3-dien-1-yl]-4-methylbenzene **355**

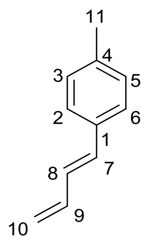

After a 6 hour reaction time, product obtained as a yellow oil (87 mg, 89%), following silica gel chromatography, eluent 1% EtOAc in hexane. ^{1}H NMR (700 MHz, $CDCl_3$): δ 2.34 (3H, s, Me), 5.15 (1H, ddt, J= 10.0, 1.6, 0.8 Hz, H_{10cis}), 5.32 (1H, ddt, J= 17.1, 1.8, 0.9 Hz, $H_{10trans}$), 6.47-6.59 (2H, m, $H_{7,8}$), 6.75 (1H, m, H_9), 7.14 (2H, d, J= 7.9 Hz, $H_{3,5}$), 7.31-7.33 (2H, m, $H_{2,6}$). ^{13}C NMR (176 MHz, $CDCl_3$): δ 21.1(C_{11}), 117.0 (C10), 126.3 ($C_{2,6}$), 128.7 (C_9), 129.3 ($C_{3,5}$), 132.8 (C_1), 134.3 (C_8), 137.3 (C_7), 137.5 (C_4); IR (ν_{max}, cm$^-$1) 1581 (m, aromatic C-C), 1630 (m, alkene C-C), 1641 (m, alkene C-C), 1659 (m, alkene C-C), *inter alia*. All spectroscopic data were consistent with those reported previously.[187]

1-[(1E)-Buta-1,3-dien-1-yl]-2-methylbenzene **363**

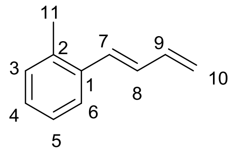

After a 25 hour reaction time, product obtained as a colourless oil (39 mg, 40%), following silica gel chromatography on silver nitrate impregnated silica, eluent 1%

EtOAc in hexane. ^{1}H NMR (700 MHz, $CDCl_3$): δ 2.81 (3H, s, Me), 5.18 (1H, ddd, J=10.0, 1.6, 0.8 Hz, H_{10cis}), 5.34 (1H, ddd, J= 17.0, 1.7, 0.8 Hz, $H_{10trans}$), 6.56 (1H, dt, J= 16.9, 10.1 Hz, H_9), 6.70 (1H, ddd, J= 15.5, 10.3, 0.8 Hz, H_8), 6.80 (1H, d, J= 15.5 Hz, H_7), 7.14-7.20 (3H, m, $H_{3,4,5}$), 7.47-7.52 (1H, m, H_6). ^{13}C NMR (151 MHz, $CDCl_3$): δ 19.8 (C_{11}), 117.4 (C_{10}), 125.2 (C_6), 126.1 (C_3), 127.5(C_5), 130.4 (C_4), 130.5 (C_7), 130.7 (C_8), 135.6 (C_2), 136.0 (C_1), 137.5 (C_9). All spectroscopic data were consistent with those reported previously.[187]

1-[(1E)-Buta-1,3-dien-1-yl]-4-nitrobenzene **364**

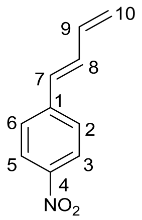

After a 6 hour reaction, product obtained as a yellow solid (78 mg, 66%), following silica gel chromatography on silver nitrate impregnated silica, eluent 1% EtOAc in hexane, mp 66.0-69.9 °C. ^{1}H NMR (400 MHz, $CDCl_3$): δ 5.35 (1H, d, J= 10.0 Hz, H_{10cis}), 5.48 (1H, d, J= 16.9 Hz, $H_{10trans}$), 6.52 (1H, dt, J= 16.9, 10.3 Hz, H_9), 6.60 (1H, d, J= 15.7 Hz, H_7), 6.93 (1H, dd, J= 15.7, 10.5 Hz, H_8), 7.50 (2H, d, J= 8.7 Hz, $H_{2,6}$), 8.16 (2H, d, J= 14.0 Hz, $H_{3,5}$). 13C NMR (176 MHz, CDCl3): δ 120.9 (C_{10}), 124.1 ($C_{3,5}$), 126.8 ($C_{2,6}$), 130.4 (C_7), 134.0 (C_8), 136.4 (C_9), 143.6 (C_4), 146.8 (C_1). All spectroscopic data were consistent with those reported previously.[204]

(E)-Methyl-2-(buta-1,3-dienyl) benzoate **365**

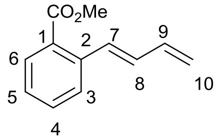

After a 23 hour reaction time, product obtained as a colourless oil containing 1:1:0.33 reference:unreacted aryl:product (29 mg, 24%), following silica gel chromatography on silver nitrate impregnated silica, eluent 1% EtOAc in hexane.

^{1}H NMR (700 MHz, $CDCl_3$): δ 3.90 (3H, s, CO_2*Me*), 5.21 (1H, ddt, J=10.0, 1.5, 0.8 Hz, H_{10} *cis* proton), 5.36 (1H, ddt, J=16.8, 1.5, 0.8 Hz, H_{10} *trans* proton), 6.58 (1H, dtd, J=16.9, 10.3, 0.8 Hz, H_9) 6.71 (1H, ddt, J=15.6, 10.5, 0.9 Hz, H_7), 7.28 (1H, td, J=7.6, 1.2 Hz, H_5), 7.40 (1H, m, H_8), 7.46 (1H, tdd, J=7.9, 1.5, 0.7 Hz, H_3), 7.59-7.69 (1H, m, H_4), 7.84-7.89 (1H, m, H_6).^{13}C NMR (151 MHz, $CDCl_3$): δ 52.1 (Me), 118.4 (C_{10}), 126.7 (C_4), 127.1 (C_5), 130.5 (C_6), 131.1 (C_8), 131.9 (C_3), 132.3 (C_7), 137.4 (C_9), 166.9 (*C*O_2Me), 167.8 (C_1); IR (ν_{max}, cm^{-1}) 1678 (w, C=C stretch), 1659 (w, C=C stretch), 1649 (w, C=C stretch), 1641 (w, C=C stretch), *inter alia*; LRMS (ASAP) 188.1; HRMS (ASAP) calculated [$C_{12}H_{12}O_2$], 189.0916, found 189.0923.

2-[(1E)-Buta-1,3-dien-1-yl]-naphthalene **354**

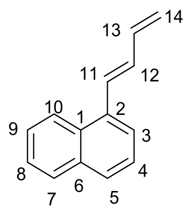

Product obtained as a colourless oil (82 mg, 68%), following silica gel chromatography on silver nitrate impregnated silica, eluent 1% EtOAc in hexane. ^{1}H NMR (400 MHz, $CDCl_3$): δ 5.25 (1H, ddt, J= 9.9, 1.4, 0.7 Hz, $H_{14\mathit{cis}}$), 5.40 (1H, ddt, J= 16.8, 1.6, 0.8 Hz, $H_{14\mathit{trans}}$), 6.67 (1H, ddt, J= 16.9, 10.31 Hz, H_{13}), 6.86 (1H, ddt, J= 15.3, 10.6, 0.9 Hz, H_{12}), 7.36 (1H, d, J= 15.3 Hz, H_{11}), 7.45-7.55 (3H, m, $H_{3,5,9}$), 7.68 (1H, dt, J= 7.3, 1.0 Hz, H_{10}), 7.76-7.83 (1H, m, H_7), 7.84-7.89 (1H, m, H_8), 8.15 (1H, dq, J=8.1, 0.9 Hz, H_4). ^{13}C NMR (151 MHz, $CDCl_3$): δ 117.9 (C_{14}), 123.4 (C_{10}), 123.6 (C_4), 125.6 (C_3), 125.7 (C_5), 126.0 (C_9), 128.0 (C_7), 128.6 (C_8), 129.6 (C_{11}), 131.2 (C_1), 132.5 (C_{12}), 133.7 (C_6), 134.5 (C_2), 137.4 (C_{13}). All spectroscopic data were consistent with those reported previously.[187]

3-[(1E)-Buta-1,3-dien-1-yl]-pyridine **356**

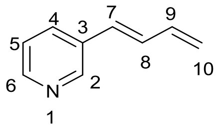

After a 24 hour reaction time, product obtained as a yellow oil containing 1.03 borate byproduct:product (78 mg, 88%), following silica gel chromatography, eluent 10-50% EtOAc in hexane. ^{1}H NMR (600 MHz, $CDCl_3$): δ 5.20-5.28 (1H, m, H_{10} *cis* proton), 5.39 (1H, dd, J=17.0, 1.4 Hz, H_{10} *cis* proton), 6.45-6.56 (2H, m, $H_{7,9}$), 6.83 (1H, dd, J=15.7 Hz, 10.5 Hz, H_8), 7.18-7.25 (1H, m, H_6), 7.66-7.77 (1H, m, H_5), 8.45 (1H, d, J=4.8 Hz, H_2), 8.61 (1H, s, H_4). ^{13}C NMR (176 MHz, $CDCl_3$): δ 119.1 (C_{10}), 123.5 (C_6), 128.9 (C_7), 131.6 (C_8), 132.6 ($C_{3,5}$), 136.6 (C_9), 148.4 (C_2), 148.5 (C_4). IR (ν_{max}, cm^{-1}) 2968 (w, alkene C-H), 1678 (m, C=C stretch), 1659 (m, C=C stretch), 1641 (m, C=C stretch), *inter alia;* LRMS (ASAP) 131.1; HRMS (ASAP) calculated [$C_9H_{10}N$], 132.0813, found 132.0817. All spectroscopic data were consistent with those reported previously.[205]

2-[(1E)-Buta-1,3-dien-1-yl]-thiophene **367**

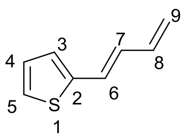

After a 23 hour reaction, product obtained as a colourless oil (42 mg, 46%), following silica gel chromatography on silver nitrate impregnated silica, eluent 1% EtOAc in hexane. ^{1}H NMR (400 MHz, $CDCl_3$): δ 5.15 (1H, ddt, J= 10.1, 1.5, 0.7 Hz, H_{9cis}), 5.31 (1H, ddt, J= 16.9, 1.6, 0.7 Hz, H_{9trans}), 6.44 (1H, dt, J=16.8, 10.0 Hz, H_7), 6.57-6.75 (2H, m, $H_{6,8}$), 6.94-6.99 (2H, m, $H_{4,5}$), 7.14-7.19 (1H, m, C_3). ^{13}C NMR (176 MHz, $CDCl_3$): δ 117.6 (C_9), 124.6 (C_3), 125.8 (C_6), 127.7 ($C_{4,5}$), 129.5 (C_8), 136.8 (C_7), 142.6 (C_2). All spectroscopic data were consistent with those reported previously.[206]

Methyl (3E, 5E)-octa-3,5,7-trienoate **348**

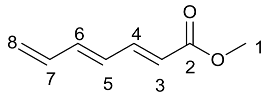

After a 4 hour reaction time, product obtained as a colourless oil (49 mg, 53%), silica gel chromatography on silver nitrate impregnated silica, eluent 0-10% ethyl acetate in hexane. ^{1}H NMR (400 MHz, $CDCl_3$): δ 3.75 (3H, s, Me), 5.32 (1H, dd, J= 9.9, 1.3 Hz, H_{8cis}), 5.42 (1H, dd, J= 16.7, 1.3 Hz, H_{8trans}), 5.91 (1H, d, J= 15.3 Hz, H_3), 6.30-6.36 (1H, m, H_7), 6.39-6.46 (1H, m, H_5) 6.56 (1H, ddt, J= 14.8, 10.7, 0.7 Hz, H_6), 7.31 (1H, ddd, J= 15.3, 11.3, 0.7 Hz, C_4). ^{13}C NMR (176 MHz, $CDCl_3$): δ 51.4 (C1), 120.9 (C_3), 121.5 (C_8), 130.2 (C_7), 136.0 (C_5), 140.8 (C_6), 144.2 (C_4), 167.2 (C_2); IR (ν_{max}, cm^{-1}) 1631 (w, alkene C-C), 1641 (w, alkene C-C), 1659 (w, alkene C-C), 1678 (w, alkene C-C), 1727 (s, ester C=O) *inter alia*; LRMS (ASAP) 138.068; HRMS (ASAP) calculated [$C_8H_{10}O_2$], 139.0752, found 139.0759.

Procedure for making silica impregnated with 10% silver(I) nitrate

A solution of silver nitrate (11.0 g) in distilled H_2O (60 mL) was added to silica (100 g) and ground for 5 minutes using a mortar and pestle. This was then dried in an oven at 150 °C overnight and stored in a beaker wrapped in aluminium in a dessicator over P_2O_5.

Potassium (1E)-buta-1,3-dien-1-yltrifluoroboranuide **349**

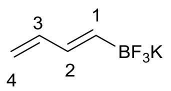

(*E*)-2-(Buta-1,3-dienyl)-4,4,6-trimethyl-1,3,2-dioxaborinane (0.10 g, 0.560 mmol) was dissolved in MeOH (1.1 mL), then MeCN (1.1 mL) was added. KF (0.130 g, 2.21 mmol) in H_2O (0.4 mL) was added dropwise at room temperature, followed by (+)-tartaric acid (0.170 g, 1.13 mmol) in THF (1.7 mL) dropwise. The resulting white suspension was stirred for 1 minute, then sonicated for 1 minute, then stirred for 5 minutes. MeCN (1.7 mL) was then added, the reaction was stirred for 2 minutes, then MeCN (0.5 mL) was added and the reaction stirred for a further 2 minutes. The suspension was filtered, the white solid was washed with MeCN (3 x 3.0 mL) and the filtrate concentrated *in vacuo* to give desired product as a white (90 mg, 100%), mp 126.6 ^{o}C (decomp); ^{1}H NMR (400 MHz, acetone-d_6): δ 4.74 (1H, dd, J=9.1, 2.5 Hz, H_{4cis}), 4.89 (1H, dd, J=16.3, 2.2 Hz, C_{4trans}), 5.63-5.73 (1H, m, H_2), 6.18-6.34 (2H, m, $H_{1,3}$); ^{11}B NMR (128 MHz, acetone-d_6): δ 2.69 (q, J=56.0 Hz); ^{19}F NMR (376 MHz, acetone-d_6): δ -142.03 (dd, J=105.8, 48.7 Hz); ^{13}C NMR (151 MH, acetone-d_6): δ 112.0 (C_4), 136.1 ($C_{2,3}$), 143.0 (C_1); IR (ν_{max}, cm^{-1}): 3186.4 (w, alkene C-H), 1591.9 (m, C=C), *inter alia*; LRMS (ESI -ve) [M-K] 120.0; HRMS (ESI -ve) calculated [$C_4H_5{}^{10}BF_3$], 120.0478, found 120.0481.

5.3 Screen conditions

5.3.1 Screens detailed in **Section 1.2**

Conditions used in SM screen on boronic acid

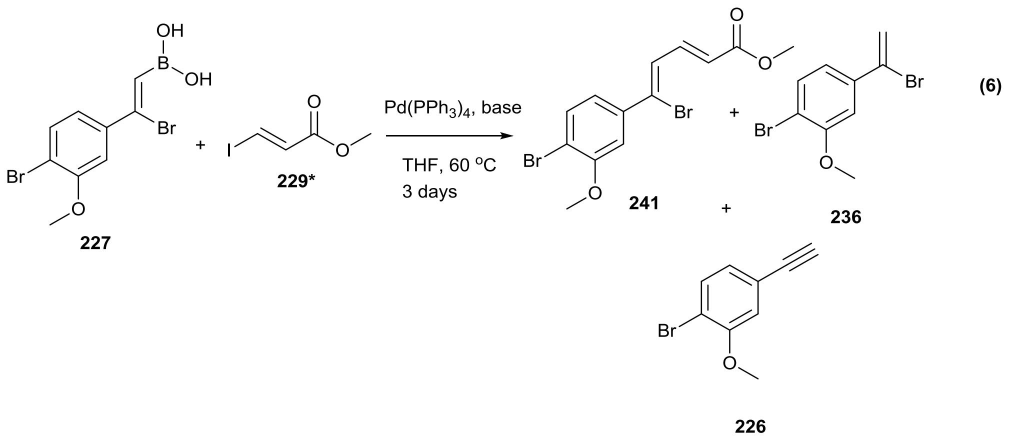

[(*Z*)-7-Bromo-7-(4-bromo-3-methoxyphenyl)ethenyl] boronic acid (20 mg, 0.0911 mmol), methyl (2*E*)-3-iodoprop-2-enoate (13mg, 0.0608 mmol), $Pd(PPh_3)_4$ (4 mg, 0.00306 mmol) and base (0.0729 mmol) were added to dry reaction tubes under argon. Degassed THF (0.53 mL) was then added, the tubes were further purged with argon for 2 minutes, and the tubes were heated to 60 °C with vigorous stirring for 4 days. A further 0.5 mL THF was added, and the reaction was analysed by ^{1}H NMR.

Conditions used in SM screen on styrenyl iodide

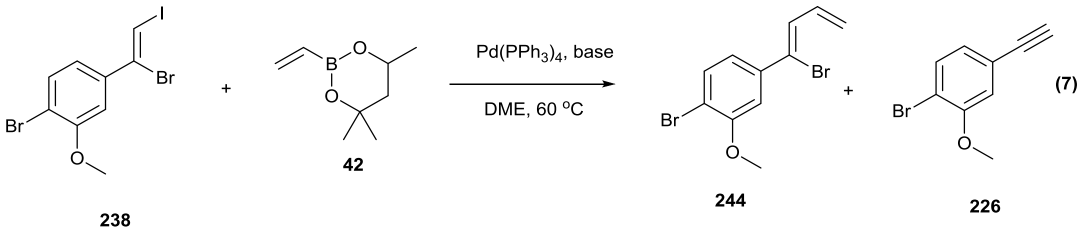

(7)

1-[(*Z*)-7-Bromo-8-iodoethenyl]-3-methoxy-4-bromobenzene (50 mg, 0.120 mmol), $Pd(PPh_3)_4$ (7 mg, 0.006 mmol) and base (0.144 mmol) were added to dry reaction tubes under argon. Dry, degassed DME (1.1 mL) was then added, followed by 4,4,6-trimethyl-2-vinyl-1,3,2-dioxaborinane (0.03 mL, 0.144 mmol), the tubes were further purged with argon for 2 minutes, and the tubes were heated to 60 °C with vigorous stirring for 3 days. The reactions were then analysed by ^{1}H NMR.

Conditions used in SM screen on 4-iodoanisole

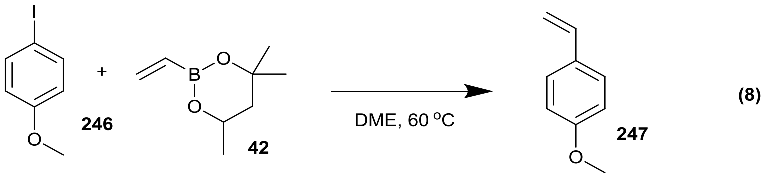

(8)

Entries **1** and **2**: 4-iodoanisole (0.309 g, 1.32 mmol), catalyst (0.066 mmol) and base (1.58 mmol) were added to a dry flask, and the flask purged with argon. 4,4,6-Trimethyl-2-vinyl-1,3,2-dioxaborinane (0.23 mL, 1.32 mmol) was added, followed by dry, degassed DME (12 mL), then the flask was purged with argon for a further 2 minutes. The reaction mixture was then stirred at 60 °C for 16.5 and 19 hours, respectively. The reactions were then analysed by ^{1}H NMR.

Entries **3** and **4**: 4-iodoanisole (0.140 g, 0.60 mmol), catalyst (0.030 mmol) and base (0.720 mmol) were added to a dry flask, and the flask purged with argon. 4,4,6-Trimethyl-2-vinyl-1,3,2-dioxaborinane (0.12 mL, 0.720 mmol) was added, followed by dry, degassed DME (5.3 mL), then the flask was purged with argon for a further 2 minutes. The reaction mixture was then stirred at 60 °C for 3 days. The reactions were then analysed by ^{1}H NMR.

Conditions used in screen on styrenyl Bpin

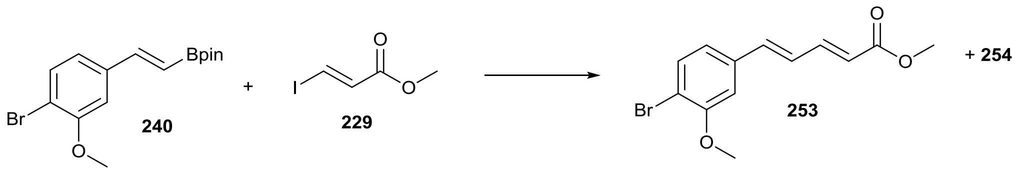

(15)

Conditions were analogous to those above.

Conditions used in screen on brominated styrenyl Bpin

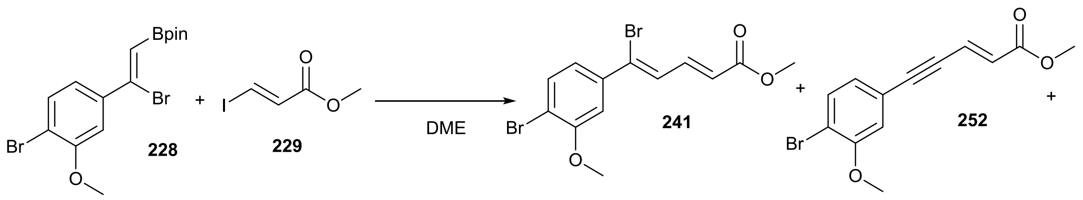

(16)

Conditions were analogous to those above.

5.3.2 Screens detailed in **Section 1.3**

Conditions used in temperature screen on tetraenyl iodide

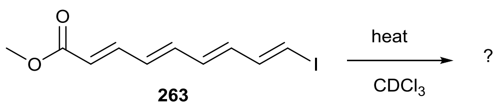

Tetraenyl iodide (50 mg) was dissolved in 5.0 mL degassed MeCN-d_6, and 0.50 mL of this solution added to 5 pre-cooled NMR tubes. 0.20 mL of a 1 M solution of TMB in degassed MeCN-d_6 was added, the tubes were degassed, and each tube was heated to the stipulated temperature for 2 hours before analysing the mixture by ^{1}H NMR.

Conditions used for HM temperature screen

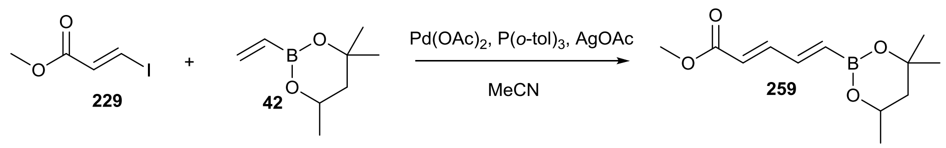

(18)

Methyl (2*E*)-3-iodoprop-2-enoate (0.141 g, 0.665 mmol), $Pd(OAc)_2$ (8 mg, 0.0340 mmol), P(*o*-tol)$_3$ (20 mg, 0.0670 mmol) and AgOAc (0.120 g, 0.721 mmol) were added to dry flasks under argon in the absence of light. Dry, degassed MeCN (4.0 mL) was added to each flask, followed by 4,4,6-trimethyl-2-vinyl-1,3,2-dioxaborinane (0.13 mL, 0.760 mmol) under a positive pressure of argon. The flasks were then purged with argon for 2 minutes, and then heated to the stipulated temperature with vigorous stirring, with conversion monitored at 3 hours and 24 hours by ^{1}H NMR. The HM:SM ratio was also determined by ^{1}H NMR.

5.3.3 Screens detailed in **Section 2.1**

General conditions used for base and ligand screen

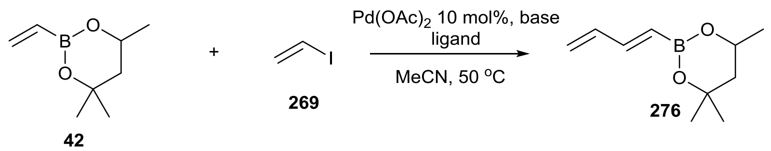

(38)

$Pd(OAc)_2$ (0.0650 mmol) monodentate ligand (0.130 mmol) or bidentate ligand (0.0650 mmol) and base (0.780 mmol) were added to reaction tubes under argon. MeCN (4.5 mL), previously degassed by the freeze-pump-thaw method (4 x cycles) was added to each tube together with vinyl iodide (0.650 mmol) and 4,4,6-trimethyl-2-vinyl-1,3,2-dioxaborinane **(**0.780 mmol). The reaction tubes were then evacuated and filled with argon, and the reaction tubes stirred at 50 °C for 3 days. An internal reference compound of naphthalene (0.0650 mmol) was used. Reaction products and conversions were identified by ^{1}H NMR.

General conditions used for boronate equivalents screen

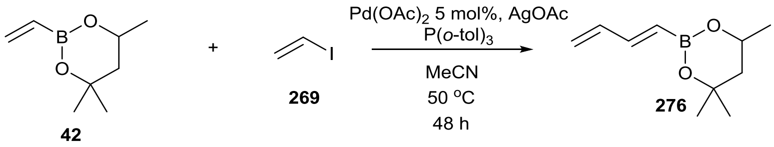

(39)

Pd(OAc)$_2$ (0.0650 mmol), P(*o*-tol)$_3$ (0.130 mmol) and AgOAc (0.780 mmol) were added to reaction tubes under argon. MeCN (4.5 mL), previously degassed by the freeze-pump-thaw method (4 x cycles) was added to each tube together with vinyl iodide (0.650 mmol) and 4,4,6-trimethyl-2-vinyl-1,3,2-dioxaborinane. The reaction tubes were then evacuated and filled with argon, and the reaction tubes stirred at 50 °C for 36 hours. Reaction products and conversions were identified by ^{1}H NMR

General conditions used for catalyst screen

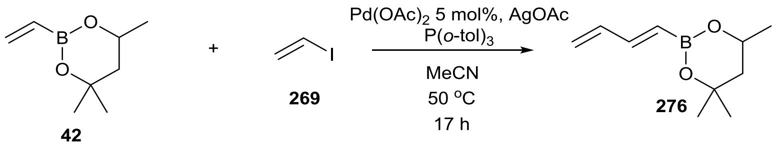

(40)

To oven dried reaction tubes under argon were added catalyst (0.0325 mmol), P(*o*-tol)$_3$ (20 mg, 0.0650 mmol), AgOAc (0.130 g, 0.780 mmol) and naphthalene (9 mg, 0.0650 mmol). Degassed MeCN (2.0 mL) was added to each tube together with vinyl iodide (0.10 g, 0.650 mmol) and 4,4,6-trimethyl-2-vinyl-1,3,2-dioxaborinane **(**0.10 g, 0.650 mmol). The reaction tubes were then heated to 50 °C for 17 hours with vigorous stirring, after which a portion was taken and analysed by GC and ^{1}H NMR. Reaction products and conversions were identified relative to naphthalene internal standard.

General conditions used for silver(I) acetate equivalent screen

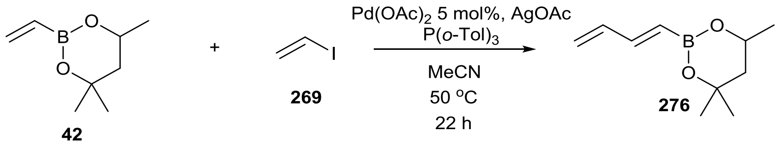

(41)

To oven dried reaction tubes under argon were added $Pd(OAc)_2$ (7 mg, 0.0325 mmol), P(*o*-tol)$_3$ (20 mg, 0.0650 mmol), AgOAc and naphthalene (9 mg, 0.0650 mmol). Degassed MeCN (2.0 mL) was added to each tube together with vinyl iodide (0.10 g, 0.650 mmol) and 4,4,6-trimethyl-2-vinyl-1,3,2-dioxaborinane **(**0.10 g, 0.650 mmol). The reaction tubes were then heated to 50 °C for 22 hours with vigorous stirring, after which a portion was taken and analysed by GC and ^{1}H NMR. Reaction products and conversions were identified relative to naphthalene internal standard.

General conditions used for initial SM couplings

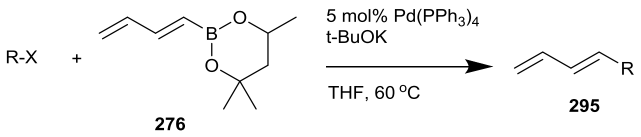

(51)

To an oven dried reaction tube were added (*E*)-2-(buta-1,3-dienyl)-4,4,6-trimethyl-1,3,2-dioxaborinane (0.146 g, 0.810 mmol), aryl or vinyl halide (0.675 mmol), *t*-BuOK (91 mg, 0.80 mmol), $Pd(PPh_3)_4$ (39 mg, 0.0338 mmol) and naphthalene (9 mg, 0.0675 mmol). The reaction tube was then purged with argon and evacuated (x2). Degassed THF (6.0 mL) was added under argon and the reaction mixture heated to 67 °C for 24 hours. The reaction mixture was allowed to cool, then diluted with Et_2O (30 mL) and passed through a short Celite/silica plug. The organic extracts were washed with H_2O (40 mL) and brine (40 mL), dried over $MgSO_4$, filtered and evaporated to yield crude product. The crude product was purified by silica chromatography to yield desired polyene.

5.3.4 Screens detailed in **Section 2.2**

Conditions for the temperature screen are detailed in **Section 5.3.2**.

Conditions used for HM ligand screen

(56)

Methyl (2*E*)-3-iodoprop-2-enoate (0.141 g, 0.665 mmol), $Pd(OAc)_2$ (15 mg, 0.0670 mmol), ligand (0.134 mmol) and AgOAc (0.120 g, 0.721 mmol) were added to dry flasks under argon in the absence of light. Degassed MeCN (4.0 mL) was added to each flask, followed by 4,4,6-trimethyl-2-vinyl-1,3,2-dioxaborinane (0.13 mL, 0.760 mmol) under a positive pressure of argon. The flasks were then purged with argon for 2 minutes, and then stirred vigorously at room temperature, with conversion monitored at 1.5 hours, 3 hours and 24 hours by ^{1}H NMR. The HM:SM ratio was also determined by ^{1}H NMR.

Conditions used for catalyst loading screen

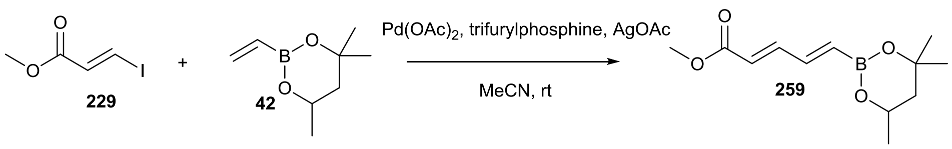

(57)

Methyl (2*E*)-3-iodoprop-2-enoate (0.141 g, 0.665 mmol), $Pd(OAc)_2$, tri(2-furyl)phosphine (2 equivalents wrt catalyst) and AgOAc (0.120 g, 0.721 mmol) were added to dry round-bottomed flasks under argon in the absence of light. Degassed MeCN (4.0 mL) was added to each flask, followed by 4,4,6-trimethyl-2-vinyl-1,3,2-dioxaborinane (0.13 mL, 0.760 mmol) under a positive pressure of argon. The flasks were then purged with argon for 2 minutes, then stirred vigorously at room temperature, with conversion monitored at 3 hours and 24 hours by ^{1}H NMR. The HM:SM ratio was also determined by ^{1}H NMR.

Conditions for substrate scope

Iodide (0.665 mmol), $Pd(OAc)_2$ (2 mg, 0.00665 mmol), tri(2-furyl)phosphine (3 mg, 0.0133 mmol)) and AgOAc (0.120 g, 0.721 mmol) were added to dry flasks under argon in the absence of light. Degassed MeCN (4.0 mL) was added to each flask, followed by 4,4,6-trimethyl-2-vinyl-1,3,2-dioxaborinane (0.13 mL, 0.760 mmol) under a positive pressure of argon. The flasks were then purged with argon for 2 minutes, then stirred vigorously at room temperature, with conversion monitored at 3 hours and 24 hours by ^{1}H NMR.

References

1 C. Thirsk and A. Whiting, *J. Chem. Soc. Perkin Trans. 1*, 2002, 999-1023

2 K. S. Madden, F. A. Mosa and A. Whiting, *Org. Biomol. Chem.*, 2014, **12**, 7877–7899.

3 A. H. Thomas, *Analyst*, 1976, **101**, 321–340.

4 C. Dugave and and L. Demange, *Chem. Rev.*, 2003, **103**, 2475–2532.

5 H. J. Bestmann, *Pure Appl. Chem.*, 1979, **51**, 515–533.

6 A. Wojtkielewicz, *Curr. Org. Synth.*, 2013, **10**, 43–66.

7 S. Gaudiano, P. Bravo, A. Quilico, B. T. Golding and R. W. Rickards, *Tetrahedron Lett.*, 1966, **7**, 3567–3571.

8 PCT Int. Appl., US005880101A, 1999.

9 B. M. Trost, J. T. Hane and P. Metz, *Tetrahedron Lett.*, 1986, **27**, 5695–5698.

10 G. Ryu, B.-W. Choi and B.-H. Lee, *Bull. Korean Chem. Soc.*, 2002, **23**, 1429–1435.

11 G. Ryu, W.-C. Choi, S. Hwang, W.-H. Yeo, A. Chong-Sam Lee and S.-K. Kim, *J. Nat. Prod.*, 1999, **62**, 917–919.

12 L. Radics, M. Incze, K. Dornberger and H. Thrum, *Tetrahedron*, 1982, **38**, 183–189.

13 G.-Q. Chen, F.-P. Lu and L.-X. Du, *J. Agric. Food. Chem*, 2008, **56**, 5057–5061.

14 B. Dorocka-Bobkowska, K. Konopka and N. Düzgüneş, *Arch. Oral Biol.*, 2003, **48**, 805–814.

15 U. I. M. Wiehart, M. Rautenbach and H. C. Hoppe, *Biochem. Pharmacol.*, 2006, **71**, 779–790.

16 L. M. Cañedo, L. Costa, L. M. Criado, J. L. F. Puentes, M. A. Moreno And K. L. Rinehart, *J. Antibiot. (Tokyo).*, 2000, **53**, 623–626.

17 Amos B. Smith, III, A. Suresh M. Pitram and M. J. Fuertes, *Org. Lett.*, 2003, **5**, 2751–2754.

18 E. M. Seco, S. Fotso, H. Laatsch and F. Malpartida, *Chem. Biol.*, 2005, **12**, 1093–1101.

19 M. Rolón, E. M. Seco, C. Vega, J. J. Nogal, J. A. Escario, A. Gómez-Barrio and F. Malpartida, *Int. J. Antimicrob. Agents*, 2006, **28**, 104–109.

20 A. Aszalos, A. Bax, N. Burlinson, P. Roller And C. McNeal, *J. Antibiot. (Tokyo).*, 1985, **38**, 1699–1713.

21 E. Borowski, J. Zieliński, L. Falkowski, T. Zimiński, J. Golik, P. Kołodziejczyk, E. Jereczek, M. Gdulewicz, Y. Shenin and T. Kotienko,

Tetrahedron Lett., 1971, **12**, 685–690.

22 J. Yamaguchi and Y. Hayashi, *Chem. - Eur. J.*, 2010, **16**, 3884–3901.

23 R. A. Hill, *Annu. Reports Sect. 'B' (Organic Chem.)*, 2006, **102**, 123–137.

24 T. Hasegawa, T. Kamiya, T. Henmi, H. Iwasaki And S. Yamatodani, *J. Antibiot. (Tokyo).*, 1975, **28**, 167–175.

25 M. Nakagawa, K. Furihata, Y. Hayakawa and H. Seto, *Tetrahedron Lett.*, 1991, **32**, 659–662.

26 M. Nakagawa, Y. Toda, K. Furihata, Y. Hayakawa And H. Seto, *J. Antibiot. (Tokyo).*, 1992, **45**, 1133–1138.

27 A. W. Kruger and A. . Meyers, *Tetrahedron Lett.*, 2001, **42**, 4301–4304.

28 A. G. Waterson, A. W. Kruger and A. Meyers, *Tetrahedron Lett.*, 2001, **42**, 4305–4308.

29 G. N. Maw, C. Thirsk, J.-L. Toujas, M. Vaultier and A. Whiting, *Synlett*, 2004, **2004**, 1183–1186.

30 J. P. Knowles, V. E. O′Connor and A. Whiting, *Org. Biomol. Chem.*, 2011, **9**, 1876.

31 A. S. Batsanov, J. P. Knowles and A. Whiting, *J. Org. Chem.*, 2007, **72**, 2525–2532.

32 H. C. Kwon, C. A. Kauffman, P. R. Jensen and W. Fenical, *J. Am. Chem. Soc.*, 2006, **128**, 1622–1632.

33 D. Amans, L. Bareille, V. Bellosta and J. Cossy, *J. Org. Chem.*, 2009, **74**, 7665–7674.

34 K. C. Nicolaou, A. L. Nold, R. R. Milburn and C. S. Schindler, *Angew. Chem. Int. Ed.*, 2006, **45**, 6527–6532.

35 K. C. Nicolaou, A. L. Nold, R. R. Milburn, C. S. Schindler, K. P. Cole and J. Yamaguchi, *J. Am. Chem. Soc.*, 2007, **129**, 1760–1768.

36 D. Amans, V. Bellosta and J. Cossy, *Org. Lett.*, 2007, **9**, 1453–1456.

37 P. A. Evans, M.-H. Huang, M. J. Lawler and S. Maroto, *Nat. Chem.*, 2012, **4**, 680–684.

38 Y. Igarashi, Y. In, T. Ishida, T. Fujita, T. Yamakawa, H. Onaka and T. Furumai, *J. Antibiot. (Tokyo).*, 2005, **58**, 523–525.

39 Y. In, H. Ohishi, H. Miyagawa, K. Kitamura, Y. Igarashi and T. Ishida, *Bull. Chem. Soc. Jpn.*, 2006, **79**, 126–133.

40 Y. In, H. Ohishi, T. Ishida and Y. Igarashi, *Chem. Commun.*, 2003, **218**, 1692–1693.

41 S. C. D. N. Lopes, E. Goormaghtigh, B. J. Costa Cabral and M. A. R. B. Castanho, *J. Am. Chem. Soc.*, 2004, **126**, 5396–5402.

42 A. C. Cope and H. E. Johnson, *J. Am. Chem. Soc.*, 1958, **80**, 1504–1506.

43 R. C. Pandey, C. C. Kalita, A. A. Aszalos, R. Geoghegan, A. L. Garretson, J. C. Cook and K. L. Rinehart, *Biol. Mass Spectrom.*, 1980, **7**, 93–98.

44 M. O. and S. S. S. Umezawa, Y. Tanaka, *J. Antibiot. Ser. A*, 1958, **11**, 26–29.

45 M. L. Dhar, V. Thaller and M. C. Whiting, *J. Chem. Soc.*, 1964, 842.

46 J. T. and G. C. V. Pozsgay, *Acta Chim. Acad. Sci. Hungaricae*, 1975, **85**, 215–219.

47 V. Pozsgay, J. Tamás, G. Czira, T. Wirthlin And A. Lévai, *J. Antibiot. (Tokyo).*, 1976, **29**, 472–476.

48 R. C. Pandey, E. C. Guenther, A. A. Aszalos And J. Brajtburg, *J. Antibiot. (Tokyo).*, 1982, **35**, 988–996.

49 T. A. U. and R. N. E. V. I. Frolova, A. D. Kuzovkov, *Khimiko-Farmatsevticheskii Zhurnal*, 1967, **1**, 36–39.

50 B. V. R. and V. I. T. T. A. Ushakova, V. I. Frolova, A. D. Kuzokova, *Khimiko-Farmatsevticheskii Zhurnal*, 1971, **5**, 18–23.

51 S. D. Rychnovsky, U. R. Khire and G. Yang, *J. Am. Chem. Soc.*, 1997, **119**, 2058–2059.

52 K. Kobinata, H. Koshino, T. Kudo, K. Isono And H. Osada, *J. Antibiot. (Tokyo).*, 1993, **46**, 1616–1618.

53 H. Maehr, R. Yang, L. N. Hong, C. M. Liu, M. H. Hatada and L. J. Todaro, *J. Org. Chem.*, 1989, **54**, 3816–3819.

54 D. A. Evans and B. T. Connell, *J. Am. Chem. Soc.*, 2003, **125**, 10899–10905.

55 S. L. Schreiber and M. T. Goulet, *Tetrahedron Lett.*, 1987, **28**, 6001–6004.

56 S. D. Dreher and J. L. Leighton, *J. Am. Chem. Soc.*, 2001, **123**, 341–342.

57 H. C. Kwon, C. A. Kauffman, P. R. Jensen and W. Fenical, *J. Org. Chem.*, 2009, **74**, 675–684.

58 C. Bonini, L. Chiummiento, M. Funicello, P. Lupattelli and V. Videtta, *Tetrahedron Lett.*, 2008, **49**, 5455–5457.

59 G. Schlingmann, L. Milne, D. B. Borders and G. T. Carter, *Tetrahedron*, 1999, **55**, 5977–5990.

60 A. Plaza, H. L. Baker and C. A. Bewley, *J. Nat. Prod.*, 2008, **71**, 473–477.

61 J. Pawlak, K. Nakanishi, T. Iwashita and E. Borowski, *J. Org. Chem.*, 1987, **52**, 2896–2901.

62 F. Song, S. Fidanze, A. B. Benowitz and Y. Kishi, *Tetrahedron*, 2007, **63**, 5739–5753.

63 J. Niggemann, N. Bedorf, U. Flörke, H. Steinmetz, K. Gerth, H. Reichenbach and G. Höfle, *Eur. J. Org. Chem.*, 2005, **2005**, 5013–5018.

64 F. Fu and T.-P. Loh, *Tetrahedron Lett.*, 2009, **50**, 3530–3533.

65 S. A. B. And and F. E. McDonald, *J. Am. Chem. Soc.*, 2004, **126**, 2495–2500.

66 B. Domínguez, B. Iglesias and A. R. de Lera, *Tetrahedron*, 1999, **55**, 15071–15098.

67 M. A. Blanchette, W. Choy, J. T. Davis, A. P. Essenfeld, S. Masamune, W. R. Roush and T. Sakai, *Tetrahedron Lett.*, 1984, **25**, 2183–2186.

68 S. E. D. and and S. Fujimori, *J. Am. Chem. Soc.*, 2005, **127**, 8971–8973.

69 M. J. Mitton- Fry, A. J. Cullen and T. Sammakia, *Angew. Chem. Int. Ed.*, 2007, **46**, 1066–1070.

70 H. Guo, M. S. Mortensen and G. A. O'Doherty, *Org. Lett.*, 2008, **10**, 3149–3152.

71 M. R. Reboll, B. Ritter, F. Sasse, J. Niggemann, R. Frank and M. Nourbakhsh, *ChemBioChem*, 2012, **13**, 409–415.

72 EP 2520292 A1, 2012.

73 I. Paterson, A. D. Findlay and C. Noti, *Chem. Commun.*, 2008, **14**, 5013–6410.

74 C. Gregg, C. Gunawan, A. W. Y. Ng, S. Wimala, S. Wickremasinghe and M. A. Rizzacasa, *Org. Lett.*, 2013, **15**, 516–519.

75 S. Newton, C. F. Carter, C. M. Pearson, L. de C Alves, H. Lange, P. Thansandote and S. V Ley, *Angew. Chem. Int. Ed. Engl.*, 2014, **53**, 4915–20.

76 M. J.Thirumalachar and S. K. Menon, *Hind. Antibiot. Bull.*, 1962, **4**, 106–108.

77 Ping Cai, Fangming Kong, Pamela Fink, Mark E. Ruppen, R. T. Williamson and T. Keiko, *J. Nat. Prod.*, 2007, **70**, 215–219.

78 H. Irschik, D. Schummer, Gerhard Höfle, Hans Reichenbach, Heinrich Steinmetz and R. Jansen, *J. Nat. Prod.*, 2007, **70**, 1060–1063.

79 B. B. G. and M. J. T. A. A. Padhye, *Hind. Antibiot. Bull.*, 1963, **5**, 74–77.

80 R. S. Gordee, T. F. Butler And N. Narasimhachari, *J. Antibiot. (Tokyo).*, 1971, **24**, 561–565.

81 US 5159002 A, 1992.

82 N. Narasimhachari And M. B. Swami, *Chemotherapy*, 1968, **13**, 181–187.

83 N. Narasimhachari And M. B. Swami, *J. Antibiot. (Tokyo).*, 1970, **23**, 566–566.

84 C. J. Sinz and S. D. Rychnovsky, *Angew. Chem. Int. Ed.*, 2001, **40**, 3224–3227.

85 C. J. Sinz and S. D. Rychnovsky, *Tetrahedron*, 2002, **58**, 6561–6576.

86 Y. Zhang, C. C. Arpin, A. J. Cullen, M. J. Mitton-Fry and T. Sammakia, *J. Org. Chem.*, 2011, **76**, 7641–7653.

87 P. Li, J. Li, F. Arikan, W. Ahlbrecht, M. Dieckmann and D. Menche, *J. Am.*

Chem. Soc., 2009, **131**, 11678–11679.

88 P. Li, J. Li, F. Arikan, W. Ahlbrecht, M. Dieckmann and D. Menche, *J. Org. Chem.*, 2010, **75**, 2429–2444.

89 S. Zotchev, *Curr. Med. Chem.*, 2003, **10**, 211–223.

90 WO2003086418 A1, 2003.

91 O. N. Ékzemplyarov, *Khim.-Farm. Zh.*, 1977, **11**, 140–145.

92 V. V. Belakhov and Y. L. Shenin, *Pharm. Chem. J.*, **41**, 314–318.

93 B. B. Gokhale, *Arch. Dermatol.*, 1963, **88**, 558–560.

94 L. Kozhuharova, A. Velizar, G. Ae and L. Koleva, *World J. Microbiol. Biotechnol.*, 2008, **24**, 1–5.

95 J. Zieliński, H. Borowy-Borowski, J. Golik, J. Gumieniak, T. Zimiński, P. Kołodziejczyk, J. Pawlak, E. Borowski, Y. Shenin and A. I. Filippova, *Tetrahedron Lett.*, 1979, **20**, 1791–1794.

96 T. Bruzzese, C. Rimaroli, A. Bonabello, E. Ferrari and M. Signorini, *Eur. J. Med. Chem.*, 1996, **31**, 965–972.

97 J. J. Wright, D. Greeves, A. K. Mallams and D. H. Picker, *J. Chem. Soc. Chem. Commun.*, 1977, 710–712.

98 US 4359462 A, 1982.

99 P. Kołodziejczyk, J. Zieliński, J. Pawlak, J. Golik, L. Falkowski and E. Borowski, *Tetrahedron Lett.*, 1976, **17**, 3603–3606.

100 J. M. T. Hamilton-Miller, 1973, **37**.

101 A. Aszalos, *ed. Modern Analysis of Antibodies. Vol. 27*, CRC Press, 1986.

102 S. Haeder, R. Wirth, H. Herz and D. Spiteller, *Proc. Natl. Acad. Sci.*, 2009, **106**, 4742–4746.

103 T. Komiri, Y. Morimoto, M. Niwa and Y. Hirata, *Tetrahedron Lett.*, 1989, **30**, 3813–3816.

104 M. P. Barros, E. Pinto, P. Colepicolo and M. Pedersén, *Biochem. Biophys. Res. Commun.*, 2001, **288**, 225–232.

105 E. Pinto, L. H. Catalani, N. P. Lopes, P. Di Mascio and P. Colepicolo, *Biochem. Biophys. Res. Commun.*, 2000, **268**, 496–500.

106 M. Oura, T. H. Sternberg And E. T. Wright, *Antibiot. Annu.*, 1955, **3**, 566–73.

107 C. Halde, V. D. Newcomer, E. T. Wright And T. H. Sternberg, *J. Invest. Dermatol.*, 1957, **28**, 217–32.

108 J. J. Torrado, R. Espada, M. P. Ballesteros and S. Torrado-Santiago, *J. Pharm. Sci.*, 2008, **97**, 2405–25.

109 V. Rajshekhar, *Neurol. India*, 2007, **55**, 267–273.

110 S. Sundar, J. Chakravarty, D. Agarwal, M. Rai and H. W. Murray, *N. Engl. J.*

Med., 2010, **362**, 504–12.

111 L. Soler, P. Caffrey and H. E. M. McMahon, *Biochim. Biophys. Acta*, 2008, **1780**, 1162–7.

112 J. Groeschke, I. Solassol, F. Bressolle and F. Pinguet, *J. Pharm. Biomed. Anal.*, 2006, **42**, 362–366.

113 K. C. Nicolaou, R. A. Daines, T. K. Chakraborty and Y. Ogawa, *J. Am. Chem. Soc.*, 1987, **109**, 2821–2822.

114 K. C. Nicolaou, R. A. Daines, Y. Ogawa and T. K. Chakraborty, *J. Am. Chem. Soc.*, 1988, **110**, 4696–4705.

115 G. Wang, S. Xu, Q. Hu, F. Zeng and E. Negishi, *Chem. - Eur. J.*, 2013, **19**, 12938–12942.

116 M. Tswell, *Deut. bot. Ges.*, 1906, **24**, 235–244.

117 F. Czapek, *Lotos*, 1912, **59**, 250–251.

118 R. Willstätter and H. J. Page, *Justus Liebig's Ann. der Chemie*, 1914, **404**, 237–271.

119 R. Bonnett, A. K. Mallams, A. A. Spark, J. L. Tee, B. C. L. Weedon and A. McCormick, *J. Chem. Soc. C Org.*, 1969, 429.

120 K. Bernard, G. P. Moss, G. Tóth and B. C. L. Weedon, *Tetrahedron Lett.*, 1976, **17**, 115–118.

121 S. Iwasaki, M. A. K. Widjaja-adhi, A. Koide, T. Kaga and S. Nakano, *Food Nutr. Sci.*, 2012, **3**, 1491–1499.

122 C. Tan and Y. Hou, *Inflammation*, 2014, **37**, 443–450.

123 A. C. Morandi, N. Molina, B. A. Guerra, A. P. Bolin and R. Otton, *Eur. J. Nutr.*, 2014, **53**, 779–792.

124 T.-W. Chung, H.-J. Choi, J.-Y. Lee, H.-S. Jeong, C.-H. Kim, M. Joo, J.-Y. Choi, C.-W. Han, S.-Y. Kim, J.-S. Choi and K.-T. Ha, *Biochem. Biophys. Res. Commun.*, 2013, **439**, 580–5.

125 S.-J. Heo and Y.-J. Jeon, *J. Photochem. Photobiol. B.*, 2009, **95**, 101–7.

126 Y. Yamano and M. Ito, *J. Chem. Soc., Perkin Trans. 1*, 1993, **93**, 1599–1610.

127 Y. Yamano and M. Ito, *Chem. Pharm. Bull.*, 1994, **42**, 410–412.

128 T. Kajikawa, S. Okumura, T. Iwashita, D. Kosumi, H. Hashimoto and S. Katsumura, 2012, **14**.

129 M. Kuba, N. Furuichi and S. Katsumura, *Chem. Lett.*, 2002, **31**, 1248–1249.

130 N. Furuichi, H. Hara, T. Osaki, H. Mori, S. Katsumura, Noriyuki Furuichi, Hirokazu Hara, Takashi Osaki, Masayuki Nakano, A. Hajime Mori and S. Katsumura, *Angew. Chem. Int. Ed.*, **41**, 1023–1026.

131 Noriyuki Furuichi, Hirokazu Hara, Takashi Osaki, Masayuki Nakano, A. Hajime Mori and S. Katsumura, *J. Org, Chem.*, 2004, **69**, 7949–7959.

132 Y. Murakami, M. Nakano, T. Shimofusa, N. Furuichi and S. Katsumura, *Org. Biomol. Chem.*, 2005, **3**, 1372–4.

133 H. Andrewes, A.G., Jenkins, C.L., Starr, M.P., Shepherd, J. and Hope, *Tetrahedron Lett.*, 1976, **45**, 4023–4024.

134 C. L. Jenkins and M. P. Starr, *Curr. Microbiol.*, 1982, **7**, 195–198.

135 L. Rajagopal, C. S. S. Sundari, D. Balasubramanian and R. V. Sonti, *FEBS Lett.*, 1997, **415**, 125–128.

136 M. Rosa-Fraile, J. Rodríguez-Granger, A. Haidour-Benamin, J. M. Cuerva and A. Sampedro, *Appl. Environ. Microbiol.*, 2006, **72**, 6367–70.

137 M. Paradas, R. Jurado, A. Haidour, J. Rodríguez Granger, A. Sampedro Martínez, M. de la Rosa Fraile, R. Robles, J. Justicia and J. M. Cuerva, *Bioorg. Med. Chem.*, 2012, **20**, 6655–61.

138 J. Kotler-Brajtburg, G. Medoff, G. S. Kobayashi, S. Boggs, D. Schlessinger, R. C. Pandey, K. L. Rinehart and Jr., *Antimicrob. Agents Chemother.*, 1979, **15**, 716–22.

139 S. Akiyama, T. Tabuki, M. Kaneko, S. Komiyama and M. Kuwano, *Antimicrob. Agents Chemother.*, 1980, **18**, 226–30.

140 Y. Shen and P. Ronald, *Microbes Infect.*, 2002, **4**, 1361–1367.

141 A. R. Poplawsky, S. C. Urban and W. Chun, *Appl.Environ.Microbiol.*, 2000, **66**, 5123–5127.

142 N. W. Poplawsky, A. R., Kawalek, M. D., Schaad, *Mol. Plant-Microbe Interact.*, 1993, **6**, 545–545.

143 W. Chun, J. Cui and A. Poplawsky, *Physiol. Mol. Plant Pathol.*, 1997, **51**, 1–14.

144 A. R. Poplawsky and W. Chun, *J. Bacteriol.*, 1997, **179**, 439–444.

145 A. R. Poplawsky, W. Chun, H. Slater, M. J. Daniels and J. M. Dow, *Mol. Paint. Interact.*, 1998, **11**, 68–70.

146 A. R. Poplawsky and W. Chun, *Mol. Plant-Microbe Interact.*, 1998, **11**, 466–475.

147 A. R. Poplawsky, D. M. Walters, P. E. Rouviere and W. Chun, *Mol. Plant Pathol.*, 2005, **6**, 653–657.

148 A. Yajima, N. Imai, A. R. Poplawsky, T. Nukada and G. Yabuta, *Tetrahedron Lett.*, 2010, **51**, 2074–2077.

149 L. Zhou, J. Y. Wang, J. Wang, A. Poplawsky, S. Lin, B. Zhu, C. Chang, T. Zhou, L. H. Zhang and Y. W. He, *Mol. Microbiol.*, 2013, **87**, 80–93.

150 L. Zhou, T.-W. Huang, J.-Y. Wang, S. Sun, G. Chen, A. Poplawsky and Y.-W. He, *Mol. Plant. Microbe. Interact.*, 2013, **26**, 1239–48.

151 A. G. Andrewes, S. Hertzberg, S. Liaaen-Jensen and M. P. Starr, *Acta Chem. Scand.*, 1973, **27**, 2383–95.

152 A. G. Andrewes, *Acta. Chem. Scand.*, 1973, **27**, 2574–2580.

153 M. L. Paret, S. K. Sharma, A. K. Misra, T. Acosta, A. S. DeSilva, T. Vowell and A. M. Alvarez, *Proc. SPIE*, 2012, **8367**, 1–9.

154 M. P. Starr, C. L. Jenkins, L. B. Bussey and A. G. Andrewes, *Arch. Microbiol.*, 1977, **113**, 1–9.

155 C. L. Jenkins and M. P. Starr, *Curr. Microbiol.*, 1982, **7**, 323–326.

156 A. K. Goel, L. Rajagopal, N. Nagesh and R. V Sonti, *J. Bacteriol.*, 2002, **184**, 3539–3548.

157 A. C. R. da Silva, J. A. Ferro, F. C. Reinach, C. S. Farah, L. R. Furlan, R. B. Quaggio, C. B. Monteiro-Vitorello, M. A. Van Sluys, N. F. Almeida, L. M. C. Alves, A. M. do Amaral, M. C. Bertolini, L. E. A. Camargo, G. Camarotte, F. Cannavan, J. Cardozo, F. Chambergo, L. P. Ciapina, R. M. B. Cicarelli, L. L. Coutinho, J. R. Cursino-Santos, H. El-Dorry, J. B. Faria, A. J. S. Ferreira, R. C. C. Ferreira, M. I. T. Ferro, E. F. Formighieri, M. C. Franco, C. C. Greggio, A. Gruber, A. M. Katsuyama, L. T. Kishi, R. P. Leite, E. G. M. Lemos, M. V. F. Lemos, E. C. Locali, M. A. Machado, A. M. B. N. Madeira, N. M. Martinez-Rossi, E. C. Martins, J. Meidanis, C. F. M. Menck, C. Y. Miyaki, D. H. Moon, L. M. Moreira, M. T. M. Novo, V. K. Okura, M. C. Oliveira, V. R. Oliveira, H. A. Pereira, A. Rossi, J. A. D. Sena, C. Silva, R. F. de Souza, L. A. F. Spinola, M. A. Takita, R. E. Tamura, E. C. Teixeira, R. I. D. Tezza, M. Trindade dos Santos, D. Truffi, S. M. Tsai, F. F. White, J. C. Setubal and J. P. Kitajima, *Nature*, 2002, **417**, 459–463.

158 T. A. T. Schöner, S. W. S. S. W. Fuchs, B. Reinhold-Hurek and H. B. Bode, *PLoS One*, 2014, **9**, e90922.

159 P. Cimermancic, M. H. Medema, J. Claesen, K. Kurita, L. C. Wieland Brown, K. Mavrommatis, A. Pati, P. A. Godfrey, M. Koehrsen, J. Clardy, B. W. Birren, E. Takano, A. Sali, R. G. Linington and M. A. Fischbach, *Cell*, 2014, **158**, 412–421.

160 S. K. Stewart and A. Whiting, *Tetrahedron Lett.*, 1995, **36**, 3929–3932.

161 S. K. Stewart and A. Whiting, *Tetrahedron Lett.*, 1995, **36**, 3925–3928.

162 S. K. Stewart and A. Whiting, *J. Organomet. Chem.*, 1994, **482**, 293–300.

163 A. P. Lightfoot, S. J. R. Twiddle and A. Whiting, *Tetrahedron Lett.*, 2004, **45**, 8557–8561.

164 A. P. Lightfoot, G. Maw, C. Thirsk, S. J. R. Twiddle and A. Whiting, *Tetrahedron Lett.*, 2003, **44**, 7645–7648.

165 A. R. Hunt, S. K. Stewart and A. Whiting, *Tetrahedron Lett.*, 1993, **34**, 3599–3602.

166 N. Hénaff, S. K. Stewart and A. Whiting, *Tetrahedron Lett.*, 1997, **38**, 4525–4526.

167 A. P. Lightfoot, S. J. R. Twiddle and A. Whiting, *Org. Biomol. Chem.*, 2005, **3**, 3167–3172.

168 B. La Roche, *Unpublished work*, .

169 B. Sansam, *Unpublished work*, .

170 D. Thompson, *Unpublished work*, .

171 N. A. Petasis and I. A. Zavialov, *Tetrahedron Lett.*, 1996, **37**, 567–570.

172 H. Zhang, F. Y. Kwong, Y. Tian and K. S. Chan, *J. Org. Chem.*, 1998, **63**, 6886–6890.

173 K. S. Madden, S. David, J. P. Knowles and A. Whiting, *Chem. Commun. (Camb).*, 2015, **51**, 11409–12.

174 M. Altendorfer, A. Raja, F. Sasse, H. Irschik and D. Menche, *Org. Biomol. Chem.*, 2013, **11**, 2116–2139.

175 M. Altendorfer and D. Menche, *Chem. Commun.*, 2012, **48**, 8267.

176 S. Garrais, J. Turkington and W. P. D. Goldring, *Tetrahedron*, 2009, **65**, 8418–8427.

177 P. S. Kalsi, *Spectroscopy of Organic Compounds*, New Age International Limited, 2004.

178 T. Kajikawa, S. Okumura, T. Iwashita, D. Kosumi, H. Hashimoto and S. Katsumura, *Org. Lett.*, 2012, **14**, 808–811.

179 Y.-J. Zhao and T.-P. Loh, *Tetrahedron*, 2008, **64**, 4972–4978.

180 G. Pattenden, A. T. Plowright, J. A. Tornos and T. Ye, *Tetrahedron Lett.*, 1998, **39**, 6099–6102.

181 J. M. Clough and G. Pattenden, *Tetrahedron Lett.*, 1978, **19**, 4159–4162.

182 G. Pattenden, B. C. L. Weedon, C. F. Garbers, D. F. Schneinder and J. P. van der Merwe, *Chem. Commun.*, 1965, 347–349.

183 N. E. Campbell and G. M. Sammis, *Angew. Chem. Int. Ed.*, 2014, **53**, 6228–6231.

184 T. Chatterjee, R. Dey and B. C. Ranu, *New J. Chem. New J. Chem*, 2011, **35**, 1103–1110.

185 J. Barluenga, M. Tomás-Gamasa, F. Aznar and C. Valdés, *Adv. Synth. Catal.*, 2010, **352**, 3235–3240.

186 J. McNulty and P. Das, *Tetrahedron Lett.*, 2009, **50**, 5737–5740.

187 D. A. Mundal, K. E. Lutz and R. J. Thomson, *Org. Lett.*, 2009, **11**, 465–468.

188 H. Hattori, M. Katsukawa and Y. Kobayashi, *Tetrahedron Lett.*, 2005, **46**, 5871–5875.

189 J. Barluenga, F. Rodríguez, L. Álvarez-Rodrigo and F. J. Fañanás, *Chem. - Eur. J.*, 2004, **10**, 101–108.

190 S. Fujii, S. Y. Chang and M. D. Burke, *Angew. Chem. Int. Ed.*, 2011, **50**, 7862–7864.

191 H. A. Dieck and R. F. Heck, *J. Org. Chem.*, 1975, **40**, 1083–1090.

192 A. P. Lightfoot, S. J. Twiddle and A. Whiting, *Synlett*, 2005, **2005**, 529–531.

193 J. P. Knowles and A. Whiting, *Org. Biomol. Chem.*, 2007, **5**, 31–44.

194 L. Eberlin, B. Carboni and A. Whiting, *J. Org. Chem.*, 2015, **80**, 6574–6583.

195 F. Tripoteau, L. Eberlin, M. A. Fox, B. Carboni and A. Whiting, *Chem. Commun.*, 2013, **49**, 5414.

196 A. J. J. Lennox and G. C. Lloyd-Jones, *Angew. Chem. Int. Ed.*, 2012, **51**, 9385–9388.

197 T.-S. Li, J.-T. Li and H.-Z. Li, *J. Chromatogr. A*, 1995, **715**, 372–375.

198 J. P. Knowles, PhD Thesis, Durham University, 2008.

199 C. E. Thirsk, PhD Thesis, Durham University, 2003.

200 J. R. Coombs, L. Zhang and J. P. Morken, *Org. Lett.*, 2015, **17**, 1708–1711.

201 C. R. Smith and T. V. RajanBabu, *Tetrahedron*, 2010, **66**, 1102–1110.

202 N. B. Das and K. B. G. Torssell, *Tetrahedron*, 1983, **39**, 2247–2253.

203 T. Chou, H.-H. Tso and L.-J. Chang, *J. Chem. Soc., Perkin Trans. 1*, 1985, 515.

204 T. Borg, P. Tuzina and P. Somfai, *J. Org. Chem.*, 2011, **76**, 8070–8075.

205 B. I. Rosen and W. P. Weber, *J. Org. Chem.*, 1977, **42**, 47–50.

206 T. Preuß, W. Saak and S. Doye, *Chem. - Eur. J.*, 2013, **19**, 3833–3837.

Appendix

(Z)-2-(2-bromo-2-(4-bromo-3-methoxyphenyl)vinyl)-4,4,5,5-tetramethyl-1,3,2-dioxaborolane **61** (13srv085)[168]

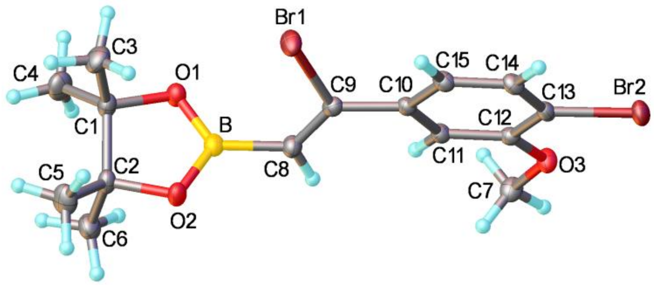

Table 1. Crystal data and structure refinement for **61**

Empirical formula	$C_{15}H_{19}BO_3Br_2$
Formula weight	417.93
Temperature/K	120
Crystal system	monoclinic
Space group	$P2_1/c$
a/Å	15.3222(8)
b/Å	8.5128(5)
c/Å	13.2436(7)
α/°	90
β/°	103.701(8)
γ/°	90
Volume/Å^3	1678.27(17)
Z	4
ρ_{calc}mg/mm^3	1.654
m/mm^{-1}	4.836
F(000)	832.0

Crystal size/mm^3	0.52 × 0.48 × 0.14
2Θ range for data collection	2.736 to 64°
Index ranges	-22 ≤ h ≤ 22, -12 ≤ k ≤ 12, -19 ≤ l ≤ 19
Reflections collected	25514
Independent reflections	5829[R(int) = 0.0294]
Data/restraints/parameters	5829/0/200
Goodness-of-fit on F^2	1.017
Final R indexes [I>=2σ (I)]	R_1 = 0.0242, wR_2 = 0.0515
Final R indexes [all data]	R_1 = 0.0407, wR_2 = 0.0568
Largest diff. peak/hole / e $Å^{-3}$	0.56/-0.45

Table 2. Fractional Atomic Coordinates (×10^4) and Equivalent Isotropic Displacement Parameters ($Å^2$×10^3) for **61**. U_{eq} is defined as 1/3 of of the trace of the orthogonalised U_{IJ} tensor.

Atom	***x***	***y***	***Z***	**U(eq)**
Br1	1868.3(2)	6888.8(2)	1324.3(2)	27.02(5)
Br2	5565.0(2)	8084.5(2)	5785.5(2)	23.92(4)
O1	2242.8(7)	4485.7(13)	-640.7(8)	21.4(2)
O2	1851.0(7)	2485.0(13)	314.0(8)	22.4(2)
O3	5951.8(7)	5991.5(13)	4166.9(8)	21.4(2)
C1	1453.9(10)	3751.5(19)	-1316.6(12)	21.5(3)
C2	1406.7(10)	2138.8(18)	-763.9(12)	20.4(3)
C3	667.8(12)	4835(2)	-1301.3(14)	32.2(4)
C4	1605.4(13)	3630(2)	-2402.1(13)	32.5(4)
C5	464.0(12)	1569(2)	-795.4(15)	33.3(4)
C6	1950.5(12)	851(2)	-	29.2(4)

			1115.4(13)	
C7	6280.8(11)	4918.2(19)	3512.9(13)	23.7(3)
C8	3043.7(10)	4390.1(18)	1307.1(11)	20.8(3)
C9	2945.9(9)	5689.9(17)	1828.8(11)	17.6(3)
C10	3558.6(9)	6308.0(17)	2781.7(11)	16.6(3)
C11	4464.5(10)	5849.7(16)	3001.1(11)	16.9(3)
C12	5062.2(9)	6358.1(16)	3898.7(11)	16.7(3)
C13	4748.8(10)	7344.1(17)	4579.0(11)	18.1(3)
C14	3862(1)	7815.2(16)	4368.4(12)	19.6(3)
C15	3266.6(10)	7306.1(17)	3469.0(12)	19.3(3)
B	2370.6(11)	3781(2)	308.3(13)	19.0(3)

Table 3. Anisotropic Displacement Parameters (Å^2×10^3) for **61**. The Anisotropic displacement factor exponent takes the form: $-2\pi^2[h^2a^{*2}U_{11}+...+2hka\times b\times U_{12}]$

Atom	**U_{11}**	**U_{22}**	**U_{33}**	**U_{23}**	**U_{13}**	**U_{12}**
Br1	18.15(7)	26.67(8)	31.88(9)	-6.61(6)	-2.78(6)	5.03(6)
Br2	23.96(8)	24.48(8)	21.30(7)	-7.25(6)	1.30(6)	-2.81(6)
O1	19.4(5)	24.2(5)	19.8(5)	-0.4(4)	2.9(4)	-4.2(4)
O2	24.7(6)	25.7(5)	15.3(5)	-0.6(4)	2.0(4)	-4.6(4)
O3	16.0(5)	24.4(5)	22.9(5)	-5.4(4)	2.7(4)	2.5(4)
C1	20.3(7)	26.2(7)	16.9(6)	-1.0(6)	2.1(5)	-2.5(6)
C2	18.9(7)	25.7(7)	16.0(6)	-2.3(5)	2.7(5)	-4.6(6)
C3	27.0(9)	36.1(9)	29.6(9)	2.0(7)	-0.8(7)	6.5(7)
C4	39.8(10)	39.9(10)	18.6(7)	0.5(7)	8.4(7)	-5.3(8)
C5	24.6(8)	41.3(10)	33.9(9)	-1.8(8)	6.9(7)	-12.4(7)
C6	31.3(9)	26.8(8)	27.3(8)	-6.8(6)	2.7(7)	0.5(7)
C7	20.3(7)	27.9(8)	23.0(7)	-2.6(6)	5.6(6)	5.4(6)

C8	19.2(7)	21.8(7)	20.1(7)	-1.8(6)	1.8(6)	0.4(6)
C9	14.4(6)	19.0(6)	19.4(6)	1.7(5)	4.2(5)	-0.4(5)
C10	16.3(6)	15.1(6)	18.5(6)	0.0(5)	4.4(5)	-1.8(5)
C11	17.6(6)	16.0(6)	17.7(6)	-1.9(5)	5.5(5)	0.3(5)
C12	15.5(6)	14.9(6)	19.8(6)	0.9(5)	4.6(5)	-0.4(5)
C13	21.1(7)	15.8(6)	17.0(6)	-1.8(5)	4.1(5)	-3.6(5)
C14	20.9(7)	17.1(7)	22.4(7)	-3.8(5)	8.4(6)	-0.5(5)
C15	17.9(7)	17.5(6)	23.4(7)	-1.7(5)	6.7(6)	0.0(5)
B	17.5(7)	21.1(8)	18.7(7)	-2.9(6)	4.7(6)	1.3(6)

Table 4. Bond Lengths for **61**.

Atom	**Atom**	**Length/Å**	**Atom**	**Atom**	**Length/Å**
Br1	C9	1.9213(14)	C2	C5	1.515(2)
Br2	C13	1.8888(14)	C2	C6	1.516(2)
O1	C1	1.4631(18)	C8	C9	1.332(2)
O1	B	1.364(2)	C8	B	1.561(2)
O2	C2	1.4587(18)	C9	C10	1.480(2)
O2	B	1.362(2)	C10	C11	1.404(2)
O3	C7	1.4303(18)	C10	C15	1.394(2)
O3	C12	1.3611(17)	C11	C12	1.387(2)
C1	C2	1.566(2)	C12	C13	1.397(2)
C1	C3	1.521(2)	C13	C14	1.380(2)
C1	C4	1.513(2)	C14	C15	1.387(2)

Table 5. Bond Angles for **61**.

Atom	Atom	Atom	Angle/°	Atom	Atom	Atom	Angle/°
B	O1	C1	107.06(12)	C8	C9	C10	127.68(13)
B	O2	C2	107.24(12)	C10	C9	Br1	115.28(10)
C12	O3	C7	117.60(11)	C11	C10	C9	118.30(13)
O1	C1	C2	102.21(11)	C15	C10	C9	122.45(13)
O1	C1	C3	105.96(13)	C15	C10	C11	119.25(13)
O1	C1	C4	108.67(13)	C12	C11	C10	120.68(13)
C3	C1	C2	113.64(13)	O3	C12	C11	124.70(13)
C4	C1	C2	114.74(14)	O3	C12	C13	116.45(13)
C4	C1	C3	110.76(14)	C11	C12	C13	118.83(13)
O2	C2	C1	102.58(11)	C12	C13	Br2	119.09(11)
O2	C2	C5	108.22(13)	C14	C13	Br2	119.79(11)
O2	C2	C6	106.48(12)	C14	C13	C12	121.09(13)
C5	C2	C1	114.65(14)	C13	C14	C15	119.90(13)
C5	C2	C6	110.49(14)	C14	C15	C10	120.23(14)
C6	C2	C1	113.66(13)	O1	B	C8	123.83(14)
C9	C8	B	125.64(14)	O2	B	O1	113.87(13)
C8	C9	Br1	117.00(11)	O2	B	C8	122.29(14)

Table 6. Hydrogen Atom Coordinates (Å×10^4) and Isotropic Displacement Parameters (Å^2×10^3) for **61**.

Atom	***x***	***y***	***z***	**U(eq)**
H3A	576	4885	-595	41(3)
H3B	124	4428	-1775	41(3)
H3C	797	5889	-1525	41(3)
H4A	1635	4686	-2686	43(4)
H4B	1108	3047	-2847	43(4)
H4C	2171	3077	-2376	43(4)
H5A	494	545	-451	44(3)
H5B	127	1469	-1520	44(3)
H5C	162	2326	-435	44(3)
H6A	2564	1225	-1067	42(3)
H6B	1672	567	-1837	42(3)
H6C	1967	-73	-669	42(3)
H7A	6204	5376	2818	28(3)
H7B	5944	3931	3463	28(3)
H7C	6920	4712	3809	28(3)
H8	3569	3781	1565	25
H11	4670	5184	2530	20
H14	3660	8487	4838	23
H15	2658	7639	3321	23

15srv238

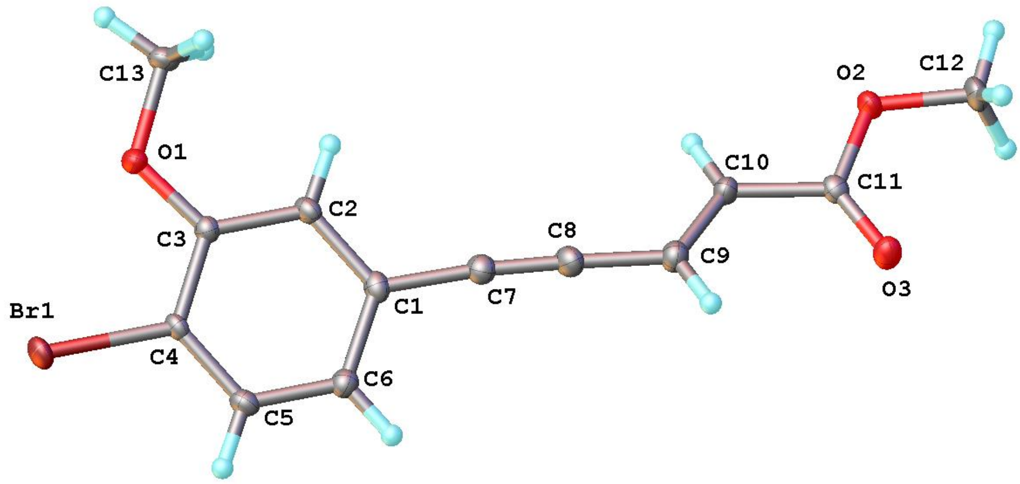

Table 1 Crystal data and structure refinement for 15srv238.

Identification code	15srv238
Empirical formula	$C_{13}H_{11}O_3Br$
Formula weight	295.13
Temperature/K	120.0
Crystal system	triclinic
Space group	P-1
a/Å	7.5029(6)
b/Å	7.7331(6)
c/Å	11.6022(9)
α/°	96.926(3)
β/°	103.697(3)
γ/°	110.372(3)
Volume/Å^3	597.69(8)
Z	2
ρ_{calc}g/cm^3	1.640

μ/mm^{-1}	3.431
F(000)	296.0
Crystal size/mm^3	0.24 × 0.22 × 0.02
Radiation	MoKα (λ = 0.71073)
2Θ range for data collection/°	5.76 to 58
Index ranges	-10 ≤ h ≤ 10, -10 ≤ k ≤ 10, -15 ≤ l ≤ 15
Reflections collected	11320
Independent reflections	3174 [R_{int} = 0.0511, R_{sigma} = 0.0585]
Data/restraints/parameters	3174/0/156
Goodness-of-fit on F^2	1.029
Final R indexes [I>=2σ (I)]	R_1 = 0.0311, wR_2 = 0.0623
Final R indexes [all data]	R_1 = 0.0441, wR_2 = 0.0660
Largest diff. peak/hole / e $Å^{-3}$	0.49/-0.42

Table 2 Fractional Atomic Coordinates ($\times10^4$) and Equivalent Isotropic Displacement Parameters ($Å^2\times10^3$) for 15srv238. U_{eq} is defined as 1/3 of of the trace of the orthogonalised U_{IJ} tensor.

Atom	***x***	***y***	***z***	**U(eq)**
Br1	2868.3(3)	6482.9(3)	842.56(19)	19.53(8)
O1	2460(2)	2503(2)	320.1(13)	18.9(3)
O2	1613(2)	-5173(2)	6709.0(13)	19.2(3)
O3	2801(2)	-2469(2)	8132.2(13)	22.0(3)
C1	2692(3)	2452(3)	3526.4(19)	16.1(4)
C2	2564(3)	1804(3)	2318.4(19)	15.8(4)
C3	2591(3)	2992(3)	1505.1(18)	14.1(4)
C4	2760(3)	4838(3)	1930.8(18)	13.4(4)

C5	2880(3)	5477(3)	3117.2(19)	16.5(4)
C6	2845(3)	4289(3)	3922.3(19)	16.9(4)
C7	2695(3)	1269(3)	4391.0(19)	18.2(4)
C8	2729(3)	399(3)	5176(2)	19.5(5)
C9	2829(3)	-548(3)	6155(2)	19.1(5)
C10	1992(3)	-2416(3)	6020.8(19)	16.4(4)
C11	2198(3)	-3291(3)	7084.3(19)	15.0(4)
C12	1738(4)	-6207(3)	7663(2)	22.2(5)
C13	2560(3)	718(3)	-98(2)	18.6(5)

Table 3 Anisotropic Displacement Parameters ($Å^2 \times 10^3$) for 15srv238. The Anisotropic displacement factor exponent takes the form: $-2\pi^2[h^2a^{*2}U_{11}+2hka^*b^*U_{12}+\ldots]$.

Atom	**U_{11}**	**U_{22}**	**U_{33}**	**U_{23}**	**U_{13}**	**U_{12}**
Br1	25.51(13)	12.63(11)	22.06(12)	9.16(8)	8.27(9)	6.84(9)
O1	30.6(9)	14.2(7)	15.8(8)	4.7(6)	9.6(7)	11.2(7)
O2	29.8(9)	12.9(7)	16.6(8)	5.9(6)	7.2(7)	9.2(7)
O3	29.6(9)	16.3(8)	16.0(8)	3.5(6)	4.7(7)	5.6(7)
C1	13.9(10)	16.6(10)	18.9(11)	7.9(8)	6.0(9)	5.4(9)
C2	18.0(11)	11.2(10)	20.5(11)	5.8(8)	8.3(9)	6.0(8)
C3	14(1)	12.8(10)	15(1)	4.0(8)	4.7(8)	4.2(8)
C4	13.2(10)	10.4(9)	16.9(10)	5.6(7)	5.2(8)	3.7(8)
C5	16.9(11)	12(1)	21.1(11)	3.5(8)	6.0(9)	6.0(8)
C6	16.9(11)	18.7(11)	15.7(10)	4.3(8)	5.5(9)	6.9(9)
C7	18.7(11)	17.4(11)	19.5(11)	4.7(8)	7.0(9)	7.1(9)
C8	22.4(12)	14.9(10)	21.5(12)	5.5(8)	8.9(10)	5.5(9)
C9	21.5(12)	19.0(11)	16.9(11)	5.4(8)	6.2(9)	7.2(9)
C10	20.4(11)	15.6(10)	13.1(10)	3.4(8)	4.5(9)	7.0(9)
C11	13.3(10)	14.4(10)	17.5(11)	4.9(8)	4.5(9)	5.2(8)
C12	32.3(13)	16.8(11)	22.1(12)	11.7(9)	10.5(10)	10.8(10)

C13	23.2(12)	12.6(10)	20.9(11)	2.3(8)	7.8(9)	7.7(9)

Table 4 Bond Lengths for 15srv238.

Atom	**Atom**	**Length/Å**	**Atom**	**Atom**	**Length/Å**
Br1	C4	1.8928(19)	C2	C3	1.392(3)
O1	C3	1.352(2)	C3	C4	1.404(3)
O1	C13	1.440(2)	C4	C5	1.376(3)
O2	C11	1.346(2)	C5	C6	1.385(3)
O2	C12	1.446(2)	C7	C8	1.197(3)
O3	C11	1.200(2)	C8	C9	1.426(3)
C1	C2	1.399(3)	C9	C10	1.331(3)
C1	C6	1.395(3)	C10	C11	1.479(3)
C1	C7	1.437(3)			

Table 5 Bond Angles for 15srv238.

Atom	**Atom**	**Atom**	**Angle/°**	**Atom**	**Atom**	**Atom**	**Angle/°**
C3	O1	C13	117.77(15)	C5	C4	C3	121.57(18)
C11	O2	C12	115.66(16)	C4	C5	C6	119.83(19)
C2	C1	C7	121.46(19)	C5	C6	C1	119.82(19)
C6	C1	C2	120.21(18)	C8	C7	C1	175.2(2)
C6	C1	C7	118.32(19)	C7	C8	C9	177.0(2)
C3	C2	C1	120.14(18)	C10	C9	C8	124.2(2)
O1	C3	C2	124.85(18)	C9	C10	C11	120.8(2)
O1	C3	C4	116.73(17)	O2	C11	C10	109.96(17)
C2	C3	C4	118.42(18)	O3	C11	O2	124.16(18)
C3	C4	Br1	118.70(15)	O3	C11	C10	125.87(19)
C5	C4	Br1	119.72(15)				

Table 6 Selected Torsion Angles for 15srv238.

A	B	C	D	Angle/°	A	B	C	D	Angle/°
C2	C3	O1	C13	-8.5(3)	C9	C10	C11	O2	-166.9(2)
C4	C3	O1	C13	171.70(18)	C9	C10	C11	O3	12.8(3)
C7	C8	C9	C10	-180(100)	C10	C11	O2	C12	-179.96(17)
C8	C9	C10	C11	178.9(2)	C12	O2	C11	O3	0.3(3)

Table 7 Hydrogen Atom Coordinates ($Å\times10^4$) and Isotropic Displacement Parameters ($Å^2\times10^3$) for 15srv238.

Atom	*x*	*y*	*z*	U(eq)
H2	2458	552	2052	19
H5	2987	6730	3384	20
H6	2924	4724	4742	20
H9	3539	201	6955	23
H10	1254	-3196	5232	20
H12A	1276	-7557	7300	33
H12B	899	-6023	8159	33
H12C	3124	-5742	8178	33
H13A	2506	563	-958	28
H13B	1431	-314	-4	28
H13C	3810	689	382	28